UNIVERSITÀ DEGLI STUDI DI CATANIA

FACOLTÀ DI SCIENZE MM.FF.NN.

DOTTORATO IN SCIENZE DEI MATERIALI XXV CICLO

DIPARTIMENTO DI SCIENZE CHIMICHE

Dott. Ivan Pietro Oliveri

Zinc(II) Schiff Base Complexes and their Aggregation/ Deaggregation Properties: Versatile and Multifunctional Materials as Chemosensors and Building Blocks for New Supramolecular Architectures

Tesi di Dottorato

Coordinatore di dottorato

Chiar.mo Prof. Antonino Licciardello

Tutor

Chiar.mo Prof. Santo Di Bella

TRIENNIO 2009-2012

Contents

Abstract

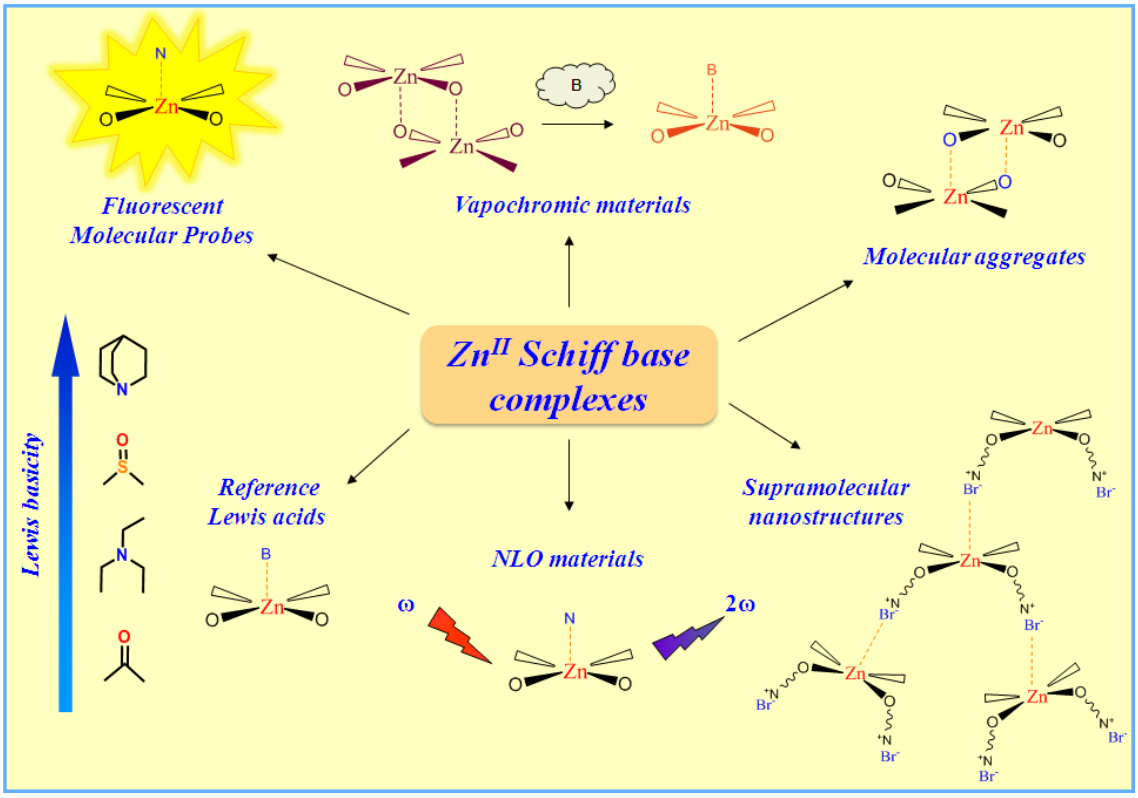

In this PhD thesis the synthesis, characterization, and study of the aggregation/deaggregation properties of a series of amphiphilic bis(salicylal-diminato)Zn^{II} Schiff base complexes, involving different bridging diamino groups, and their applications as molecular probes, nonlinear optical (NLO) and vapochromic materials, as well as synthons for the formation of new fibrillar and branched supramolecular nanostructures, are reported.

Through detailed ^{1}H NMR, DOSY NMR and optical spectroscopic studies, it is found that these species always form aggregates in solution of non-coordinating solvents. The degree of aggregation is related to the nature of the bridging diamine. Solutions of complexes where the bridging diamine contains the naphthalene or the pyridine nucleus are always characterized by the presence of defined dimer aggregates, oligomeric aggregates are likely formed for complexes having the benzene bridge, whereas for complexes with the 2,3-diaminomaleonitrile, the degree of aggregation is concentration dependent, influencing also their second-order NLO response. Finally, for the complexes having as bridging diamine the ethane group,

the existence of equilibrium between two different types of dimers is observed, related to the non-conjugated, conformational flexible nature of the bridge. In coordinating solvents or in the presence of coordinating species, a complete deaggregation of all complexes occurs because of the axial coordination to the Zn^{II} ion, accompanied by considerable changes of the ^{1}H NMR and optical absorption and fluorescence spectra. Moreover, an easy switch-on of the NLO response upon addition of a Lewis base, such a pyridine, with formation of a 1:1 adduct, or 1,2-bis-(4-pyridyl)ethane, with formation of a 2:1 adduct, is observed. As the amount of the coordinating species for the complete deaggregation of the complexes is dependent of the Lewis character of the Zn^{II} ion, an order of the Lewis acidic character, Zn^{II}(2,3-diaminomaleonitrile) > Zn^{II}(2,3-diaminopyridine) > Zn^{II}(2,3-diaminonaphthalene) > Zn^{II}(1,2-diaminobenzene) > Zn^{II}(1,2-ethylendiamine), can be established for the aggregate species in non-coordinating solvents. The effect of the alkyl chain length seems to play a minor role in the aggregation properties, since ^{1}H NMR data, optical absorption and fluorescence spectra remain almost unaltered upon changing the chain lengths. The Zn^{II}(1,2-diaminobenzene) complexes form fibrillar nanostructures whose width is influenced by the degree of interdigitation of side alkyl chains.

The Lewis acid properties of the Zn^{II}(2,3-diaminomaleonitrile) complexes, with respect a series of primary, secondary and tertiary aliphatic amines, and several alkaloids, are also investigated. Through the analysis of fluorescence titrations, it is found that the binding interaction, the selectivity and the sensitivity of these complexes are strongly influenced by the steric characteristics of the nitrogen based donors and then by their Lewis basicity, leading to high selectivity, in the micromolar range, and sensitivity for pyridine-based, cinchona alkaloids, primary and alicyclic amines. A distinct selectivity is also observed along the series of secondary or tertiary amines, paralleling the increasing steric hindrance at the nitrogen atom. Moreover, these complexes have been also involved as reference Lewis acids, to build up a reliable Lewis basicity scale in dichloromethane for amines and various common solvents whose trend is influenced by the steric hindrance of both the Lewis bases and the reference Lewis acid. The Zn^{II}(2,3-diaminomaleonitrile) complexes have also investigated as vapochromic materials, able to change their colour upon exposure to

volatile Lewis bases, allowing their application as chemosensors for volatile Lewis bases in the solid state.

Finally, new branched nanostructures have been achieved for a Zn^{II} Schiff base complex having an alkyl ammonium bromide in the alkyl side chains. Unlike to studies on the aforementioned amphiphilic complexes, in this case the control of the supramolecular architecture is governed by intermolecular Zn···Br interactions.

1 General Introduction

Tetracoordinated Schiff base metal complexes play an important role in the coordination chemistry.[1] These complexes can be obtained by condensation of a diamine with a salicylaldehyde derivative, followed by complexation with a metal ion. In relation to the kind of diamine, it is possible to distinguish two classes of complexes: the "*salen*" species, if the diamine is aliphatic, and the "*salphen"* or "*salophen*" species in the case of aromatic diamines.

Schiff base ligands coordinate the metal ions in their dianionic form because they possess four coordinative sites, two phenolate anions and two iminic nitrogen atoms. This N_2O_2-donor "pocket" is capable to stabilize various metal cations in different oxidation states.[3] This feature resembles the porphyrins but, from a synthetic point of view, the Schiff base ligands are more versatile.[3] In fact, the large amount of commercial diamines and salicylaldehydes and the various synthetic routes of their functionalization allow the achievement of a larger number of ligands and then metal complexes, with properties easily fine-tunable.

The type and the coordination geometry of the metal centre are crucial in determining the properties of the Schiff base complexes. The coordination of the metal centre in the N_2O_2-donor "pocket" of ligand occurs in the equatorial plane, leaving unsaturated the apical sites of the metal ion.

Among various Schiff base metal complexes, Zn^{II} derivatives have only recently been studied for their various photophysical, catalytic, supramolecular, and sensing properties,[4] while other metal complexes such as Mn,[5] Fe,[6] Al,[7] Cr,[8] Co,[9] Cu,[10] Ni,[11] Pt[12] etc. have been widely investigated.

A peculiarity of Zn^{II} Schiff base complexes is the tendency of the Zn^{II} ion to expand its coordination sphere through the axial coordination. This is due to the constrain of the Zn^{II} ion in the square-planar N_2O_2-donor "pocket" of the Schiff base ligand since the favoured coordination of Zn^{II} is tetrahedral. This constrain forces the Zn^{II} ion to a

position little above the plane formed by the N_2O_2-donor "pocket"[13] and the axial coordination implies square pyramidal coordination geometry.

The axial coordination of the Zn^{II} ion can be satisfied through two ways, *i)* by intermolecular interactions between the Zn^{II} of an unit with the phenolic oxygen of another unit; *ii)* coordination of the solvent or other coordinating species. In the first case, this implies the formation of aggregate species, through Zn···O intermolecular interactions, while a pentacoordinated monomer is formed in the presence of a coordinating species. In other words, the Zn^{II} ion in Schiff base complexes is a Lewis acid capable to coordinate various neutral or anionic Lewis bases or, in their absence, to form aggregate species in solution and in the solid state, allowing a "control" of the supramolecular aggregation both in solution and in the solid state.[14]

These features open multiple ways involving Zn^{II} Schiff base complexes in various fields such as catalysis, supramolecular chirality, sensing, nanostructured materials, etc. In the following discussion, it will be discussed several fields of application of these complexes, highlighting how the tendency of metal centre to axial coordination, hence their Lewis acidic character, plays a crucial role in each application.

1.1 Catalysis

Schiff base metal complexes have been extensively studied in homogeneous catalysis.[3c,d,3f,3h,4,15] They have been used as catalytic species in numerous organic reactions including, lactide polymerization, asymmetric ring opening of epoxides, Michael reactions, the epoxidation of olefins, etc..

In spite of numerous studies about the catalytic properties of Schiff base metal complexes, the application of Zn^{II} complexes is yet limited, even if their efficiency as catalyst has been well demonstrated. For example, the demand of Zn^{II} ion in Schiff base complexes to saturate its coordination sphere permits to immobilize a species, allowing the correct approaching of another species, thus speeding up the reaction. Kleij and co-workers have investigated various Zn^{II} Schiff base complexes as catalysts for the synthesis of cyclic carbonate, under mild conditions, by coupling of CO_2 with terminal epoxides in presence of tetrabutylammonium (TBA) halide as co-catalyst.[16] Both the Zn^{II} Schiff base complex and co-catalyst are indispensable for the catalysis of reaction since the absence/lowering of either components virtually gives none or very low conversion. The catalytic mechanism is based on the axial coordination of terminal

epoxides on the Zn^{II} Schiff base complex. In particular, the epoxide coordination to the complex blocks the epoxide, allowing the subsequent epoxide ring opening by the halide anion. Then, insertion of carbon dioxide in the $Zn\cdots O_{epoxide}$ bond and cyclization by internal attack of the carbonate oxygen on the C-halide bond with regeneration of the halide co-catalyst, take place (Figure 1.1).

One peculiarity of Zn^{II} Schiff base complexes is the ability to act both as Lewis acid and base, respectively, through the metal centre and the oxygen atoms of the ligand framework. Cozzi uses this bifunctional ability of Lewis acid/base of chiral Zn^{II} Schiff base complexes for the catalytic enantioselective addition of alkynes to ketones.[17] This reaction occurs between an aliphatic or aromatic ketone and a zinc alkyne. The zinc alkynides are prepared in situ by stirring $(CH_3)_2Zn$ and alkyne, then the Zn^{II} complexes and the ketones are added in the reaction mixture. The catalysis mechanism involves the double interactions between the Zn^{II} ion of the Schiff base complexes with the carbonyl oxygen of the ketone and the Zn^{II} of the zinc alkyne with the phenolate oxygen atom of Schiff base ligand framework. This implies the formation of a transition state (Figure 1.2) in which the carbon atom bound to Zn^{II} of the zinc alkyne reacts with the carbonyl carbon of the ketone to obtain the corresponding tertiary alcohol derivative. Aromatic ketones are less reactive than aliphatic ketones, and the enantiomeric excess of the product depends by steric hindrance of ketone, whereas electronic effects play only a minor role. This indicates that the $Zn\cdots O$ interaction between the Zn^{II} ion of the Schiff base complex with the oxygen atom of the ketone is dependent of the steric hindrance of ketone.

Zn^{II} Schiff base complexes can be functionalized with a cavitand in peripherical position building a catalyst that can include a specific guest, able to interact both with the cavitand and the Zn^{II} complex. Rebek and co-workers use a catalyst, obtained by fusion of a cavitand of resorcin-[4]-arene with a Zn^{II} salophen complex, in the reactions of hydrolysis of para-nitrophenyl choline carbonate (PNPCC) by the water present in CH_2Cl_2 and esterification of choline with various anhydrides (Figure 1.3).[18]

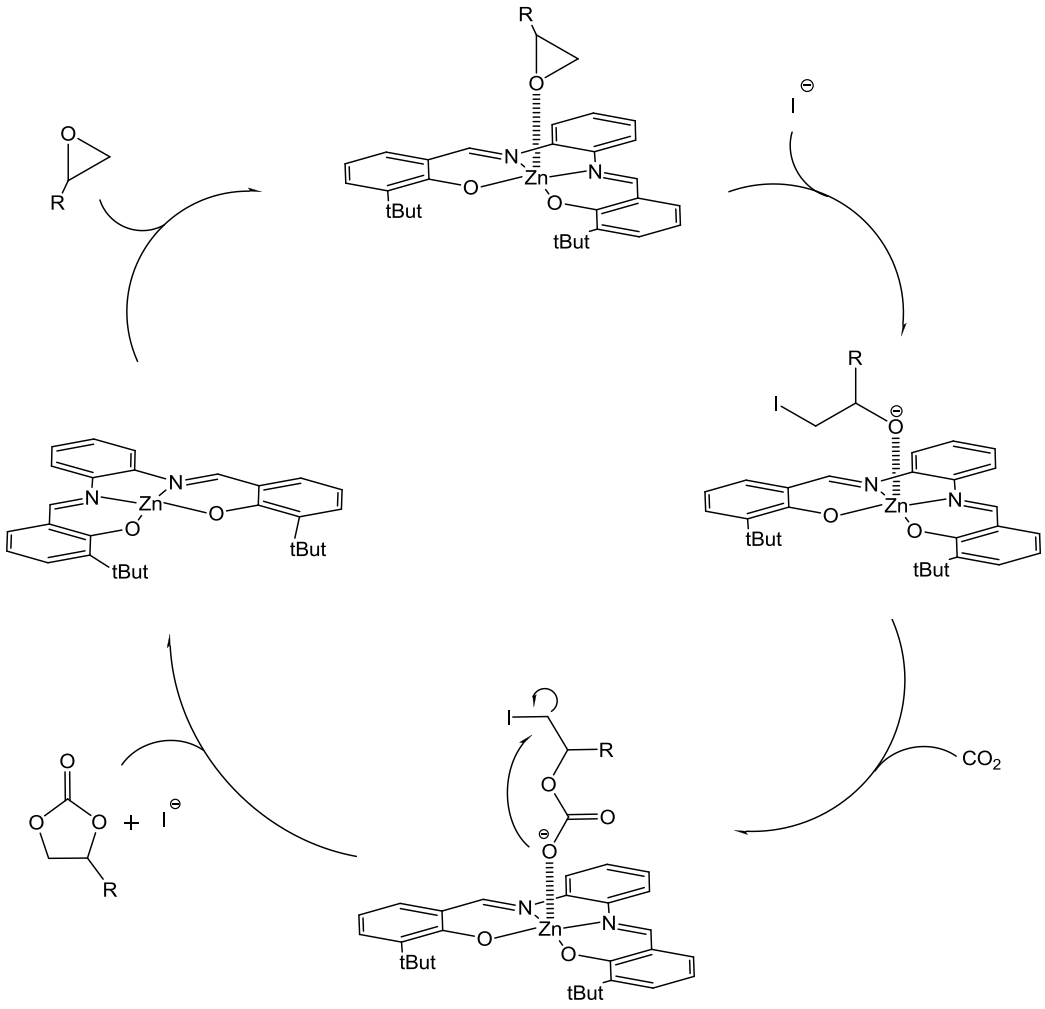

Figure 1.1 Representation of the catalytic cycle proposed in the synthesis of cyclic carbonate.

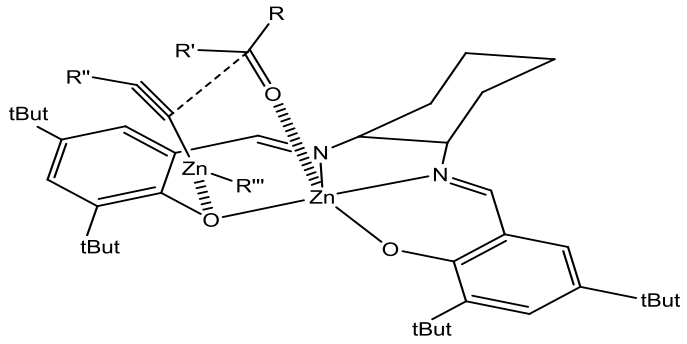

Figure 1.2 Representation of the catalytic mechanism of a chiral Zn^{II} Schiff base complex in the reaction of addition of alkynes to ketones.

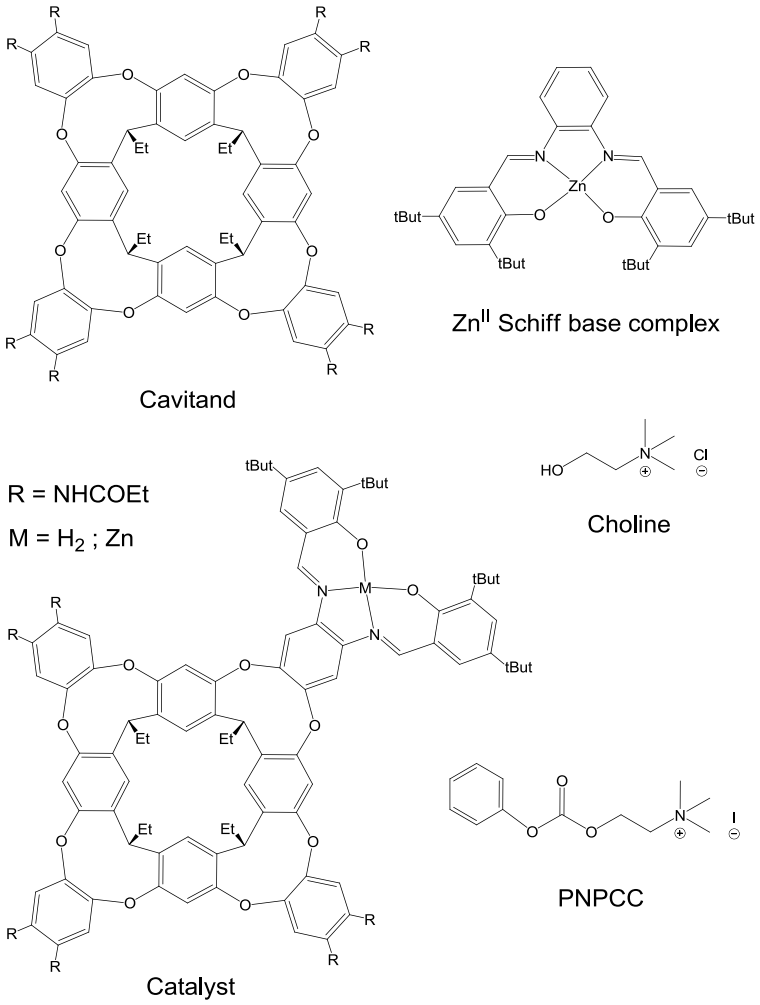

Figure 1.3 Structures of the catalyst, its building blocks and the substrates involved in the reaction of hydrolysis and esterification.

In the hydrolysis reaction, the guest (PNPCC) interacts with host (catalyst) through the cation-π interaction between alkyl ammonium group and benzene rings of the resorcin-[4]-arene cavity and the Zn···O interactions between carbonyl oxygen atom of carbonate and Zn^{II} ion of the Schiff base complex. These interactions occur simultaneously, thus allowing the dramatic acceleration of hydrolysis of PNPCC. However, the Zn···O interaction plays a crucial role in the catalytic mechanism. In fact, no acceleration is observed with the metal-free salophen cavitand, whereas, when the Zn^{II} salophen without cavitand is used as catalyst, the Zn^{II} ion plays its Lewis acid role and, interacting with carbonilyc oxygen of PNPCC, the reaction rate is increased, even if is five times slower than the reaction catalyzed with Zn^{II} salophen fused with cavitand.

In the esterification of choline with anhydrides, the catalytic mechanism is quite different (Figure 1.4).

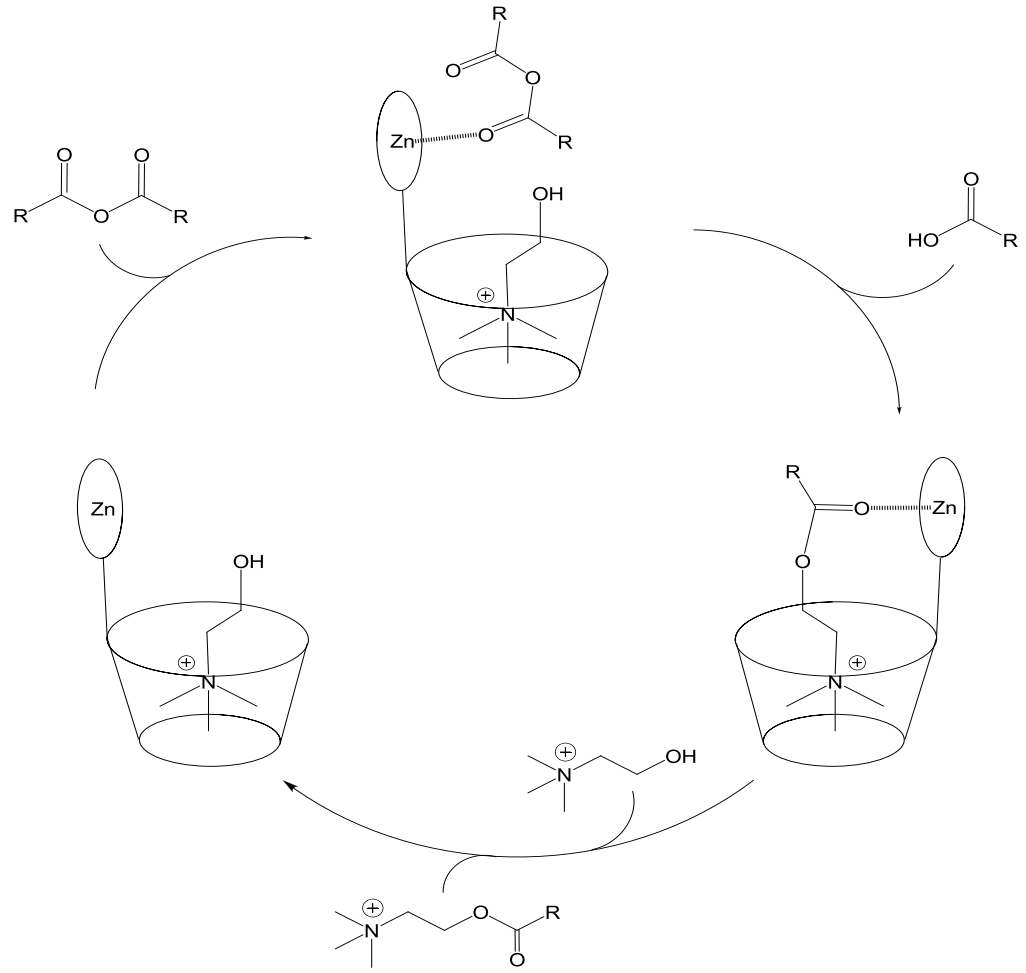

Figure 1.4 Representation of the catalytic cycle proposed in the esterification of choline.

The alkyl ammonium group of choline is included in the cavity of the resorcin-[4]-arene through cation-π interaction, whereas the anhydride interacts with catalyst through Zn···O interaction between carbonyl oxygen and Zn^{II} ion of the Schiff base complexes. These interactions lock both substrates so as to be sufficiently close to allowing the attack of alcoholic oxygen of cholyne to the carbonyl carbon of anhydrides to form acylcholine derivative, which leaves the binding pocket of cavitand restoring the catalyst. Also in this case, the Zn···O interaction plays a crucial role, in fact no reaction occur with cavitand without Zn^{II} salophen complexes. Moreover, the reaction is slow considering more encumbered anhydrides according to the strongly dependence from steric hindrance of axial coordination in the Zn^{II} Schiff base complexes.

1.2 Chirogenesis

Chirogenesis is defined as the induction of chirality by chiral guest able to lock non-chiral host substrates in a determinate chiral configuration[19]. Natural system such as proteins, DNA, etc. transfer chiral information through supramolecular interactions and the chirogenesis is involved in various fields, for example in enantioselective catalysis[20] and material science.[20a,21] An interesting application of chirogenesis is the determination of the absolute configuration of various chiral substrates.[22]

Zn^{II} Schiff base complexes are suitable substrates useful for the induction of chirality because the Zn^{II} ion can interact, through axial coordination, with various chiral substrates allowing the determination of their chiral configuration. In this context, Kleij and co-workers have investigated the chirogenesis of a new series of Zn^{II} bis-salophen complexes **1**-**6** (Figure 1.5).[23]

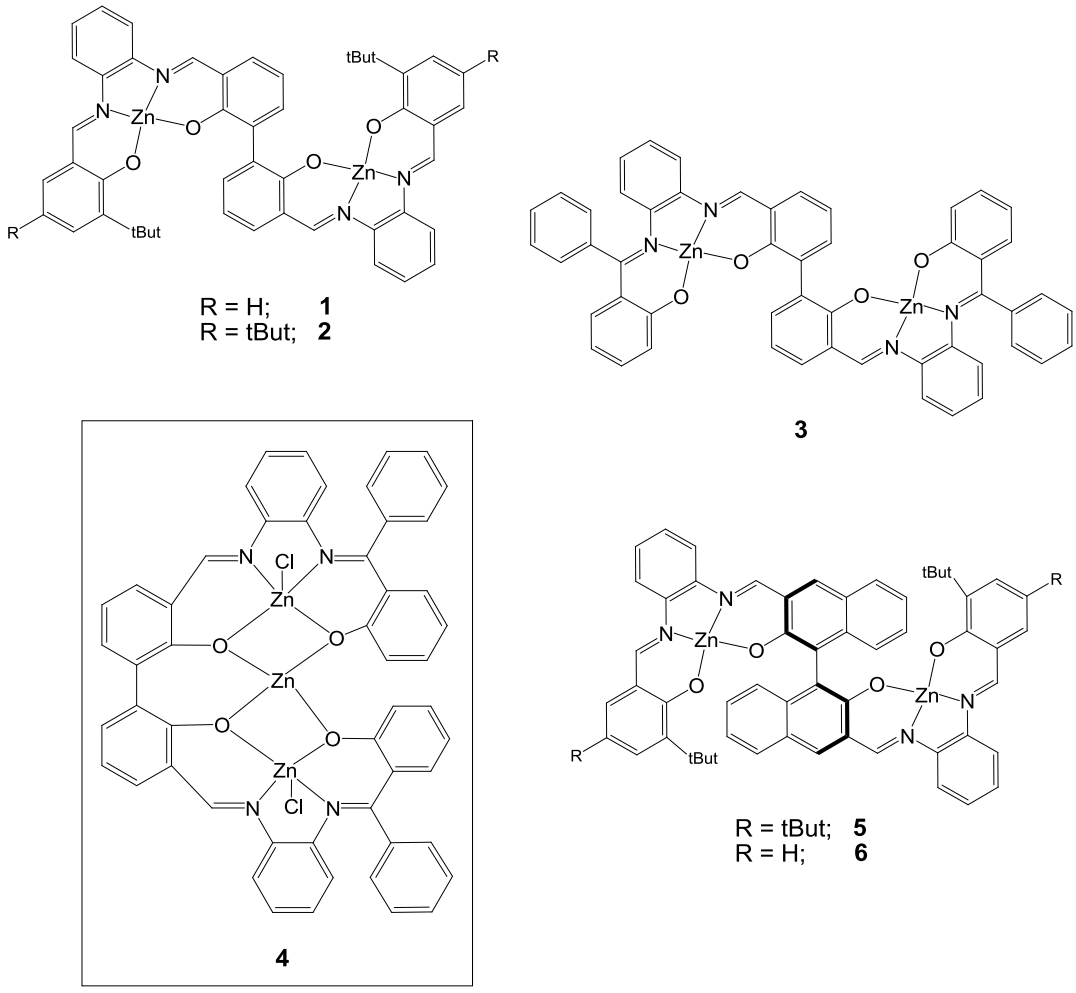

Figure 1.5 Structures of Zn^{II} bis-salophen complexes **1**-**6**.

These binuclear complexes have been synthesized in one step reaction of two equivalent of monoimine precursors and $Zn(CH_3COO)_2$ and one equivalent of bis-salicylaldehyde in the presence of organic base. Their peculiarity is the presence of a biphenyl bridging group that permits the rotation of the two metal complex units, allowing a dynamic equilibrium between two possible enantiomers (Figure 1.6).

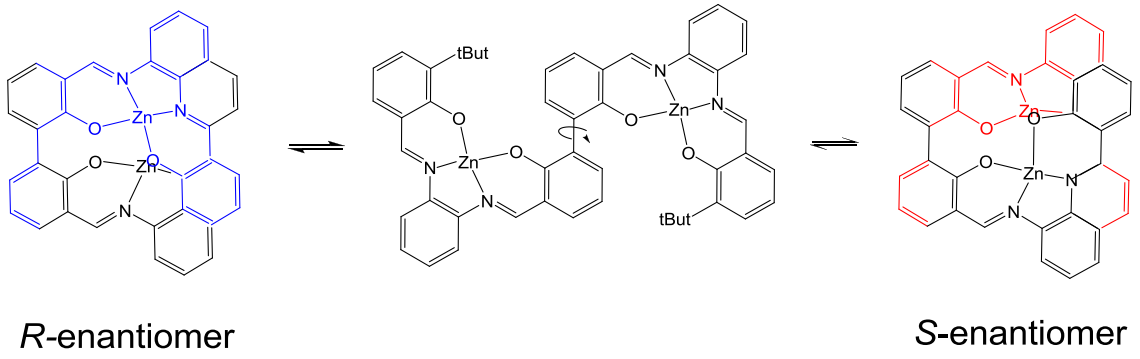

Figure 1.6 Conformational isomerism of complex **1**. The t-But groups in the enantiomers structures are omitted for clarity.

Complex **1** has been investigated through single crystal X-ray diffraction, 1D, 2D ^1H NMR, circular dichroism (CD) experiments and DFT calculations. It is found that acetic acid (AcOH), side product of the synthesis, blocks the rotation of two complex units coordinating the two Zn^{II} ions with two oxygen atoms of AcOH,[14d] with the formation of racemic mixture of *R* and *S* enantiomers. These Zn···O interactions are very strong, in fact, even using pyridine that bind strongly the Zn^{II} ion in Schiff base complexes[13], a stoichiometric excess is required to displace the AcOH. However, in presence of another carboxylic acid, the displacement of AcOH occurs with the stoichiometric amount of competitive carboxylic acid. This allows the determination of the absolute configuration of various chiral α-carboxylic acids. Through CD experiments in solution, it is found that the chirogenesis with the chiral α-carboxylic acid implies the stabilization of the *R* enantiomer, if the organic acid is in *S* configuration, and vice versa. The increment of molar ellipticity is related of the steric hindrance of the chiral α-carboxylic acid, because the Zn···O interaction is less efficient.

In general, the induction of chirality in a non-chiral host occurs through a ditopic chiral guest.[24] Despite the validity of this approach, the chirogenesis of a non-chiral host through monotopic chiral guest is highly desirable,[22f,25] because it permits the

achievement of new chiral supramolecular ligands and the determination of absolute configuration of a larger variety of chiral substrates. Kleij and co-workers have synthesized complex **3** through metalation of the corresponding free bis-salophen ligand with $ZnEt_2$ as Zn^{II} ion source, thus avoiding the formation of the adduct with AcOH,[23c] and then allowing the chirogenesis without the presence of competitive species.[23b] In absence of guest, **3** possesses four free oxygen atoms of the ligand framework able to bind another Zn^{II} ion. In fact, upon addition of ethereal solution of $ZnCl_2$, the coordination of a third Zn^{II} ion by four oxygen atoms of the framework and the axial coordination of the other two Zn^{II} ion with chloride anions, occur with formation of trinuclear Zn_3 bis-salophen complex **4**. As expected, the chirogenesis of **3** occurs with ditopic chiral guests[23c] whereas for **4**, the chirogenesis occurs with the monotopic chiral guests, because there is only the central Zn^{II} ion able to axially coordinate the chiral guest. In other words, the availability for axial coordination of one or two Zn^{II} metal centres implies a differentiation of the kind of chiral guest able to transfer chiral information, thus allowing the possibility to determinate the chiral configuration of a wider variety of chiral guests.

The common non-chiral host molecules useful for chirogenesis applications does not include competitor salts that can compete for the chiral guest.[23b] To take a broad view on the effect of salt observed for **1** in the chirogenesis for these systems,[23c] Kleij and co-workers have investigated the complexes **2**, **3**, **5** and **6** synthesized with/without, excess/defect of $Zn(CH_3COO)_2$.[23a] Through X-ray diffraction, ^1H, DOSY NMR and MALDI(+) mass spectrometry experiments, it is found that the complexes **2**, **3**, **5** and **6** are stable as hexanuclear complexes having two $Zn(CH_3COO)_2$ molecules, using a slight excess of $Zn(CH_3COO)_2$, and two $Zn(OH)_2$ molecules using $ZnEt_2$ as Zn^{II} ion source molecules.[26] The authors have also investigated the role the stoichiometric reaction to understand factors which control the formation of multinuclear or AcOH adducts complexes. It is found that in slight defect of $Zn(CH_3COO)_2$, Zn^{II} bis-salophen·AcOH adducts are obtained, whereas the achievement of multinuclear Zn^{II} bis-salophen complexes requires a slight excess of $Zn(CH_3COO)_2$.

1.3 Sensing

The deaggregation process of Zn^{II} Schiff base complexes upon coordination of neutral or ion Lewis bases implies dramatic variations in terms of ^{1}H NMR chemical shift, optical absorption, enhancement/quenching of fluorescence etc., and the magnitude of spectroscopic properties changes are related to Lewis basicity of coordinating species.[14] These features are suitable to design molecular sensors to various Lewis bases. For example, Kleij and co-workers have investigated the sensing properties of a series of mononuclear and binuclear Zn^{II} salophen complexes **7**-**10** *vs.* a series of nicotine alkaloids derivatives in coordinating and non-coordinating solvents (Figure 1.7).[14e]

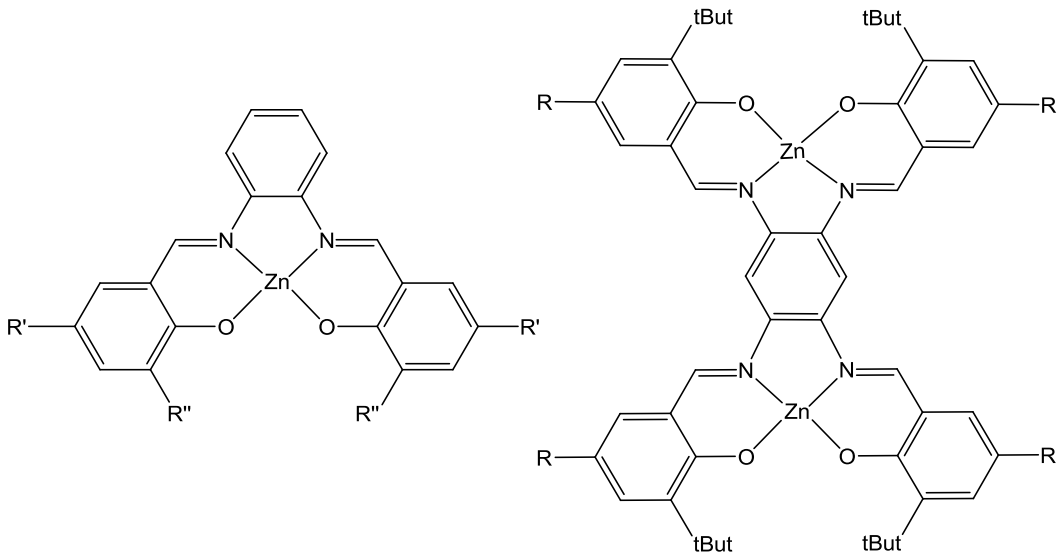

R' = R" = tBut **7**
R' = H; R" = tBut **8**

R = tBut **9**
R = H **10**

Figure 1.7 Structures of Zn^{II} salophen complexes **7**-**10**.

In absence of coordinating Lewis bases, the Zn^{II} Schiff base complexes tend to form aggregate species by intermolecular axial Zn···O interactions (vide supra). However, the t-But groups of the ligand frameworks of complexes **7**-**10** avoid axial coordination interactions for their steric hindrance, therefore these complexes in solution are in a monomeric form in solution.[27] Through ^{1}H, NOE NMR, UV-vis and X-ray diffraction experiments, it is found that complexes **7** and **8** coordinate one molecule of alkaloid, whereas the complexes **9** and **10** are capable to coordinate two molecules of alkaloid,

according with the number of metal centre available for axial coordination. The Zn···N axial interactions involving the pyridine nitrogen atom of alkaloid are very strong, with binding constant values typically up to an order of 10^5. Moreover, the formation of complex·alkaloid implies dramatic changes in terms of optical properties, suitable in sensing application. Noteworthy, the Zn···N axial interactions between Zn^{II} complexes and the alkaloids is influenced by electronic effects.[13a,28] In particular, for the complexes **9** and **10**, the first binding constant is comparable with those of the complexes **7** and **8**, but, after the coordination of the first molecule of alkaloid, the second binding constant is almost two times smaller, as compared to the first binding constant, according to the electronic conjugation between the two Zn^{II} complex units.

The axial coordination in the Zn^{II} Schiff base complexes is also influenced by steric effects. This dependence is well demonstrated by Kleij and co-workers that have investigated the remetalation process of Zn^{II} complexes **7** and **9** with isoquinoline *N*-heterocycles derivatives after demetalation.[29] The demetalation process of Zn^{II} Schiff base complexes occurs in presence of water. In particular, if the solvent is not enough dried, the water can coordinate the Zn^{II} ion allowing the formation of $Zn(OH)_2$ and then the demetalation of complex.[29] The addition of strong Lewis bases, such as *N*-heterocycles, permits the restoring of the Zn^{II} complex since the ability of nitrogen based compounds to coordinate the Zn^{II} ion of Schiff base complexes.[3i,13,14e,27a,28b] Through ^{1}H NMR and UV-vis experiments, it is found that the axial interactions between Zn^{II} complexes and the isoquinoline *N*-heterocycle derivatives investigated are strongly influenced by the steric hindrance of the Lewis base. In fact, through UV-vis experiments, it is noted that a quasi-complete restoring is obtained using *N*-heterocycles derivatives less encumbered, whereas no remetallation occurs with alkaloids more encumbered.

The crucial role of the steric hindrance of the Lewis base on axial coordination of Zn^{II} Schiff base complexes is also demonstrated by Dalla Cort and co-workers in a study of discrimination of tertiary amines with Zn^{II} complexes **11-13** (Figure 1.8).[30] In spite the complexes are in aggregate form, since the presence of isopropylic groups does not avoid the Zn···O intermolecular interactions,[27,30] it is found that the axial coordination of tertiary amines is strongly dependent by steric hindrance of amines and not by their Brønsted basicity.

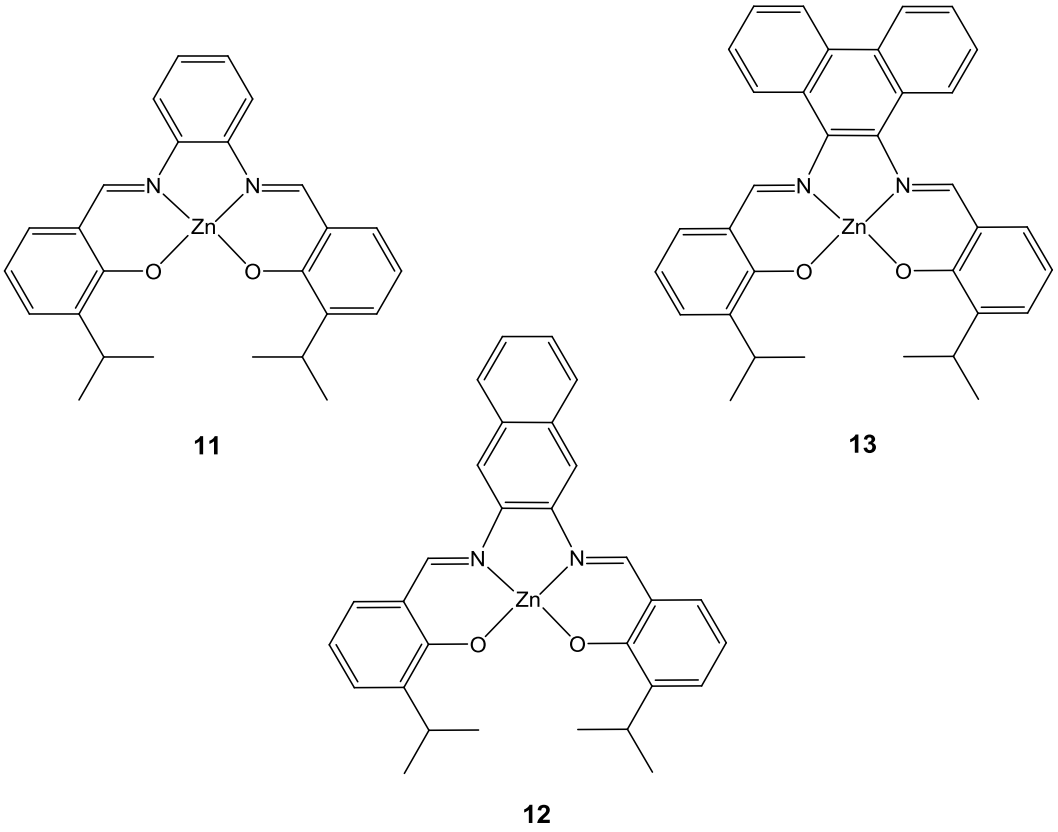

Figure 1.8 Structures of Zn^{II} salophen complexes **11**-**13**.

In fact, despite its greater Brønsted basicity, the binding constant of diisopropylamine is lower than that of quinuclidine, because the quinuclidine steric hindrance is less than that of diisopropylamine. This permits the application of complexes **11**-**13** as molecular probing of tertiary amines in relation of their steric hindrance.

The Zn^{II} Schiff base complexes are able to coordinate not only neutral Lewis bases, but also anions. Supramolecular recognition of anions is of increasing interest in various applications, since anions are ubiquitous.[31] Dalla Cort and co-workers have investigated the Zn^{II} Schiff base complexes **11** and **12** as receptors of inorganic phosphates PO_4^{3-}, $P_2O_7^{4-}$, and $P_3O_{10}^{5-}$ and adenosine nucleotides AMP^{2-}, ADP^{3-}, and ATP^{4-}.[32] Through ^{31}P NMR and ESI mass spectrometry experiments, it is found that both inorganic phosphates and adenosine nucleotides coordinate the Zn^{II} ion of the Schiff base complexes forming 1:1 adducts. However, there are optical absorption spectra and ^{1}H NMR chemical shift variations and quenching of fluorescence only for adenosine nucleotides[33], allowing the application of these complexes for molecular recognition of

adenosine nucleotides. The binding constants, calculated through UV-vis and fluorescence spectroscopy, for both complexes are almost identical and their order is $ADP^{3-} > ATP^{4-} > AMP^{2-}$. Noteworthy, this order does not depend by anions's charge, but from the secondary interaction π-π between the aromatic framework of the Zn^{II} Schiff base complexes and the adenosine moiety of the nucleotide.

The ability of Zn^{II} Schiff base complexes to axially coordinate both neutral and ion Lewis bases and the possibility of functionalization with groups that allow the solubilisation in a variety of solvents allow the application of these systems for molecular recognition in water. For example, Dalla Cort and co-workers have synthesized a Zn^{II} salophen complex, **14**, having D-glucose units in the 5-positions of benzene rings of salicylaldehyde moieties and investigated the chiral recognition properties *vs.* α-aminoacids in water (Figure 1.9).[34]

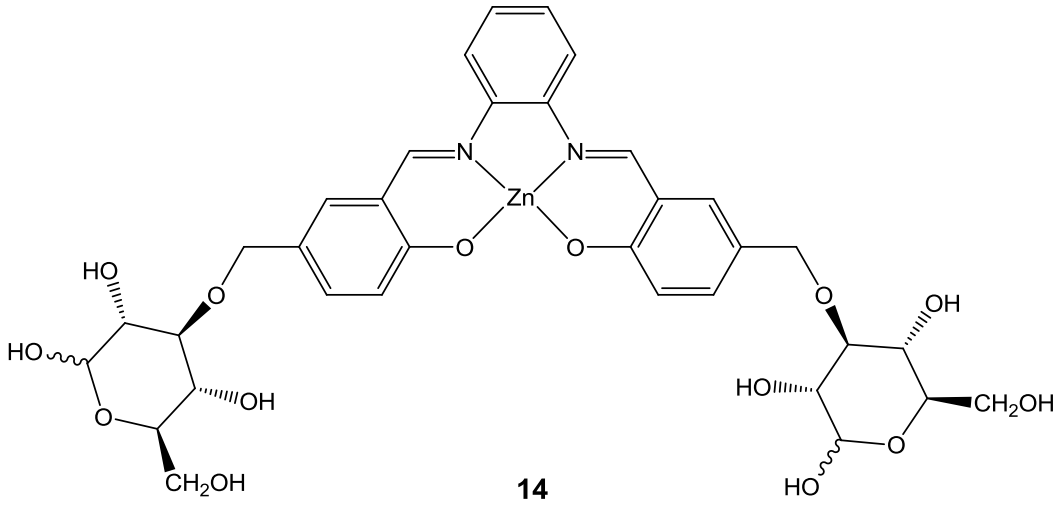

14

Figure 1.9 Structure of the Zn^{II} salophen complex **14**.

Through UV-vis experiments, it is found that the coordination of α-aminoacid occurs through the carboxylate group and it is strongly dependent of the steric hindrance of the side chain of the α-aminoacid. In fact, glycine, having a hydrogen atom as side chain, showed the highest binding constant, while tryptophan, having more encumbered indole group in the side chain, shows the lowest binding affinity. Moreover, the simultaneous hydrogen bond interaction between the ammonium group of α-aminoacid and two oxygen atoms of D-glucose moiety allows the discrimination of L and D α-aminoacids.

1.4 Supramolecular building blocks

In supramolecular chemistry, the achievement of 3D-structures through intermolecular interactions between small building blocks is very important, because these structures have different properties respect their building blocks. For example, 3D supramolecular structures may have internal cavities able to include several small organic or metallo-organic molecules.[35]

The demand of the Zn^{II} ion in the Schiff base complexes to axially coordinate Lewis bases to saturate their coordination sphere allows the possibility to use these complexes as building blocks to achievement new supramolecular 3D structures. In particular, linear or branched multitopic Lewis bases can coordinate several Zn^{II} complex units, obtaining new 3D structures with different properties respect to the building block, useful for various applications.[14c,36] Reek and co-workers have investigated the supramolecular architectures, obtained using Zn^{II} Schiff base complexes **15**-**18** and two pyridylphosphanes $P(py)_3$-**1**, and $P(py)_3$-**2** as a template, and their catalytic properties (Figure 1.10).[28b].

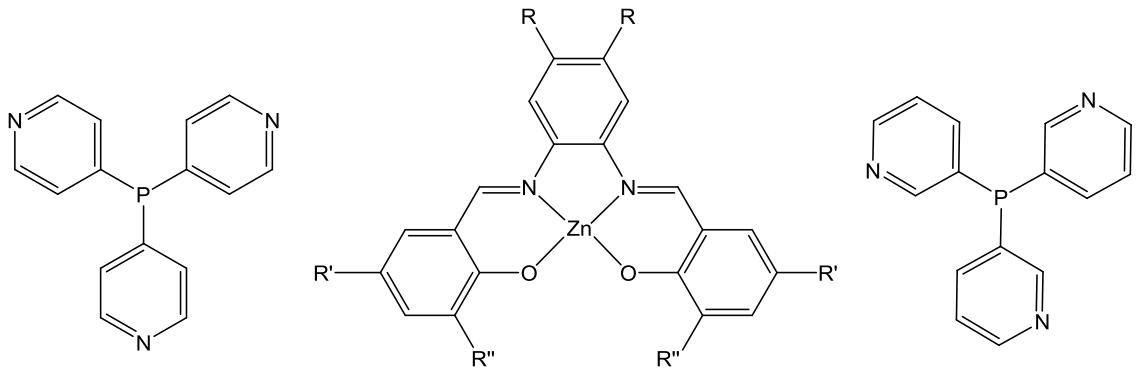

Figure 1.10 Structures of Zn^{II} Schiff base complexes **15-18** and pyridylphosphanes $P(py)_3$-**1**, $P(py)_3$-**2**.

Through UV-vis, ^1H NMR and X-ray experiments, it is found that three units of Zn^{II} Schiff base complex are coordinated to the pyridine groups of $P(py)_3$-**1** and $P(py)_3$-**2** by Zn···N axial interaction,[3i,13,14e,27a,28b] allowing the formation of supramolecular adducts (**Zn**)$_3$P(py)$_3$-**1**, and (**Zn**)$_3$P(py)$_3$-**2** (Zn = complexes **15-18**) in which the phosphorous is

encapsulated into three molecules of the complex. However, the degree of encapsulation of the phosphorous atom in the two supramolecular systems is different. In particular, even if (**Zn**)$_3$P(py)$_3$-**1** adduct is rather encumbered, the phosphorous atom is accessible and tends to form P···P interactions, with formation of the structure [(**Zn**)$_3$P(py)$_3$-**1**]$_2$. On the other hand, the phosphorous atom is better encapsulated in the (**Zn**)$_3$P(py)$_3$-**2** adduct than (**Zn**)$_3$P(py)$_3$-**1**, thus avoid the formation of P···P interactions. These structural differences are reflected in their catalytic properties.[37] (**Zn**)$_3$P(py)$_3$-**1** and (**Zn**)$_3$P(py)$_3$-**2** have been used as ligands in the rhodium-catalyzed hydroformylation of 1-octene at ambient temperature and their catalytic efficiency has been compared with respect to their parent precursors P(py)$_3$-**1** and P(py)$_3$-**2**. Since the minor accessibility of phosphorous atom to metal centre of rhodium complex, the (**Zn**)$_3$P(py)$_3$-**1** is less efficient than parent P(py)$_3$-**1**. Conversely, the phosphorous atom in the (**Zn**)$_3$P(py)$_3$-**2** is more accessible to the rhodium metal centre, therefore (**Zn**)$_3$P(py)$_3$-**2** is more efficient than P(py)$_3$-**2**.

Another approach, followed by Reek and co-workers to build a ligand useful for catalytic applications, is to use the rigid dinuclear Zn^{II} Schiff base complex **9** (Figure 1.7) as a template, to bind two mono pyridyl phosphorous ligands and forming a supramolecular structure useful for catalysis (Figure 1.11).[38]

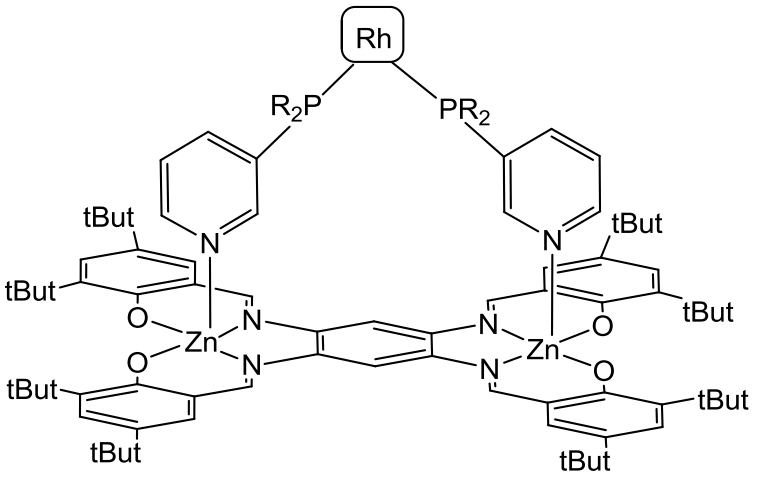

Figure 1.11 Structure of the template **9** coordinated with two generic mono pyridyl phosphorous ligands and a rhodium complex.

The formation of the supramolecular architecture is monitored by UV-vis, ^{1}H NMR spectroscopy and X-ray analysis and it is found that these templates improve the

selectivity in asymmetric hydroformylation and hydrogenation reactions compared to their non-templated mono pyridyl phosphorous ligands.

Zn^{II} Schiff base complexes have been involved in the achievement of porous materials through axial coordination of ditopic nitrogen ligands to the Zn^{II} metal centre. The goal of this strategy is the control of channel size of the material through the length of the ditopic ligand. Reek and co-workers have investigated the molecular assembly of the Zn^{II} Schiff base complex of **9** (Figures 1.7) with a series of bis-pyridine ligands.[13a] It is observed that the axial coordination of Zn^{II} ion by ligands occurs also in polar solvents, in contrast with Zn^{II} porphyrins,[39] according to the major Lewis acidic character of the Zn^{II} ion in Schiff base complexes respect to Zn^{II} porphyrins.[13a] Moreover, if the complex **9** axially coordinate the ditopic ligand such as 4,4′-bipyridine or 1,2-bis(4-pyridyl)ethane or 1,4-bis(4-pyridyl)benzene, it is possible the achievement of supramolecular box assemblies with different size channel according with the different molecular length of the ditopic ligands (Figure 1.12).

Another approach to obtain porous materials by intermolecular interactions between Zn^{II} Schiff base building blocks is the synthesis of a complex having a Lewis base within the ligand frameworks, thus allowing the Lewis acid/base interactions without external mono/multi-topic ligands.[40] Reek and co-workers have investigated the self-assembly of a Zn^{II} Schiff base complex **19** having 3,4 diaminopyridine as diamino bridging group (Zn^{II} salpyr) (Figure 1.13a).[41] The pyridine nitrogen atom of the diamine is a suitable Lewis base able to coordinate Zn^{II} metal centre of another unit of complex to obtain a supramolecular architecture.[3i,13,14e,27a,28b] Through ^1H NMR and X-ray analysis, it is found that cooperative interactions Zn···N between units of complex **19** stabilize the self-assembled tetrameric structure $[\mathbf{19}]_4$ with a vase shape with wide and narrow rim (Figure 1.13b). The complex **19** is achiral, but not the tetrameric aggregate that in solid state is present in both conformers. This $[\mathbf{19}]_4$ structure possesses regular square channel occupied by solvent and it is very stable, in fact an excess of pyridine is required to deaggregation of $[\mathbf{19}]_4$ to obtain the monomeric adduct **19**·py.

(a)

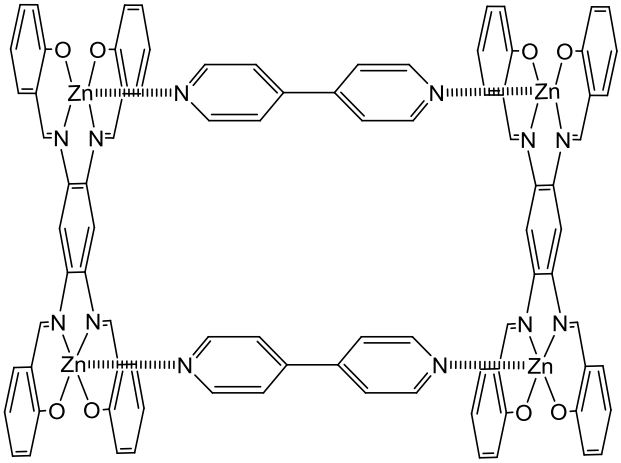

(b)

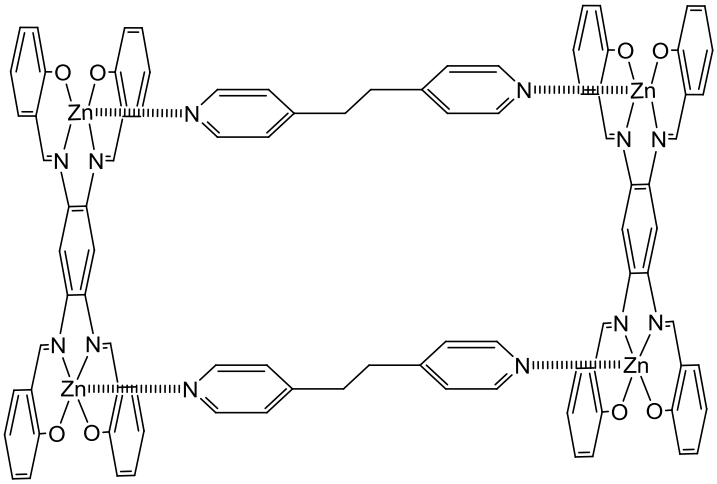

(c)

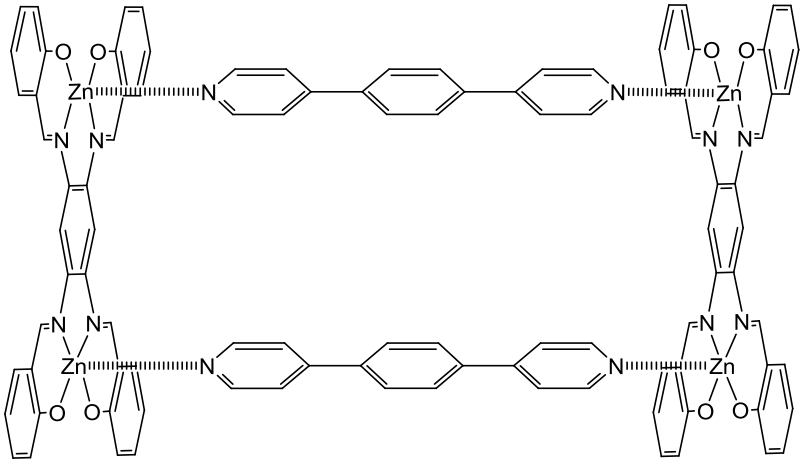

Figure 1.12 Structures of *(a)* [(**9**)$_2$·4,4′-bipyridine], *(b)* [(**9**)$_2$·1,2-bis(4-pyridyl)ethane)] and *(c)* [(**9**)$_2$·1,4-bis(4-pyridyl)benzene]. The diameters of three boxes are: *(a)* 13.9 Å, *(b)* 15.4 Å and *(c)* 17.4 Å. The t-But groups of **9** are omitted for clarity.

(a) *(b)*

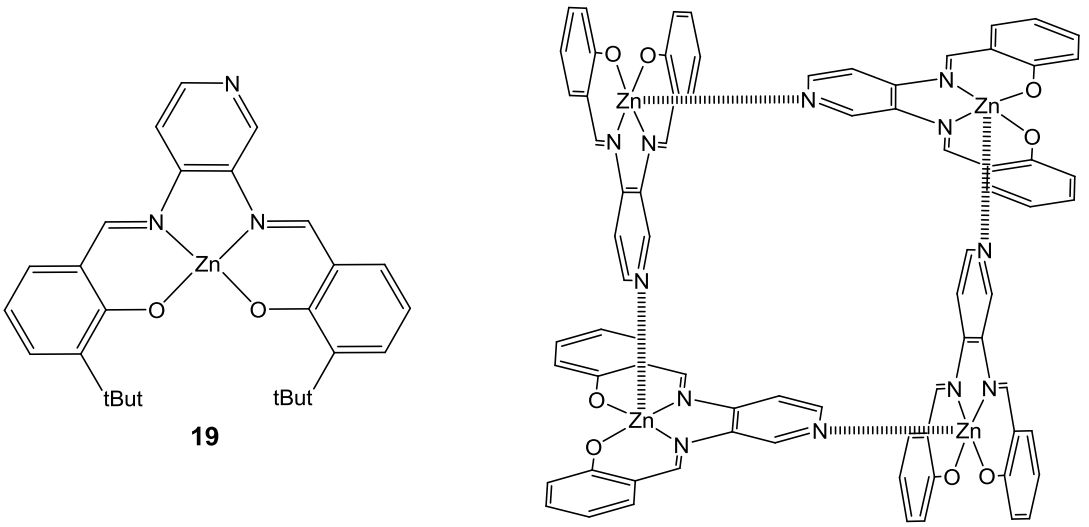

Figure 1.13 Structures of *(a)* Zn^{II} Schiff base complex **19** and *(b)* [**19**]$_4$·tetrameric assembly. The t-But groups of [**19**]$_4$ are omitted for clarity.

The ability of the pyridine nitrogen atom of Zn^{II} salpyr complexes to axially coordinate the metal ion of other complex allows the possibility to build new supramolecular heteromultimetallic structures. Kleij and co-workers have studied the supramolecular heteromultimetallic structure available by self assembly of the complexes **7**, **9**, **20**-**26** one each other, through ^{1}H, COSY, NOESY; DOSY NMR and X-ray measurements (Figure 1.14).[42] It is found that by stoichiometric reaction between **7** and **9** with **22** and **23** and **26** carries out to formation of 1:1 assembly **7**·**22** and **7**·**23**, 1:2 assembly **9**·(**22**)$_2$ and **9**·(**23**)$_2$ and 2:2 assembly (**9**)$_2$·(**26**)$_2$ in which the nitrogen atom of the pyridine moieties of complexes **22**, **23** and **26** axially coordinated by Zn···N intermolecular interactions the complexes **7** and **9**. The same heteromultimetallic assembly can be obtained using **20** with different features due to different length of Zn-N_{pyr} and Ru-N_{pyr}. A cooperative effect, with formation of various heteromultimetallic assemblies, occurs if the position of building blocks is correct and this can be more easily obtained using as scaffold dinuclear rigid complexes like **9**. Noteworthy, (**9**)$_2$·(**26**)$_2$ is highly stable and have an overall association constant of $\sim 10^{20}$. However, by NMR analysis, it is found that in solution it can be found in a different isomeric 2:2 assembly, in which units of complex **26** stay in different relative positions, in slow equilibrium with "open" structure (Figure 1.15).

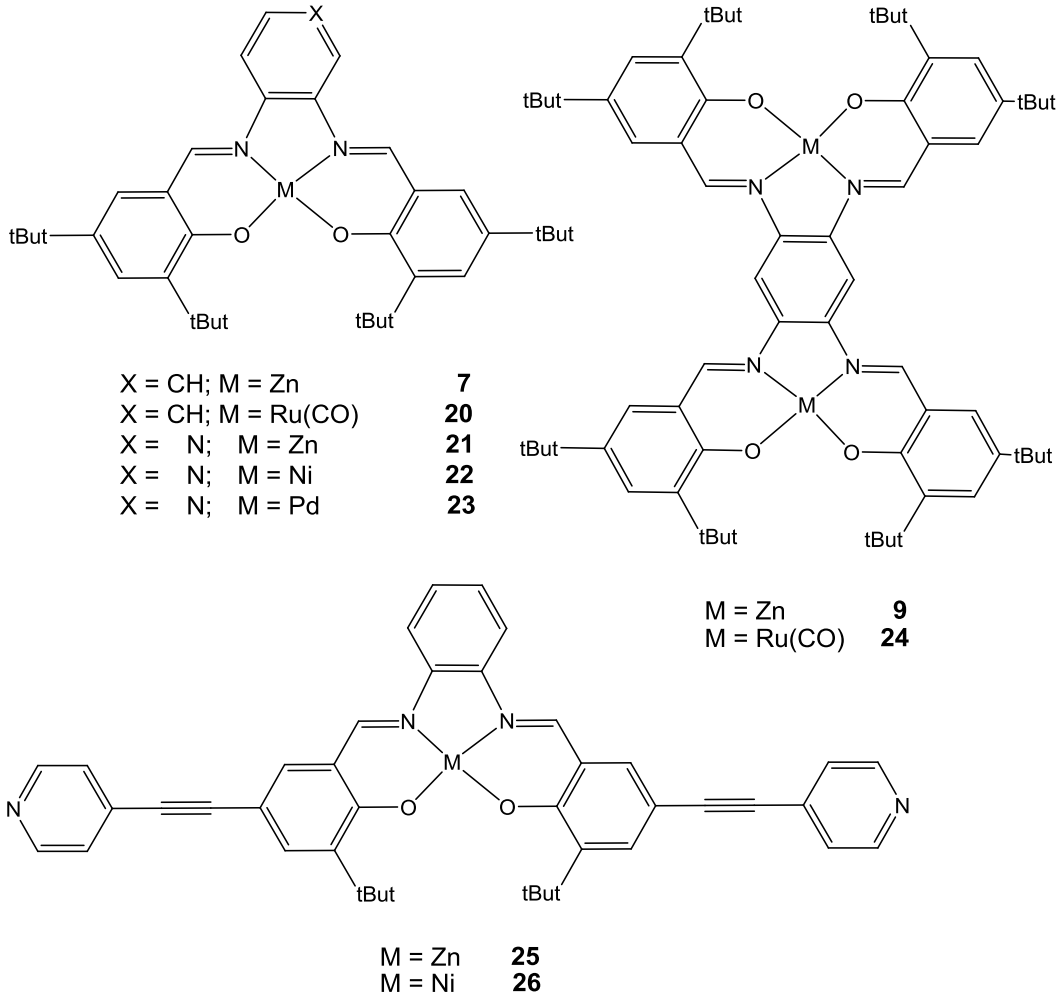

Figure 1.14 Structures of Zn^{II} Schiff base complexes **7**, **9**, **20**-**26**.

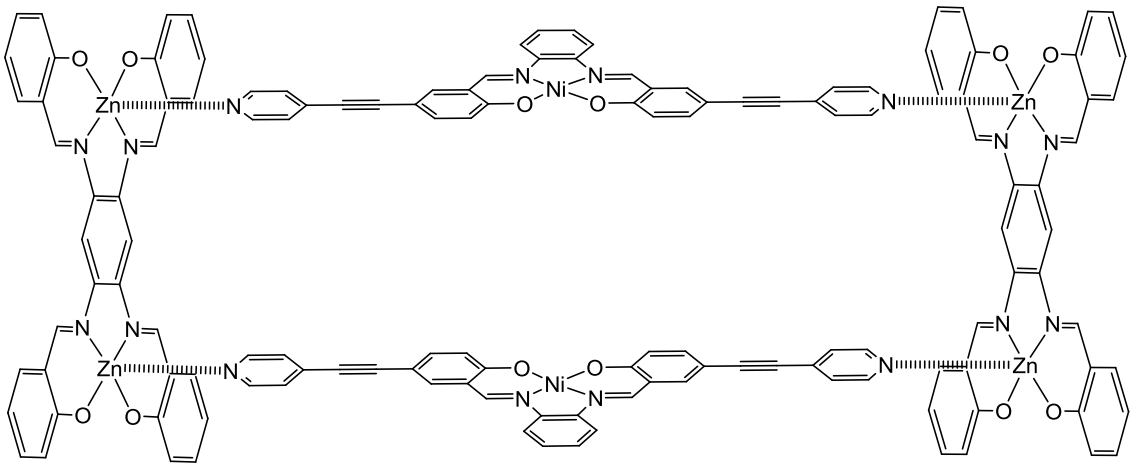

Figure 1.15 Structure of 2:2 assembly $(\mathbf{9})_2 \cdot (\mathbf{26})_2$. The t-But groups of **9** are omitted for clarity.

Zn^{II} Schiff base complexes can coordinate not only neutral Lewis base but also anions (see paragraph **1.3**). This feature paves the way in the design of supramolecular assembly using anions as template. Kleij and co-workers have studied the self assembly of complexes **7** and **8** (Figure 1.7) using acetate (OAc) ion as template.[14d] X-ray, ^{1}H NMR and UV-vis experiments showed that **7** and **8** coordinate the acetate ion through Zn···O axial interactions and the formation of 1:1 or 2:1 adducts is concentration dependent (Figure 1.16a). In particular, **8** forms more easily adduct 2:1 adducts with acetate ion respect to complex **7**, because the steric hindrance of **8** is less than **7**. The acetate ion has also been involved in the formation of trinuclear Zn^{II} complexes with methanolpyridine (mpy) (Figure 1.16b). In particular, the structure $(\mathbf{7})_2\cdot(OAc)_2\cdot(mpy)_2Zn$ is obtained by a stoichiometric mixture three components, in which a Zn^{II} ion forms a hexanuclear complex with two molecules of mpy on the equatorial plane and two molecules of acetate ions through axial coordination with the carbonylic oxygen atoms. The two units of **7** in the $(\mathbf{7})_2\cdot(OAc)_2\cdot(mpy)_2Zn$ are coordinate through Zn^{II} axial coordination with the carboxylate oxygen atoms of acetate.

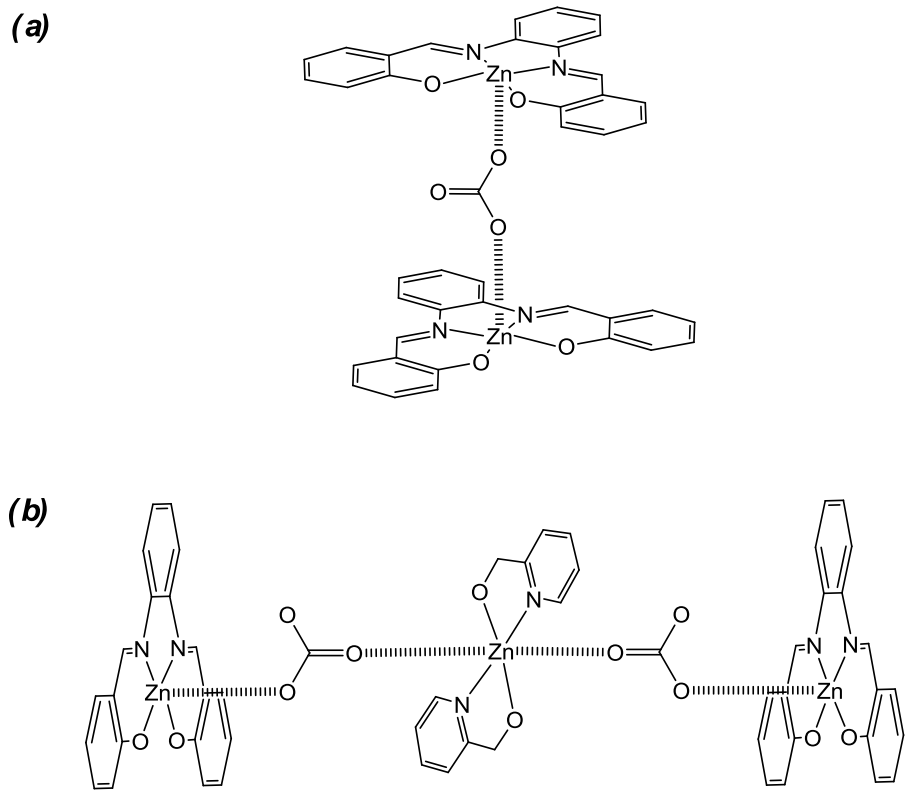

Figure 1.16 Structures of *(a)* 2:1 adducts between complexes **7** or **8** with OAc *(b)* $(\mathbf{7})_2\cdot(OAc)_2\cdot(mpy)_2Zn$ self assembly. The t-But groups of **7** and **8** are omitted for clarity.

Another example of formation of supramolecular architecture by ion coordination is demonstrated by Kleij and co-workers that have studied the supramolecular assembly between complex **8** and the OH^- ion (Figure 1.17).[43]

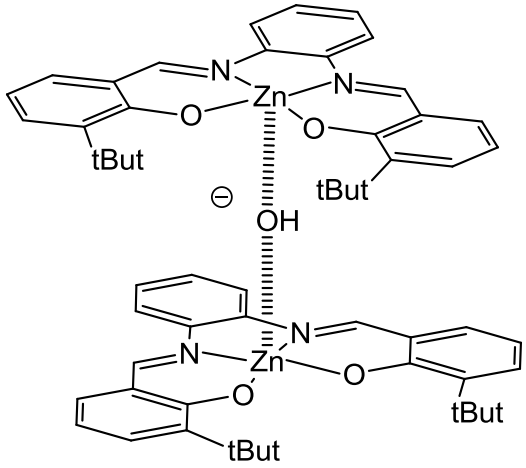

Figure 1.17 Structure of $(\mathbf{8})_2 \cdot OH$.

The OH^- ion can axially coordinate two Zn^{II} complex units, allowing the achievement of $(\mathbf{8})_2 \cdot OH$ assembly. This supramolecular structure is very stable, in fact even in a polar coordinating solvent, such as acetone and DMSO, its deaggregation is only partial.

1.5 Nanostructured materials

The supramolecular self assembly of building blocks is a powerful tool to obtain complex hierarchical nanoscale materials with significant functions and properties.[44] The versatility of the "bottom up " approach for the achievement of nanostructured material is due to the control of shape and functionality through the choice of precursors able to self organize in, for example, nanocapsules or one dimensional structures.[45] In the paragraph **1.4**, the discussion has been focused on the different strategies for the achievement of 3D supramolecular assembly using Zn^{II} Schiff base complexes as building blocks. In this paragraph, the discussion will be focused on the achievement and characterization of nanostructured materials, such as self assembly layers on solid support and nanofibers[46] obtained by Zn^{II} Schiff base complexes.

The self-assembled monolayers (SAMs) based on π-conjugated systems are highly desirable in electronic applications.[47] In this type of materials, the alignment of the

molecular components and the overall stability of the system are crucial for their application, however it is difficult to obtain both features. Elemans, Kleij, and Feyter have investigated the self assembly behaviour of amphiphilic Zn^{II} Schiff base complexes **28** and **30**, both in the solution phase as well as at the solid-liquid interface on highly oriented pyrolytic graphite (HOPG), in comparison to Ni^{II} analogous complexes **27** and **29** (Figure 1.18).[48] The complex **27** forms lamellar monolayers highly regular in which the side alkyl are interdigitating one each other along a main symmetry axes of grafite. The preferential orientation is head-to-tail, where the units of complex **27** are aligned or in opposite direction, but, within the defect of lamellae, there are rather domains where the units of **27** are oriented tail-to-tail. Conversely, the complex **28** forms bilayers less regular and well resolved than complex **27**. This is in full agreement with the tendency of Zn^{II} Schiff base complexes to form dimers through Zn···O intermolecular interactions.[14] In fact, upon addition of pyridine, a regular monolayer is observed, according to the deaggregation process and formation of **28**·py adduct.[14]

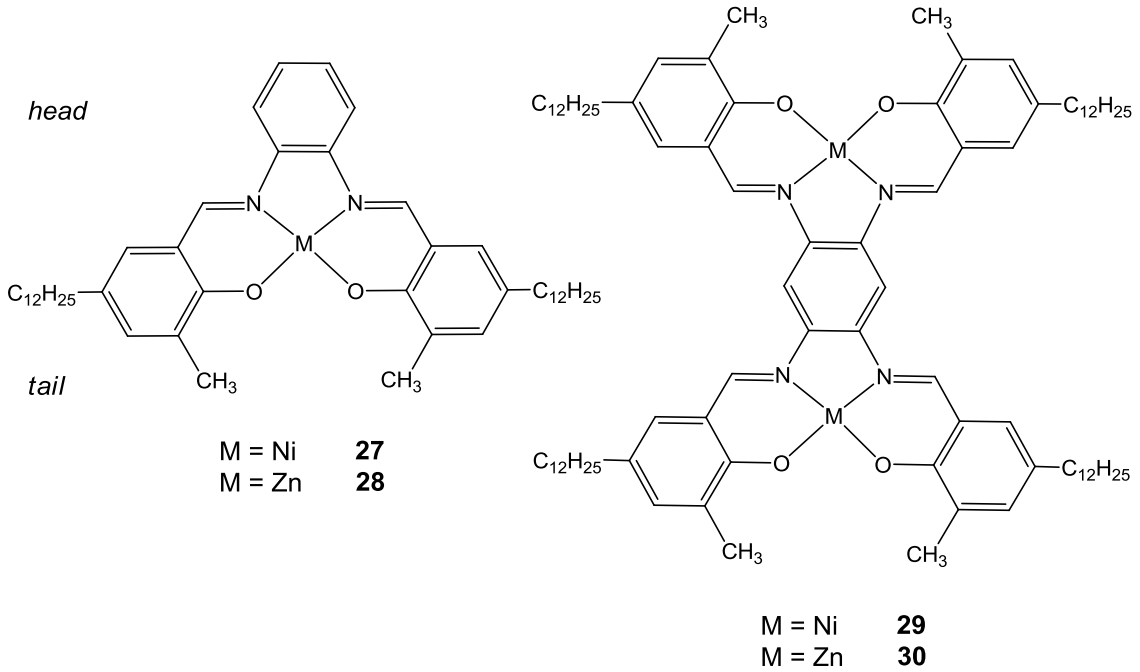

Figure 1.18 Structures of Zn^{II} Schiff base complexes **27**-**30**.

In the case of complex **30**, it is found unusual aggregation behaviour. In fact, the more extended aromatic system implies the stabilization of oligomeric aggregates via Zn···O

interactions. These oligomers are formed perpendicularly with respect to the interface and are very stable. In fact, a large amount of pyridine for the total deaggreation of oligomer is required respect to **28**. The aggregation is not influenced by the side chain, in fact only the presence of encumbered groups avoids the Zn···O interactions.[27]

Nanofibers[46] are supramolecular aggregates, linear or helical,[49] having useful features for use in nanosized mechanics,[50] electronics[51] and in the construction of biomimetic fibrous structures where they might have medically relevant applications.[52] Furthermore, the various nanofibers interact with each other forming a network able to entrap solvent molecules with the formation of gels.[53] Gels are interesting materials and in relation of their nature, they can be used in various fields such as catalysis, biomedical, drug delivery, sensing etc..[54] MacLachlan and co-workers have investigated a series of Zn^{II} Schiff base complexes **31**-**41** (Figure 1.19) able to forms nanofibers and gels with features dependent by groups of ligand framework and aggregation/deaggregation properties.[14f,55]

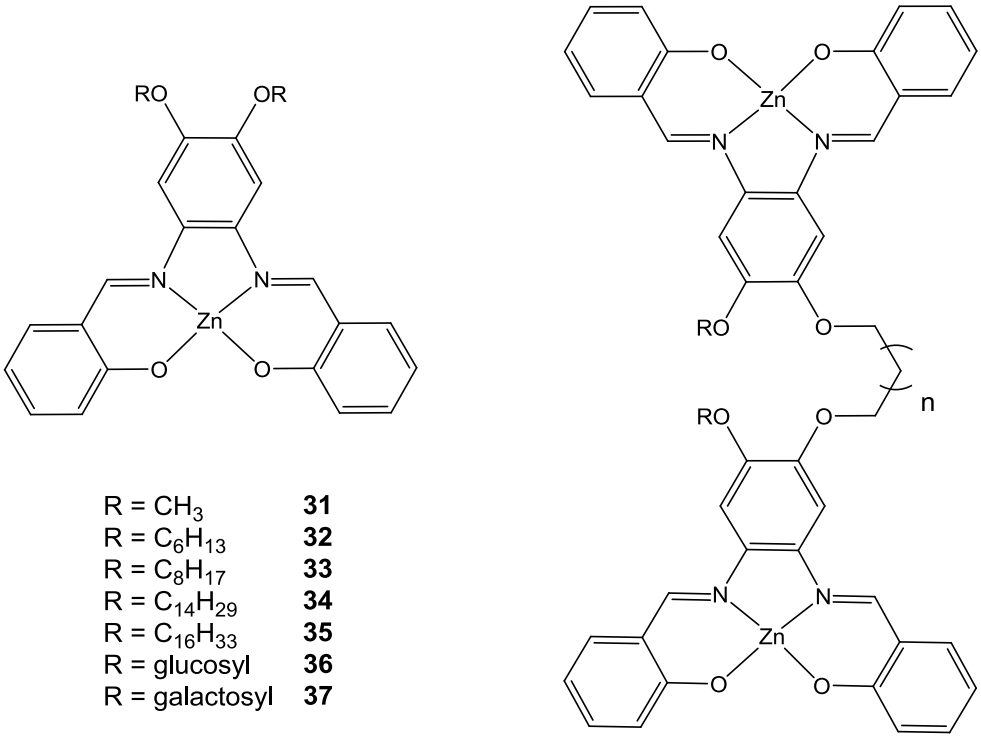

Figure 1.19 Structures of Zn^{II} Schiff base complexes **31**-**41**.

The amphiphilic complexes **31**-**35** form gels in aromatic solvent as toluene, o-xylene and benzene. Moreover, the complex **34** also forms luminescence gels in methanol solutions. The gel formation is thermoreversible and can be disrupted by deaggregation with small amount of pyridine.[14] Through TEM and ESI mass experiments, it is found that, by methanolic solutions of the complexes **31**-**35**, 1D nanofibers are formed and their formation is independent from the hydrophobicity of substituent groups. In fact, nanofibers are also observed in complexes **36** and **37** having hydrophilic groups such as glucose and galactose. The nanofibers have a helical conformation and, in the case of **36** and **37**, this conformation is more pronounced. In particular, the helical fibers are left-handed due to the presence of chiral carbohydrate substituents that induce the orientation of various fibers in an unique direction.[55b] The driving force for the formation of 1D nanofibers is the intermolecular Zn···O interaction between the units of complexes and not the π-π interactions as in the case of porphyrins.[56] In fact, in analogue complexes to **34** having t-But groups in 3 and 5 position of salicylaldehyde moieties or thiolic groups, instead than phenolic groups, no nanofibers are observed for the reason that the aggregation of the complex is prevented.[27] Moreover, the nanofibers are disrupted by addition of pyridine, according to the deaggregation of complexes and formation of pyridine adducts.[3i,13,14e,f,27a,28b] Even dinuclear complexes **38**-**41** form 3D nanofibers through Zn···O interactions, but the morphology is dependent by solvent.[55a] In particular, while in methanolic and methanol-chloroform mixture solutions a bundle of helical nanofibers is observed, in chloroform solutions the nanofibers are narrower and no prominent bundle of fibers or helical arrangement are observed by electron microscopy. In methanol and methanol-chloroform mixtures, the helical conformation is well definite because the linker permits a better flexibility respect to mononuclear complexes **31**-**35**. Finally, the addition of 4,4′-bipyridine implies the formation of nanofibers with different morphology, according to deaggregation process of complexes.

1.6 Macrocycles

Macrocyclic systems are functional materials useful to various applications, such as catalysis, synthetic mimics for ionconducting channels, tubular structures and porous materials.

Metal Schiff base macrocycles can be obtained through a metal template approach[14k,57] using opportune bis-aldehydes and diamine as building blocks, allowing to achieve new metallo-macrocyclic structures. This strategy allows a simple fine-tuning of properties of these systems through variation of the peripheral groups of these building blocks, opening up the ways at various potential applications.[58]

Metallo-macrocyclic structures obtained by fusion of Zn^{II} Schiff base complex units can form aggregate structures through intermolecular Zn···O interactions. Moreover, the addition of Lewis base implies a deaggregation of aggregate species. MacLachlan and co-workers have investigated the aggregation/deaggregation properties of Zn^{II} Schiff base macrocycles **42** and **43** and their potential sensing application (Figure 1.20).[14k]

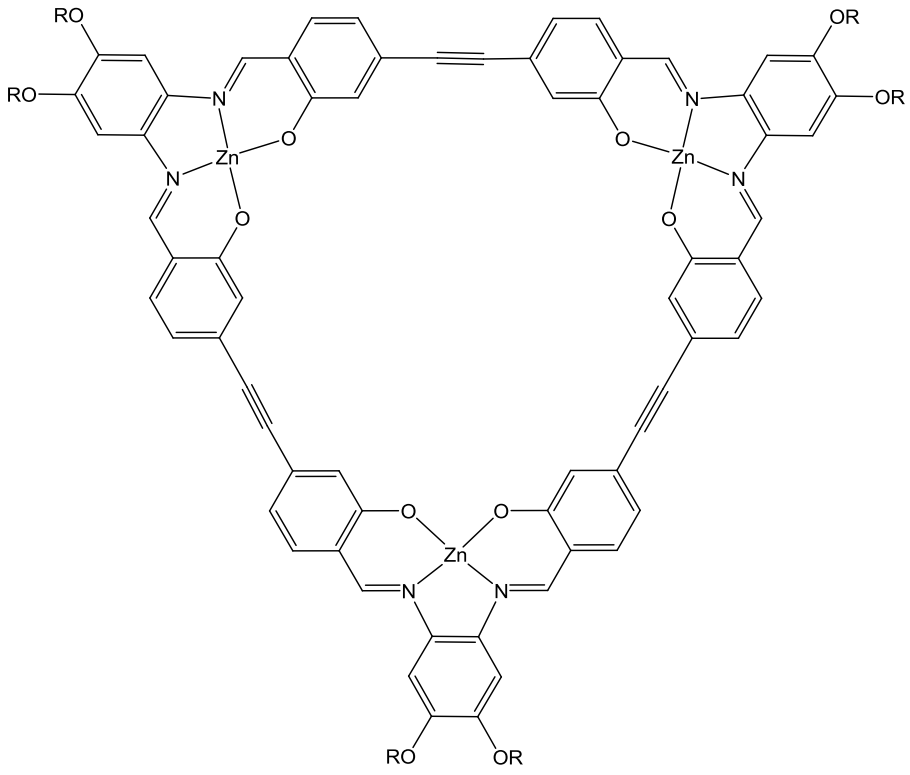

R = n-C_8H_{17} **42**
R = C_8H_{17} **43**

Figure 1.20 Structures of Zn^{II} Schiff base macrocycles **42** and **43**.

Through ^1H NMR, UV-vis and fluorescence spectra, it is found that in non-coordinating solvent the macrocycles form aggregate species, while in coordinating solvent they are present in solution as monomer axially coordinate with the solvent. The

driving force of aggregation of these systems is not only π-π interactions, otherwise the tendency to form aggregate should be stronger for analogous macrocycles of Ni^{II} and Cu^{II} that adopt a square-planar coordination respect to Zn^{II} macrocycles in which the Zn^{II} ion does not adopt square-planar coordination. The main driving force for aggregation of these systems is intermolecular Zn···O interactions between the Zn^{II} of a unit of macrocycle with the phenolic oxygen of another unit. This is confirmed because the addition of coordination species that can compete with phenolic oxygen for the axial coordination of Zn^{II} ion implies variations of spectroscopic properties only for **42** and **43** and not for analogous macrocycles of Ni^{II} and Cu^{II}. The magnitude of spectroscopic properties is consistent with the deaggregation of aggregate macrocycles and this process is strongly dependent from the Lewis basicity of coordinating species.[14] In fact, pyridine and quinuclidine species coordinate strongly the Zn metal centre, whereas lutidine cannot coordinate Zn^{II} ion for its steric hindrance. This permits to use this macrocycles for sensing Lewis bases in relation of their steric hindrance (see paragraph **1.3**).[58]

The stability of Zn^{II} Schiff base macrocycles aggregates is greater than that of analogous aggregate species of monometallic complexes. The presence of multiple units of complex within a macrocycle results in multivalency[59] and consequently cooperative binding, making more stable aggregates. This has been well demonstrated by Kleij and co-workers through the comparison of spectroscopic titrations with pyridine of Zn^{II} macrocycle **44** with the precursors complexes **45** and **46** (Figure 1.21).[60] It is found that the order of the amount of pyridine required to full deaggregation, normalized respect of numbers of Zn^{II} ion in **44**-**46**, is **44** (63 equiv) > **45** (38 equiv) > **46** (10 equiv), according to the cooperative binding that stabilizes the macrocyclic aggregate.

Macrocycle systems are reliable candidates for the creation of dynamic molecular assemblies that, by external stimuli,[61] can be switched between two stable states in the prospect for applications as memory units for information storage of a single bit in binary code.[62] Dalla Cort and co-workers have synthesized a Zn^{II} salophen complex having a hexaethylene glycol chain in the 5,5′ positions, **47**, and have investigated if this macrocycle can act as a wheel in the formation of [2]-pseudorotaxanes feasible of a pH promoted translocation[61b,63] of a secondary dialkylammonium axle between two stations (Figure 1.22).[64]

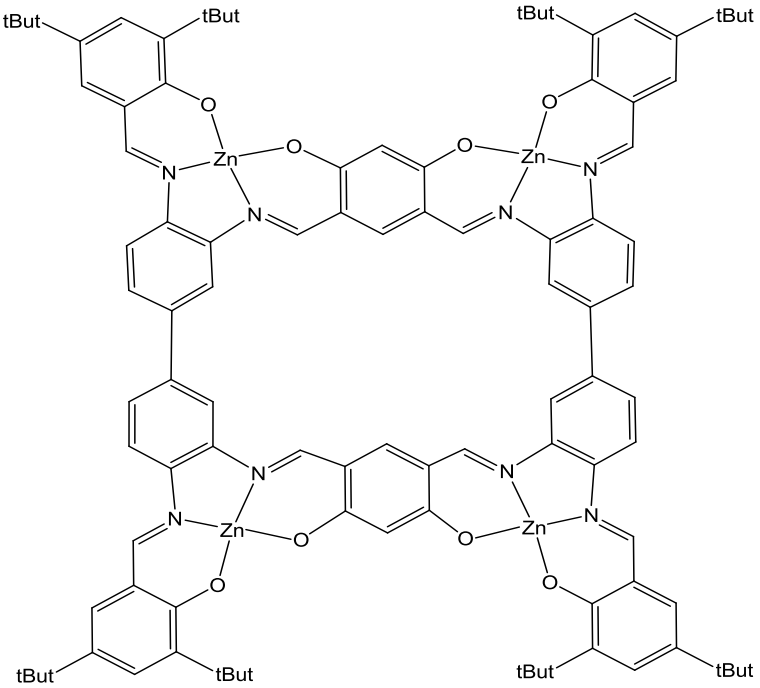

44

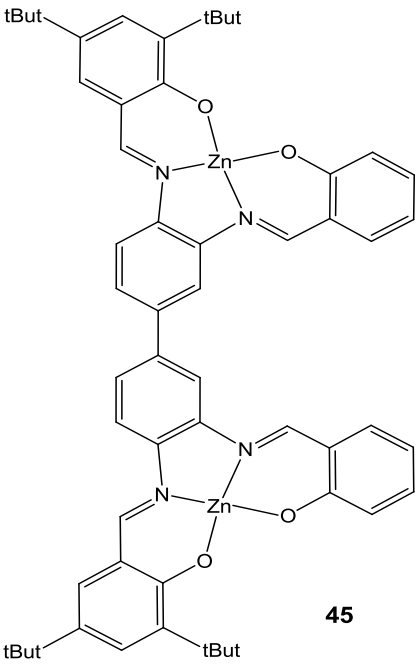

45

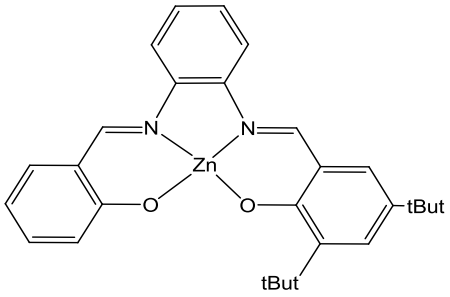

46

Figure 1.21 Structures of Zn^{II} Schiff base macrocycles **44** and analogous dinuclear **45** and mononuclear **46** complexes.

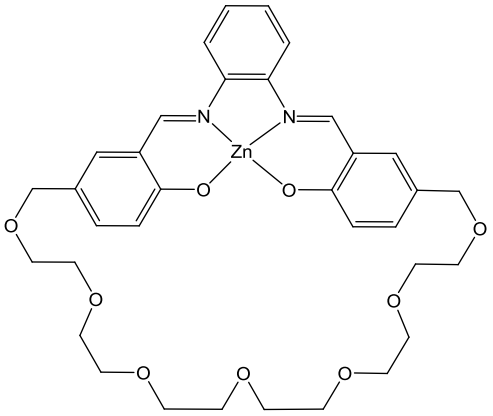

47

Figure 1.22 Structure of Zn^{II} Schiff base macrocycle **47**.

The macrocycle **47** have two binding sites. In particular, the Zn^{II} ion able to coordinate the amine[30] through Zn···O axial coordination and the polyoxyethylene chain able to bind the dialkylammonium cation axle through hydrogen bonds. The axial site of Zn^{II} salophen moieties of macrocycle is oriented inside the cavity and pointing the chain. The status of the system can be easily monitored because the coordination of amine implies variation of spectroscopic properties and an enhancement of fluorescence.[14] These feature are the prerequisite for application of **47** as [2]-pseudorotaxane of dialkylammonium cation. Through ^{1}H NMR, UV-vis and fluorescence spectra, it is found that both a secondary amine and a secondary alkylammonium cation bind the macrocycle **47**. Moreover, this process is reversible; in fact the addition of acid/base[61b] implies the traslocation of axle in two sites of macrocycle (Figure 1.23).

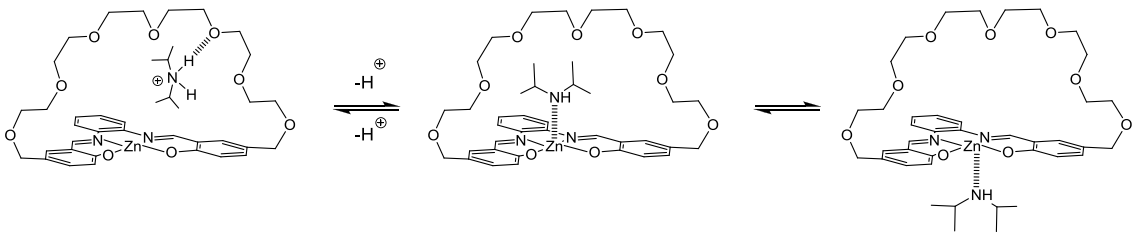

Figure 1.23 Representation of pH-driven dynamic equilibrium between Zn^{II} Schiff base macrocycle **47** and diisopropylamine.

Therefore, the macrocycle **47** behaves as a wheel in the formation of [2]-pseudorotaxanes with secondary ammonium ions.

1.7 The aim of PhD thesis

In the previous paragraphs has been presented a panoramic view on various applications of Zn^{II} Schiff base complexes, which shows how the aggregation/deaggregation properties of these complexes and then the demand of Zn^{II} to saturate its coordination sphere through axial interactions allows the use of this kind of complexes in each application examined.

By literature analysis it is found that the Zn^{II} ion in the Schiff base complexes is a Lewis acid that in absence of coordinating species form stable aggregates, through intermolecular Zn···O interactions with another units.[14] The stability of these aggregates can be modulated by peripherical groups of the ligand framework or by cooperative effects, if the complexes have multiple Zn^{II} metal centres.[59,60] Moreover, the aggregation can be also prevented by functionalizing the ligand framework with encumbered groups. On the other hand, in coordinating solvents or upon addition of coordinating species, the Zn^{II} ion can axially coordinate various Lewis bases forming monomeric species. The deaggregation process is strongly influenced by the Lewis basicity of the coordinating species because both electronic[13a,14,28] and steric effects[14,30] play a crucial role in the axial coordination to the Zn^{II} ion. Moreover, the deaggregation process implies variations of spectroscopic properties of the complexes, allowing the monitoring through various spectroscopic techniques. Therefore these systems are used in catalysis to coordinate various substrates, thus locking in a specific position useful to allow a reaction with another substrate to speed up the reaction (see paragraph **1.1**), or in molecular recognition and supramolecular chemistry, since the Zn^{II} ion can coordinate various kind of species to form various supramolecular architectures and that the deaggregation process is influenced by their Lewis basicity of the coordinating species, this allows for their discrimination (see paragraphs **1.3** and **1.4**).

In spite of all studies about Zn^{II} Schiff base complexes and their applications, the factors that influence the Lewis acidic character of Zn^{II} ion and then the aggregation/deaggregation properties are almost unexplored. In particular, the role of the ligand framework on Lewis acidity of Zn^{II} ion is almost unknown. This is an important aspect in the application of these complexes because their Lewis acidic character modulates the degree of aggregation and the stability of the aggregate species or supramolecular assemblies. Moreover, in relation to the Lewis character of the Zn^{II}

ion, the reactivity of complexes with respect to various Lewis bases can change, for example, allowing the modulation of sensing properties or the reactivity respect to other building blocks for the formation of new supramolecular systems.

In this contest, the research activity developed in PhD course and described in this PhD thesis has been focused on the following topics:

- Synthesis and characterization of new amphiphilic Schiff base complexes
- Study of the influence of ligand framework on their aggregation/deaggregation properties
- Study of their sensing and vapochromic properties for application as chemosensors
- Control of their molecular aggregation through the design of the ligand framework

An accurate study of the molecular aggregation of these complexes necessarily requires that they should be soluble in a large variety of coordinating and non-coordinating solvents of different polarities. Therefore, the synthesis of amphiphilic Zn^{II} Schiff base complexes, having different side alkyl chains length, has been accomplished, thus allowing the study of their aggregation in a large range of concentration, both in polar/non-polar, coordinating/non-coordinating solvents. The study of the influence of ligand framework on the aggregation/deaggregation properties of Zn^{II} Schiff base complexes has been carried out through the investigation of optical and structural properties of a series of amphiphilic complexes having conjugated and non-conjugated bridging diamino groups. With this approach, it has been possible to obtain a complete prospectus on how the nature of diamino bridge group influences the molecular aggregation, both in solution and in the solid state. Moreover, being all amphiphilic species, the role of the side alkyl chains on the aggregation properties of these complexes has been also investigated.

The sensing and vapochromic properties of Zn^{II} Schiff base complexes have been investigated respect to a series of amines and alkaloids compounds, having different steric and electronic features, considering the affinity of Zn^{II} Schiff base complexes *vs.* nitrogen based Lewis bases (see paragraph **1.3** and **1.4**). Through this study, it has been possible to rationalize the influence of the steric hindrance of the Lewis base upon the axial coordination to Zn^{II} Schiff base complexes, opening up the possibility to use these complexes as chemosensors, both in solution and in the solid state.

Finally, the control of the molecular aggregation has carried out through the design of a complex having a Lewis base in the ligand framework capable to coordinate the Zn^{II} metal centre. The presence of a Lewis base in the ligand framework implies that the aggregation does not occur through the usual intermolecular Zn···O interactions (see paragraph **1.4**), thus allowing the possibility to obtain new supramolecular architectures both in solution and in the solid state.

1.8 References

1. Vigato, P. A.; Tamburini, S. *Coord. Chem. Rev.* **2004**, *248*,1717.
2. Kleij, A. W. *Eur. J. Inorg. Chem.* **2009**, 193.
3. *(a)* Holbach, M.; Zheng, X.; Burd, C.; Jones, C. W.; Weck, M. *J. Org. Chem.* **2006**, *71*, 2903. *(b)* Kleij, A. W.; Tooke, D. M.; Spek, A. L.; Reek, J. N. H. *Eur. J. Inorg. Chem.* **2005**, 4626. *(c)* McGarrigle, E. M.; Gilheany, D. G. *Chem. Rev.* **2005**, *105*, 1563. *(d)* Cozzi, P. G. *Chem. Soc. Rev.* **2004**, *33*, 410. *(e)* Larrow, J. F.; Jacobsen, E. N. *Top. Organomet. Chem.* **2004**, *6*, 123. *(f)* Katsuki, T. *Chem. Soc. Rev.* **2004**, *33*, 437. *(g)* Katsuka, T. *AdV. Synth. Catal.* **2002**, *344*, 131. *(h)* Atwood, D. A.; Harvey, M. J. *Chem. Rev.* **2001**, *101*, 37. *(i)* Morris, G. A.; Zhou, H.; Stern, C. L.; Nguyen, S.-T. *Inorg. Chem.* **2001**, *40*, 3222.
4. *(a)* Whiteoak, C. J.; Salassa, G.; Kleij, A. W. *Chem. Soc. Rev.* **2012**, *41*, 622. *(b)* Wezenberg, S. J.; Kleij, A. W. *Angew. Chem. Int. Ed.* **2008**, *47*, 2354.
5. See for example: *(a)* Nasr-Esfahani, M.; Moghadam, M.; Valipour, G. *Synth. Commun.* **2009**, *39*, 3867. *(b)* Tong, J.; Zhang, Y.; Li, Z.; Xia, C. *J. Mol. Catal. A: Chem.* **2006**, *249*, 47. *(c)* Mirkhani, V.; Tangestaninejad, S.; Moghadam, M.; Mohammadpoor-Baltork, I. P.; Kargar, H. *J. Mol. Catal. A: Chem.* **2005**, *242*, 251. *(d)* Doctrow, S. R.; Huffman, K.; Marcus, C. B.; Tocco, G.; Malfroy, E.; Adinolfi, C. A.; Kruk, H.; Baker, K.; Lazarowych, N. et al. *J. Med. Chem.* **2002**, *45*, 4549. *(e)* Melov, S.; Ravenscroft, J.; Malik, S.; Gill, M. S.; Walker, D. W.; Clayton, P. E.; Wallace, D. C.; Malfroy, B.; Doctrow, S. R.; Lithgow, G. J. *Science* **2000**, *289*, 1567. *(f)* Zhang, W.; Loebach, J. L.; Wilson, S. R.; Jacobsen, E. N. *J. Am. Chem. Soc.* **1990**, *112*, 2801.
6. See for example: *(a)* Mayilmurugan, R.; Stoeckli-Evans, H.; Suresh, E.; Palaniandavar, M. *Dalton Trans.* **2009**, 5101. *(b)* Lange, T. S.; Kim, K. K.; Singh, R. K.; Strongin, R. M.; McCourt, C. K.; Brard, L. *PLoS One* **2008**, *3*, e2303, 1.

7. See for example: *(a)* Sessler, J. L.; Gale, P. A.; Cho, W.-S. *Anion Receptor Chemistry*, Royal Society of Chemistry, Cambridge, UK, 2006. *(b)* Beer, P. D.; Gale, P. A. *Angew. Chem. Int. Ed.* **2001**, *40*, 486.
8. See for example: Gale, P. A. *Coord. Chem. Rev.* **2001**, *213*, 79.
9. See for example: Gale, P. A. *Chem. Commun.* **2011**, *47*, 82.
10. See for example: Dunn, T. J.; Chiang, L.; Ramogida, C. F.; Webb, M. I.; Savard, D.; Sakaguchi, M.; Ogura, T.; Shimazaki, Y.; Storr, T. *Dalton Trans.* **2012**, *41*, 7905.
11. See for example: Dunn, T. J.; Chiang, L.; Ramogida, C. F.; Webb, M. I.; Savard, D.; Sakaguchi, M.; Ogura, T.; Shimazaki, Y.; Storr, T. *Inorg. Chem.* **2011**, *50*, 6746.
12. See for example: *(a)* Rudkevich, D. M.; Stauthamer, W. P. R. V.; Verboom, W.; Engbersen, J. F. J.; Harkema, S. Reinhoudt, D. N. *J. Am. Chem. Soc.* **1992**, *114*, 9671. *(b)* Bandoli, G.; Clemente, D. A.; Croatto, U.; Vidali, M.; Vigato, P. A. *J. Chem. Soc. D* **1971**, 1330.
13. *(a)* Kleij, A. W.; Kuil, M.; Tooke, D. M.; Lutz, M.; Spek, A. L.; Reek J. N. H. *Chem. Eur. J.* **2005**, *11*, 4743. *(b)* Singer, A. L.; Atwood, D. A. *Inorg. Chim. Acta* **1998**, *277*, 157.
14. See for example: *(a)* Bhattacharjee, C. R.; Das, G.; Mondal, P.; Prasad, S. K.; Rao, D. S. S. *Eur. J. Inorg. Chem.* **2011**, 1418. *(b)* Martínez Belmonte, M.; Wezenberg, S. J.; Haak, R. M.; Anselmo, D.; Escudero-Adán, E. C.; Benet-Buchholz, J.; Kleij, A W *Dalton Trans.* **2010**, *39*, 4541. *(c)* Kleij, A. W. *Dalton Trans.* **2009**, 4635. *(d)* Wezenberg, S. J.; Escudero-Adán, E. C.; Benet-Buchholz J.; Kleij, A. J. *Chem. Eur. J.* **2009**, *15*, 5695. *(e)* Escudero-Adán, E. C.; Benet-Buchholz, J.; Kleij, A. W. *Inorg. Chem.* **2008**, *47*, 4256. *(f)* Hui, J. K.-H.; Yu, Z.; MacLachlan, M. J. *Angew. Chem. Int. Ed.* **2007**, *46*, 7980. *(g)* Leung, A. C. W.; MacLachlan, M. J. *J. Mater. Chem.* **2007**, *17*, 1923. *(h)* Gallant, A. J.; Chong, J. H.; MacLachlan, M. J. *Inorg. Chem.* **2006**, *45*, 5248. *(i)* Kleij, A. W.; Kuil, M.; Lutz, M.; Tooke, D. M.; Spek, A. L.; Kamer, P. C. K.; van Leeuwen, P. W. N. M.; Reek, J. N. H. *Inorg. Chim. Acta.* **2006**, *359*, 1807. *(j)* Odoko, M.; Tsuchida, N.; Okabe, N. *Acta Crystallogr., Sect. E: Struct. Rep. Online* **2006**, *E62*, m708. *(k)* Ma, C. T. L.; MacLachlan, M. J. *Angew. Chem. Int. Ed.* **2005**, *44*, 4178. *(l)* Matalobos, J. S.; García-Deibe, A. M.; Fondo, D. N.; Bermejo, M. R. *Inorg. Chem. Commun.* **2004**, *7*, 311. *(m)* Reglinski, J.; Morris S.; Stevenson, D. E. *Polyhedron* **2002**, *21*, 2175.

15. For reviews see: *(a)* Haak, R. M.; Wezenberg, S. J.; Kleij, A. W. *Chem. Commun.* **2010***, 46,* 2713. *(b)* Farlow, J. F.; Jacobsen, E. N. *Top. Organomet. Chem.* **2004**, *7*, 123. *(c)* Katsuki, T. *Synlett* **2003**, 281. *(d)* Jacobsen, E. N. *Acc. Chem. Res.* **2000**, *33*, 421. *(e)* Canali, L.; Sherrington, D. C. *Chem. Soc. Rev.* **1999**, *28*, 85. *(f)* Jacobsen, E. N. in *Comprehensive Organometallic Chemistry II*, Vol. 12 (Hrsg.: E. W. Abel, F. G. A. Stone, E. Willinson), Pergamon, New York, 1995, S. 1097. *(g)* Katsuki, T. *Coord. Chem. Rev.* **1995**, *140*, 189.
16. Decortes, A.; Martínez Belmonte, M.; Benet-Buchholz, J.; Kleij, A. W. *Chem. Commun.* **2010**, *46*, 4580.
17. Cozzi, G. *Angew. Chem. Int. Ed.* **2003**, *42*, 2895.
18. *(a)* Zelder, F. H.; Rebek, J. J. *Chem. Commun.* **2006**, 753. *(b)* Richeter, S.; Rebek, J. J. *J. Am. Chem. Soc.* **2004**, *126*, 16280.
19. *(a)* Hembury, G. A.; Borovkov, V. V.; Inoue, Y. *Chem. Rev.* **2008**, *108*, 1. *(b)* Borovkov, V. V.; Inoue, Y. *Top. Curr. Chem.* **2006**, *265*, 89. *(c)* Borovkov, V. V.; Hembury, G. A.; Inoue, Y. *Acc. Chem. Res.* **2004**, *37*, 449.
20. For recent works see: *(a)* Escárcega-Bobadilla, M. V.; Kleij, A. W. *Chem. Sci.* **2012**, *3*, 2421. *(b)* Dydio, P.; Rubay, C.; Gadzikwa, T.; Lutz, M.; Reek, J. N. H. *J. Am. Chem. Soc.* **2011**, *133*, 17176. *(c)* van Leeuwen, P. W. N. M.; Rivillo, D.; Raynal, M.; Freixa, Z. *J. Am. Chem. Soc.* **2011**, *133*, 18562.
21. *(a)* Borovkov, V. V.; Harada, T.; Hembury, G. A.; Inoue, Y.; Kuroda, R. *Angew. Chem. Int. Ed.* **2003**, *42*, 1746. *(b)* Valli, L.; Casilli, S.; Giotta, L.; Pignataro, B.; Conoci, S.; Borovkov, V. V.; Inoue, Y.; Sortino, S. *J. Phys. Chem. B* **2006**, *110*, 4691.
22. *(a)* Li, X.; Borhan, B. *J. Am. Chem. Soc.* **2008**, *130*, 16126. *(b)* Li, X.; Tanasova, M.; Vasileiou, C.; Borhan, B. *J. Am. Chem. Soc.* **2008**, *130*, 1885. *(c)* Etxebarria, J.; Vidal-Ferran, A.; Ballester, P. *Chem. Commun.* **2008**, 5939. *(d)* Proni, G.; Pescitelli, G.; Huang, X.; Nakanishi, K.; Berova, N. *J. Am. Chem. Soc.* **2003**, *125*, 12914. *(e)* Yang, Q.; Olmsted, C.; Borhan, B. *Org. Lett.* **2002**, *4*, 3423. *(f)* Borovkov, V. V.; Lintuluoto, J. M.; Inoue, Y. *J. Am. Chem. Soc.* **2001**, *123*, 2979. *(g)* Huang, X.; Rickman, B. H.; Borhan, B.; Berova, N.; Nakanishi, K. *J. Am. Chem. Soc.* **1998**, *120*, 6185.

23. *(a)* Escárcega-Bobadilla, M. V.; Anselmo, D.; Wezenberg, S. J.; Escudero-Adán, E. C.; Martínez Belmonte, M.; Martin, E.; Kleij, A. W. *Dalton Trans.* **2012**, *41*, 9766. *(b)* Escárcega-Bobadilla, M. V.; Salassa, G.; Martínez Belmonte, M.; Escudero-Adán, E. C.; Kleij, A. W. *Chem. Eur. J.* **2012**, *18*, 6805. *(c)* Wezenberg, S. J.; Salassa, G.; Escudero-Adán, E. C.; Benet-Buchholz, J.; Kleij, A. W. *Angew. Chem.* **2011**, *123*, 739.
24. For a review, see: Borovkov, V. *Symmetry* **2010**, *2*, 184.
25. Lintuluoto, J. M.; Borovkov, V. V.; Inoue, Y. *J. Am. Chem. Soc.* **2002**, *124*, 13676.
26. The authors have supposed that the $Zn(OH)_2$ may have been produced by partial hydrolysis of the $ZnEt_2$.
27. *(a)* Kamer, P. C. J.; van Leeuwen, P.W. N. M.; Reek, J. N. H. *Inorg. Chim. Acta* **2006**, *359*, 1807. *(b)* Kleij, A. W.; Tooke, D. M.; Spek, A. L.; Reek, J. N. H. *Eur. J. Inorg. Chem.* **2005**, 4626.
28. *(a)* Kleij, A. W.; Kuil, M.; Lutz, M.; Tooke, D. M.; Spek, A. L.; Kamer, P. C. J.; van Leeuwen, P. W. N. M.; Reek, J. N. H. *Inorg. Chim. Acta*, **2006**, *359*, 1807. *(b)* Kleij, A. W.; Lutz, M.; Spek, A. L.; van Leeuwen, P. W. N. M.; Reek, J. N. H. *Chem. Commun.* **2005**, 3661. *(c)* Kleij, A. W.; Kuil, M.; Tooke, D. M.; Spek, A. L.; Reek, J. N. H. *Inorg. Chem.* **2005**, *44*, 7696.
29. Wezenberg, S. J.; Escudero-Adán, E. C.; Benet-Buchholz, J.; Kleij, A. W. *Org. Lett.* **2008**, *10*, 3311.
30. Dalla Cort, A; Mandolini, L.; Pasquini, C.; Rissanen, K.; Russo, L.; Schiaffino, L. *New J. Chem.* **2007**, *31*, 1633.
31. *(a)* Dalla Cort, A.; De Bernardin, P.; Forte, G.; Yafteh Mihan, F. *Chem. Soc. Rev.* **2010***, 39,* 3863. *(b)* Sessler, J.-L.; Gale, P. A.; Cho. W.-S. *Anion Receptor Chemistry*; RCS Publishing: Baltimore, MD, 2006. *(c)* Katayev, E. A.; Ustynyuk, Y. A.; Sessler, J. L. *Coord. Chem. Rev.* **2006**, 250, 3004. *(d)* Kang, S. O.; Begum, R. A.; Bowman-James, K. *Angew. Chem. Int. Ed.* **2006**, *45*, 7882. *(e)* Amendola, V.; Bonizzoni, M.; Esteban-Gómez, D.; Fabbrizzi, L.; Licchelli, M.; Sancenón, F.; Taglietti, A. *Coord. Chem. Rev.* **2006**, *250*, 1451. *(f)* Schmidtchen, F. P. *Coord. Chem. Rev.* **2006**, 250, 2918. *(g)* Ilioudis, C. A.; Tocher, D. A.; Steed, J. W. *J. Am. Chem. Soc.* **2004**, *126*, 12395. *(h)* Suksai, C.; Tuntulani, T. *Chem. Soc. Rev.* **2003**, *32*, 192. *(i)* P. D. Beer, Gale, P. A. *Angew. Chem. Int. Ed.* **2001**, *40*, 486. *(j)* Bianchi,

A., Bowman-James, K., García-Espãna, E. *Supramolecular Chemistry of Anions*; Eds.; Wiley-VCH: New York, 1997.

32. Cano, M.; Rodríguez, L.; Lima, J. C.; Pina, F.; Dalla Cort, A; Pasquini, C.; Schiaffino, L. *Inorg. Chem.* **2009**, *48*, 6229.
33. *(a)* Wang, H.; Chan, W.-H. *Org. Biomol. Chem.* **2008**, *6*, 162. *(b)* Bazzicaluppi, C.; Bencini, A.; Bianchi, A.; Danesi, A.; Faggi, E.; Giorgi, C.; Lodeiro, C.; Oliveira, E.; Pina, F.; Valtancoli, B. *Inorg. Chim. Acta* **2008**, *361*, 3410. *(c)* Gunnlaugsson, T.; Davis, A. P.; Hussey, G. M.; Tierney, J.; Glynn, M. *Org. Biomol. Chem.* **2004**, *2*, 1856. *(d)* Albelda, M. T.; Aguilar, J.; Alves, S.; Aucejo, R.; Díaz, P.; Lodeiro, C.; Lima, J. C.; García-Espãna, E.; Pina, F.; Soriano, C. *Helv. Chim. Acta* **2003**, *86*, 3118.
34. Dalla Cort, A; De Bernardin, P.; Schiaffino, L. *Chirality* **2009**, *21*, 104.
35. Kleij, A. W.; Reek, J. N. H. *Chem. Eur. J.* **2006**, *12*, 4218.
36. *(a)* Crane, A. K.; MacLachlan, M. J. *Eur. J. Inorg. Chem.* **2012**, 17. *(b)* Kleij, A. W. *Chem. Eur. J.* **2008**, *14*, 10520.
37. Slagt, V. F.; Reek, J.N.H.; Kamer, P. J. C.; van Leeuwen, P. W. N.M. *Angew. Chem. Int. Ed.* **2001**, *40*, 4271.
38. Kuil, M.; Goudriaan, P. E.; Kleij, A. W.; Tooke, D. M.; Spek, A. L.; van Leeuwen, P. W. N. M.; Reek, J. N. H. *Dalton Trans.* **2007**, 2311.
39. *(a)* Twyman, L. J.; King, A. S. H. *Chem. Commun.* **2002**, 910. *(b)* Wilson, G. S.; Anderson, H. L. *Chem. Commun.* **1999**, 1539. *(c)* Okumura, A.; Funatsu, K.; Sasaki, Y.; Imamura, T. *Chem. Lett.* **1999**, 779. *(d)* Funatsu, K.; Imamura, T.; Ichimura, A.; Sasaki, Y. *Inorg. Chem.* **1998**, 37, 4986. *(e)* Stibrany, R. T.; Vasudevan, J.; Knapp, S.; Potenza, J. A.; Emge, T.; Schugar, H. J. *J. Am. Chem. Soc.* **1996**, *118*, 3980. *(f)* Kobuke, Y.; Miyaji, H. *J. Am. Chem. Soc.* **1994**, *116*, 4111.
40. *(a)* Chichak, K.; Jacquemard, U.; Branda, N. R. *Eur. J. Inorg. Chem.* **2002**, 357. *(b)* Morris, G. A.; Nguyen, S. T. *Tetrahedron Lett.* **2001**, *42*, 2093.
41. Kleij, A. W.; Kuil, M.; Tooke, D. M.; Spek, A. L.; Reek J. N. H. *Inorg. Chem.* **2007**, *46*, 5829.
42. Wezenberg, S. J.; Escudero-Adán, E. C.; Benet-Buchholz, J.; Kleij, A. W. *Inorg. Chem.* **2008**, *47*, 2925.

43. Anselmo, D.; Escudero-Adán, E. C.; Benet-Buchholz, J.; Kleij, A. W. *Dalton Trans.* **2010**, *39*, 8733.

44. Ozin, G. A. *Adv. Mater.* **1992**, *4*, 612.

45. *(a)* Frischmann, P. D.; Gallant, A. J.; Chong, J. H.; MacLachlan, M. J. *Inorg. Chem.* **2008,** *47*, 101. *(b)* Frischmann, P. D.; MacLachlan, M. J. *Chem. Commun.* **2007**, 4480. *(c)* Peroukidis, S. D.; Vanakaras, A. G.; Photinos, D. J. *J. Chem. Phys.* **2005**, *123*, 164904. *(d)* Tschierske, C. *Nature* **2002**, *419*, 681.

46. Hui, J. K.-H.; MacLachlan, M. J. *Coord. Chem. Rev.* **2010**, 524, 2363.

47. *(a)* Elemans, J. A. A. W.; Lei, S.; De Feyter, S. *Angew. Chem. Int. Ed.* **2009**, *48*, 7298. *(b)* Elemans, J. A. A. W. *Mater. Today* **2009**, *12*, 34. *(c)* Piot, L.; Bonifazi, D.; Samorí, P. *Adv. Funct. Mater.* **2007**, *17*, 3689.

48. *(a)* Salassa, G.; Coenen, M. J. J.; Wezenberg, S. J.; Hendriksen, B. L. M.; Speller, S.; Elemans, J. A. A. W.; Kleij, A. W. *J. Am. Chem. Soc.* **2012**, *134*, 7186. *(b)* Elemans, J. A. A. W.; Wezenberg, S. J.; Coenen, M. J. J.; Escudero-Adán, E. C.; Benet-Buchholz, J.; den Boer, D.; Speller, S.; Kleij, A. W.; De Feyter, S. *Chem. Commun.* **2010**, *46*, 2548.

49. *(a)* Ikkala, O.; Ras, R. H. A.; Houbenov, N.; Ruokolainen, J.; Pääkkö, M.; Laine, J.; Leskelä, M.; Berglund, L. A.; Lindström, T.; ten Brinke, G.; Iatrou, H.; Hadjichristidis, N.; Faul, C. F. J. *Faraday Discuss.* **2009**, *143*, 95. *(b)* Lee, C. C.; Grenier, C.; Meijer, E. W.; Schenning, A. P. H. J. *Chem. Soc. Rev.* **2009**, *38*, 671.

50. *(a)* Koenders, M. M. J. F.; Yang, L.; Wismans, R. G.; van der Werf, K. O.; Reinhardt, D. P.; Daamen, W.; Bennink, M. L.; Dijkstra, P. J.; Van Kuppevelt, T. H.; Feijen, J. *Biomaterials* **2009**, *30*, 2425. *(b)* Carlisle, C. R.; Coulais, C.; Namboothiry, M.; Carroll, D. L.; Hantgan, R. R.; Guthold, M. *Biomaterials* **2009**, *30*, 1205. *(c)* Roosma, J.; Mes, T.; Lèclere, P.; Palmans, A. R. A.; Meijer, E. W. *J. Am. Chem. Soc.* **2008**, *130*, 1120.

51. *(a)* Kume, S.; Kuroiwa, K.; Kimizuka, N. *Chem. Commun.* **2006**, 2442. *(b)* Schenning, A. P. H. J.; Meijer, E. W. *Chem. Commun.* **2005**, 3245. *(c)* Schenning, A. P. H. J.; Jonkheijm, P.; Hoeben, F. J. M.; Van Herrikhuyzen, J.; Meskers, S. C. J.; Meijer, E. W.; Herz, L. M.; Daniel, C.; Silva, C.; Phillips, R. T.; Friend, R. H.; Beljonne, D.; Miura, A.; De Feyter, S.; Zdanowska, M.; Uji-i, H.; De Schryver, F.

C.; Chen, Z.; Würthner, F.; Mas-Torrent, M.; den Boer, D.; Durkut, M.; Hadley, P. *Synth. Met.* **2004**, *147*, 43. *(d)* Kimizuka, N. *Adv. Mater.* **2000**, *12*, 1461.

52. *(a)* Kenawy, E.-R.; Abdel-Hay, F. I.; El-Newehy, M. H.; Wnek, G. E. *Mater. Chem. Phys.* **2009**, *113*, 296. *(b)* Huang, Z.-M.; Zhang, Y.-Z.; Kotaki, M.; Ramakrishna, S.; *Compos. Sci. Technol.* **2003**, 63, 2223. *(c)* Hartgerink, J. D.; Beniash, E.; Stupp, S. I. *Science* **2001**, 294, 1684.
53. *(a)* Westcott, A.; Sumby, C. J.; Walshaw, R. D.; Hardie, M. J. *New J. Chem.* **2009**, *33*, 902. *(b)* Jung, J. H.; Shinkai, S. *Top. Curr. Chem.* **2004**, *248*, 223.
54. *(a)* Rodríguez-Llansola, F.; Escuder, B.; Miravet, J. F. *J. Am. Chem. Soc.* **2009**, *131*, 11478. *(b)* Hirst, A. R.; Escuder, B.; Miravet, J. F., Smith, D. K. *Angew. Chem. Int. Ed.* **2008**, *47*, 8002. *(c)* Fages, F. *Angew. Chem. Int. Ed.* **2006**, *45*, 1680. *(d)* Sugiyasu, K.; Fujita, N., Shinkai, S. *J. Mater. Chem.* **2005**, *15*, 2747. *(e)* Motulsky, A.; Lafleur, M.; Couffin-Hoarau, A.-C.; Hoarau, D.; Boury, F.; Benoit, J.-P.; Leroux, J.-C. *Biomaterials* **2005**, *26*, 6242.
55. *(a)* Hui, J. K.-H.; MacLachlan, M. J. *Dalton Trans.* **2010**, *39*, 7310. *(b)* Hui, J. K.-H.; Yu, Z.; Mirfakhrai, T.; MacLachlan, M. J. *Chem. Eur. J.* **2009**, *15*, 13456.
56. *(a)* Kishida, T.; Fujita, N.; Hirata, O.; Shinkai, S. *Org. Biomol. Chem.* **2006**, *4*, 1902. *(b)* Kishida, T.; Fujita, N.; Sada, K.; Shinkai, S. *J. Am. Chem. Soc.* **2005**, *127*, 7298. *(c)* Kishida, T.; Fujita, N.; Sada, K.; Shinkai, S. *Langmuir* **2005**, *21*, 9432. *(d)* Abraham, R. J.; Fell, S. C.; Pearson, H.; Smith, K. M. *Tetrahedron* **1979**, *35*, 1759.
57. *(a)* Frischmann, P. D.; Jiang, J.; Hui, J. K.-H.; Grzybowski, J. J.; MacLachlan, M. J. *Org. Lett.* **2008**, *10*, 1255. *(b)* Hui, J. K.-H.; MacLachlan, M. J. *Chem. Commun.* **2006**, 2480. *(c)* Akine, S.; Hashimoto, D.; Saiki, T.; Nabeshima, T. *Tetrahedron Lett*. **2004**, *45*, 4225. *(d)* Gallant, A. M.; MacLachlan, M. J. *Angew. Chem. Int. Ed.* **2003**, 42, 5307.
58. Germain, M. E.; Knapp, M. J. J. *J. Am. Chem. Soc.* **2008**, *130*, 5422.
59. *(a)* Hunter, C. A.; Anderson, H. L. *Angew. Chem. Int. Ed.* **2009**, *48*, 7488. *(b)* Mulder, A.; Huskens, J.; Reinhoudt, D. N. *Org. Biomol. Chem.* **2004**, *2*, 3409. *(c)* Ercolani, G. *J. Am. Chem. Soc.* **2003**, *125*, 16097. *(d)* Mammen, M.; Choi, S.-K.; Whitesides, G. M. *Angew. Chem. Int. Ed.* 1998, *37*, 2754.
60. Salassa, G.; Castilla, A. M.; Kleij, A. W. *Dalton Trans.* **2011**, *40*, 5236.

61. *(a)* Kinbara, K.; Aida, T. *Chem. Rev.* **2005**, *105*, 1377. *(b)* Balzani, V.; Credi, A.; Venturi, M. *Molecular Devices and Machines-A Journey into the Nano World*, Wiley-VCH, Weinheim, Germany, 2003.
62. *(a)* Leigh, D. A.; Morales, M. A. F.; Pérez, E. M.; Wong, J. K. Y.; Saiz, C. G.; Slawin, A. M. Z.; Carmichael, A. J.; Haddleton, D. M.; Brouwer, A. M.; Buma, W. J.; Wurpel, G. W. H.; León, S.; Zerbetto, F. *Angew. Chem. Int. Ed.* **2005**, *44*, 3062. *(b)* Andrasson, J.; Terazono, Y.; Albinsson, B.; Moore, T. A., Moore, A. L.; Gust, D. *Angew. Chem. Int. Ed.* **2005**, *44*, 7591.
63. Balzani, V.; Clemente-León, M.; Credi, A.; Lowe, J. N.; Badjić, J. D.; Stoddart, J. F.; Williams, D. J. *Chem. Eur. J.* **2003**, *9*, 5348.
64. Dalla Cort, A; Mandolini, L.; Pasquini, C.; Schiaffino, L. *Org. Biomol. Chem.* **2006**, *4*, 4543.

2 *Syntheses*

2.1 Introduction

Tetracoordinated Schiff bases metal complexes are systems achievable by complexation between a metal ion and a Schiff base ligand framework, which it can obtained through a condensation between a diamine and a salicylaldehyde. This kind of ligand coordinate the metal ion through imine nitrogens and the phenolic oxygens of the salicylaldehyde, thus allowing the coordination of various metal ions in various oxidation states, controlling the performance of metals in a large variety of properties, such as catalysis.[1]

The symmetrical Schiff base metal complexes derivatives can be easily obtained by reaction between the ligand and the metal acetate. In particular, the acetate ion deprotonates the phenolic groups of ligand framework, so that the metal ion can be complexed. The achievement of metal complexes can be carrying out with or without[2] the isolation of the ligand.

The unsymmetrical Schiff base ligands and relative metal complex derivatives can be obtained through a different approach. In particular, the synthesis can be carried out through the direct combination of the two different salicylaldehydes and the diammine, or the use of appropriate protector groups, or via monoimine precursors.[3]

The versatility of Schiff base metal complexes consists in the possibility to functionalize the diamine bridge, the salicylaldehyde moieties or both, thus allowing a fine tuning of properties of these species.

In this chapter, the synthetic procedure and the characterization of all the salicylaldehydes, Schiff base ligands and Zn^{II} Schiff base complexes synthesized are reported (Chart 2.1).

Among symmetrical complexes, with exception of complex **5i**, the synthesis was accomplished via template method[2] in a three-step approach involving a nucleophilic substitution reaction (the Williamson ether synthesis procedure) between 2,4-dihydroxybenzaldehyde and appropriate halogenated hydrocarbons to form the 2-

hydroxy-4-(alkoxy)benzaldehyde derivative, followed by a condensation reaction with diamine and, finally, complexation with the Zn^{II} cation. In the case of complex **5i**, before the complexation with Zn^{II} cation, the tetracoordinated ligand **5'** has been isolated.

Among the unsymmetrical Zn^{II} complexes **1e** and **1f**, the synthetic approach used implies the isolation of monoimine tridentate Schiff base **1'**[3] followed by condensation with salicylaldehydes **2** and **5** and complexation with the Zn^{II} cation.

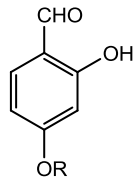

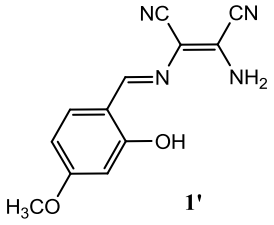

1'

$R = C_2H_5$	**1**
$R = C_{10}H_{21}$	**2**
$R = (CH_2)_9CH=CH_2$	**3**
$R = (CH_2)_{12}Br$	**4**
$R = (CH_2)_{12}N^+(CH_3)_3Br^-$	**5**
$R = C_{16}H_{33}$	**6**
$R = C_{20}H_{41}$	**7**

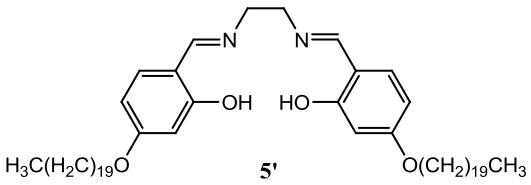

5'

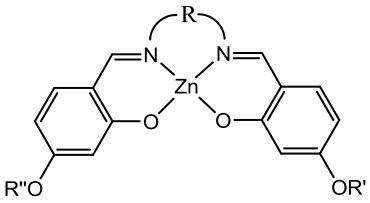

1 R = 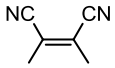

$R'' = R' = (CH_2)_9CH=CH_2$	**1a**
$R'' = R' = C_{16}H_{33}$	**1b**
$R'' = R' = (CH_2)_{12}Br$	**1c**
$R'' = R' = (CH_2)_{12}N^+(CH_3)_3Br^-$	**1d**
$R'' = CH_3 \quad R' = C_{10}H_{21}$	**1e**
$R'' = CH_3 \quad R' = (CH_2)_{12}N^+(CH_3)_3Br^-$	**1f**

2 R = 

$R'' = R' = C_{16}H_{33}$	**2b**
$R'' = R' = C_{10}H_{21}$	**2g**
$R'' = R' = C_2H_5$	**2h**

3 R = 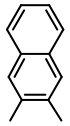

$R'' = R' = C_{16}H_{33}$	**3b**
$R'' = R' = C_{10}H_{21}$	**3g**
$R'' = R' = C_2H_5$	**3h**

4 R = 

$R'' = R' = C_{16}H_{33}$	**4b**
$R'' = R' = C_{10}H_{21}$	**4g**
$R'' = R' = C_2H_5$	**4h**

5 R = 

$R'' = R' = C_{20}H_{41}$	**5i**
$R'' = R' = C_{16}H_{33}$	**5b**
$R'' = R' = C_{10}H_{21}$	**5g**
$R'' = R' = C_2H_5$	**5h**

Chart 2.1

2.2 Syntheses of salicylaldehydes 1-7

2.2.1 General procedure for the synthesis of 4-alkoxy-2-hydroxybenzaldehyde 1-3, 6 and 7.

4-alkoxy-2-hydroxybenzaldehydes have been prepared by a modification of the literature procedure.[4] To a solution of 2,4-dihydroxybenzaldehyde (0.690 g, 5.00 mmol) in acetone (20 mL), have been added potassium carbonate (0.691 g, 5.00 mmol), 18-crown-6 (0.0661 g, 0.250 mmol) and 1-iodoethane (0.780 g, 5.00 mmol), or 1-iododecane (1.341 g, 5.00 mmol), or 11-bromo-1-undecene (1.166 g, 5.00 mmol), or 1-bromohexadecane (1.527 g, 5.00 mmol) or 1-bromoicosane (1.807g, 5.00 mmol). The resulting mixture has been heated at reflux with stirring for 48 h, under a nitrogen atmosphere. After evaporating the solvent, the brown residue has been portioned between 30 mL of diethyl ether (ethyl acetate for aldehyde **1**) and 20 mL of 1.0 M hydrochloric acid. The organic phase has been washed with brine (2 × 10 mL), dried over anhydrous sodium sulphate and evaporated under vacuum. The oily-brown residue has been purified by column chromatography.

4-ethoxy-2-hydroxybenzaldehyde (1). This has been prepared by the above general procedure using 1-iodoethane and purified by column chromatography (silica gel, eluent: cyclohexane/ethyl acetate, 97:3 vol/vol) to afford a colourless oily product (yield 35%). $C_9H_{10}O_3$ (166.17): calcd. C, 65.05; H, 6.07; found C, 65.01; H, 6.09. ^{1}H NMR (500 MHz, $CDCl_3$, TMS, 27°C): δ = 1.44 (t, $^3J_{HH}$ = 7.0 Hz, 3H; C*H*$_3$), 4.09 (q, $^3J_{HH}$ = 7.0 Hz, 2H; C*H*$_2$), 6.41 (d, $^4J_{HH}$ = 2.0 Hz, 1H; Ar*H*), 6.52 (dd, $^4J_{HH}$ = 2.0 Hz, $^3J_{HH}$ = 8.5 Hz, 1H; Ar*H*), 7.41 (d, $^3J_{HH}$ = 8.5 Hz, 1H; Ar*H*), 9.71 (s, 1H; C*H*O), 11.47 (s, 1H; O*H*).

4-decyloxy-2-hydroxybenzaldehyde (2). This has been prepared by the above general procedure using 1-iododecane, and purified by column chromatography (silica gel, eluent: cyclohexane/ethyl acetate, 97:3 vol/vol) to afford a colourless oily product (yield 36%). $C_{17}H_{26}O_3$ (278.39): calcd. C, 73.34; H, 9.41; found C, 73.29; H, 9.40. ^{1}H NMR (500 MHz, $CDCl_3$, TMS, 27°C): δ = 0.88 (t, $^3J_{HH}$ = 7.0 Hz, 3H; C*H*$_3$), 1.27-1.39 (m, 12H; C*H*$_2$), 1.45 (m, 2H; C*H*$_2$), 1.79 (m, 2H; C*H*$_2$), 4.00 (t, $^3J_{HH}$ = 7.0 Hz, 2H; OC*H*$_2$), 6.41 (d, $^4J_{HH}$ = 2.0 Hz, 1H; Ar*H*), 6.52 (dd, $^4J_{HH}$ = 2.0 Hz, $^3J_{HH}$ = 8.5 Hz, 1H; Ar*H*), 7.41 (d, $^3J_{HH}$ = 8.5 Hz, 1H; Ar*H*), 9.70 (s, 1H; C*H*O), 11.47 (s, 1H; O*H*).

4-(undec-10-enyloxy)-2-hydroxybenzaldehyde (3). This has been prepared by the above general procedure using 11-bromo-1-undecene and purified by column

chromatography (silica gel, eluent: cycloexane/ethyl acetate, 95 : 5 vol/vol) to afford a pale-yellow oily product (yield 23%). $C_{18}H_{26}O_3$ (290.40): calcd. C, 74.45; H, 9.02; found C, 75.01; H, 9.12. ^{1}H NMR (500 MHz, $CDCl_3$, TMS, 27°C): δ = 1.30-1.48 (m, 12H; CH_2), 1.80 (m, 2H; CH_2), 2.03 (q, $^3J_{HH}$ = 6.5 Hz, 2H; CH_2-CH), 4.00 (t, $^3J_{HH}$ = 6.5 Hz, 2H; OCH_2), 4.93 (dd, $^4J_{HH}$ = 2.0, $^3J_{HH}$ = 10.0 Hz, 1H; CH=CH_2), 4.99 (dd, $^4J_{HH}$ = 2.0, $^3J_{HH}$ = 17.0 Hz, 1H; CH=CH_2), 5.81 (m, 1H, CH=CH_2), 6.41 (d, $^4J_{HH}$ = 2.0 Hz, 1H; ArH), 6.53 (dd, $^4J_{HH}$ = 2.0, $^3J_{HH}$ = 8.5 Hz, 1H; ArH), 7.41 (d, $^3J_{HH}$ = 8.5 Hz, 1H; ArH), 9.70 (s, 1H; CHO), 11.48 (s, 1H; OH).

4-hexadecyloxy-2-hydroxybenzaldehyde (6). This has been prepared by the general above procedure using 1-bromohexadecane and purified by column chromatography (silica gel, eluent: cyclohexane/ethyl acetate, 98:2 vol/vol) to afford a colourless oil, which solidified on standing (yield 45%). $C_{23}H_{38}O_3$ (362.55): calcd. C, 76.20; H, 10.56; found C, 76.32; H, 10.58. ^{1}H NMR (500 MHz, $CDCl_3$, TMS, 27°C): δ = 0.88 (t, $^3J_{HH}$ = 7.0 Hz, 3H; CH_3), 1.20-1.40 (m, 24H; CH_2), 1.46 (m, 2H; CH_2), 1.81 (m, 2H; CH_2), 4.02 (t, $^3J_{HH}$ = 6.5 Hz, 2H; OCH_2), 6.42 (d, $^4J_{HH}$ = 2.0 Hz, 1H; ArH), 6.53 (dd, $^4J_{HH}$ = 2.0 Hz, $^3J_{HH}$ = 8.5 Hz, 1H; ArH), 7.41 (d, $^3J_{HH}$ = 8.5 Hz, 1H; ArH), 9.71 (s, 1H; CHO), 11.47 (s, 1H; OH).

4-icosyloxy-2-hydroxybenzaldehyde (7). This has been prepared by the general above procedure using 1-bromoicosane and purified by column chromatography (silica gel, eluent: cyclohexane/ethyl acetate, 98:2 vol/vol) to afford a colourless oil, which solidified on standing (yield 54%). $C_{27}H_{46}O_3$ (418.66): calcd. C, 77.46; H, 11.07; found C, 77.32; H, 11.02. ^{1}H NMR (500 MHz, $CDCl_3$, TMS, 27°C): δ = 0.88 (t, $^3J_{HH}$ = 6.5 Hz, 3H; CH_3), 1.20-1.40 (m, 32H; CH_2), 1.44 (m, 2H; CH_2), 1.79 (m, 2H; CH_2), 4.00 (t, $^3J_{HH}$ = 6.5 Hz, 2H; OCH_2), 6.41 (d, $^3J_{HH}$ = 2.5 Hz, 1H; ArH), 6.52 (dd, $^4J_{HH}$ = 2.5 Hz, $^3J_{HH}$ = 9.0 Hz, 1H; ArH), 7.41 (d, $^3J_{HH}$ = 9.0 Hz, 1H; ArH), 9.70 (s, 1H; CHO), 11.47 (s, 1H; OH).

4-(12-Bromododecyloxy)-2-hydroxybenzaldehyde (4). A solution of 2,4 dihydroxybenzaldehyde (0.691 g, 5.00 mmol), 1,12-dibromododecane (1.641 g, 5.00 mmol) and potassium carbonate (0.346 g, 2.50 mmol) in acetonitrile (200 mL) has been heated at reflux with stirring for 4 h under a nitrogen atmosphere. The reaction has been followed by TLC (silica gel; eluent: cyclohexane/ethyl acetate 90:10 vol/vol). The solution has been concentrated and the product has been purified by column

chromatography (silica gel; eluent: cyclohexane/ethyl acetate from 98:2 to 95:5 vol/vol) to obtain a white solid product (yield 39%). $C_{19}H_{29}BrO_3$ (385.34): calcd. C, 59.22; H, 7.59; found C, 59.25; H, 7.55. ^{1}H NMR (500 MHz, DMSO-d_6, TMS, 27°C): δ = 1.26-1.39 (m, 16H; CH_2), 1.69-1.80 (m, 4H; CH_2), 3.51 (t, $^3J_{HH}$ = 6.5 Hz, 2H; CH_2-Br), 4.01 (t, $^3J_{HH}$ = 6.5 Hz, 2H; OCH_2), 6.46 (d, $^4J_{HH}$ = 2.0 Hz, 1H; Ar*H*), 6.55 (dd, $^4J_{HH}$ = 2.0 Hz, $^3J_{HH}$ = 8.5 Hz, 1H; Ar*H*), 7.61 (d, $^3J_{HH}$ = 8.5 Hz, 1H; Ar*H*), 9.99 (s, 1H; C*H*O).

12-(4-Formyl-3-hydroxyphenoxy)-N,N,N-trimethyldodecan-1-ammonium bromide (5). In a two necked-flask, closed by a $CaCl_2$ tube, a solution of aldehyde **4** (0.475 g, 1.23 mmol) in ethanol (40.0 mL) has been saturated with trimethylamine. The yellow-brine solution has been heated at 50°C with stirring for 12 h and then concentrated to obtain a yellow solid product (quantitative yield). $C_{22}H_{38}BrNO_3$ (444.45): calcd. C, 59.45; H, 8.62; N, 3.15; found C, 59.35; H, 8.72; N, 3.25. ^{1}H NMR (500 MHz, DMSO-d_6, TMS, 27°C): δ = 1.39-1.42 (m, 16H; CH_2), 1.64-1.72 (m, 4H; CH_2), 3.03 (s, 9H; N(CH_3)$_3^+$), 3.03-3.27 (m, 2H; CH_2-N(CH$_3$)$_3^+$), 4.02 (t, $^3J_{HH}$ = 6.5 Hz, 2H; OCH_2), 6.46 (d, $^4J_{HH}$ = 2.0 Hz, 1H; Ar*H*), 6.54 (dd, $^4J_{HH}$ = 2.0 Hz, $^3J_{HH}$ = 8.5 Hz, 1H; Ar*H*), 7.61 (d, $^3J_{HH}$ = 8.5 Hz, 1H; Ar*H*), 9.99 (s, 1H; C*H*O).

2.3 Syntheses of uncomplexed ligands 1' and 5'

2-amino-3-((E)-2-hydroxy-4-methoxybenzylideneamino)maleonitrile (1'): The monoimine **1'** has been prepared by a modification of the literature procedure.[5] To a solution of 2,3-diaminomaleonitrile (0.108 g, 1.00 mmol) and 2-hydroxy-4-methoxybenzaldehyde (0.152 g, 1.00 mmol) in methanol (20 mL) has been added 2-3 drops of glacial acetic acid. The resulting mixture has been heated at reflux with stirring for 2 h, under a nitrogen atmosphere. After cooling, the orange product obtained has been filtered, washed with methanol and dried under vacuo at 80°C (yield 60%). $C_{12}H_{10}N_4O_2$ (242.23): calcd. C, 59.50; H, 4.16; N, 23.13; found C, 59.40; H, 4.12; N, 23.16. ^{1}H NMR (500 MHz, DMSO-d_6, TMS, 27°C): δ = 3.78 (s, 3H; OCH_3), 6.47 (d, $^4J_{HH}$ = 2.5 Hz, 1H; Ar*H*), 6.51 (dd, $^4J_{HH}$ = 2.5 Hz, $^3J_{HH}$ = 8.8 Hz, 1H; Ar*H*), 7.65 (s, 2H; NH_2), 7.93 (d, $^3J_{HH}$ = 8.8 Hz, 1H; Ar*H*), 8.48 (s, 1H; C*H*=N), 10.63 (s, 1H; O*H*)

N,N-Bis(4-icosyloxy-2-hydroxybenzylidene)-1,2-ethylenediamine (5'). To a solution of 4-icosyloxy-2-hydroxybenzaldehyde (0.209 g, 0.500 mmol) in hot ethanol (25 mL), ethylenediamine (17 µL, 0.250 mmol) has been added under stirring. The mixture heated at reflux with stirring for 1 h, under a nitrogen atmosphere. After cooling, the

precipitated product has been collected by filtration, has been washed with ethanol, and dried. The white solid product has been purified by crystallization from ethanol/cyclohexane (yield 55%). $C_{56}H_{96}N_2O_4$ (861.39): calcd. C, 78.08; H, 11.23; N, 3.25; found C, 78.14; H, 11.25; N, 3.21. ESI-MS: m/z = 861 $[M+H]^+$. ^{1}H NMR (500 MHz, $CDCl_3$, TMS, 27°C): δ = 0.89 (t, $^3J_{HH}$ = 7.0 Hz, 6H; C*H*$_3$), 1.23-1.38 (m, 64H; C*H*$_2$), 1.43 (m, 4H; C*H*$_2$), 1.77 (m, 4H; C*H*$_2$), 3.85 (s, 4H, NC*H*$_2$C*H*$_2$N), 3.95 (t, $^3J_{HH}$ = 7.0 Hz, 4H; OC*H*$_2$), 6.38 (dd, $^4J_{HH}$ = 2.5 Hz, $^3J_{HH}$ = 9.0 Hz, 2H; Ar*H*), 6.41 (d, $^4J_{HH}$ = 2.5 Hz, 2H; Ar*H*), 7.07 (d, $^3J_{HH}$ = 8.5 Hz, 2H; Ar*H*), 8.20 (s, 2H; C*H*=N), 13.67 (s, 2H; O*H*).

2.4 Syntheses of Zn^{II} complexes 1a-5i

2.4.1 General procedure for the synthesis of complexes 1a-d, 2b, 2g, 2h, 3b, 3g, 3h, 4b, 4g, 4h, 5b, 5g and 5h.

The complexes have been prepared by a template method.[2] To a solution of 4-alkoxy-2-hydroxybenzaldehyde (1.00 mmol) in ethanol (20 mL) (30 mL for complex **1d**), diamine (0.500 mmol) has been added under stirring. The mixture has been heated at reflux with stirring for 1 h, under nitrogen atmosphere. To the solution so obtained, zinc acetate dihydrate (0.1095 g, 0.500 mmol) has been added and the mixture has been heated at reflux with stirring for 1h under a nitrogen atmosphere. After cooling, the precipitated product has been collected by filtration, washed with ethanol and dried.

[2,3-bis[[2-hydroxy-4-(undec-10-enyloxy)benzylidene]amino]-2-butenedinitrilato]-Zn^{II} (1a). Purple powder (yield 75%). $C_{40}H_{50}N_4O_4Zn$ (716.24): calcd. C, 67.08; H, 7.04; N, 7.82; found C, 67.50; H, 6.99; N, 7.94. MALDI-TOF: m/z = 715 ($[M+H]^+$, 100%). ^{1}H NMR (500 MHz, THF-d_8, TMS, 27°C): δ = 1.33-1.50 (m, 24H; C*H*$_2$), 1.77 (m, 4H; C*H*$_2$), 2.04 (m, 4H; C*H*$_2$-CH), 4.00 (t, $^3J_{HH}$ = 6.5 Hz, 4H; OC*H*$_2$), 4.95 (m, 4H; CH=C*H*$_2$), 5.79 (m, 2H; C*H*=CH$_2$), 6.20 (dd, $^4J_{HH}$ = 2.5 Hz, $^3J_{HH}$ = 9.0 Hz, 2H; Ar*H*), 6.26 (d, $^4J_{HH}$ = 2.5 Hz, 2H; Ar*H*), 7.17 (d, $^3J_{HH}$ = 9.0 Hz, 2H; Ar*H*), 8.40 (s, 2H; C*H*=N).

[2,3-bis[[2-hydroxy-4-(undec-10-enyloxy)benzylidene]amino]-2-butenedinitrilato]-Zn^{II} (1b). Purple powder (yield 41%). $C_{50}H_{74}N_4O_4Zn$ (860.56): calcd. C, 69.78; H, 8.67; N, 6.51; found C, 69.95; H, 8.56; N, 6.48. MALDI-TOF: m/z = 860 ($[M+H]^+$, 100%). ^{1}H NMR (500 MHz, THF-d_8, TMS, 27°C): δ = 0.91 (t, $^3J_{HH}$ = 7.0 Hz, 6H; C*H*$_3$), 1.25-1.45 (m, 48H; C*H*$_2$), 1.50 (m, 4H; C*H*$_2$), 1.80 (m, 4H; C*H*$_2$), 4.01 (t, $^3J_{HH}$ = 7.0 Hz,

4H; OCH_2), 6.22 (dd, $^4J_{HH}$ = 2.5 Hz, $^3J_{HH}$ = 9.0 Hz, 2H; Ar*H*), 6.29 (d, $^4J_{HH}$ = 2.5 Hz, 2H; Ar*H*), 7.19 (d, $^3J_{HH}$ = 9.0 Hz, 2H; Ar*H*), 8.42 (s, 2H; C*H*=N). ^{13}C NMR (125 MHz, THF-d_8, TMS, 27°C): δ = 13.42, 22.55, 26.03, 29.07, 29.30, 29.38, 29.59, 29.60, 29.61, 29.65, 31.87, 67.73, 104.42, 107.82, 111.32, 114.29, 120.44, 137.15, 160.39, 167.24, 177.65.

[2,3-bis[[2-hydroxy-4(12-bromododecyloxy)benzylidene]amino]-2-butenedinitrilato]Zn^{II} (1c). Purple powder (yield 74%). $C_{42}H_{56}Br_2N_4O_4Zn$ (906.14): calcd. C, 55.67; H, 6.23; N, 6.18; found C, 55.61; H, 6.33; N, 6.12. ^{1}H NMR (500 MHz, DMSO-d_6, TMS, 27°C): δ = 1.26-1.40 (m, 32H; CH_2), 1.79-1.70 (m, 8H; CH_2), 3.51 (t, $^3J_{HH}$ = 7.0 Hz, 4H; CH_2-Br), 4.00 (t, $^3J_{HH}$ = 7.0 Hz, 4H; OCH_2), 6.20 (d, $^4J_{HH}$ = 2.5 Hz, 2H; Ar*H*), 6.22 (dd, $^4J_{HH}$ = 2.5 Hz, $^3J_{HH}$ = 9.0 Hz, 2H; Ar*H*), 7.34 (d, $^3J_{HH}$ = 9.0 Hz, 2H; Ar*H*), 8.38 (s, 2H; C*H*=N).

[2,3-Bis[[2-hydroxy-4-(1-N,N,N,N-trimethyldodecyl-12-oxyammonium bromide) benzylidene]amino]-2-butenedinitrilato]Zn^{II} (1d). Purple powder (yield 60%). $C_{48}H_{74}Br_2N_6O_4Zn$ (1024.35): calcd. C, 56.28; H, 7.28; N, 8.20%; found C, 56.73; H, 7.34; N, 8.30%. ESI: m/z = 1024 $[M]^+$. MALDI-TOF: m/z = 1968 $[(M)_2\text{-Br}]^+$. ^{1}H NMR (500 MHz, DMSO-d_6, TMS, 27°C): δ = 1.27-1.40 (m, 32H; CH_2), 1.64-1.73 (m, 8H; CH_2), 3.02 (s, 18H; N(CH_3)$_3^+$), 3.23-3.26 (m, 4H; CH_2-N(CH$_3$)$_3^+$), 3.99 (t, $^3J_{HH}$ = 6.5 Hz, 4H; OCH_2), 6.17 (d, $^4J_{HH}$ = 2.0 Hz, 2H; Ar*H*), 6.21 (dd, $^4J_{HH}$ = 2.0 Hz, $^3J_{HH}$ = 8.5 Hz, 2H; Ar*H*), 7.33 (d, $^3J_{HH}$ = 8.5 Hz, 2H; Ar*H*), 8.36 (s, 2H; C*H*=N).

[N,N-Bis(4-hexadecyloxy-2-hydroxybenzylidene)-1,2-phenylenediaminato]Zn^{II} (2b). Yellow powder (yield 40%). $C_{52}H_{78}N_2O_4Zn$ (860.60): calcd. C, 72.57; H, 9.14; N, 3.26; found C, 69.61; H, 7.81; N, 4.00. ESI-MS: m/z = 1722 ($[(M)_2+H]^+$, 100%). ^{1}H NMR (500 MHz, DMSO-d_6, TMS, 27°C): δ = 0.84 (t, $^3J_{HH}$ = 7.0 Hz, 6H; CH_3), 1.23-1.40 (m, 50H; CH_2), 1.69-1.79 (m, 6H; CH_2), 3.96 (t, $^3J_{HH}$ = 6.5 Hz, 4H; OCH_2), 6.13 (dd, $^4J_{HH}$ = 2.5 Hz, $^3J_{HH}$ = 9.0 Hz, 2H; Ar*H*), 6.16 (d, $^4J_{HH}$ = 2.5 Hz, 2H; Ar*H*), 7.28 (m, 4H; Ar*H*), 7.78 (m, 2H; Ar*H*), 8.86 (s, 2H; C*H*=N).

[N,N-Bis(4-decyloxy-2-hydroxybenzylidene)-1,2-phenylenediaminato]Zn^{II} (2g). Yellow powder (yield 84%). $C_{40}H_{54}N_2O_4Zn$ (692.28): calcd. C, 69.40; H, 7.86; N, 4.05; found C, 69.61; H, 7.81; N, 4.00. ESI-MS: m/z = 1385 ($[(M)_2+H]^+$, 100%). ^{1}H NMR (500 MHz, DMSO-d_6, TMS, 27°C): δ = 0.86 (t, $^3J_{HH}$ = 7.0 Hz, 6H; CH_3), 1.23-1.45 (m, 28H; CH_2), 1.71 (m, 4H; CH_2), 3.96 (t, $^3J_{HH}$ = 6.5 Hz, 4H; OCH_2), 6.14 (dd, $^4J_{HH}$ = 2.5

Hz, $^3J_{HH}$ = 9.0 Hz, 2H; Ar*H*), 6.16 (d, $^4J_{HH}$ = 2.5 Hz, 2H; Ar*H*), 7.27 (d, $^3J_{HH}$ = 9.0 Hz, 2H; Ar*H*), 7.29 (m, 2H; Ar*H*), 7.79 (m, 2H; Ar*H*), 8.86 (s, 2H; C*H*=N).

[N,N-Bis(4-ethoxy-2-hydroxybenzylidene)-1,2-phenylenediaminato]Zn^{II} (2h). Yellow powder (yield 70%). $C_{24}H_{22}N_2O_4Zn$ (467.85): calcd. C, 61.61; H, 4.74; N, 5.99; found C, 61.69; H, 4.79; N, 5.51. ESI-MS: m/z = 937 ($[(M)_2+H]^+$, 100%). ^{1}H NMR (500 MHz, DMSO-d_6, TMS, 27°C): δ = 1.33 (t, $^3J_{HH}$ = 7.0 Hz, 6H; CH_3), 4.03 (t, $^3J_{HH}$ = 7.0 Hz, 4H; OCH_2), 6.14 (dd, $^4J_{HH}$ = 2.5 Hz, $^3J_{HH}$ = 8.5 Hz, 2H; Ar*H*), 6.17 (d, $^4J_{HH}$ = 2.5 Hz, 2H; Ar*H*), 7.27 (d, $^3J_{HH}$ = 8.5 Hz, 2H; Ar*H*), 7.29 (m, 2H; Ar*H*), 7.79 (m, 2H; Ar*H*), 8.86 (s, 2H; C*H*=N).

[N,N-Bis(4-hexadecyloxy-2-hydroxybenzylidene)-2,3-naphthalenediaminato]Zn^{II} (3b). Yellow powder (yield 95%).$C_{56}H_{80}N_2O_4Zn$ (910.66): C, 73.86; H, 8.85; N, 3.08; found C, 73.76; H, 8.95; N, 3.18. ^{1}H NMR (500 MHz, DMSO-d_6, TMS, 27°C): δ = 0.84 (t, $^3J_{HH}$ = 6.5 Hz, 6H; CH_3), 1.23-1.41 (m, 52H; CH_2), 1.71 (m, 4H; CH_2), 3.97 (t, $^3J_{HH}$ = 6.5 Hz, 4H; OCH_2), 6.15-6.18 (m, 4H; Ar*H*), 7.31 (d, $^3J_{HH}$ = 9.0 Hz, 2H; Ar*H*), 7.44-7.46 (m, 2H; Ar*H*), 7.87-7.89 (m, 2H; Ar*H*), 8.21 (s, 2H; Ar*H*), 9.00 (s, 2H; C*H*=N).

[N,N-Bis(4-decyloxy-2-hydroxybenzylidene)-2,3-naphthalenediaminato]Zn^{II} (3g). Yellow powder (yield 97%). $C_{44}H_{56}N_2O_4Zn$ (742.34): calcd. C, 71.19; H, 7.60; N, 3.77; found C, 71.25; H, 7.63; N, 3.75. ESI-MS: m/z = 1486 ($[(M)_2+H]^+$, 100%). ^{1}H NMR (500 MHz, DMSO-d_6, TMS, 27°C): δ = 0.86 (t, $^3J_{HH}$ = 7.0 Hz, 6H; CH_3), 1.24-1.35 (m, 28H; CH_2), 1.72 (m, 4H; CH_2), 3.98 (t, $^3J_{HH}$ = 7.0 Hz, 4H; OCH_2), 6.15-6.19 (m, 4H; Ar*H*), 7.31 (d, $^3J_{HH}$ = 8.5 Hz, 2H; Ar*H)*, 7.43-7.47 (m, 2H; Ar*H*), 7.86-7.90 (m, 2H; Ar*H*), 8.22 (s, 2H; Ar*H*), 9.01 (s, 2H; C*H*=N).

[N,N-Bis(4-ethoxy-2-hydroxybenzylidene)-2,3-naphthalenediaminato]Zn^{II} (3h). Yellow powder (yield 93%).$C_{28}H_{24}N_2O_4Zn$ (517.91): calcd. C, 64.93; H, 4.67; N, 5.41; found C, 64.83; H, 4.77; N, 5.21. ^{1}H NMR (500 MHz, DMSO-d_6, TMS, 27°C): δ = 1.34 (t, $^3J_{HH}$ = 7.0 Hz, 6H; CH_3), 4.04 (q, $^3J_{HH}$ = 7.0 Hz, 4H; OCH_2), 6.16-6.18 (m, 4H; Ar*H*), 7.32 (d, $^3J_{HH}$ = 8.5 Hz, 2H; Ar*H*), 7.45-7.46 (m, 2H; Ar*H*), 7.88-7.89 (m, 2H; Ar*H*), 8.22 (s, 2H; Ar*H*), 9.01 (s, 2H; C*H*=N).

[N,N-Bis(4-hexadecyloxy-2-hydroxybenzylidene)-2,3-pyridinediaminato]Zn^{II} (4b). Yellow powder (yield 98%). $C_{51}H_{77}N_3O_4Zn$ (861.58): calcd. C, 71.10; H, 9.01; N, 4.88; found C, 71.07; H, 9.02; N, 4.90. ESI-MS: m/z = 1723 ($[(M)_2+H]^+$, 100%). ^{1}H NMR (500 MHz, DMSO-d_6, TMS, 27°C): δ = 0.84 (t, $^3J_{HH}$ = 7.0 Hz, 6H; CH_3), 1.22-1.43 (m,

52H; CH_2), 1.71 (m, 4H; CH_2), 3.97 (q, $^3J_{HH}$ = 6.5 Hz, 4H; OCH_2), 6.13-6.18 (m, 2H; Ar*H*), 6.18 (s, 2H; Ar*H*), 7.26 (d, $^3J_{HH}$ = 9.0 Hz, 1H; Ar*H*), 7.30-7.33 (m, 2H; Ar*H*), 8.21 (d, $^3J_{HH}$ = 8.5 Hz, 1H; Ar*H*), 8.27 (dd, $^4J_{HH}$ = 1.5 Hz, $^3J_{HH}$ = 5.0 Hz, 1H; Ar*H*), 8.93 (s, 1H; C*H*=N), 9.29 (s, 1H; C*H*=N).

[N,N-Bis(4-decyloxy-2-hydroxybenzylidene)-2,3-pyridinediaminato]Zn^{II} (4g). Yellow powder (yield 90%). $C_{39}H_{53}N_3O_4Zn$ (693.27): calcd. C, 67.57; H, 7.71; N, 6.06; found C, 67.49; H, 7.74; N, 6.01. ESI-MS: m/z = 1387 ([$(M)_2$+H]$^+$, 100%). ^{1}H NMR (500 MHz, DMSO-d_6, TMS, 27°C): δ = 0.86 (t, $^3J_{HH}$ = 7.0 Hz, 6H; CH_3), 1.22-1.45 (m, 28H; CH_2), 1.72 (m, 4H; CH_2), 3.95-4.00 (m, 4H; OCH_2), 6.14-6.20 (s, 4H; Ar*H*), 7.27 (d, $^3J_{HH}$ = 9.0 Hz, 1H; Ar*H*), 7.31-7.34 (m, 2H; Ar*H*), 8.22 (d, $^3J_{HH}$ = 7.0 Hz, 1H; Ar*H*), 8.27 (dd, $^4J_{HH}$ = 1.5 Hz, $^3J_{HH}$ = 5.0 Hz, 1H; Ar*H*), 8.93 (s, 1H; C*H*=N), 9.30 (s, 1H; C*H*=N).

[N,N-Bis(4-ethoxy-2-hydroxybenzylidene)-2,3-pyridinediaminato]Zn^{II} (4h). Yellow powder (yield 60%). $C_{23}H_{21}N_3O_4Zn$ (468.84): calcd. C, 58.92; H, 4.51; N, 8.96; found C, 58.99; H, 4.49; N, 8.90. ESI-MS: m/z = 939 ([$(M)_2$+H]$^+$, 100%). ^{1}H NMR (500 MHz, DMSO-d_6, TMS, 27°C): δ = 1.34 (t, $^3J_{HH}$ = 7.5 Hz, 6H; CH_3), 4.03-4.06 (m, 4H; OCH_2), 6.15-6.19 (m, 2H; Ar*H*), 6.20 (s, 2H; Ar*H*), 7.27 (d, $^3J_{HH}$ = 8.5 Hz, 1H; Ar*H*), 7.31-7.35 (m, 2H; Ar*H*), 8.22 (d, $^3J_{HH}$ = 8.5 Hz, 1H; Ar*H*), 8.27 (d, $^3J_{HH}$ = 4.5 Hz, 1H; Ar*H*), 8.94 (s, 1H; C*H*=N), 9.30 (s, 1H; C*H*=N).

[N,N-Bis(4-hexadecyloxy-2-hydroxybenzylidene)-1,2-ethylenediaminato]Zn^{II} (5b). White powder (yield 95%). $C_{48}H_{78}N_2O_4Zn$ (812.56): calcd. C, 70.95; H, 9.68; N, 3.45; found C, 71.03; H, 9.69; N, 3.47. ESI-MS: m/z = 1625 [$(M)_2$+H]$^+$. ^{1}H NMR (500 MHz, DMSO-d_6, TMS, 27°C): δ = 0.85 (t, $^3J_{HH}$ = 6.5 Hz, 6H; CH_3), 1.19-1.45 (m, 52H; CH_2), 1.67 (m, 4H; CH_2), 3.62 (s, 4H; NCH_2CH_2N), 3.89 (t, $^3J_{HH}$ = 6.5 Hz, 4H; OCH_2), 6.02 (d, $^3J_{HH}$ = 8.5 Hz, 2H; Ar*H*), 6.08 (s, 2H; Ar*H*), 7.00 (d, $^3J_{HH}$ = 8.5 Hz, 2H; Ar*H*), 8.28 (s, 2 H; C*H*=N).

[N,N-Bis(4-decyloxy-2-hydroxybenzylidene)-1,2-ethylenediaminato]Zn^{II} (5g). White powder (yield 90%). $C_{36}H_{54}N_2O_4Zn$ (644.24): calcd. C, 67.12; H, 8.45; N, 4.35; found C, 67.22; H, 8.47; N, 4.38. ESI-MS: m/z = 1289 [$(M)_2$+H]$^+$. ^{1}H NMR (500 MHz, DMSO-d_6, TMS, 27°C): δ = 0.86 (t, $^3J_{HH}$ = 6.5 Hz, 6H; CH_3), 1.22-1.45 (m, 28H; CH_2), 1.68 (m, 4H; CH_2), 3.63 (s, 4H; NCH_2CH_2N), 3.90 (t, $^3J_{HH}$ = 6.5 Hz, 4H; OCH_2), 6.02

(dd, $^4J_{HH}$ = 2.5 Hz, $^3J_{HH}$ = 8.5 Hz, 2H; Ar*H*), 6.08 (d, $^4J_{HH}$ = 2.5 Hz, 2H; Ar*H*), 7.00 (d, $^3J_{HH}$ = 8.5 Hz, 2H; Ar*H*), 8.28 (s, 2H; C*H*=N).

[N,N-Bis(4-ethoxy-2-hydroxybenzylidene)-1,2-ethylenediaminato]Zn^{II} (5h). White powder (yield 85%). $C_{20}H_{22}N_2O_4Zn$ (419.80): calcd. C, 57.22; H, 5.28; N, 6.67; found C, 57.19; H, 5.29; N, 6.69. ESI-MS: m/z = 841 $[(M)_2+H]^+$. ^{1}H NMR (500 MHz, DMSO-d_6, TMS, 27°C): δ = 1.31 (t, $^3J_{HH}$ = 7.0 Hz, 6H; CH_3), 3.63 (s, 4H; NCH_2CH_2N), 3.96 (q, $^3J_{HH}$ = 7.0 Hz, 4H; OCH_2), 6.03 (dd, $^4J_{HH}$ = 2.5 Hz, $^3J_{HH}$ = 8.5 Hz, 2H; Ar*H*), 6.08 (d, $^4J_{HH}$ = 2.5 Hz, 2H; Ar*H*), 7.01 (d, $^3J_{HH}$ = 8.5 Hz, 2H; Ar*H*), 8.28 (s, 2H; C*H*=N).

[N,N-Bis(4-icosyloxy-2-hydroxybenzylidene)-1,2-ethylenediaminato]Zn^{II} (5i). A suspension of **5'** (0.152 g, 0.18 mmol) in refluxing ethanol (50 mL) has been dissolved by addition of the minimum amount of cyclohexane. To the solution obtained, an ethanolic solution of zinc acetate dihydrate (0.040 g, 0.18 mmol) has been added. The mixture has been heated at reflux with stirring for 2 h, under nitrogen atmosphere. The precipitated product has been collected by filtration, has been washed with ethanol, and dried to give a white powder (yield 95%). $C_{56}H_{94}N_2O_4Zn$ (924.77): calcd. C, 72.73; H, 10.25; N, 3.03; found C, 72.68; H, 10.23; N, 3.00. ESI-MS: m/z = 1850 $[(M)_2+H]^+$. ^{1}H NMR (500 MHz, 5 × 10^{-4} M, $CDCl_3$/DMSO-d_6 83:17 vol/vol, TMS, 27°C): δ = 0.79 (t, $^3J_{HH}$ = 7.0 Hz, 6H; CH_3), 1.10-1.30 (m, 64H; CH_2), 1.33 (m, 4H; CH_2), 1.66 (m, 4H; CH_2), 3.61 (s, 4H, NCH_2CH_2N), 3.82 (t, $^3J_{HH}$ = 6.5 Hz, 4H; OCH_2), 6.00 (dd, $^4J_{HH}$ = 3.0 Hz, $^3J_{HH}$ = 9.0 Hz, 2H; Ar*H*), 6.29 (d, $^4J_{HH}$ = 3.0 Hz, 2H; Ar*H*), 6.86 (d, $^3J_{HH}$ = 9.0 Hz, 2H; Ar*H*), 8.12 (s, 2H; C*H*=N).

[2-((E)-4-(decyloxy)-2-hydroxybenzylideneamino)-3-((E)-2-hydroxy-4-methoxy-benzylideneamino)maleonitrilato]Zn^{II} (1e). The complex has been prepared following the literature procedure.[6] A mixture of monoimine **1'** (0.242 g, 1.00 mmol), aldehyde **2** (0.278 g, 1.00 mmol), $Zn(OAc)_2{\cdot}2H_2O$ (0.220 g, 1.00 mmol) and neat NEt_3 (2 mL) in ethanol (50 mL) has been stirred at room temperature for 24 h. Then the product has been collected by filtration and dried under vacuo at 120°C using sulfuric acid as a desiccant agent (yield 60 %). $C_{29}H_{32}N_4O_4Zn$ (566) calcd. C, 61.54; H, 5.70; N, 9.90; found C, 61.64; H, 5.50; N, 9.80. ^{1}H NMR (500 MHz, DMSO-d_6, TMS, 27°C): δ = 0.86 (t, $^3J_{HH}$ = 7.0 Hz, 3H; CH_3), 1.25-1.40 (m, 14H; CH_2), 1.71 (m, 2H; CH_2), 3.79 (s, 3H; OCH_3), 4.00 (t, $^3J_{HH}$ = 6.5 Hz, 2H; OCH_2), 6.21-6.25 (m, 4H; Ar*H*), 7.35 (d, $^3J_{HH}$ = 8.5

Hz, 1H; Ar*H*), 7.36 (d, $^3J_{HH}$ = 8.5 Hz, 1H; Ar*H*), 8.38 (s, 1H; C*H*=N), 8.39 (s, 1H; C*H*=N).

[2-((E)-4-(1-N,N,N,N-trimethyldodecyl-12-oxyammoniumbromide)-2-hydroxybenzylideneamino)-3-((E)-2-hydroxy-4-methoxybenzylideneamino)maleonitrilato]Zn^{II} (1f). A solution of monoimine **1'** (0.055 g, 0.22 mmol) and aldehyde **5** (0.100 g, 0.22 mmol) in ethanol (20.0 mL) has been heated at reflux with stirring for 1 h, under nitrogen atmosphere. At the red solution, zinc acetate dihydrate (0.049 g, 0.022 mmol), has been added and the mixture has been heated at reflux with stirring for 2 h, under nitrogen atmosphere. After cooling, a purple precipitate product has been collected by filtration, has been washed with methanol, and dried in vacuo (yield 30%). $C_{34}H_{44}BrN_5O_4Zn$ (732.06): calcd. C, 55.78; H, 6.06; N, 9.57; found C, 55.48; H, 6.16; N, 9.67. ^{1}H NMR (500 MHz, DMSO-d_6, TMS, 27°C): δ = 1.28-1.41 (m, 16H; CH_2), 1.66-1.73 (m, 4H; CH_2), 3.03 (s, 9H; N(CH_3)$_3^+$), 3.23-3.27 (m, 2H; CH_2-N(CH$_3$)$_3^+$), 3.79 (s, 3H; OCH_3), 4.00 (t, $^3J_{HH}$ = 6.5 Hz, 2H; OCH_2), 6.20-6.24 (m, 4H; Ar*H*), 7.35 (d, $^3J_{HH}$ = 9.0 Hz, 1H; Ar*H*), 7.36 (d, $^3J_{HH}$ = 9.0 Hz, 1H; Ar*H*), 8.38 (s, 1H; C*H*=N), 8.39 (s, 1H; C*H*=N).

2.5 References

1. For reviews see: *(a)* McGarrigle, E. M.; Gilheany, D. G. *Chem. Rev.* **2005**, *105*, 1563. *(b)* Farlow, J. F.; Jacobsen, E. N. *Top. Organomet. Chem.* **2004**, *7*, 123. *(c)* Cozzi, P. G. *Chem. Soc. Rev.* **2004**, *33*, 410.*(d)* Katsuki, T. *Chem. Soc. Rev.* **2004**, *33*, 437. *(e)* Katsuki, T. *Synlett* **2003**, 281. *(f)* Atwood, D. A.; Harvey, M. J. *Chem. Rev.* **2001**, *101*, 37. *(g)* Jacobsen, E. N. *Acc. Chem. Res.* **2000**, *33*, 421. *(h)* Canali, L.; Sherrington, D. C. *Chem. Soc. Rev.* **1999**, *28*, 85. *(i)* Katsuki, T. *Coord. Chem. Rev.* **1995**, *140*, 189.
2. Di Bella, S.; Consiglio, G.; Leonardi, N.; Failla, S.; Finocchiaro P.; Fragalà, I. *Eur. J. Inorg. Chem.*, **2004**, 2701.
3. Kleij, A. W. *Eur. J. Inorg. Chem.* **2009**, 193.
4. Bhattacharjee, C. R.; Das, G.; Mondal, P.; Rao, N. V. S. *Polyhedron* **2010**, *29*, 3089.
5. Singh, L. P.; Bhatnagar J. M. *Talanta* **2004**, *64*, 313.
6. Kleij, A. W.; Tooke, D. M.; Spek, A. L.; Reek J. N. H. *Eur. J. Inorg. Chem.* **2005**, 4626.

3 *Aggregation/Deaggregation Properties of Zn^{II} Schiff Base Complexes and their Lewis Acidic Character*

3.1 Introduction

Molecular aggregation is the capacity of molecules to self-organize, self-assemble, and self-control into supramolecular systems with new properties, which are not given from the individual molecules but arise upon aggregation.[1] It plays an important role in various biological systems and in supramolecular chemistry and finds applications in various fields, such as molecular biology,[2] materials science, chemical recognition and sensing.[1]

The main driving forces for the formation of supramolecular structures are the hydrophobic, electrostatic, hydrogen bond, van der Waals, cation-π and π-π stacking interactions, and the total intermolecular force acting between two or more molecules is the sum of all the forces they exert on each other.[3] As the molecular aggregation can occur through various mechanisms, its control depends upon the fine molecular structure and environmental conditions.[3,4]

Tetracoordinated Zn^{II} Schiff base complexes are remarkable precursors in supramolecular chemistry, which have been broadly studied for their diverse catalytic, optical, and photophysical properties.[5] The molecular aggregation of these systems occurs in a different way respect to various mechanisms abovementioned. In particular, the driving force to aggregation is the axial coordination to the Zn^{II} metal centre. This pentacoordination can be achieved by the axial coordination of a coordinating species or, in their absence, through intermolecular Zn···O axial coordination.[6-8] In other terms, in these complexes the Zn^{II} ion is a Lewis acid, which saturate its coordination sphere by coordinating a large variety of neutral and anionic Lewis bases or, in their absence, can be stabilized through intermolecular Zn···O axial coordination involving the phenolic oxygen atoms of the ligand framework. Thus allowing a different control of the supramolecular architecture and, a variety of aggregate molecular architectures,[7] supramolecular assemblies[9] and nanostructures[10] have been found. Zn^{II} Schiff base

complexes have also been investigated for their fluorescent features, which are related to the structure of the salen template[11] and the axial coordination,[4,12,13] and second-order nonlinear optical (NLO) properties.[14]

In spite of these studies, the role of the ligand framework upon the aggregation behaviour of these species in solution in the presence/absence of coordinating species is still almost undefined.[12] It is, therefore, of interest to investigate structural factors determining the aggregation of these complexes in solution in the absence of coordinating species and their spectroscopic/photophysical properties in relation to the nature of the aggregate and upon deaggregation.

In this chapter, the aggregation/deaggregation properties in solution of a series of Schiff base complexes, upon changing the bridging diamine group, and their Lewis acidic character, through detailed ^{1}H NMR, diffusion ordered (DOSY) NMR and optical spectroscopic studies, are investigated. To ensure suitable solubility, both in coordinating and non-coordinating solvents, a series of amphiphilic species have been considered, also with changing the length of the alkyl chains.

This chapter is divided in three main sections, in relation to the typology of complexes discussed. In the first section, it will be discussed the aggregation/deaggregation properties of amphiphilic Zn^{II} Schiff base complexes having 2,3-diaminomaleonitrile as bridging diamino group. In the second section, it will discussed the aggregation behaviour of Zn^{II} complexes where the bridging diamine contains the benzene, naphthalene, and pyridine nucleus, to further extend the study on aggregation of complexes having conjugated bridging diamine. Finally, in the last section of chapter, it will discussed the molecular aggregation of Zn^{II} complexes having as bridging groups an aliphatic diamine, in particular 1,2-ethylendiamine, which is a non-conjugated, conformational flexible system, to highlight any analogies and differences, in terms of aggregation properties, with respect to complexes having conjugated bridging diamine.

3.2 Zn^{II} (2,3-diaminomaleonitrile) complexes

In this section, the complexes investigated are complexes **1a** and **1b** (see Chart 3.1).

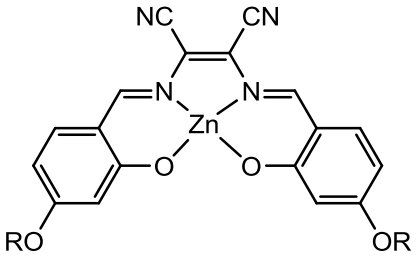

R = $(CH_2)_9CH=CH_2$ **1a**
R = $C_{16}H_{33}$ **1b**

Chart 3.1 Structure of investigated complexes.

The complex **1a** has already been investigated by Di Bella S., Cricenti A. and co-workers.[13b] In particular, this complex has been anchored onto Si(100), through the direct covalent grafting of alkene groups of **1a** with the hydrogen-terminated surface, and the self-assembly monolayers (SAMs) obtained have been characterized by UV-vis, fluorescence and AFM/SNOM measurements. It has been found that the photoluminescent properties of the monolayer can be related to its ordered structure.[13b]

The following discussion is centred on the investigation of this kind of complexes in solution. The aggregation/deaggregation and NLO properties in solution of the Zn^{II} Schiff base complexes **1a** and **1b** have been carry out through detailed ^1H NMR, DOSY NMR, optical spectroscopy and electric field induced second harmonic generation (EFISH) technique. The results and discussion will be focused essentially on complex **1a** because the complex **1b** possesses almost identical properties.

3.2.1 Results

The complex **1a** is moderately soluble in low-polarity solvents, such as dichloromethane (DCM) and tetrachloroethane (TCE), and in some coordinating solvents, such as dimethyl sulfoxide (DMSO) and tetrahydrofuran (THF), and low soluble in non polar solvents, *e.g.*, toluene (TOL) and mesitylene (MES).

Matrix-assisted laser desorption ionization-time-of-flight (MALDI-TOF) mass spectrometry analysis indicates the presence of defined signals corresponding to the protonated dimer, in addition to the protonated molecular ion (Figure 3.1).

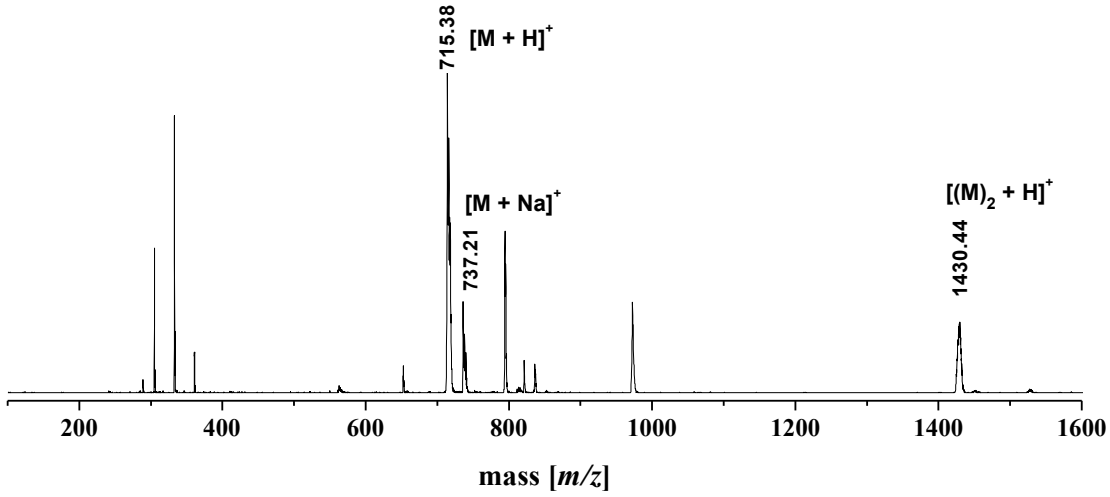

Figure 3.1 MALDI-TOF spectrum of **1a** (unassigned peaks refer to the matrix signals).

3.2.1.1 ^{1}H NMR studies

^{1}H NMR spectra of **1a** in solutions of coordinating solvents, such as DMSO-d_6 or THF-d_8, recorded at the concentration of ≈4 × 10^{-4} M, indicate the presence of sharp signals with the expected multiplicity, according to its molecular structure and consistent with the existence of monomeric species (Figure 3.2). As expected, these ^{1}H NMR spectra are independent from the concentration of the solution.

On switching to non-coordinating solvents, such as DCM-d_2 or TCE-d_2, ^{1}H NMR spectra of **1a**, recorded at the same above concentration, show a slightly broadening of the H_3 and H_5 peaks and a significant upfield shift (with respect to coordinating solvents) of the H_1 (0.15-0.35 ppm), H_3 (up to 0.65 ppm), and -OCH_2 (0.26-0.40 ppm) signals (Figure 3.2). These relevant upfield shifts, indicating that the involved hydrogens lie under the shielding zone of the π electrons of a conjugated system,[3b,15] and the observed peak broadening are both consistent with the existence of aggregate species of **1a** in non-coordinating solvents.

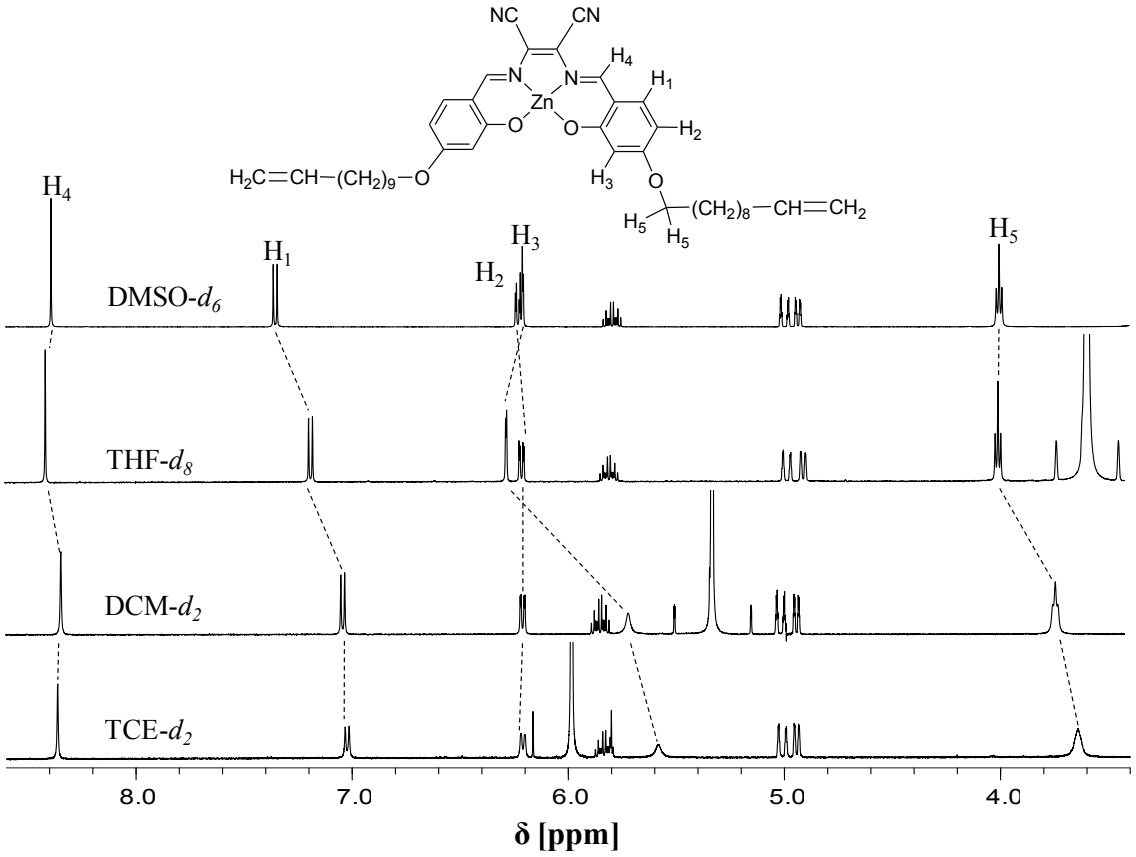

Figure 3.2 ^{1}H NMR spectra of **1a** (≈4.0 × 10^{-4} M) in various solvents.

^{1}H NMR signals of **1a** in non-coordinating solvents are concentration dependent. In particular, in the case of TCE-d_2 solutions with concentrations higher than 1 × 10^{-3} M, a progressive peak broadening of all aromatic hydrogens signals is observed, including those related to the -OCH_2 and CH=N groups, the latter of which is also upfield shifted, along with less shielding of H_3 aromatic protons (Figure 3.3a). On the other hand, on going to lower concentrations, ≤1 × 10^{-3} M, ^{1}H NMR spectra are independent from the concentration. A similar behaviour is observed in the case of DCM-d_2 solutions (Figure 3.3b). In fact, for concentrations higher than 4 × 10^{-4} M, the abovementioned ^{1}H NMR signals become concentration dependent. Thus, ^{1}H NMR spectra recorded in almost saturated solutions of these non-coordinating solvents (≈2 × 10^{-3} M in DCM-d_2 and ≈1 × 10^{-2} M in TCE-d_2) are virtually identical, consisting of very broad signals involving all protons, with the exception of those related to alkyl chains, and this is typical of the presence of large aggregate species (Figure 3.3).[8b]

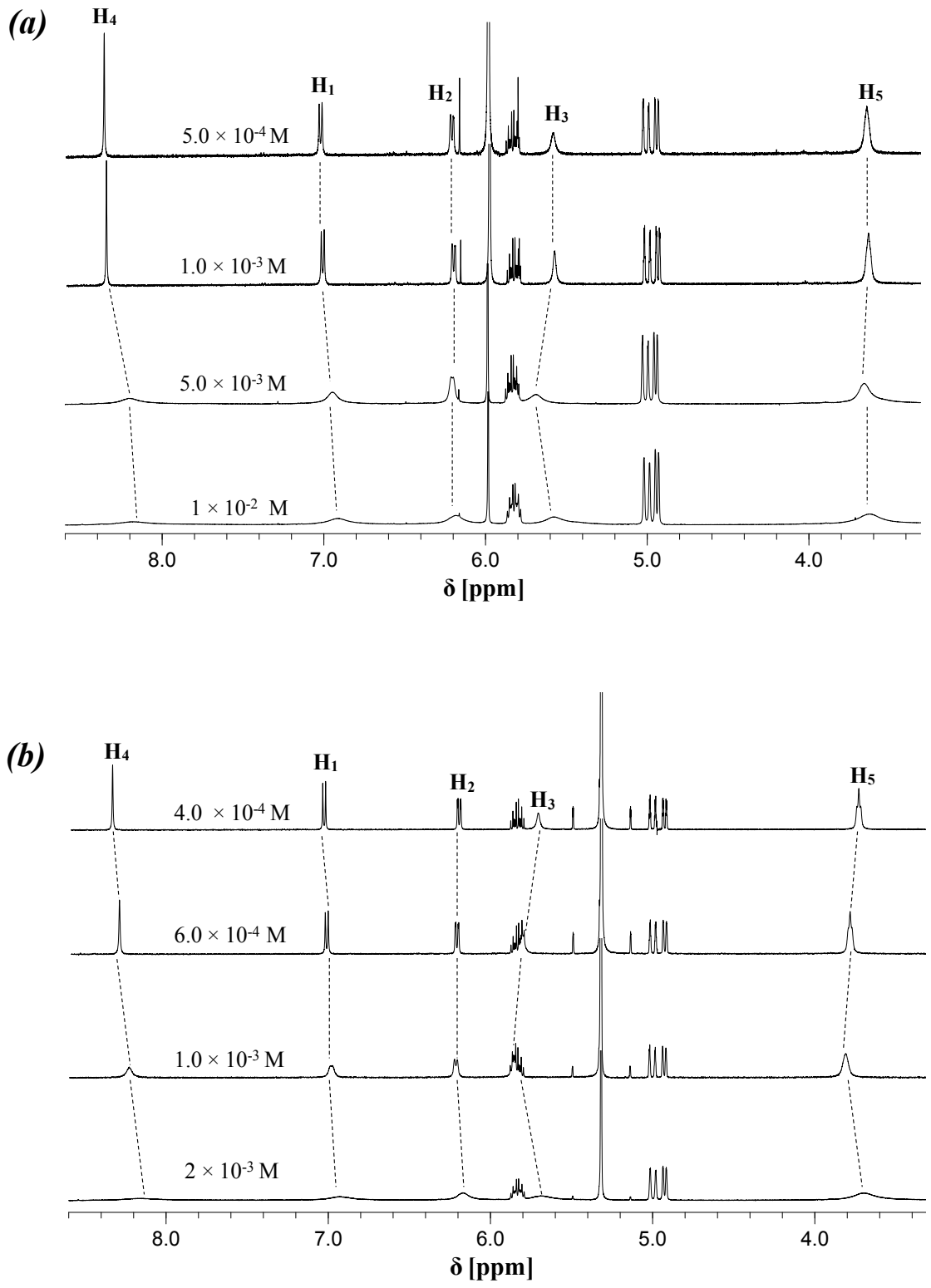

Figure 3.3 Concentration dependence of ^{1}H NMR spectra of **1a** in *(a)* TCE-d_2 and *(b)* DCM-d_2 solutions.

DOSY[16] has been used as an independent method to estimate the degree of aggregation and the molecular mass of **1a**, through the measurement of the diffusion

coefficient, D. This technique plays an important role in the identification of supramolecular species in solution owing to the straightforward two-dimensional (2D) representation of the components of the system. Equilibria between the aggregates are usually established in solution and, if the interconversion rate is fast compared to the chemical shift NMR time-scale, then a single set of resonances is observed. This implies that the average diffusion value obtained from diffusion NMR experiments contains information about the level of aggregation.[17]

2D DOSY data collected from different concentrations of **1a** in coordinating (DMSO-d_6) and non-coordinating (TCE-d_2) solvents are reported in Table 3.1 and are used to investigate the degree of aggregation of **1a**, through an estimate of the molecular mass (see paragraph **7.12**).

Table 3.1 Diffusion coefficients, *D*, and estimated molecular mass, *m*, of **1a** at 27°C in non-coordinating (TCE-d_2) and coordinating (DMSO-d_6) solvents.

Concentration [a] ($\times 10^{-3}$ M)	*D* (**1a**) ($\times 10^{-10}$ m^2 s^{-1})	*D* (solvent) ($\times 10^{-10}$ m^2 s^{-1})	*m* [b] (Da)
5.0	2.37	8.05 (TCE-d_2)	1948
1.0	2.88	8.30 (TCE-d_2)	1402
1.0	3.55	8.01 (TCE-d_2)	860[c]
0.5	3.11	8.68 (TCE-d_2)	1315
5.0	2.15	6.80 (DMSO-d_6)	832
1.0	2.30	7.20 (DMSO-d_6)	815

[a]The quasi-saturation regime of 1×10^{-2} M solutions of **1a** in TCE-d_2 precluded the achievement of reliable DOSY data at these concentrations. [b]Estimated molecular mass with eq. 5 (see paragraph **7.12**). [c]Upon addition of a stoichiometric amount of pyridine.

They clearly indicate that the estimated molecular mass in DMSO-d_6 is independent from the concentration of the solution, consistent with a monomeric DMSO axially coordinated species. In contrast, on switching to the TCE-d_2 non-coordinating solvent, a concentration dependence of the diffusion coefficient is observed. In particular, while for concentrations $\leq 1 \times 10^{-3}$ M the estimated molecular mass is independent upon dilution and consistent with a dimeric structure, for higher concentrations larger aggregates are predicted.

^{1}H NMR studies of **1a** in mixtures of non-coordinating/coordinating solvents (*e.g.*, TCE-d_2/DMSO-d_6 or DCM-d_2/THF-d_8) further support the existence of aggregates in the former solvent. In fact, even in a mixture 1% vol/vol of the coordinating DMSO-d_6

(or THF-d_8) solvent are observed almost identical ^{1}H NMR signals, in terms of peaks position and shape, as those recorded in pure DMSO-d_6 (or THF-d_8) solutions, indicating that the presence of coordinating species leads to a complete deaggregation of complex **1a** in solution (Figure 3.4).

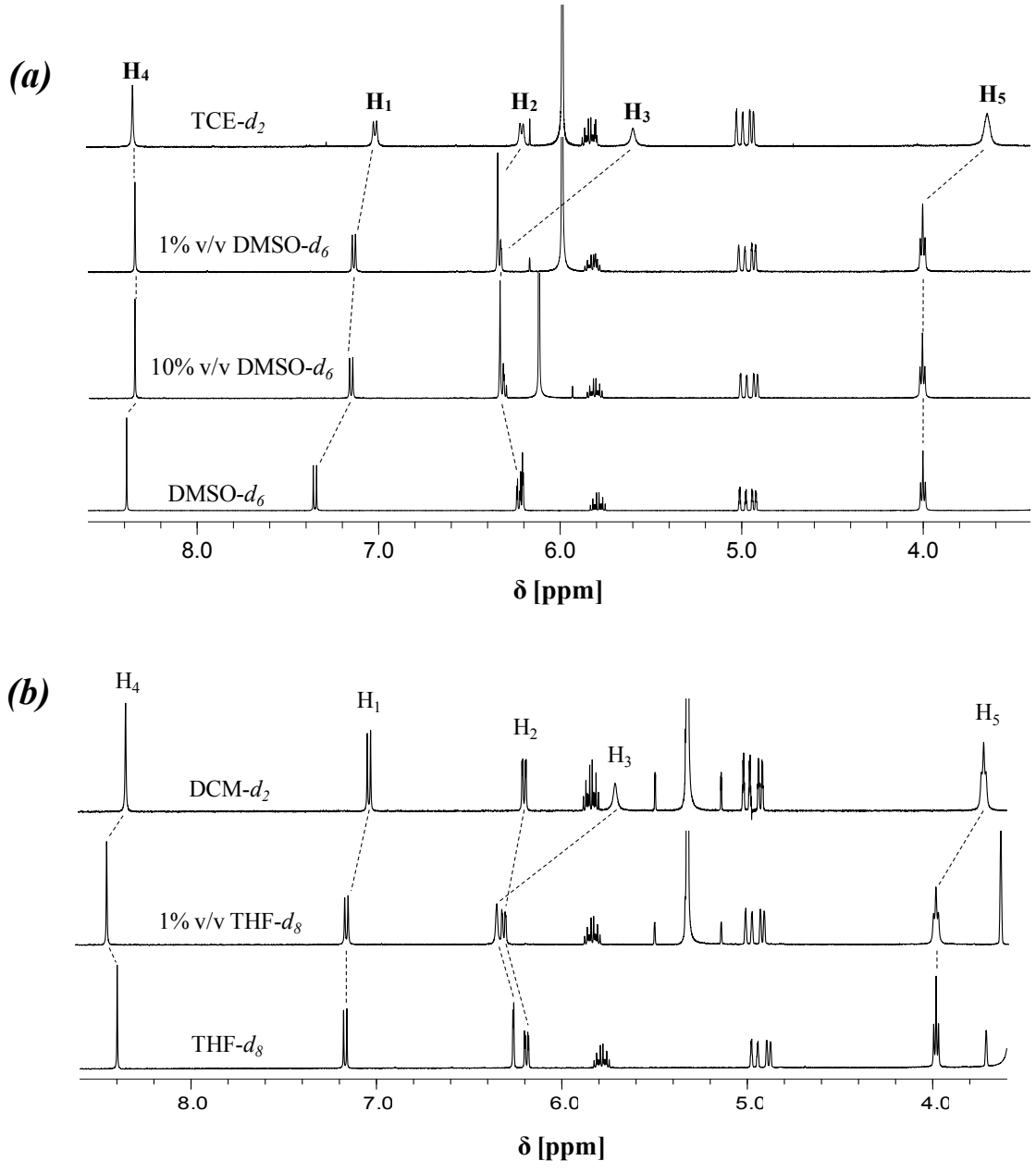

Figure 3.4 ^{1}H NMR spectra upon progressive addition of *(a)* DMSO-d_6 to a TCE-d_2 solution of **1a** (1.0×10^{-3} M) and *(b)* THF-d_8 to a DCM-d_2 solution of **1a** (5.0×10^{-4} M). The ^{1}H NMR spectra of **1a** in *(a)* DMSO-d_6 and *(b)* THF-d_8 are reported for comparison.

The deaggregation observed in solvent mixtures implies a large stoichiometric excess of the coordinating added species. Thus, it would be interesting to probe this effect with the addition of a stoichiometric amount of other coordinating species, such as pyridine (py). In fact, starting from a TCE-d_2 solution of **1a**, the progressive addition of pyridine (Figure 3.5) results in a downfield shift and in a sharpening of H_1, H_3, and the -OCH_2 signals, which become almost identical to those observed in a THF-d_8 solution, upon addition of an equimolar amount of pyridine.

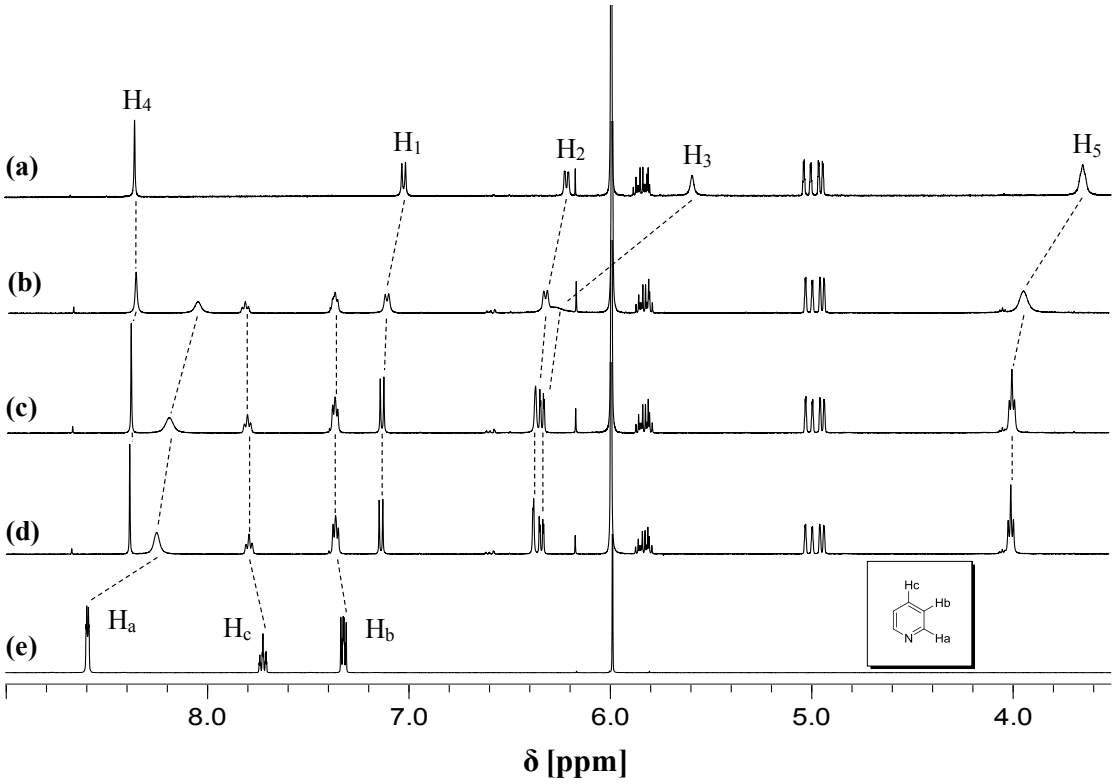

Figure 3.5 ^{1}H NMR titration spectra of *(a)* **1a** (1.0×10^{-3} M in TCE-d_2) with addition of pyridine. The concentration of pyridine added has been *(b)* 5.0×10^{-4} M, *(c)* 1.0×10^{-3} M, and *(d)* 1.5×10^{-3} M. *(e)* The ^{1}H NMR spectrum of pyridine in TCE-d_2 is reported as reference.

Noteworthy, analysis of this ^{1}H NMR spectrum (Figure 3.5) shows a substantial upfield shift and a broadening of the signal related to the ortho-hydrogen atoms of the pyridine. This clearly indicates an axial coordination of pyridine to the complex. DOSY experiments further support these data. In fact, upon addition of a stoichiometric amount of pyridine to a 1.0×10^{-3} M solution of **1a**, the increased diffusion coefficient and the estimated molecular mass are consistent with the formation of a monomeric, **1a**·py species (Table 3.1). The addition of a stoichiometric excess of pyridine does not

involve further changes in the ^{1}H NMR spectrum as far as the peaks assigned to complex **1a** are concerned (Figure 3.5).

The effect of a coordinating ditopic ligand, such as the 1,2-bis(4-pyridyl)ethane (dpe), on the deaggregation of a TCE-d_2 solution of **1a** has been also investigated (Figure 3.6). An analogous behaviour, as that above observed upon addition of pyridine, can be verified. Actually, the ^{1}H NMR spectrum obtained upon addition of a half molar amount of dpe is almost identical to that observed in a THF-d_8 solution (Figure 3.7). Moreover, the ortho-hydrogen signals of dpe exhibit a substantial upfield shift and a broadening, indicating again an axial coordination of the ditopic dpe ligand to the complex.

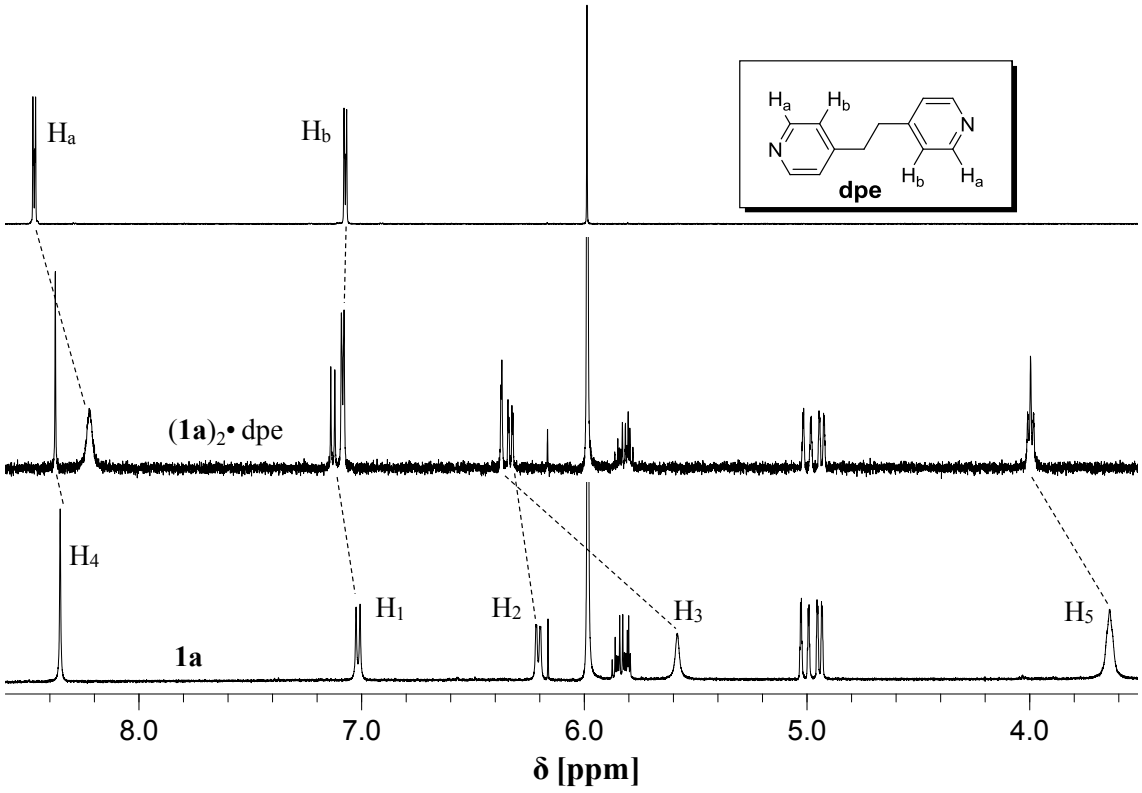

Figure 3.6 ^{1}H NMR spectra of **1a** and (**1a**)$_2$·dpe in TCE-d_2 upon addition of half molar amount of dpe to a solution 1.0×10^{-3} M of **1a**. The ^{1}H NMR spectrum of dpe in TCE-d_2 is reported as reference.

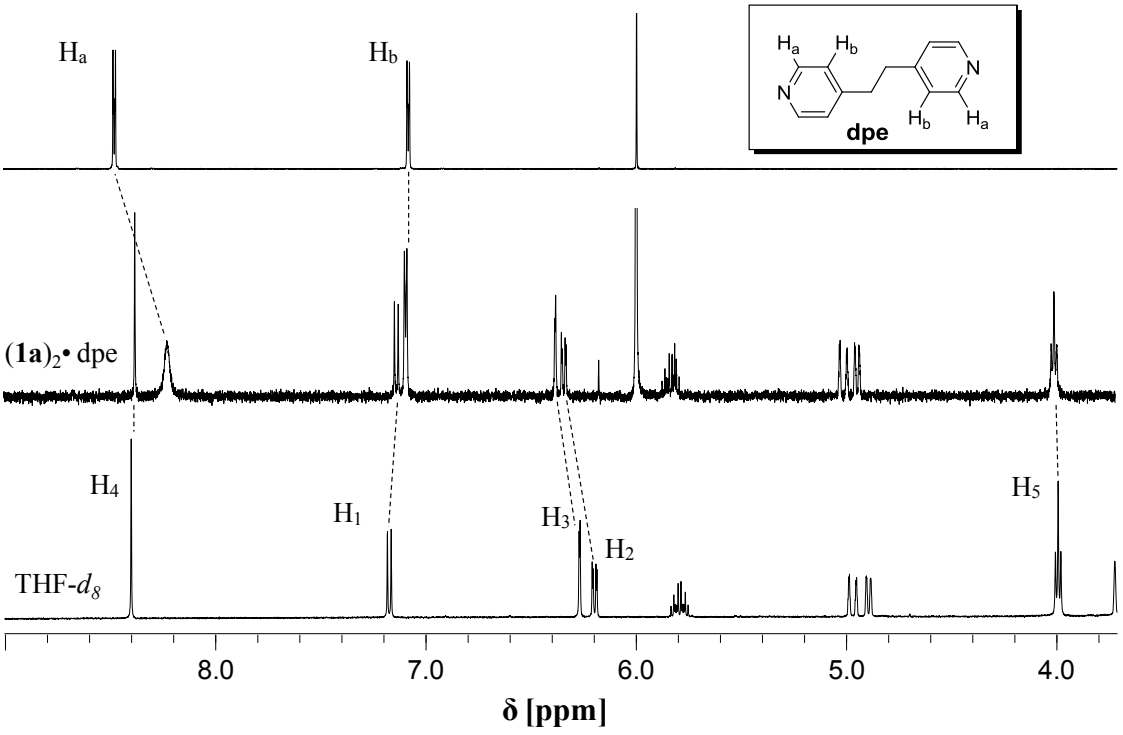

Figure 3.7 ^{1}H NMR spectra of **1a** in THF-d_8 and (**1a**)$_2$·dpe adduct in TCE-d_2. The ^{1}H NMR spectrum of dpe in TCE-d_2 is reported for comparison.

3.2.1.2 Optical absorption and fluorescence spectroscopy studies

The UV-vis and emission spectra of **1a** in a range of solvents of different polarities are shown in (Figure 3.8), while relevant absorption and emission parameters are collected in Table 3.2.

Table 3.2 Absorption and emission parameters for compound **1a** in various solvents.

solvent	absorption		emission	
	λ_{max} (nm) [a]	ε (M^{-1} cm^{-1})	λ_{max} (nm)[a,b]	Φ^c
MES	536	11200	582	0.12
	501	12600		
TOL	536	19600	590	0.16
	507	24400		
TCE	541	26800	598	0.11
	515	25900		
DCM	529	27500	597	0.08
THF	551	45000	593	0.24
ACN	542	36500	599	0.07
Py	562	45000	615	0.18
DMSO	557	35700	616	0.08

[a]Absorption and emission maxima are referred to 1.0×10^{-5} M solutions. [b]λ_{exc} = 461 nm; [c]Fluorescence quantum yields have been determined in 2.5×10^{-6} M solutions.

The absorption spectra in non-coordinating solvents (Figure 3.8a) consist of three main bands: an envelope between 300 and 400 nm, a band at ≈430 nm, and a feature between 500 and 540 nm. Moreover, on decreasing the solvent polarity, a progressive hypochromism of all bands is observed, accompanied by a marked change of the longer wavelength feature. In particular, the band centred at ≈537 nm in DCM splits in two defined peaks, whose new component appears to higher energy. These characteristics are consistent with the existence of various aggregate species. On switching to coordinating solvents, independently of their degree of polarity (Figure 3.8b), a more resolved structure between 300 and 400 nm is observed, with the appearance of two defined peaks and with the formation of a new, more intense band at ≈550 nm, which can be referred to the evolution of the longer wavelength feature observed in non-coordinating solvents. These substantial changes are all indicative of monomeric species in solution upon axial coordination of the coordinating solvent to the Zn^{II} metal center.

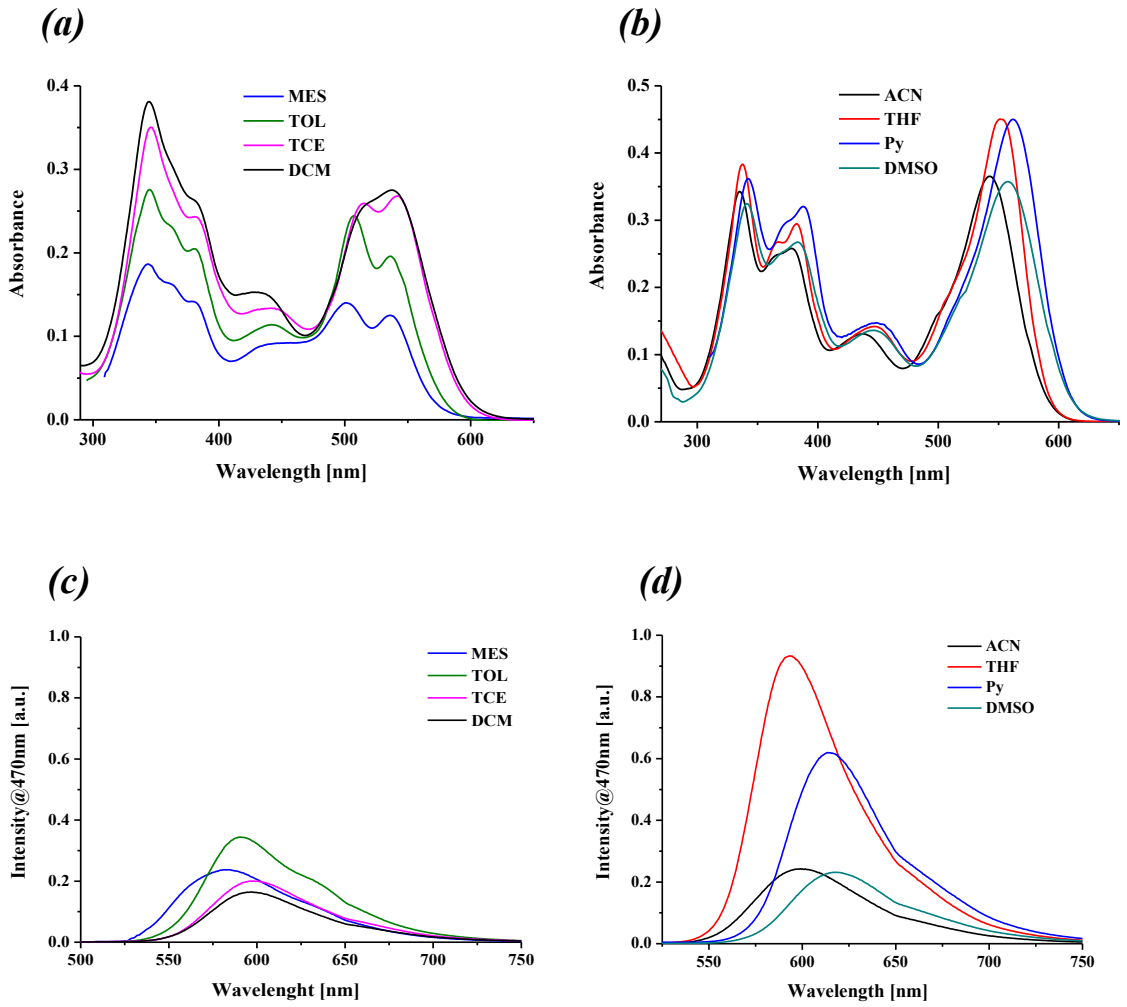

Figure 3.8 UV-vis absorption (*a* and *b*) and fluorescence (*c* and *d*) (λ_{exc} = 470 nm) spectra of **1a** (1.0×10^{-5} M) in non-coordinating and coordinating solvents of different polarities.

Steady-state fluorescence studies of **1a**, in the same range of solvents, indicate the presence of an unstructured band with a maximum between 580 and 620 nm, independent from the excitation wavelength (Table 3.2; Figure 3.8c,d). In the case of non-coordinating solvents, emission features do not reflect the changes observed in optical absorption spectra. Fluorescence quantum yields, Φ_F, determined in a regime of low concentration, indicate variable, relatively low, values (Φ_F = 0.08-0.16). Analogously, on going to coordinating solvents, the emission band maximum does not reflect the relative position of the lowest-energy band in the absorption spectra, and in the case of THF solutions, a sizable quantum yield value, Φ_F = 0.24, is achieved.

Optical absorption spectra in non-coordinating solvents are strongly concentration dependent. For example, in the case of mesitylene solutions, a progressive, dramatic

change of spectral features between 400 and 600 nm is observed in the range of concentration between 1.0×10^{-4} and 1.0×10^{-6} M (Figure 3.9a). In particular, starting from dilute solutions and proceeding to higher concentrations, a continuous evolution of the two defined peaks at 501 and 536 nm can be observed, which coalesce in a structureless, blue-shifted feature. The most marked change occurs between 1.0×10^{-5} and 2.5×10^{-5} M, accompanied by a naked-eye observation of colour change (Figure 3.9c). An analogous concentration-dependence effect is observed in toluene solutions (Figure 3.10). However, in low-polarity solvents, *e.g.*, DCM, this effect is almost negligible, with a linear relationship of absorbance *vs.* concentration plot. Some changes of optical absorption spectra can be observed just to higher concentrations $\geq 5.0 \times 10^{-4}$ M, where the maximum of the lowest-energy band shifts to 518 nm (Figure 3.11).

Related fluorescence response on varying the concentration of **1a** in mesitylene solutions, in the above investigated range of concentrations, is rather variable in terms of λ_{em} maxima and related intensities and does not reflect the changes observed in optical absorption spectra (Figura 3.9b,d).

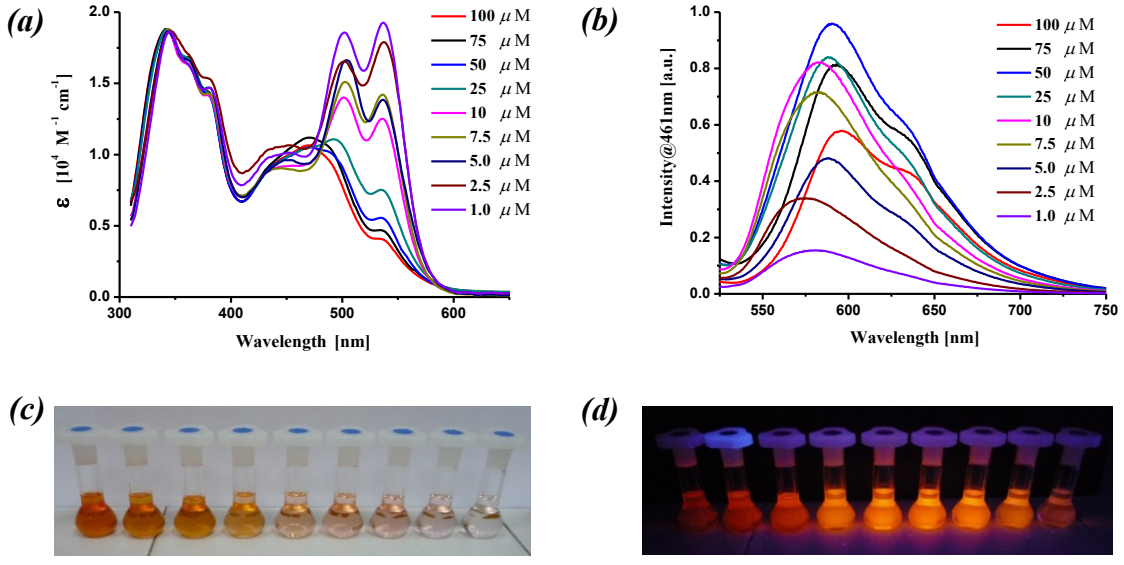

Figure 3.9 Concentration dependence (1.0-100 μM range) of *(a)* UV-vis absorption and *(b)* fluorescence spectra of **1a** in mesitylene solutions. *(c)* Visual colour changes and *(d)* fluorescence (upon irradiation with a 366 nm UV lamp) of **1a** (1.0-100 μM range, from right to left).

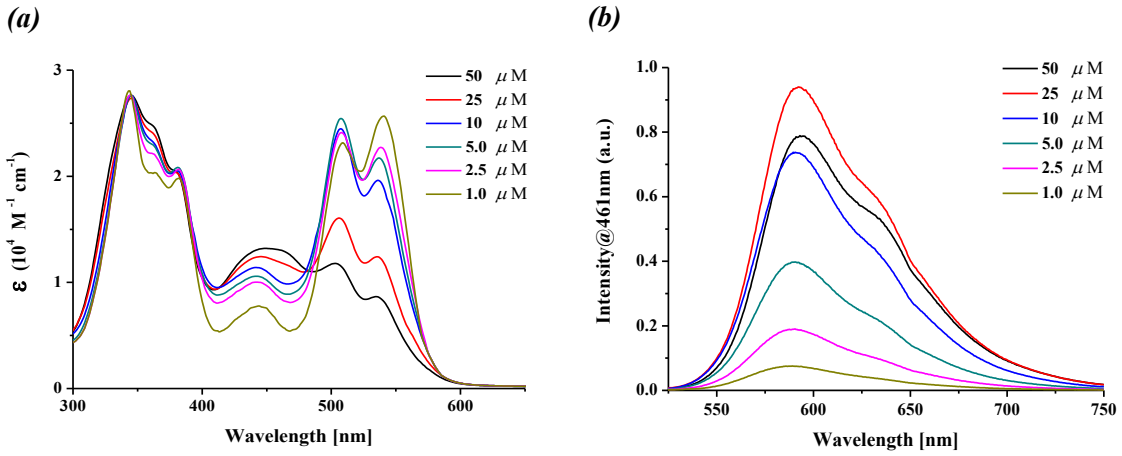

Figure 3.10 Concentration dependence (1.0-50 μM range) of *(a)* UV-vis absorption and *(b)* fluorescence (λ_{exc} = 461 nm) spectra of **1a** in toluene solutions.

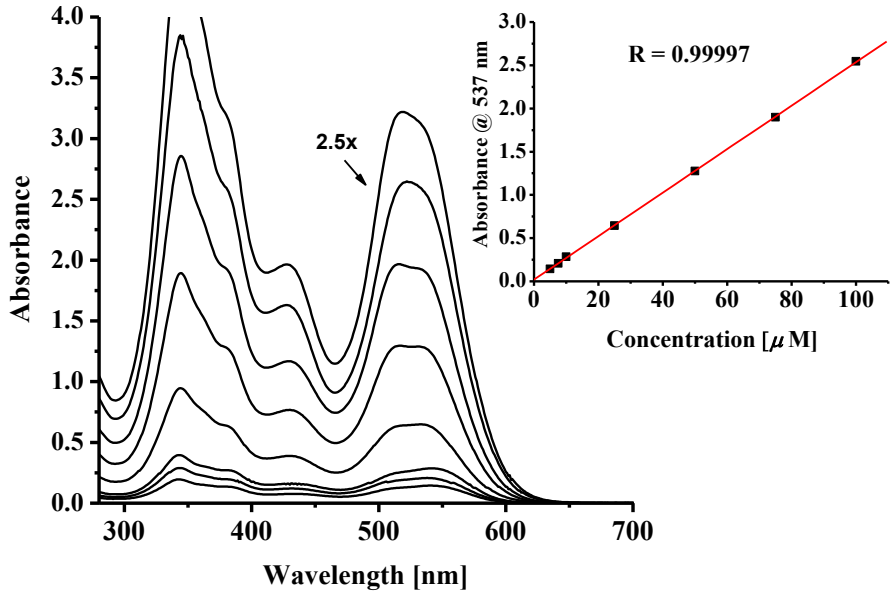

Figure 3.11 Concentration dependence (5.0-500 μM range) of UV-vis absorption spectra of **1a** in DCM solutions. The UV-vis spectrum of the 500 μM solution has been recorded with a 1-mm path length cuvette. The absorbance values have been corrected to a 1 cm path length equivalence. Inset: plot of absorbance (band at 537 nm) *vs.* concentration (5.0-100 μM range).

Fluorescence excitation spectra indicate an almost similar profile for all considered concentrations (Figure 3.12a), which can be essentially related to optical absorption spectra recorded at lower concentrations ($\leq 1.0 \times 10^{-5}$ M) (Figure 3.12b). In other words, even if absorption spectra indicate the existence of various aggregates of **1a** in

mesitylene, the emission can be mostly related to one species, while those observed in optical absorption spectra at higher concentrations seem to be less emissive. In fact, by increasing the concentration of the mesitylene solution results in a progressive attenuation of the fluorescence (Figure 3.9b,d).

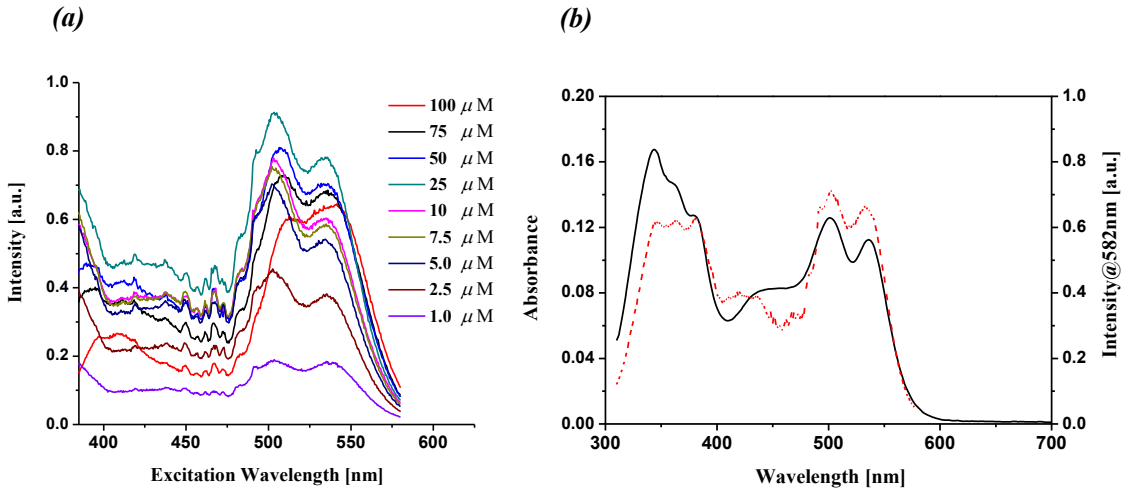

Figure 3.12 *(a)* Concentration dependence (1.0-100 μM range) of fluorescence excitation spectra of **1a** in mesitylene solutions recorded at the related λ_{em} maximum for each concentration (see, Figure 3.9b). *(b)* Optical absorption (—) and fluorescence excitation (---) spectra of **1a** (1.0×10^{-5} M) in mesitylene solution (λ_{em} = 582 nm).

Deaggregation of **1a** in solutions of non-coordinating solvents can be achieved by the addition of coordinating species. It involves dramatic changes in optical and fluorescence properties. For example, the addition of an equimolar amount of pyridine to a DCM solution of **1a** leads to an optical absorption spectrum analogous to that observed in coordinating solvents, accompanied by a large enhancement of fluorescence, about one order of magnitude larger, in terms of integrated intensity (Figure 3.13). An analogous behaviour is observed by adding DMSO, THF, or CH_3CN to a solution of **1a** in DCM, even if the phenomenon occurs for a large stoichiometric excess of the coordinating added species (Figure 3.14). In all cases, however, almost identical optical absorption spectra, fluorescence emission maxima and intensities, are achieved, presumably due to the complete deaggregation of complex **1a** in solution upon axial coordination of the involved coordinating species to the Zn^{II} ion.

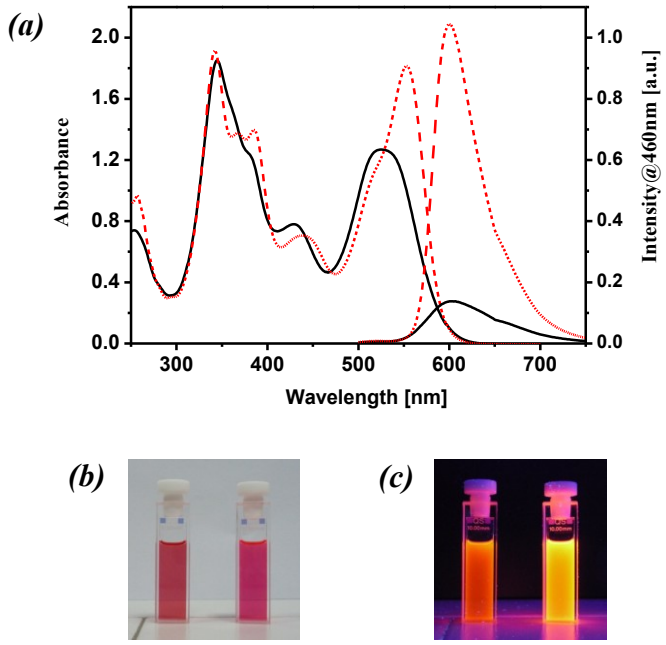

Figure 3.13 *(a)* UV-vis absorption and fluorescence (λ_{exc} = 460 nm) spectra of **1a** (5.0×10^{-5} M) in DCM solutions before (—) and after (---) the addition of an equimolar amount of pyridine. *(b)* Visual colour changes and *(c)* fluorescence (upon irradiation with a 366 nm UV lamp) before *(left)* and after *(right)* the addition of an equimolar amount of pyridine.

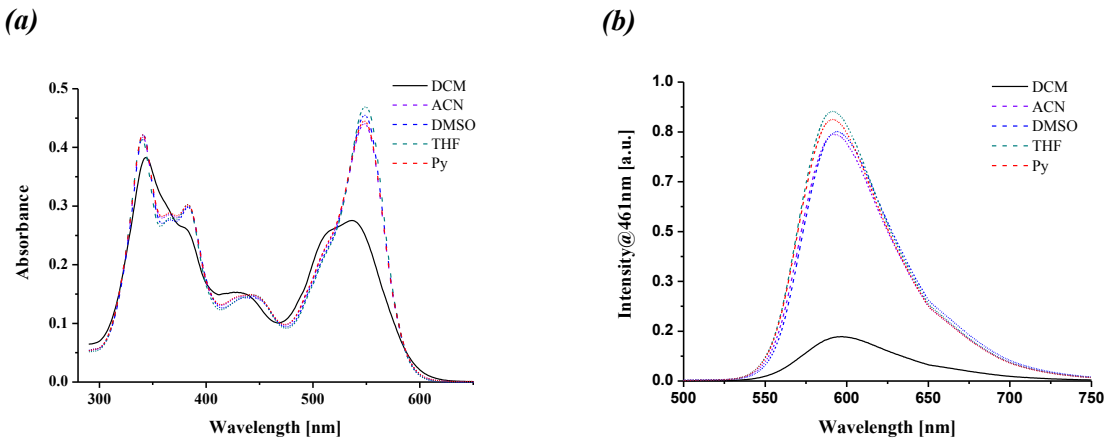

Figure 3.14 *(a)* UV-vis absorption and *(b)* fluorescence (λ_{exc} = 461 nm) spectra of **1a** (1.0×10^{-5} M; 3.0×10^{-8} mol) in DCM solutions, before (—) and after (---) the addition of various coordinating solvents: Py = 3.0×10^{-8} mol; DMSO = 3.0×10^{-6} mol; THF = 1.5×10^{-5} mol; ACN = 3.0×10^{-4} mol.

A comparable effect is observed upon addition of a large stoichiometric excess of pyridine in mesitylene solutions of **1a** (Figure 3.15), thus indicating an identical final state independent from the initial aggregate species. Moreover, the deaggregation process in mesitylene solutions (>1.0×10^{-5} M) involves an evident colour change accompanied, however, by a less enhancement of fluorescence.

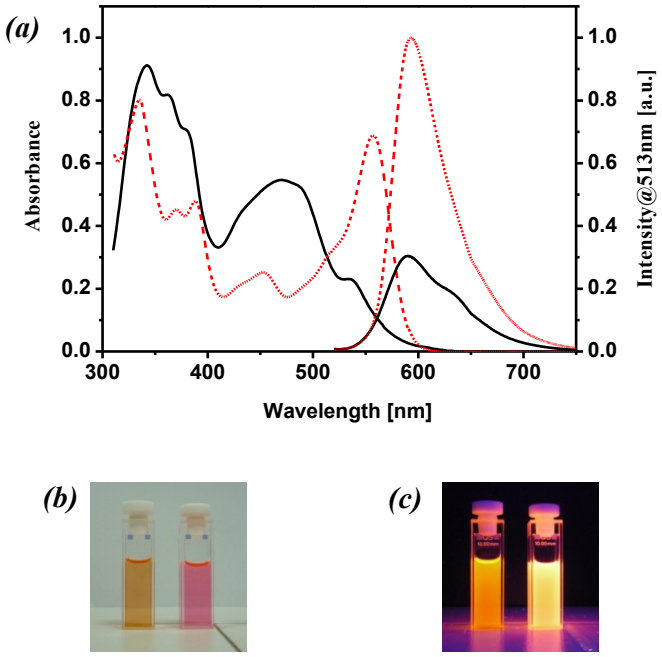

Figure 3.15 *(a)* UV-vis absorption and fluorescence (λ_{exc} = 513 nm) spectra of **1a** (5.0×10^{-5} M) in mesitylene solutions before (—) and after (---) the addition of a 10-fold mole excess of pyridine. *(b)* Visual colour changes and *(c)* fluorescence (upon irradiation with a 366 nm UV lamp) before *(left)* and after *(right)* the addition of a 10-fold mole excess of pyridine.

The effect of a coordinating ditopic ligand on the deaggregation of a DCM solution of **1a** has been also investigated. To this end, spectrophotometric and fluorimetric titrations have been performed using dpe as titrant (Figure 3.16).

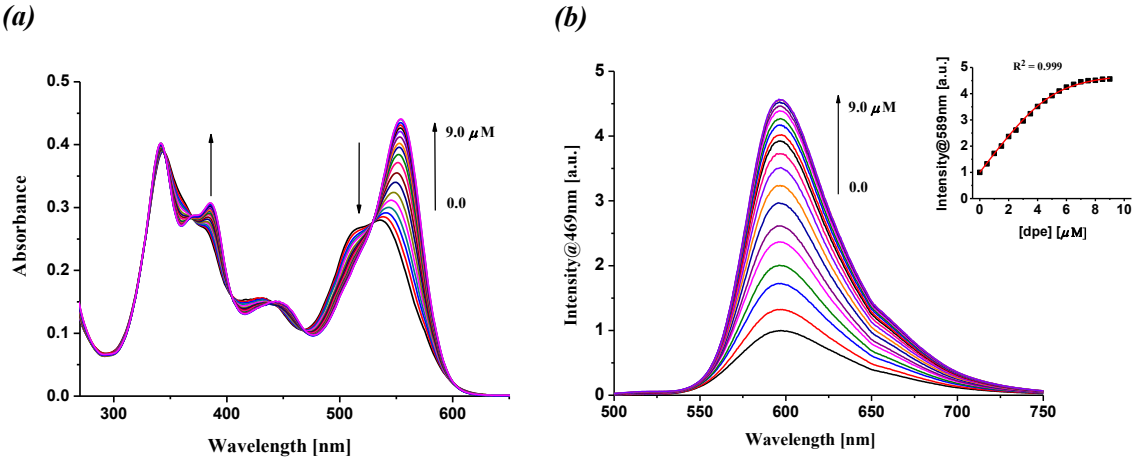

Figure 3.16 *(a)* UV-vis absorption *(b)* and fluorescence (λ_{exc} = 469 nm) titration curves of **1a** (10 μM solution in DCM) with addition of dpe. The concentration of dpe added varied from 0 to 9.0 μM. Inset: variation of fluorescence intensity at 598 nm as a function of the concentration of dpe added. The solid line represents the curve fitting analysis with eq. 2 (see paragraph **7.3**).

The changes of optical absorption spectra upon titration with dpe clearly indicate the formation of a defined single final species, as can be assessed by the presence of various isosbestic points. Moreover, a fluorescence enhancement is observed upon the addition of dpe. Interesting, both the absorption and fluorescence spectra at the end of the titration are identical to those observed upon addition of pyridine. This further confirms the same nature of the species in solution upon axial coordination.

To determine the binding stoichiometry between the complex **1a** and the dpe, the continuous variation method with fluorescence data has been used.[18] Job's plot analysis (Figure 3.17) clearly indicates the formation of a supramolecular 2:1 structure, $(\mathbf{1a})_2$·dpe, according with the ditopic nature of dpe. Estimation of the binding constants from fluorescence titration data for a 2:1 binding model (see paragraph **7.3**) indicates similar constants (log K_1 = 5.1 and log K_2 = 5.4).

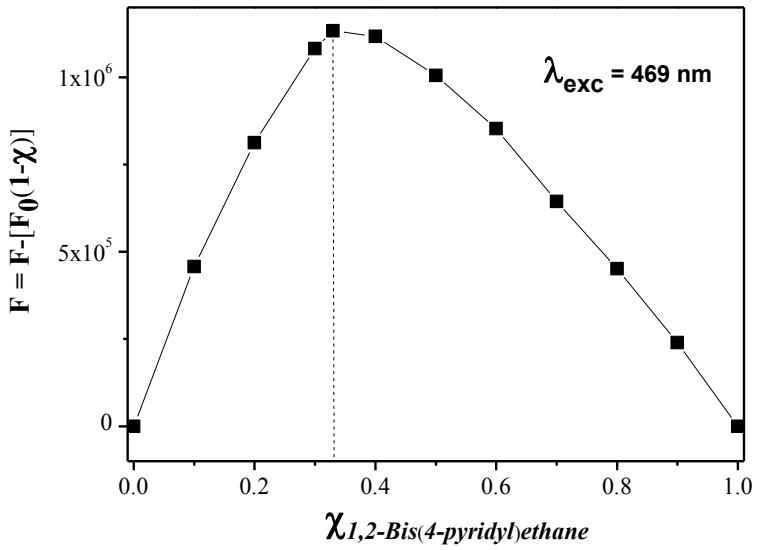

Figure 3.17 Job's plot for the binding of **1a** with dpe in DCM. The total concentration of **1a** and dpe is 10 μM.

3.2.1.3 NLO studies

The EFISH technique can provide direct information about the intrinsic molecular NLO properties through eq. 1:

$$\gamma_{\text{EFISH}} = \left(\frac{\mu\beta_{\lambda}}{5kT}\right) + \gamma(-2\omega;\omega,\omega,0) \quad (1)$$

where $\mu\beta_{\lambda}/5kT$ is the dipolar orientational contribution and $\gamma(-2\omega;\ \omega,\ \omega,\ 0)$, a third order term corresponding to the mixing of two optical fields at ω and the DC poling field at $\omega = 0$, is the electronic cubic contribution to γ_{EFISH}. This latter term is usually negligible in this kind of metal complex. β_{λ} is the projection along the dipole moment axis of the vector component of the quadratic hyperpolarizability β tensor, at a specific incident wavelength, λ.[5f,19]

Table 3.3 reports the $\mu\beta_{1.907}$ values for complex **1a** measured in a DCM solution at different concentrations, with an incident wavelength of 1.907 μm. It turns out that the $\mu\beta_{1.907}$ value of complex **1a** is strongly concentration dependent. Working at a concentration of 1.0×10^{-3} M, it is nearly 0; however, it becomes negative with an absolute value that increases rapidly upon dilution down to 3×10^{-4} M.

The deaggregation process of **1a** with py and dpe, with formation of **1a**·py and (**1a**)$_2$·dpe adducts respectively, implies a dramatic variation of $\mu\beta_{1.907}$ values, which is larger with the formation of **1a**·py adduct.

For the adducts **1a**·py and (**1a**)$_2$·dpe, it has been possible to determine the dipole moment using the Guggenheim technique[20] and, therefore, to evaluate the $\beta_{1.907}$ value, which has been found to be -518 and -105×10^{-30} esu, respectively (Table 3.4).

Table 3.3 Values of $\mu\beta_{1.907}$ for complex **1a** in DCM without and with the addition of pyridine or 1,2-bis-(4-pyridyl)ethane.

Concentration of complex **1a** ($\times 10^{-3}$ M)	$\mu\beta_{1.907}$ ($\times 10^{-48}$ esu)	$\mu\beta_{1.907}$ ($\times 10^{-48}$ esu) with py[a]	$\mu\beta_{1.907}$ ($\times 10^{-48}$ esu) with dpe[b]
1.0	≈0	-2070	-420
0.7	-526		
0.5	-1010		
0.3[c]	-1120	-1950	-347

[a]Molar ratio py:**1a** = 1.2:1. [b]Molar ratio dpe:**1a** = 0.6:1. [c]At this concentration a dimeric species is formed.

Table 3.4 Absorption maximum and NLO properties for adducts **1a**·py and (**1a**)$_2$·dpe in DCM.

	Adduct **1a**·py	Adduct (**1a**)$_2$·dpe
λ_{max} [a] (nm)	555	554
$\mu\beta_{1.907}$ [b] ($\times 10^{-48}$ esu)	-2070	-420
μ [c] ($\times 10^{-18}$ esu)	4	4
$\beta_{1.907}$ ($\times 10^{-30}$ esu)	-518	-105
β_0 ($\times 10^{-30}$ esu)	-313	-64
$\mu\beta_0$ ($\times 10^{-48}$ esu)	-1250	-254

[a]see Figure 3.14 and 3.17. [b]By working with a concentration of 10^{-3} M; the error on the EFISH measurements is ±10%. [c]Determined in $CHCl_3$; the error on the dipole moment is ± 1 × 10^{-18} esu.

Besides, as EFISH measurements are performed in a non resonant regime ($\lambda_{harm} >> \lambda_{max}$), we applied the simple two-level approximation[21,22] to extrapolate the zero-frequency static quadratic hyperpolarizability, β_0, from the experimental $\beta_{1.907}$ EFISH using the following eq.2:

$$\beta_0 = \beta_{1.907}\left(1-\left(\frac{2\lambda_{max}}{\lambda}\right)^2\right)\left(1-\left(\frac{\lambda_{max}}{\lambda}\right)^2\right) \qquad (2)$$

where λ is the fundamental wavelength of the incident photon (1907 nm) and λ_{max} is the maximum absorption value (Table 3.4). Thus, a β_0 value of -313 and -64 × 10^{-30} esu, for adducts **1a**·py and (**1a**)$_2$·dpe, respectively, may be calculated.

3.2.1 Discussion

The achievement of a simple dipolar Schiff base Zn^{II} complex having dipodal alkyl side chains in the salicylidene rings, relatively soluble even in low-polarity non-coordinating solvents, allowed us to perform a detailed study on its spectroscopic properties that, in turn, can be related to the aggregation/deaggregation process in solution. ^{1}H NMR and DOSY studies indicate the existence of dimers of **1a** in dilute solutions of non-coordinating solvents. In fact, the observed slightly broadening and upfield shift of some signals, on switching from coordinating to non-coordinating solvents, are in accord with definite aggregate species. The observed relevant upfield shift for H_1 and H_3 signals, which does not involve the H_2 and H_4 protons, indicates that these hydrogens lie under the shielding zone of the π electrons of a conjugated system. This view supports the formation of defined dimer species in dilute solutions, *e.g.*, in a staggered conformation,[14] in which both Zn atoms mutually interact through the Zn···O axial coordination, thus fulfilling the coordination sphere of the Zn^{II} ion (Chart 3.2).

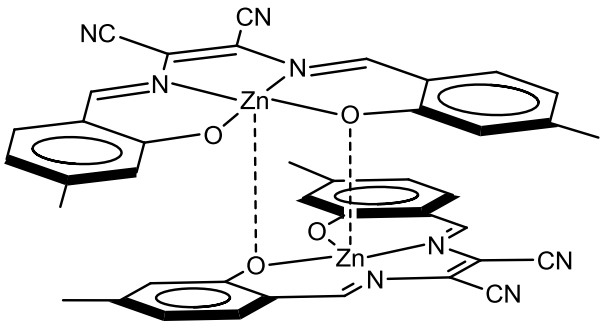

Chart 3.2 Proposed structure for dimeric aggregate of **1a**.

Actually, selected 1D ROESY experiments of **1a** in TCE-d_2 solutions (1.0×10^{-3} M) indicate absence of intermolecular Overhauser effects (*e.g.*, H_3-H_4 through-space interactions), while only intramolecular Overhauser enhancements (*e.g.*, H_1-H_4) are observed (Figure 3.18). This implies the existence of aggregate structures in staggered conformations with the H_3 hydrogens lying over the CN groups of the adjacent units. This view is in agreement with the X-ray derived structures of some dimeric related Zn-salen complexes.[7d,h]

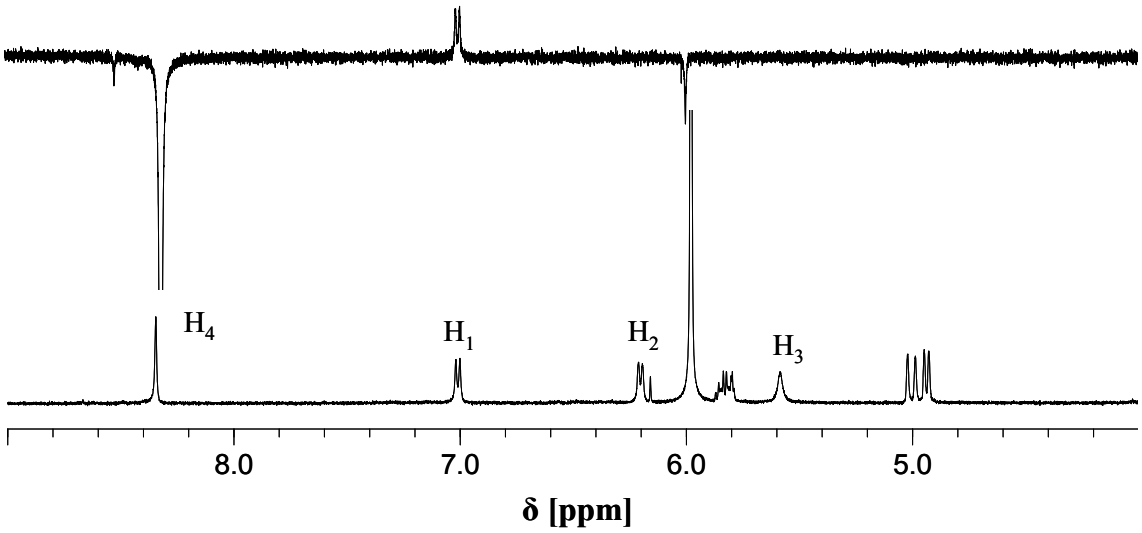

Figure 3.18 ^{1}H NMR (lower trace) and 1D T-ROESY (upper trace, upon irradiation on H_4) spectra of **1a** in TCE-d_2 solutions (1.0×10^{-3} M).

On going to higher concentrations, the observed decrease of diffusion coefficients, hence larger molecular masses, and the progressive and generalized peak broadening, involving all aromatic and imine ^{1}H NMR signals indicate the existence of larger aggregates. In fact, the formation of oligomeric aggregates causes a broadening[8b,23] due to a significant decrease in the T_2 relaxation time.[24] The different concentration threshold (>4×10^{-4} M for DCM and >1×10^{-3} M for TCE solutions) to observe formation of larger aggregates is dependent by the solvent polarity. This is consistent with the formation of larger oligomeric aggregates, involving an intermolecular Zn···O···Zn bridging coordination (Chart 3.3), presumably having an overall lower dipole moment than the dimers involved at lower concentrations, thus minimizing electrostatic interactions in concentrate solutions of low-polarity solvents. The involvement of the nitrile groups in the formation of larger aggregates is ruled out because the CN-stretching frequency of **1a** in DCM is unaffected by concentration. FT-IR spectra of **1a** in DCM solutions recorded at different concentrations (4.0×10^{-4}; 1.0×10^{-3} M) indicate an identical frequency (2220 cm^{-1}) as far as the CN-stretching mode is concerned.[25] The band remains almost unchanged (2218 cm^{-1}), even with the addition of a stoichiometric excess of pyridine. This indicates that the CN groups are not involved in the aggregation/deaggregation processes of **1a** in non-coordinating solvents.

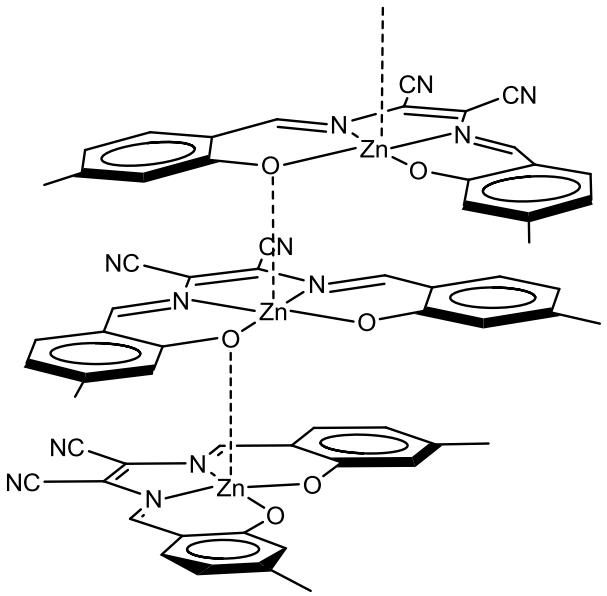

Chart 3.3 Proposed structure for oligomeric aggregate of **1a**.

Optical absorption spectra also indicate the existence of aggregate species in non-coordinating solvents, as they are characterized by structureless features, with larger bandwidths and blue-shifted, compared to monomer ones in coordinating solvents. Moreover, they exhibit a marked concentration-dependence behaviour that can be related to the solvent polarity. DCM solutions are characterized by the presence of a single species in a wide (1.0×10^{-6} - 1.0×10^{-4} M) range of concentration, according with the observed linear relationship of absorbance *vs.* concentration (Figure 3.11) and the ^{1}H NMR spectra recorded at low concentration ($\leq 4.0 \times 10^{-4}$ M) (Figure 3.3b). The existence of defined species in dilute DCM solutions is corroborated by spectrophotometric titrations with dpe, which indicate the presence of multiple isosbestic points (Figure 3.16a). Conversely, in the same range of concentration of mesitylene or toluene solutions, both being almost non polar solvents, is observed a substantial change of optical absorption and fluorescence properties, consistent with the presence of different types of aggregates by varying the concentration. The absence of any isosbestic point in the concentration-dependent optical absorption spectra (Figure 3.9a and 3.10a) supports this hypothesis. In particular for dilute solutions ($\leq 1.0 \times 10^{-5}$ M), optical absorption spectra and, hence, the nature of the aggregate species can be related to those observed in DCM or TCE solutions; the optical behaviour at higher concentrations indicates the existence of different kinds of aggregates. Unfortunately,

the relatively low solubility of **1a** ($\leq 1.0 \times 10^{-4}$ M) in mesitylene or toluene solutions, together with a concomitant slightly demetalation[26] under these conditions, precluded reliable ^{1}H NMR measurements in these deuterated solvents. To improve the solubility in non polar solvents, the synthesis of the related 4-(hexadecyloxy) derivative, **1b**, has been accomplished. Complex **1b**, possessing an almost identical, as to **1a**, optical behaviour on switching from non-coordinating to coordinating solvents (Figure 3.19), is still insufficiently soluble in non polar solvents to achieve accurate ^{1}H NMR data.

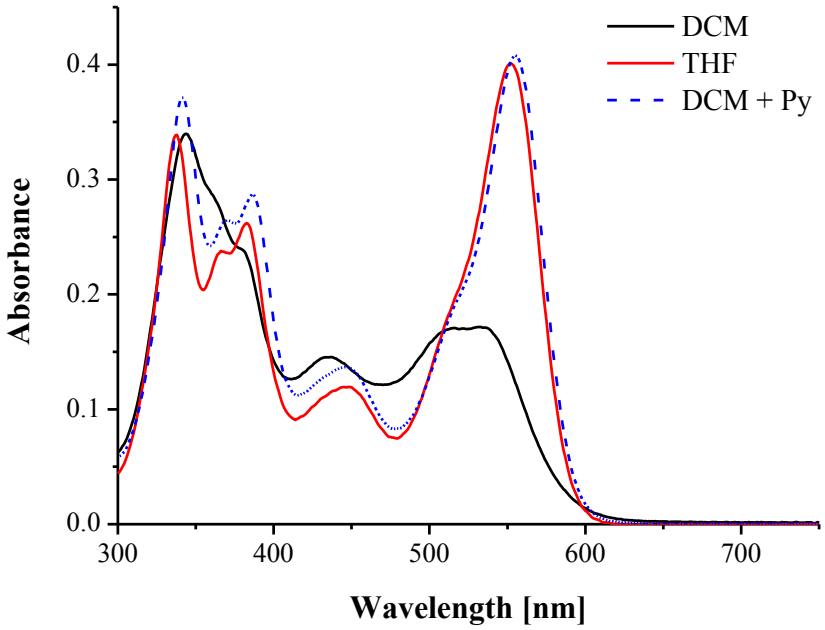

Figure 3.19 *(a)* UV-vis absorption and fluorescence (λ_{exc} = 460 nm) spectra of **1b** (1.0×10^{-5} M) in DCM (—) and THF(—)and after (---) the addition of an equimolar amount of pyridine.

On switching to coordinating solvents, ^{1}HNMR, DOSY, and optical spectroscopy data clearly indicate the presence of monomeric species of **1a** in solution, because of the axial coordination of the solvent to the Zn^{II} ion. Deaggregation of **1a** in solutions of non-coordinating solvents, by addition of coordinating species, involves dramatic changes in optical and fluorescence properties. Thus, in the case of DCM solutions, the addition of an equimolar amount of pyridine leads to an optical spectrum analogous to that obtained in coordinating solvents and, more importantly, a remarkable enhancement of fluorescence (Figure 3.13).

Deaggregation can be achieved with the addition of any coordinating species, even if it requires a variable stoichiometric amount of the latter (Figure 3.14). In any case, however, the system presumably reaches the same final electronic state, as almost identical optical absorption spectra, fluorescence emission maxima, and intensities are obtained. This is again owing to the complete deaggregation of complex **1a** in solution upon axial coordination to the Zn^{II} ion by the involved coordinating species. An analogous behaviour is observed for mesitylene solutions of **1a**, although in this case, the deaggregation process requires a large stoichiometric excess of pyridine (Figure 3.15). Actually, the deaggregation of **1a** upon axial coordination to the Zn^{II} ion necessarily involves formation of a polar species; hence, the deaggregation process becomes unfavourable in non polar solvents.

The use of a ditopic ligand as coordinating species offers the possibility to build new supramolecular architectures. Thus, the formation of a defined 2:1 supramolecular structure, $(\mathbf{1a})_2$·dpe, is demonstrated by ^{1}H NMR analysis and the existence of multiple isosbestic points in optical absorption spectra upon spectrophotometric titrations (Figure 3.16) and is further confirmed by Job's plot analysis (Figure 3.17). As expected from the two independent binding sites of dpe to complex **1a**, similar binding constants (log K_1 = 5.1 and log K_2 = 5.4) have been estimated according to the intermediate value found for the **1a**·py binding constant (log K = 5.3).[4d]

The NLO properties are dependent by aggregation/deaggregation properties of **1a**. In particular, the very low NLO response with the most concentrated solution can be reasonably explained by the presence of oligomeric aggregates,[4d] which have an expected almost centric arrangement. Upon dilution to 3-5 $\times$ 10^{-4} M, there is the formation of defined dimers,[4d] characterized by a negative but quite high $\mu\beta_{1.907}$ value. Remarkably, the addition of a stoichiometric amount of pyridine to the concentrated solution of **1a** (1.0×10^{-3} M) switches on the NLO response and $\mu\beta_{1.907}$ becomes -2070 $\times$ 10^{-48} esu (Table 3.3 and Figure 3.20) due to the deaggregation of the Zn^{II} complex and the formation of a 1:1 pyridine adduct, **1a**·py.[4d] As expected, the addition of pyridine to the dimeric Zn^{II} species (3×10^{-4} M) also affords adduct **1a**·py with a similar $\mu\beta_{1.907}$ value (Table 3.3). Unfortunately, various attempts to restore aggregate complex **1a**, by addition of a stoichiometric amount of various acids in DCM (trifluoroacetic acid, p-toluenesulphonic acid and HCl) to adduct **1a**·py, failed due to demetallation, followed

by partial hydrolysis of the Schiff base. Actually, the subsequent addition of pyridine, even in a stoichiometric excess, led only to a partial restoration of the pyridine adduct, **1a**·py.

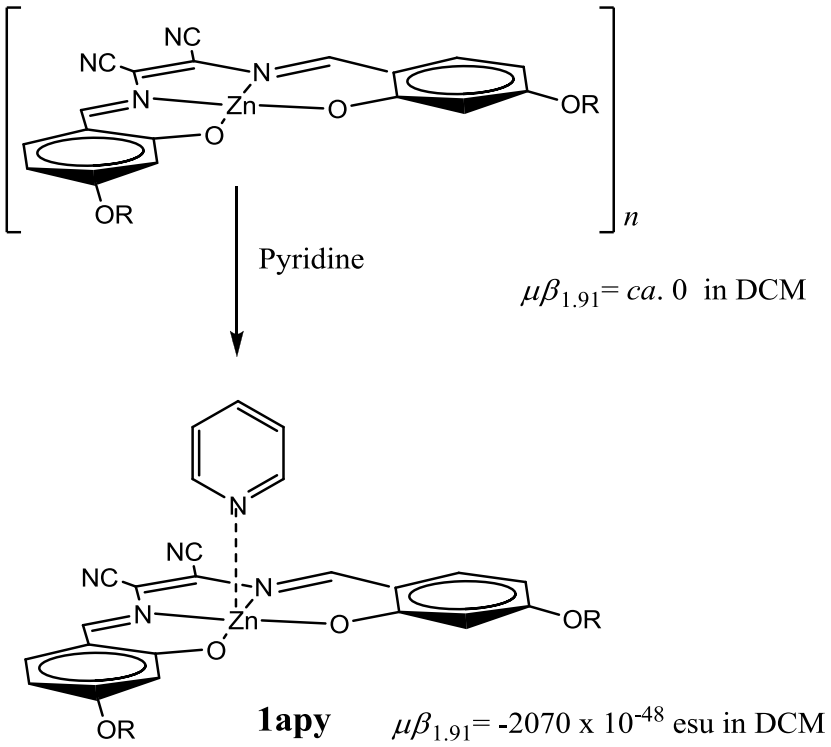

Figure 3.20 Switching on the second-order NLO response for the complex **1a** by addition of pyridine.

It has been established that the addition of a ditopic ligand as a coordinating species, such as 1,2-bis-(4-pyridyl)ethane (dpe), leads to the formation of the supramolecular 2:1 adduct, (**1a**)$_2$·dpe (Chart 3.4).[4d] We found that this designed adduct is also characterized by a good absolute $\mu\beta_{1.907}$ value, although it is found to be lower than that of adduct **1a**·py (Table 3.3). This is likely to be due to the presence of some centric conformers (Chart 3.4).

It is worth pointing out that the negative sign of the $\mu\beta_{1.907}$ value observed for adducts **1a**·py and (**1a**)$_2$·dpe and for the dimer of complex **1a** suggests that the dipole moment is lower in the excited state than in the ground state,[27] and this is common for M^{II} Schiff base complexes.[28] Actually, a negative quadratic hyperpolarizability has recently been reported for a Zn^{II} complex with an unsymmetrical Schiff base of S-methylisothiosemicarbazide.[28b] As the static hyperpolarizability is not frequency dependent, it represents the most important figure of merit when comparing the

molecular second-order NLO response of different chromophores. Remarkably, the absolute value of $\mu\beta_0$ (-1250 × 10^{-48} esu) for adduct **1a**·py is among the highest reported for metal complexes.[19] For comparison, the azo dye Disperse Red 1 (4-[N-ethyl-N-(2-hydroxyethyl) amino-4′-nitroazobenzene), which is currently used as a dopant molecule in polymeric matrices for electro-optic applications, has a $\mu\beta_0$ = 500 × 10-48 esu.[29]

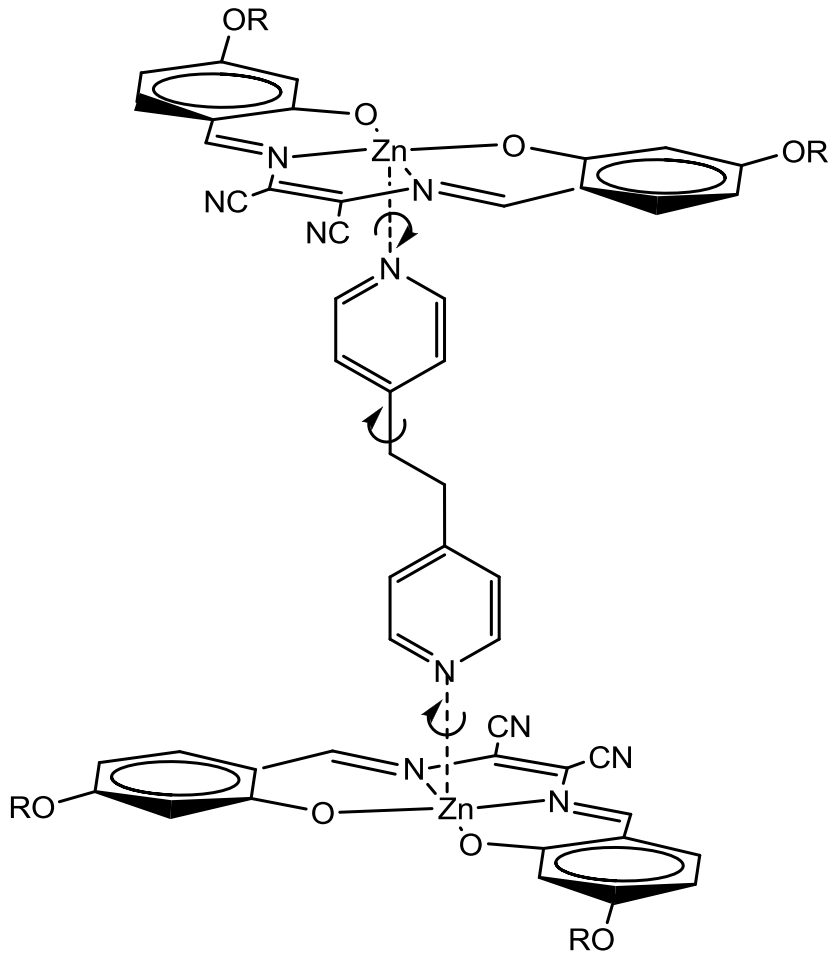

$(1a)_2$dpe

Chart 3.4 Proposed structure for the supramolecular adduct (**1a**)$_2$·dpe.

3.3 Zn^{II} (salophen) complexes

In this section, the complexes investigated are **2g**-**4g**, **2b**, **2h**, **4b**, and **4h** (Chart 3.5). To further extend the study on aggregation/deaggregation properties of Zn^{II} complexes having conjugated bridging diamine, various comparisons with complex **1a** (see section **3.2**) have been discussed.

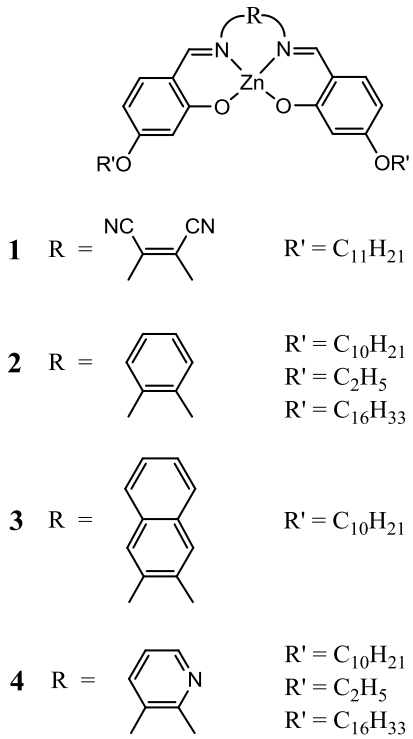

Chart 3.5 Structures of investigated complexes.

3.3.1 Results

Complexes **2**-**4** are moderately soluble in low-polarity solvents, such as chloroform, and in various coordinating solvents, such as DMSO and THF, and less soluble in non polar solvents, *e.g.*, MES and CCl_4.

The complexes have been characterized by ESI-mass spectrometry and ^1H NMR spectroscopy (vide infra). Mass spectrometry analysis always indicates the presence of defined signals corresponding to the protonated dimer.

3.3.1.1 ^{1}H NMR studies

^{1}H NMR spectra of the present Zn^{II} Schiff base complexes (**2g-4g**) in a solution of coordinating solvents (DMSO-d_6, ≈5 × 10^{-4} M), indicate the presence of sharp signals with the expected multiplicity, in accord with their molecular structures and consistent with the existence of monomeric species (Figure 3.21). As expected, these ^{1}H NMR spectra are concentration-independent, as has been previously found for **1a** (see paragraphs **3.2.1.1** and **3.2.2**).[4d]

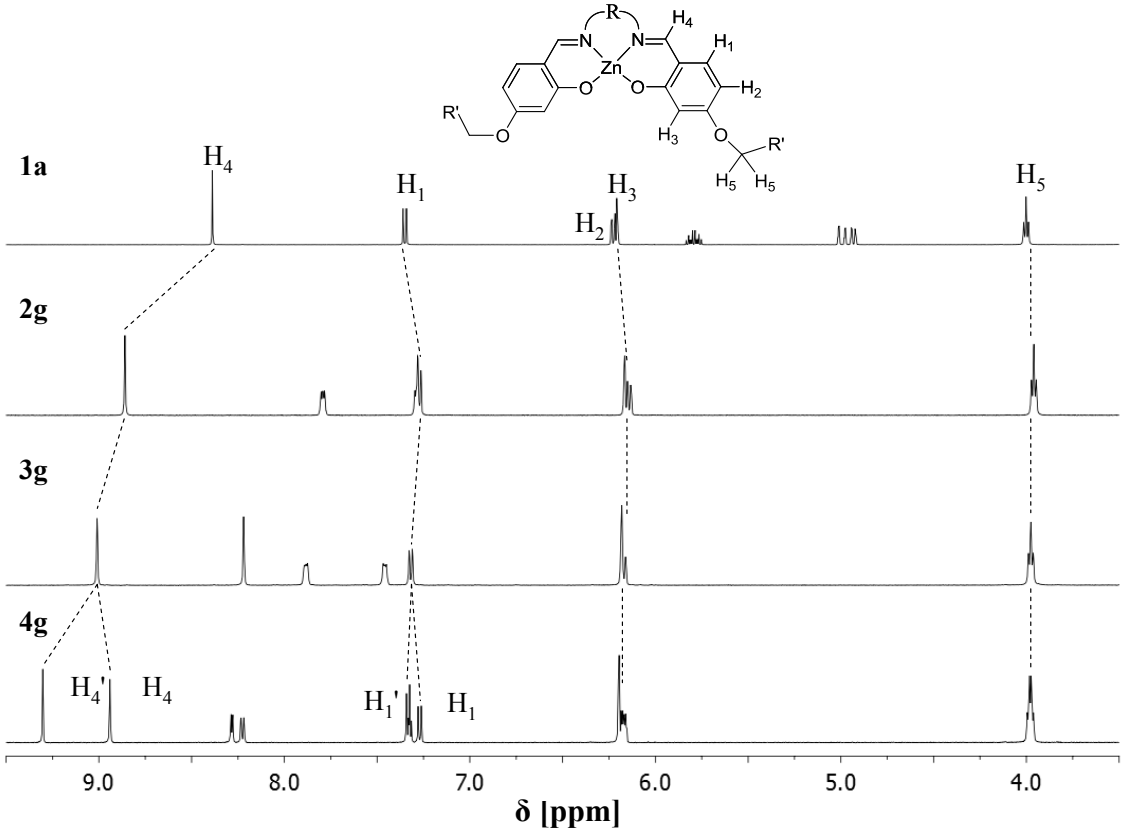

Figure 3.21 ^{1}H NMR spectra of **2g-4g** in DMSO-d_6 recorded at the concentration ≈5 × 10^{-4} M. The ^{1}H NMR spectrum of **1a** is reported for comparison.

Analyzing the ^{1}H NMR spectra of **1a** and **2g-4g** complexes, it is noted that there is a very similar chemical shift for the salicylidene aromatic and -OCH_2 hydrogens, while the CH=N signal is strongly dependent on the nature of the bridging diamine. In fact, the chemical shift of the azomethine protons of **1a** is to higher field compared to that of compounds **2g-4g**, where the conjugation of the π electrons between the two salicylidene moieties and the diamino bridge is much more extensive. This is because of the proximity of the azomethine protons to the salicylidene and the bridging diamine

aromatic rings. In fact, the shielding by the ring current of the two adjacent aromatic nucleus on the CH=N chemical shift is a function of the molecular conformation.[30] Thus, the dramatic downfield shift observed in the series **2g**-**4g** (Figure 3.21) indicates that the azomethine protons lie on the side of the salicylidene and the bridged diamine aromatic rings.

The ^{1}H NMR spectra of **4b**, **4g** and **4h** complexes are interesting enough (Figure 3.22 top).

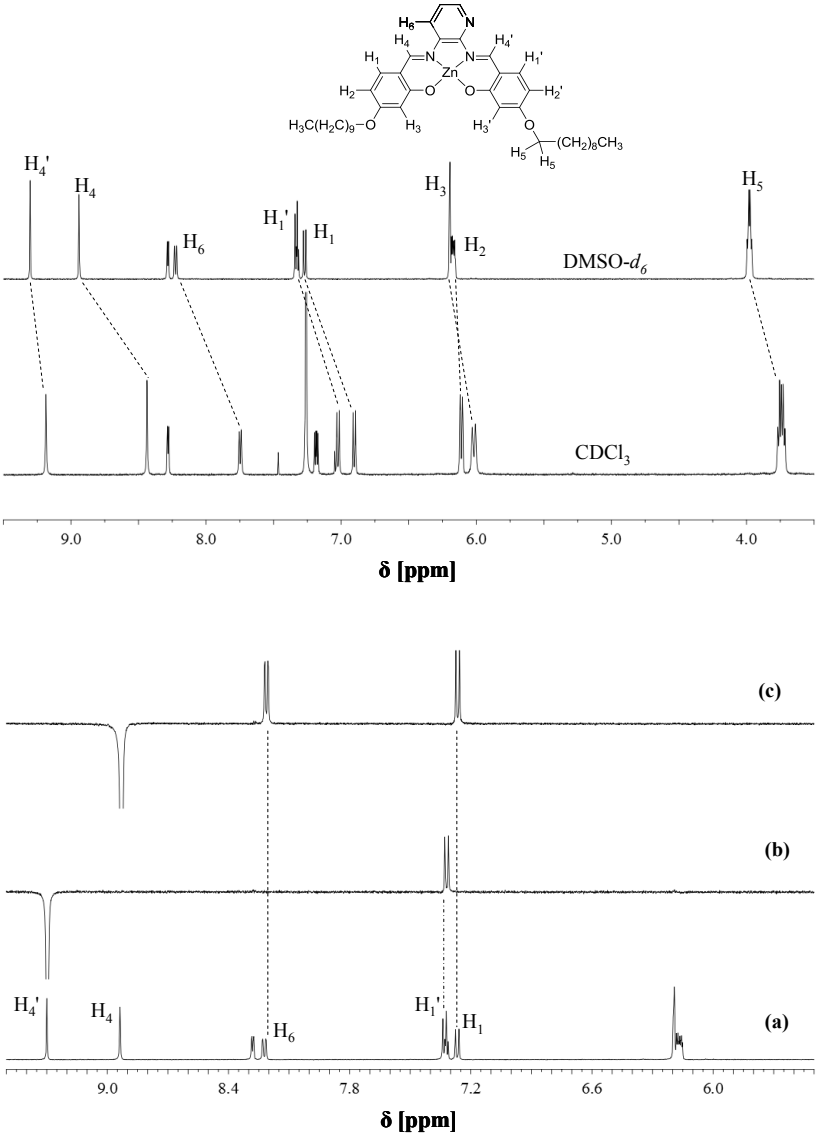

Figure 3.22 *(Top)* Comparison of ^{1}H NMR spectra of **4g** in DMSO-d_6 and $CDCl_3$ solutions (≈5 × 10^{-4} M). *(Bottom) (a)* ^{1}H NMR and *(b)* 1D T-ROESY spectra of **4g** in $CDCl_3$ solution (1.0 × 10^{-3} M) upon selective irradiation of H_4' and *(c)* H_4, respectively.

In fact, unlike complexes **1-3**, they are lacking the local C_2 axis passing through the diamine-bridged unit and the Zn^{II} ion. Then, the aromatic protons of the salicylidene units, as well as the azomethine protons are no longer homotopic, giving rise to two different sets of signals in the ^1H NMR spectra. Therefore, the chemical shifts of the 1D spectra of compound **4g** have been assigned to specific atomic positions by means of COSY and selected 1D T-ROESY measurements, which reveals that the H_4 proton is spatially close to the H_1 and H_6 hydrogens, while the H_4' proton (9.23 ppm) is spatially close to H_1' (d, 7.30 ppm) (Figure 3.22 bottom).

On switching to non-coordinating solvents ($CDCl_3$ ≈5 × 10^{-4} M), a substantial change of ^1H NMR spectra is noted (Table 3.5; Figure 3.22 and 3.23).

Table 3.5 ^1H NMR $\Delta\delta^a$ chemical shifts (ppm) of selected protons for complexes **1-4**.

Complex	H_1	H_1'	H_2	H_3	H_4	H_4'	H_5	H_6
1a	0.38	-	<0.1	0.63	0.05	-	0.35	-
2g	*b*	-	*b*	*b*	0.39	-	*b*	*b*
3g	0.41	-	<0.1	<0.1	0.55	-	0.25	0.55
4g	0.38	0.31	<0.1	0.26 [c]	0.51	0.12	0.25	0.48
4h	0.34	0.29	<0.1	0.19 [c]	0.48	0.10	0.23	0.45
4b	0.33	0.26	<0.1	0.29 [c]	0.43	0.04	0.28	0.42

[a]Difference of chemical shifts between DMSO-d_6 and $CDCl_3$ solutions. [b]The peak broadening do not allowed a quantitative evaluation of Δδ values. [c]H_3 and H_3' signals are isochrones in DMSO-d_6 solution.

In particular, while for **3g** and **4g** a strong upfield shift is found, with respect to the coordinating solvent, of the H_1 (0.38, 0.41 ppm), H_4 (up to 0.55 ppm), H_5 (0.25 ppm) and the H_6 (up to 0.55 ppm) signals, for complex **2g** a substantial broadening of all ^1H NMR signals is also observed, in addition to the upfield shift of the H_4 (0.39 ppm) peak (Figure 3.23a). Moreover, these ^1H NMR characteristics are almost concentration-independent, as ^1H NMR signals remains roughly unaltered in the explorable range of concentrations (Figure 3.24).

These relevant upfield shifts upon switching from coordinating to non-coordinating solvents, indicating that the involved hydrogens lie under the shielding zone of the π electrons of a conjugated system,[15] and the observed peak broadening for compound **2g** are both consistent with the existence of aggregate species[4d,8b] of **2g-4g** in solutions of non-coordinating solvents (see paragraphs **3.2.1.1** and **3.2.2**).

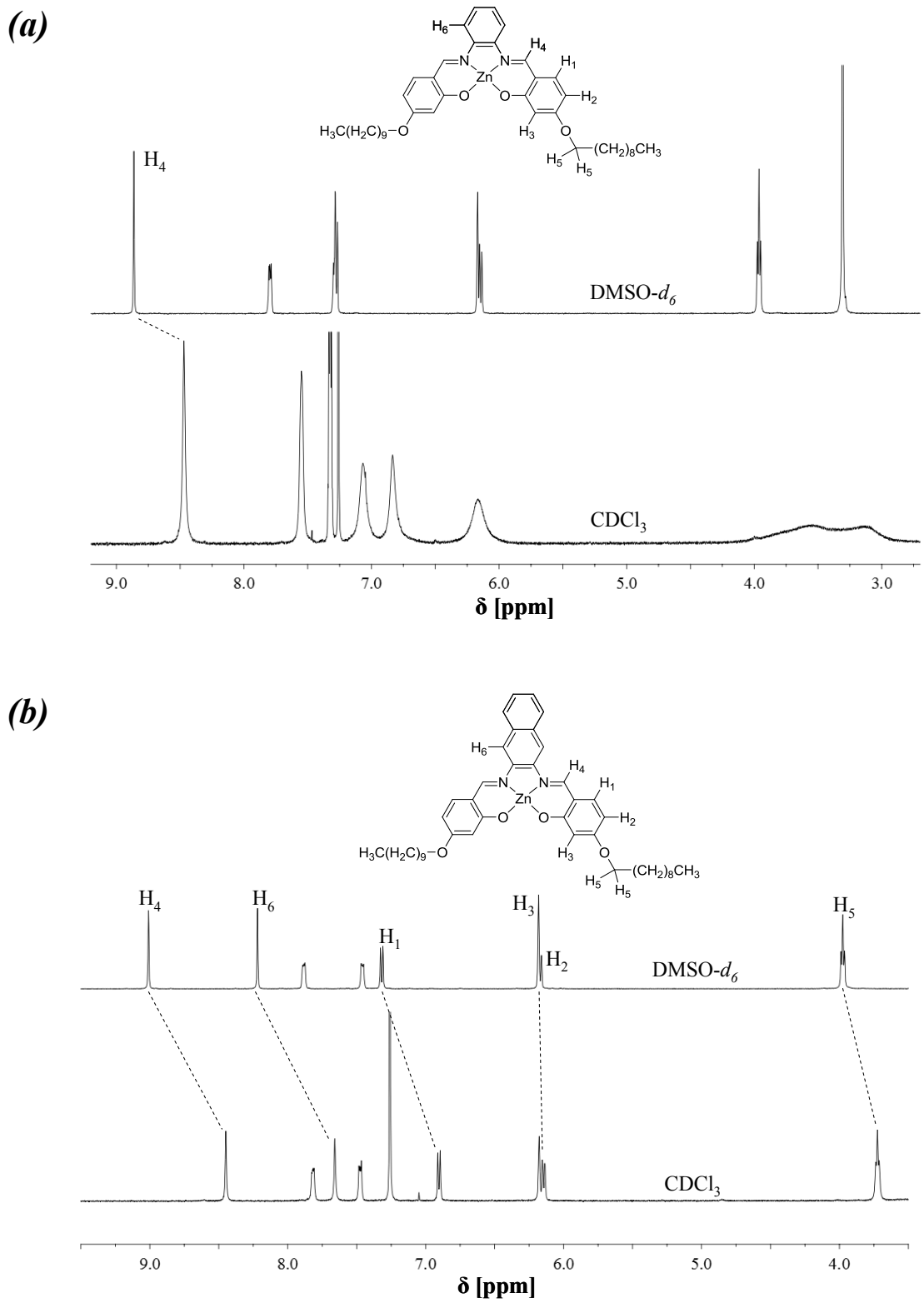

Figure 3.23 Comparison of ^{1}H NMR spectra of *(a)* **2g** and *(b)* **3g** in DMSO-d_6 and $CDCl_3$ solutions (≈5 × 10^{-4} M).

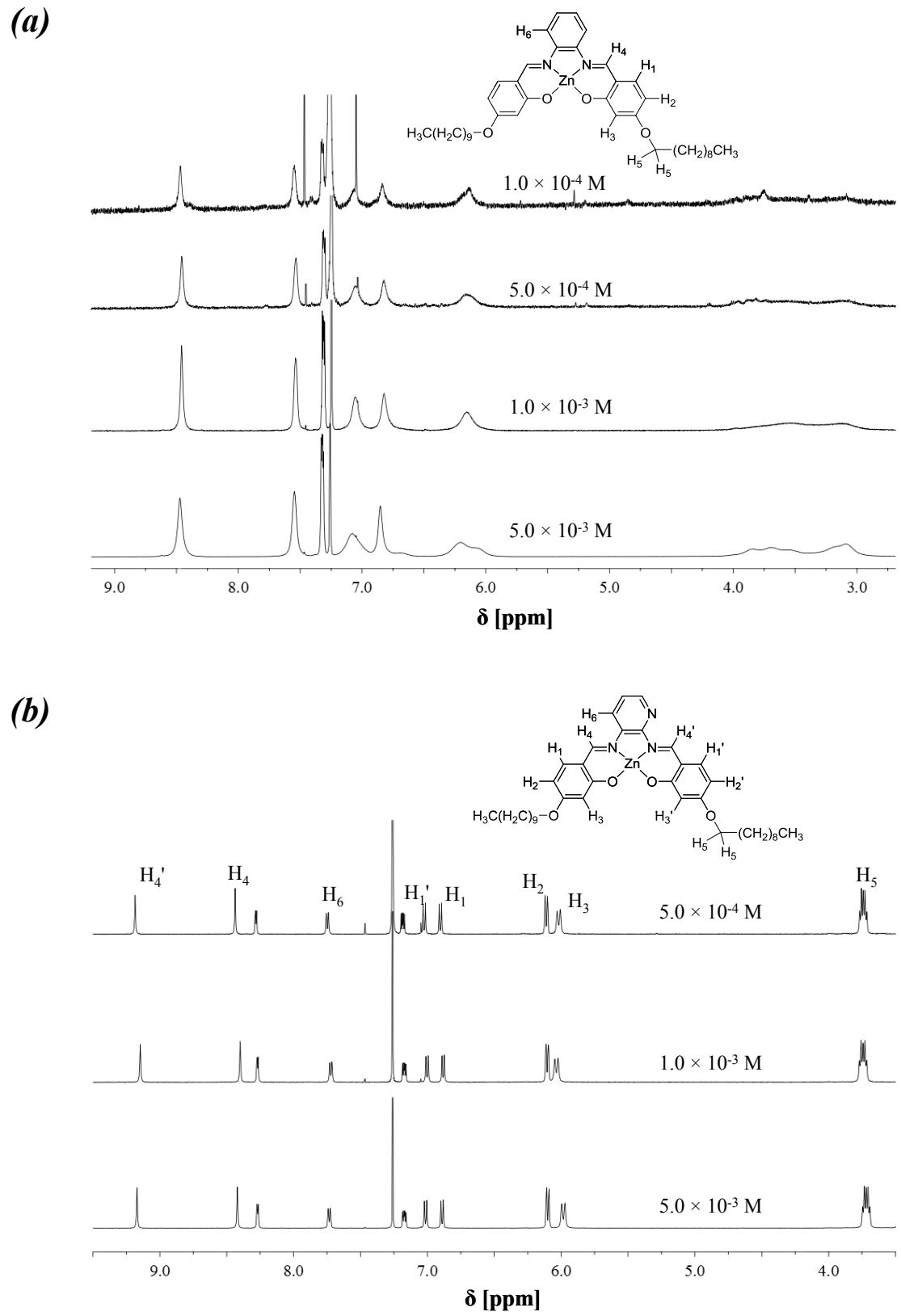

Figure 3.24 Concentration dependence of ^{1}H NMR spectra of *(a)* **2g** and *(b)* **4g** in DMSO-d_6 and $CDCl_3$ solutions.

The effect of the alkyl chains length has been analysed for the alkyl derivatives of **4**. The alkyl chains length for compounds **4b**, **4g** and **4h** (Figure 3.25a) is expected to play a very minor role, as the chemical shifts of the aromatic, CH=N and the -OCH_2 hydrogens remain almost unaltered. As expected, an analogous behaviour is also observed in coordinating solvents (Figure 3.25b).

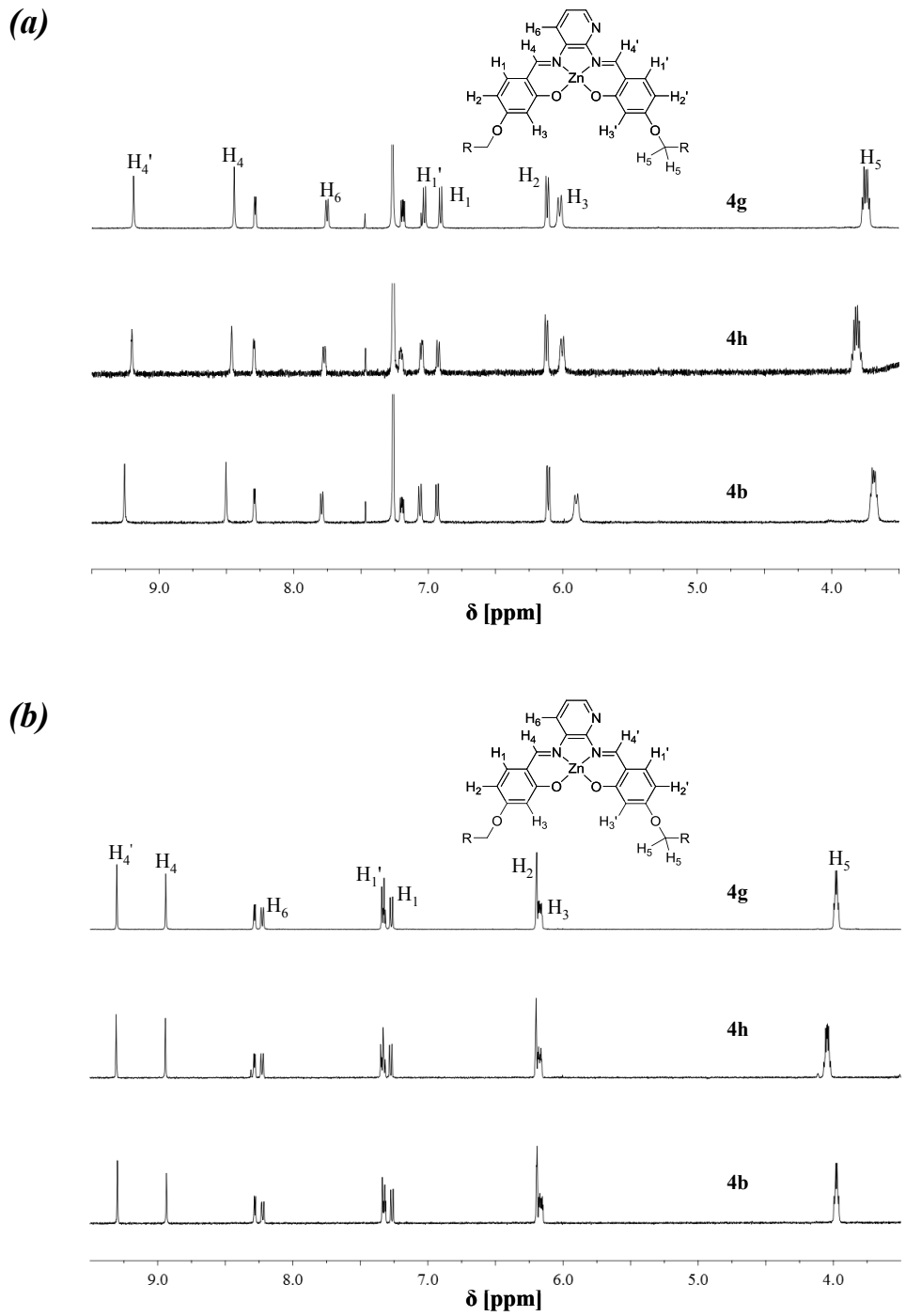

Figure 3.25 ^{1}H NMR spectra of complexes **4g**, **4h** and **4b** in *(a)* $CDCl_3$ *(b)* DMSO-d_6 solutions.

Diffusion-ordered NMR spectroscopy (DOSY)[16] has been used as an independent method to estimate the degree of aggregation and the molecular mass of complexes **2**-**4** through the measurement of the diffusion coefficient, D.

2D DOSY data collected from different complexes in coordinating (DMSO-d_6) and non-coordinating ($CDCl_3$) solvents are reported in Table 3.6 and are used to investigate the degree of aggregation present in solution through an estimate of the molecular mass (see paragraph **7.12** for further details). They clearly indicate that for all of the investigated complexes, the estimated molecular mass in DMSO-d_6 is consistent with a monomeric species with a DMSO molecule axially coordinated. In contrast, on switching to the $CDCl_3$ non-coordinating solvent, the estimated molecular mass for **3g** and **4g** is consistent with a dimeric structure (see paragraphs **3.2.1.1** and **3.2.2**), while for compound **2g** a mixture of oligomers are predicted, according to the observed broadening in the ^{1}H NMR spectra.

Table 3.6 Diffusion coefficients, *D*, and estimated molecular mass, *m*, of **1**-**4** at 27°C in non-coordinating ($CDCl_3$; TCE-d_2) and coordinating (DMSO-d_6) solvents.

Complex	Concentration ($\times 10^{-3}$ M)	*D* (complex) ($\times 10^{-10}$ m^2 s^{-1})	*D* (solvent) ($\times 10^{-10}$ m^2 s^{-1})	m^a (Da)
1a[b]	1.0	2.88	8.30 (TCE-d_2)	1402
1a[b]	1.0	2.30	7.20 (DMSO-d_6)	815
2g	1.0	2.35	7.25 (DMSO-d_6)	791
2g	1.0	6.42	27.01 ($CDCl_3$)	2130
3g	0.5[c]	7.68	27.21 ($CDCl_3$)	1511
3g	0.5[c]	2.29	7.30 (DMSO-d_6)	845
4g	1.0	2.30	7.22 (DMSO-d_6)	819
4g	5.0	2.24	6.90 (DMSO-d_6)	789
4g	1.0	7.78	27.05 ($CDCl_3$)	1455
4g	5.0	7.52	26.85 ($CDCl_3$)	1534

[a]Estimated molecular mass with eq. 5 (see paragraph **7.12**). [b]From Table 3.1. [c] Concentration maximum achievable in $CDCl_3$ and DMSO-d_6 solvents.

^{1}H NMR studies of **2g** in mixtures of non-coordinating/coordinating ($CDCl_3$/DMSO-d_6) solvents further support the existence of aggregates in the former solvent. Actually, the addition of defined amounts of DMSO-d_6 to $CDCl_3$ solutions of **2g** leads to substantial ^{1}H NMR spectral changes. In particular, upon the addition of a 3000-fold mole excess of DMSO-d_6 the resulting solution shows a ^{1}H NMR spectrum comparable to that recorded in DMSO-d_6 (Figure 3.26).

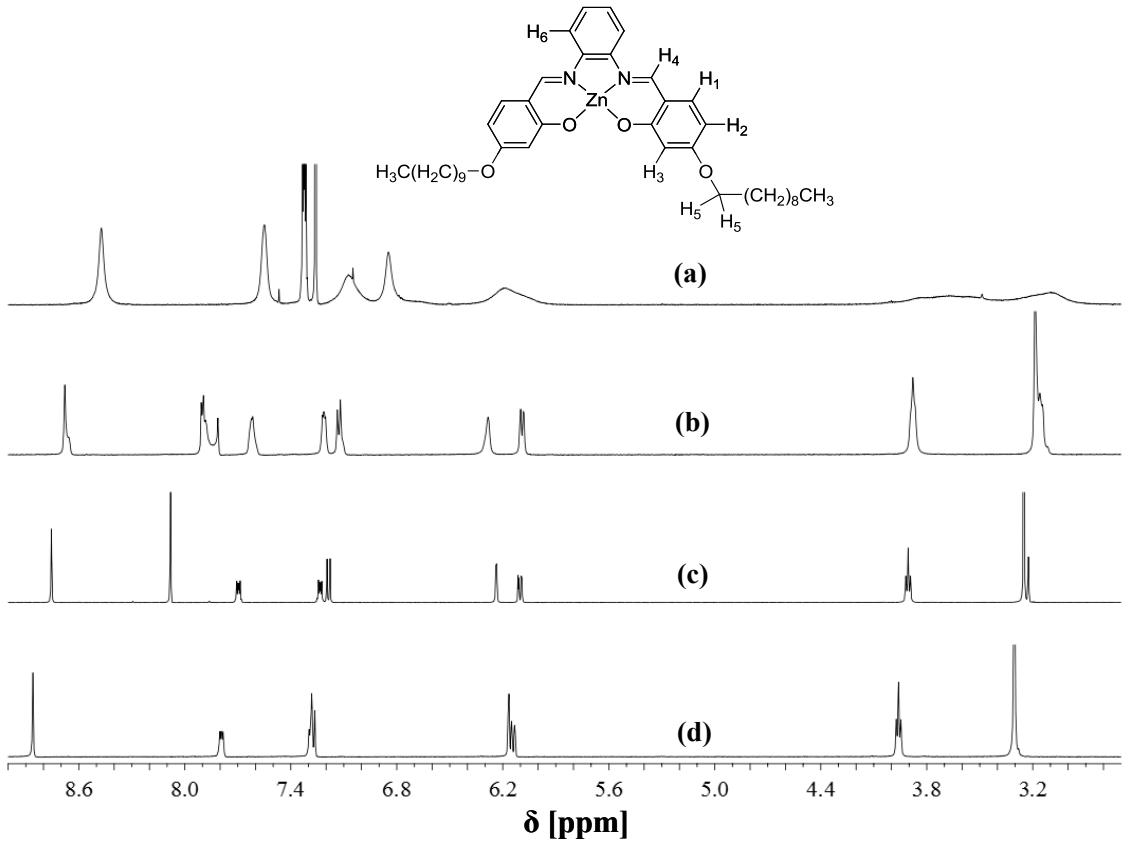

Figure 3.26 ^{1}H NMR spectra of **2g** in *(a)* $CDCl_3$ (1.0×10^{-3} M; 6.0×10^{-7} mol) and with addition of *(b)* 9.0×10^{-4} mol and *(c)* 1.8×10^{-3} mol of DMSO-d_6. *(d)* The ^{1}H NMR spectrum of **2g** in DMSO-d_6 is reported for comparison.

3.3.1.2 Optical absorption and fluorescence spectroscopy studies

The UV-vis and fluorescence emission spectra of complexes **2g**-**4g** in various solvents are shown in Figure 3.27, while the relevant absorption and emission parameters of all of the investigated complexes are collected in Table 3.7.

The absorption spectra of **2g**-**4g** in dilute solutions of non-coordinating solvents ($CHCl_3$, 10 μM) consist of two main overlapped bands at ≈315 nm and between 380-400 nm, with a shoulder at longer wavelengths, according to the existence of aggregate species in solution. These features are concentration independent, as they remain substantially unaltered up to a concentration of 5.0×10^{-4} M (Figure 3.28). Moreover, on decreasing the solvent polarity negligible variations of the optical absorption spectra are observed (Figure 3.29). For complexes **4b**, **4g** and **4h**, optical absorption spectra indicate almost identical features on changing the alkyl chains length (Figure 3.30).

Table 3.7 Optical absorption and fluorescence emission parameters for complexes **2**-**4** in various solvents.

Complex	Solvent	Absorption		Emission
		λ_{max} (nm)[a]	ε (M^{-1} cm^{-1})	λ_{max} (nm)
2g	$CHCl_3$	378 (410)	36000	483
	MES	381 (416)	25500	486
	CCl_4	381 (416)	31800	486
	THF	393, 430	37000, 22000	485
	DMSO	388, 426	36900, 22500	489
3g	$CHCl_3$	382 (412)	41100	504
	THF	402 (422)	49000	484
	DMSO	402 (420)	39500	495
4g	$CHCl_3$	398 (435)	26200	512
	THF	407 (446)	40200	486
	DMSO	408 (444)	36000	500
4h	$CHCl_3$	392 (432)	25200	510
	DMSO	407 (443)	36100	495
4b	$CHCl_3$	389 (432)	23000	511
	DMSO	405 (445)	[b]	485

[a]Values in parentheses refer to the higher wavelength shoulder (see text). [b]The very low solubility of **4b** derivative in DMSO avoided the achievement of quantitative data.

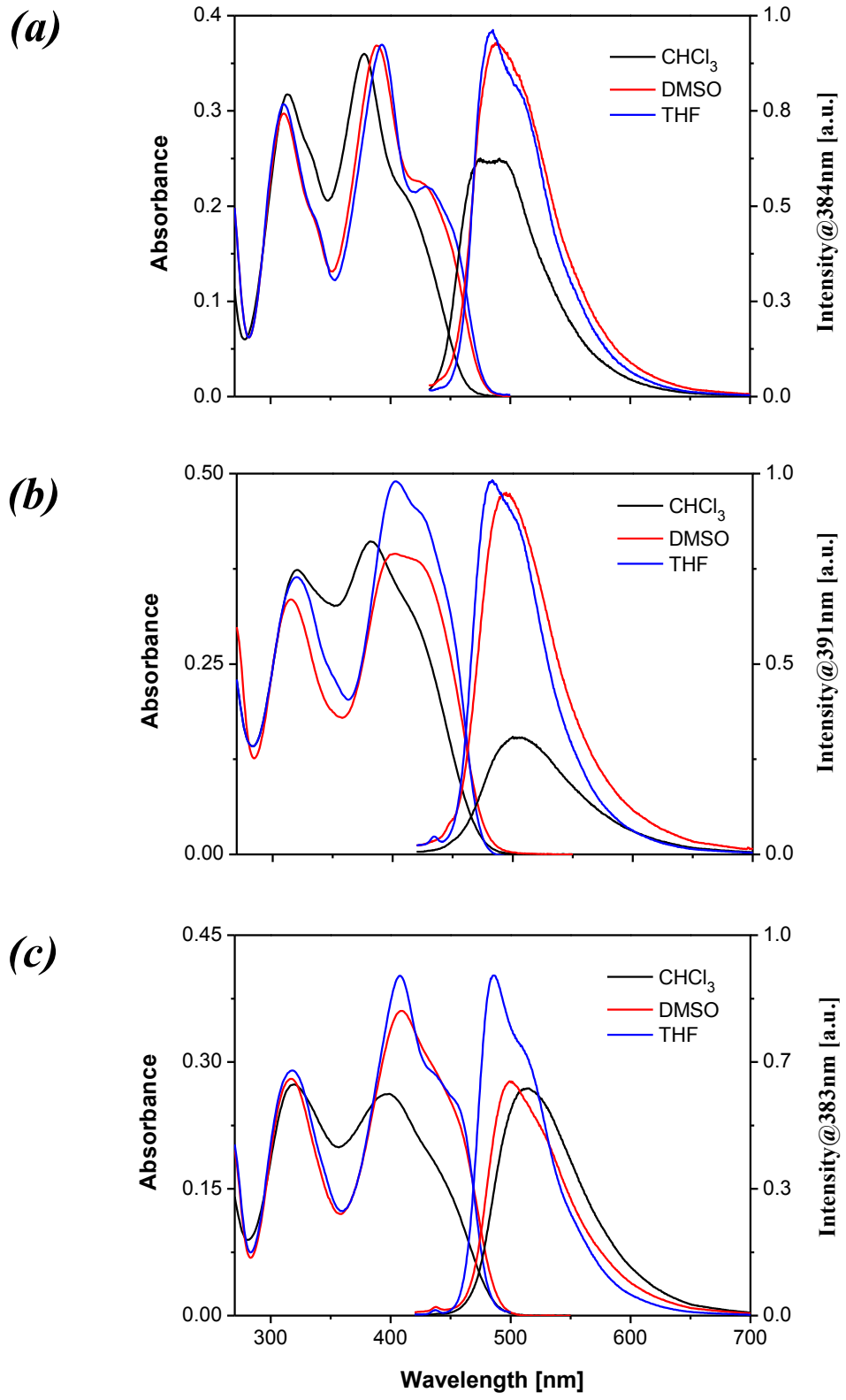

Figure 3.27 UV-vis absorption and fluorescence spectra of *(a)* **2g**, *(b)* **3g**, and *(c)* **4g** (10 μM solutions) in non-coordinating $CHCl_3$ (—) and coordinating DMSO (—), THF (—) solvents.

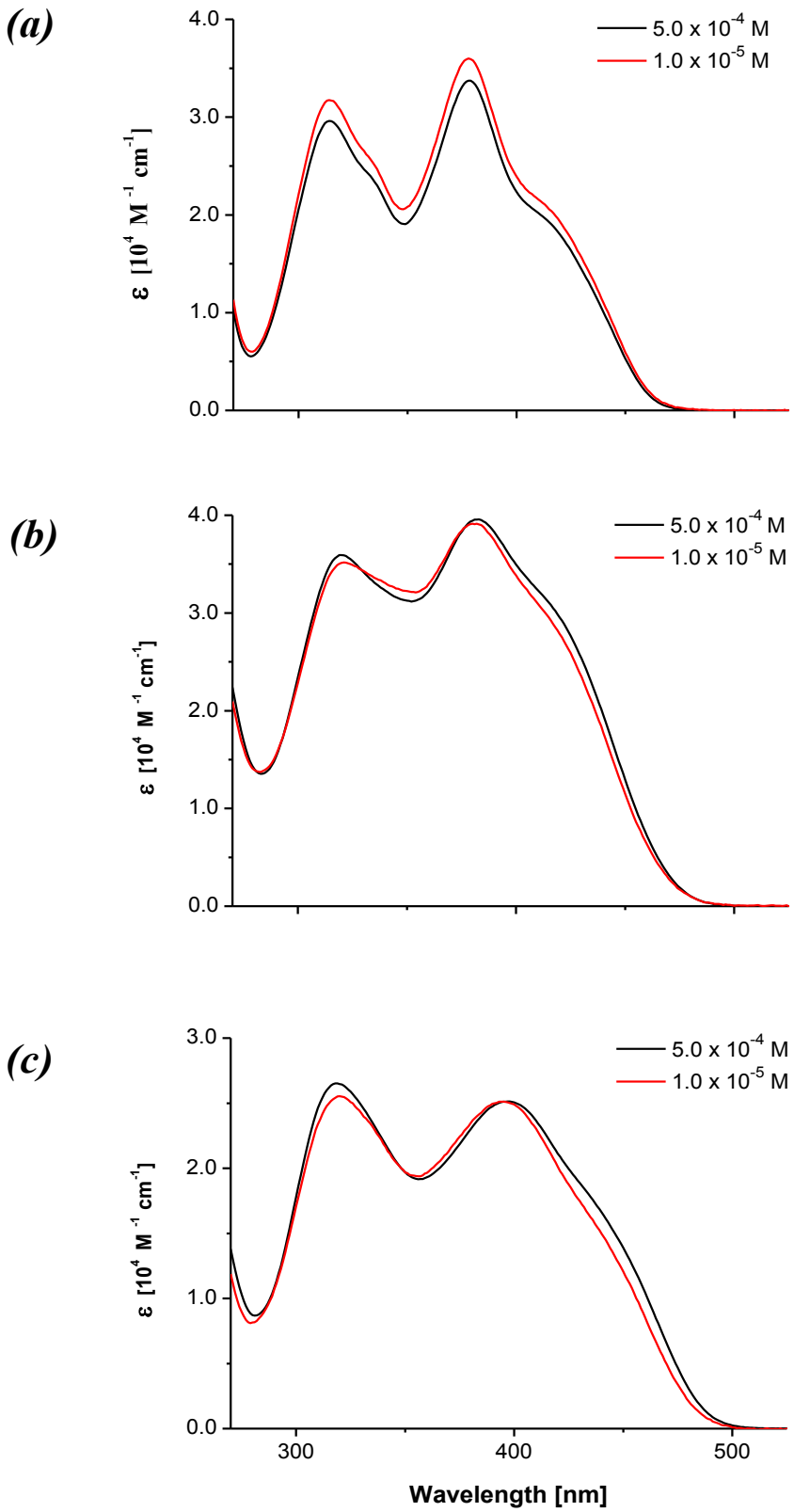

Figure 3.28 Concentration dependence of UV-vis absorption spectra of *(a)* **2g**, *(b)* **3g** and *(c)* **4g** in $CHCl_3$ solutions.

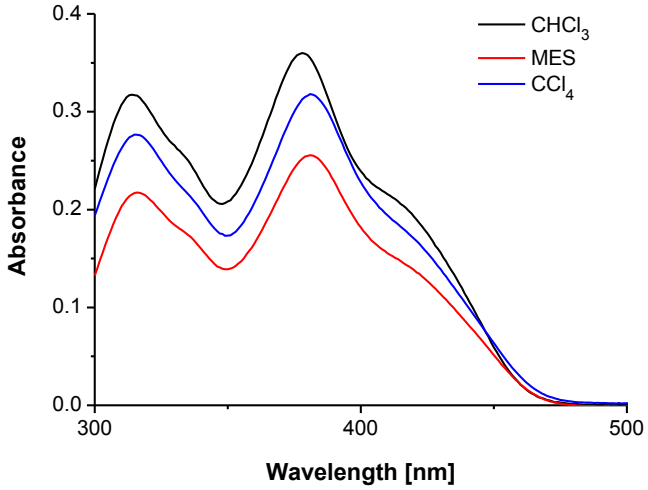

Figure 3.29 UV-vis absorption spectra of **2g** (10 μM) in non-coordinating solvents of different polarities.

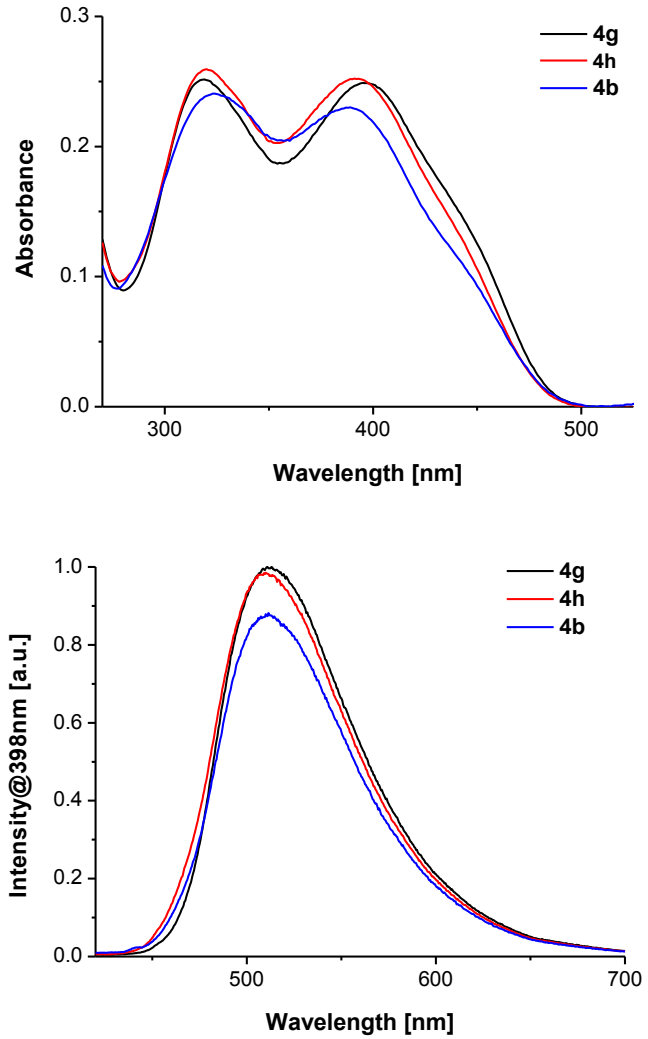

Figure 3.30 UV-vis absorption *(top)* and fluorescence *(bottom)* spectra of complexes **4g**, **4h** and **4b** (10 μM) in $CHCl_3$ solutions.

On switching to coordinating solvents (Figure 3.27), independent of their degree of polarity, *e.g.*, DMSO or THF, a red-shift (≈10 nm) of the longer wavelength feature is observed, which is much more pronounced in the case **3g** (≈20 nm), while the shoulder, in $CHCl_3$, of the phenylene derivative **2g** appears as a new defined band. These significant changes are all indicative of monomeric species in solution upon axial coordination of the coordinating solvent to the Zn^{II} metal center.

The addition of defined amounts of a coordinating species to $CHCl_3$ solutions of complexes **2g**-**4g** leads to optical changes analogous to those observed on switching to solutions of coordinating solvents. Actually, upon the addition of DMSO in 3000-, 600- or 300-fold mole excess, for **2g**-**4g**, respectively, optical absorption spectra of the resulting solutions are comparable to those recorded in the coordinating solvents (Figure 3.31). However, while the optical absorption spectra of **3g**-**4g** indicate the presence of multiple isosbestic points upon spectrophotometric titrations with DMSO, those of **2g** do not show clear isosbestic points.

The present complexes exhibit a moderate cyan fluorescence, as characterized by relatively low fluorescence quantum yield values ($\Phi \leq 0.1$). Steady-state fluorescence studies of **2g**-**4g** in a solution of non-coordinating solvents indicate the presence of an unstructured band, with a maximum between 480-515 nm, independent of the excitation wavelength (Table 3.7; Figure 3.27). Analogous to the observed small variations in the optical absorption spectra of **4b**, **4g** and **4h**, the alkyl chain length also involves negligible variation of the fluorescence emission.

On switching to coordinating solvents, the emission band maximum does not reflect the relative changes observed in the lowest energy band of the absorption spectra. In particular, a blue-shifted emission (≈10 nm), with respect to non-coordinating solvents, is found for **3g** and **4g** derivatives, while a sizable fluorescence intensity increase, up to three times larger, is observed for the **3g** derivative. Again, these data are consistent with a deaggregation of the complexes and the formation of 1:1 adducts. Actually, the deaggregation with DMSO of $CHCl_3$ solutions of **3g** leads to changes of the fluorescence emission, analogous to that observed on changing from non-coordinating to coordinating solvents (Figure 3.31).

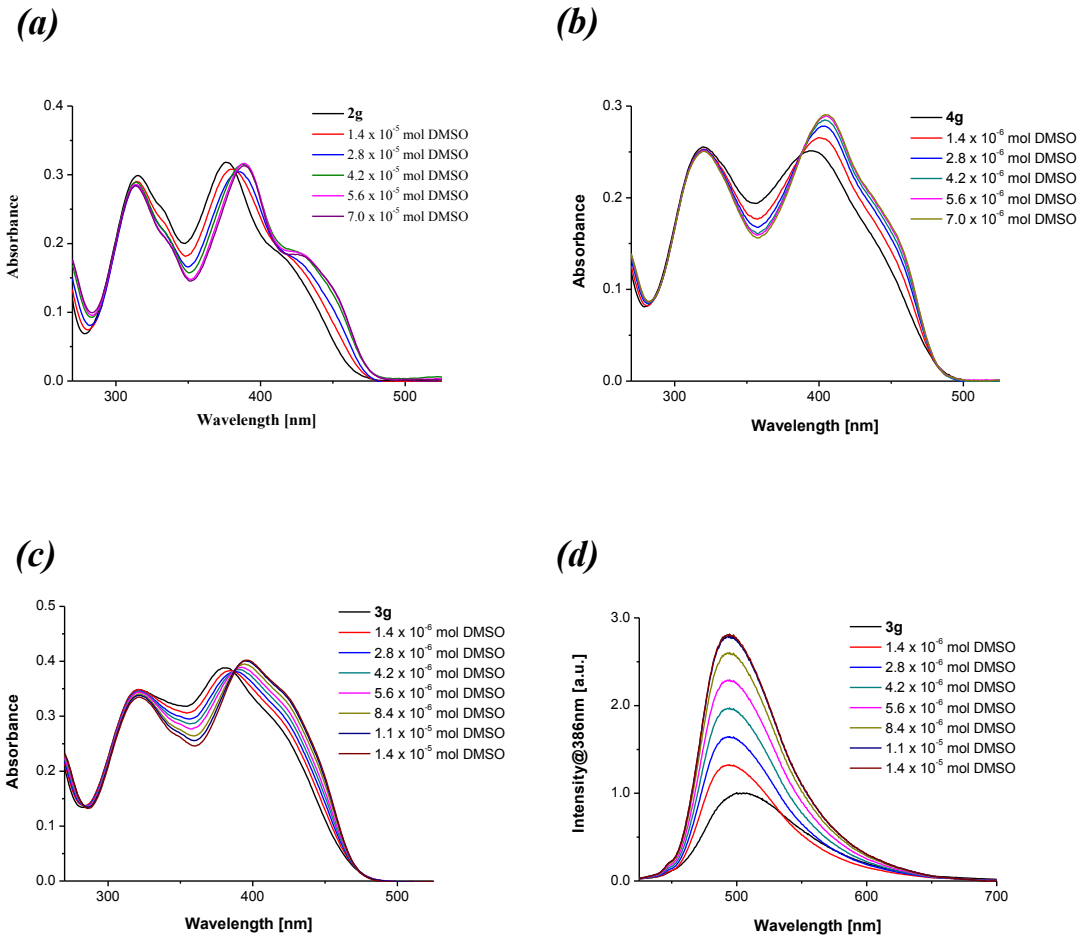

Figure 3.31 UV-vis absorption spectra of *(a)* **2g**, *(b)* **4g** and *(c)* **3g** (10 μM; 2 × 10^{-8} mol) in $CHCl_3$ with addition of DMSO. *(d)* Fluorescence spectra (λ_{exc} = 386 nm) of **3g** in $CHCl_3$ with addition of DMSO.

3.3.1.3 Field emission scanning electron microscopy (FE-SEM) and X-ray diffraction (XRD) studies

FE-SEM images of **2h**, **2g** and **2b** films, obtained by drop-casting of 1.0 × 10^{-3} M and 5.0 × 10^{-4} M THF solutions onto cleaned Si(100) substrates, are shown in Figures 3.32-3.34.

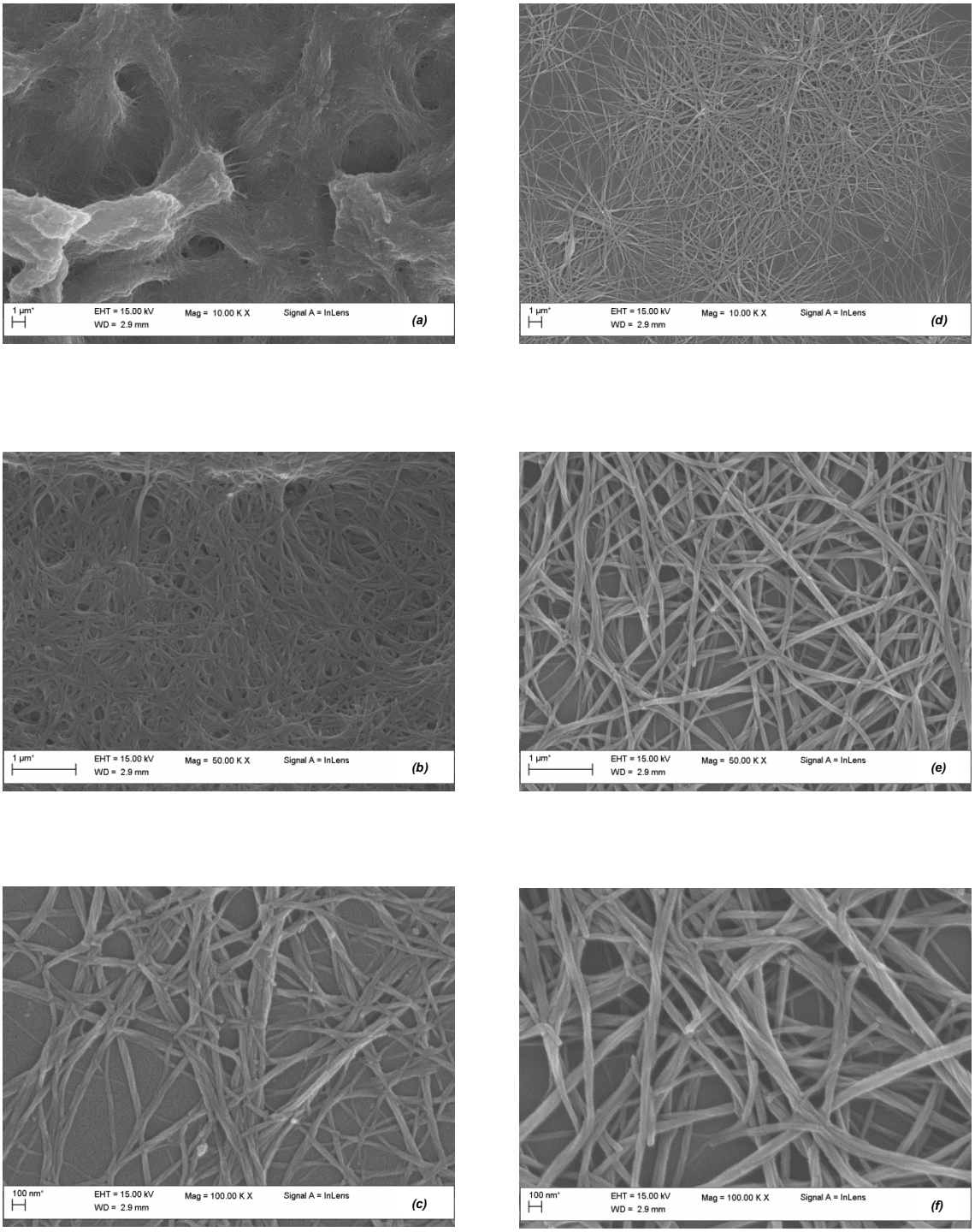

Figure 3.32 FE-SEM images of **2h** deposited by casting from *(a-c)* 1.0×10^{-3} M and *(d-f)* 5.0×10^{-4} M THF solutions at different magnifications.

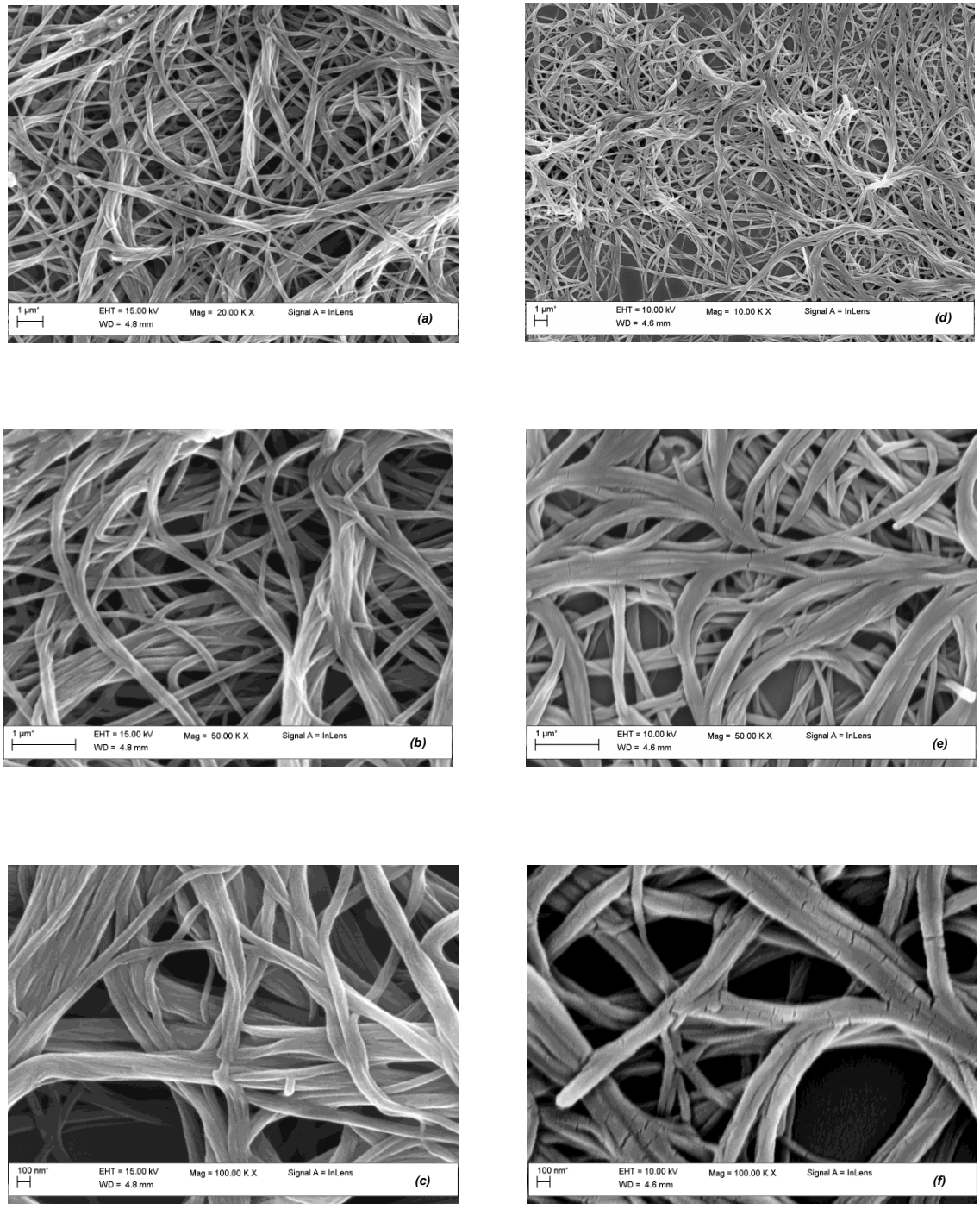

Figure 3.33 FE-SEM images of **2g** deposited by casting from *(a-c)* 1.0×10^{-3} M and *(d-f)* 5.0×10^{-4} M THF solutions at different magnifications.

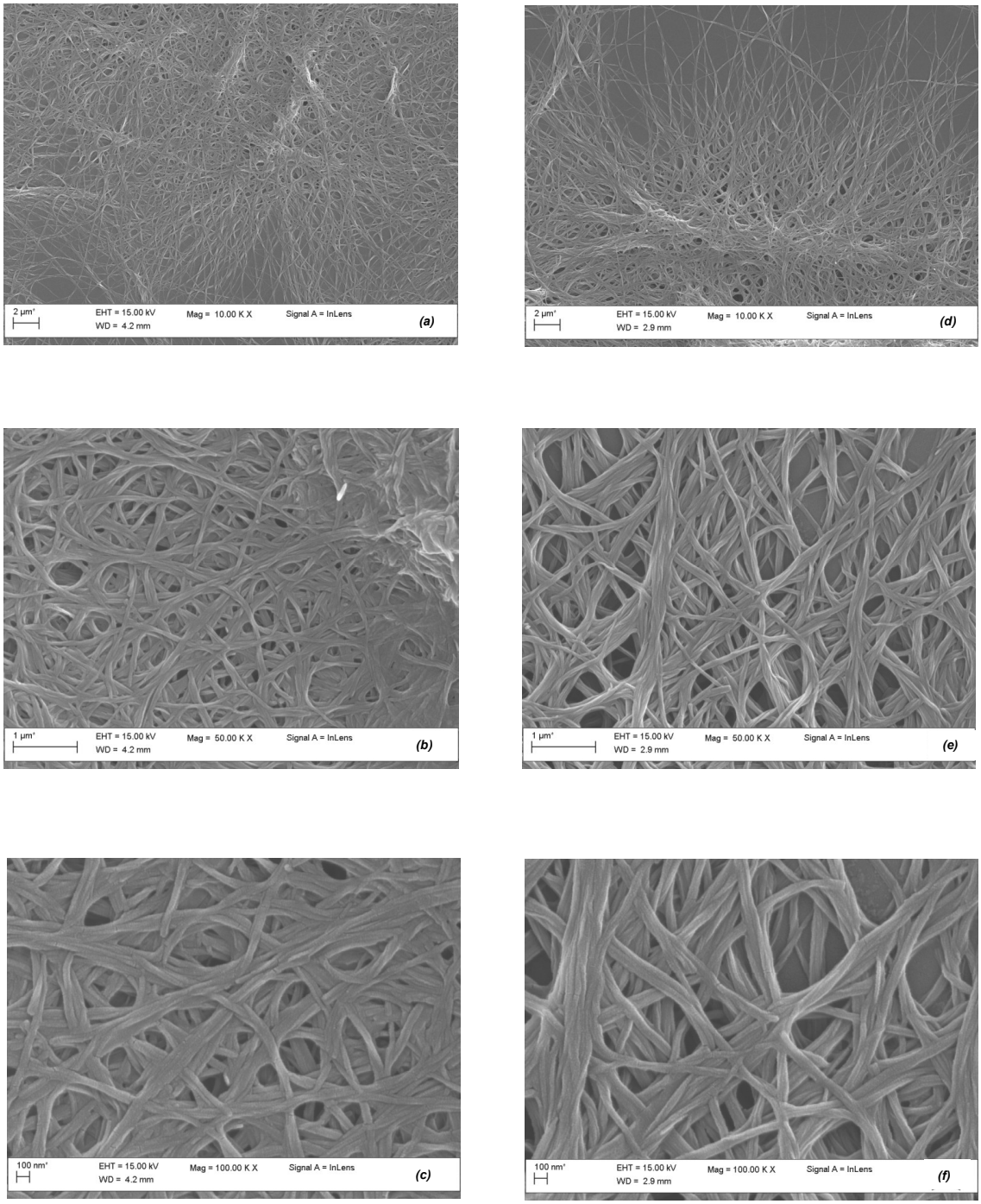

Figure 3.34 FE-SEM images of **2b** deposited by casting from *(a-c)* 1.0×10^{-3} M and *(d-f)* 5.0×10^{-4} M THF solutions at different magnifications.

FE-SEM images show that complexes **2h**, **2g** and **2b** form in the solid state, by drop-casting on Si(100) substrates, well-defined fibrillar nanostructures with bundle widths of ~100-300 nm. The bundles of nanofibers are very dense and tangled with each other and cover almost the entire surface of the material support.

On the other hand, drop-casting films obtained from $CHCl_3$ solutions possess a uniform surface without any nanostructure compared to those obtained by drop-casting from THF solutions (*e.g.*, **2g**; Figure 3.35).

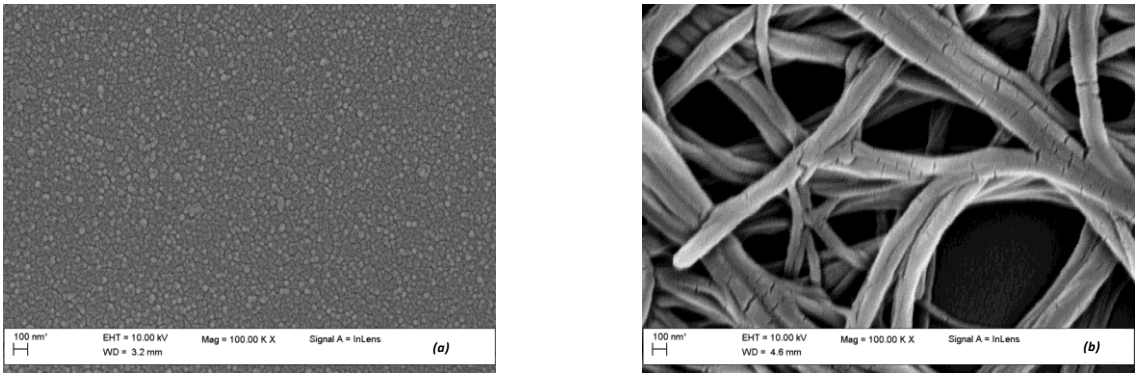

Figure 3.35 Comparison of FE-SEM images of **2g** deposited by casting from 5.0×10^{-4} M solutions in *(a)* $CHCl_3$ and *(b)* THF at the same magnification.

The formation and the morphology of these nanofibers are almost independent from concentration of the cast solution and the differences between the images obtained by drop-casting 1.0×10^{-3} M and 5.0×10^{-4} M THF solutions for complexes **2h**, **2g** and **2b** are consistent with the different amount of complex deposited on the substrate. In fact, structures obtained by casting dilute 5.0×10^{-4} M THF solutions are better definite and less dense than those obtained from 1.0×10^{-3} M THF solutions (Figure 3.32-3.34).

Slight differences of the nanofibers width can be observed on passing from **2h**, having ethyl side alkyl chains, to **2g**, having decyl side alkyl chains (Figure 3.36). In particular, larger nanofibers are observed in the latter case. Instead, on passing from **2g** to **2b**, no appreciable differences in the nanofibers width are observed.

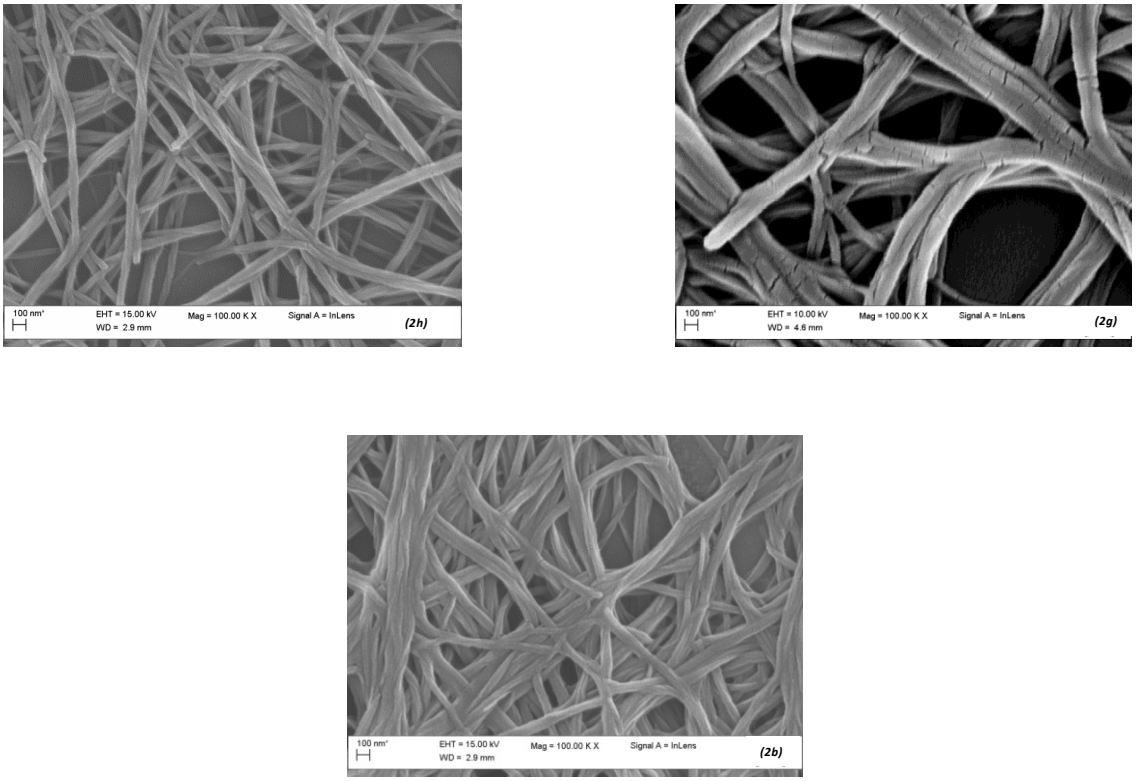

Figure 3.36 Comparison of FE-SEM images of **2h**, **2g** and **2b** deposited by casting from 5.0×10^{-4} M THF solutions at the same magnification.

XRD patterns and interplanar spacings of cast films of complexes **2h**, **2g** and **2b** are reported in Figure 3.37 and Table 3.8.

The XRD patterns for **2h**, **2g** and **2b** show broad peaks corresponding to 100, 200, 300 and 400 reflections of the assembled structure. The reflection angles do not change with the concentration of the cast solution. In fact, the diffraction patterns of the samples obtained from 1.0×10^{-3} M and 5.0×10^{-4} M THF solutions remain almost identical (Figure 3.37a-c).

Conversely a distinct effect of the side alkyl chain in XRD patterns, obtained by drop-casting of THF solutions at 1.0×10^{-3} M (Figure 3.37d), is observed. In particular, the position of the first diffraction peak, and then the interplanar spacing, is different for **2h**, **2g** and **2b** complexes and increase on passing from the ethyl to hexadecyl alkyl chain (Table 3.8), despite the analogous observed nanofibrillar morphology (Figure 3.32-3.34). Note that, the interplanar spacing deduced from XRD for **2h** is comparable with its molecular length (15.8 Å) achieved from (PM3) geometry optimization.

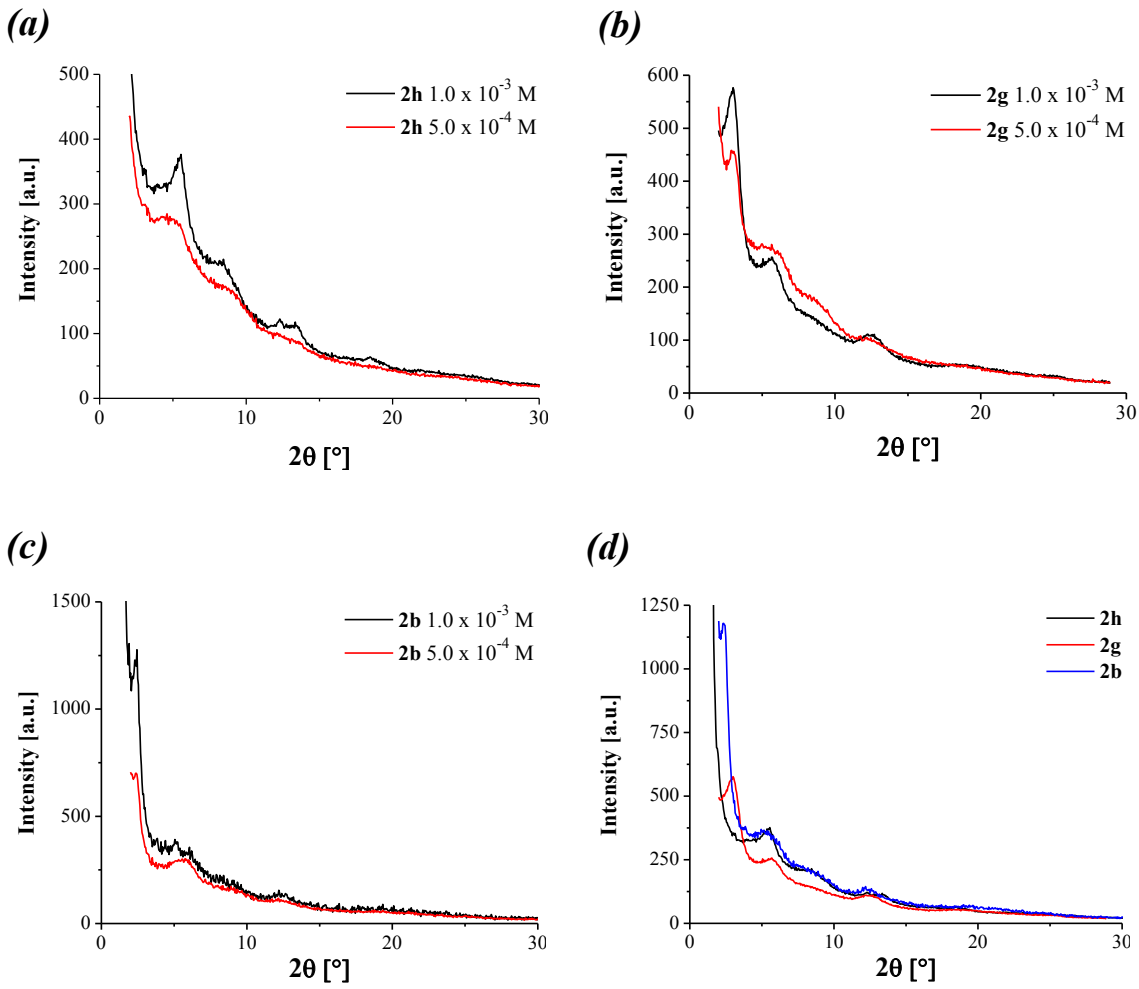

Figure 3.37 XRD patterns of samples of *(a)* **2h**, *(b)* **2g** and *(c)* **2b** obtained by drop-casting of THF solutions at different concentrations. *(d)* Comparison of XRD pattern of **2h**, **2g** and **2b** samples obtained by drop-casting of 1.0×10^{-3} M THF solutions.

Table 3.8 Interplanar spacings for **2h**, **2g** and **2b** films obtained by drop-casting of 1.0×10^{-3} M THF solutions.

Sample	2θ (°)	d (Å)
2h	5.55	15.91
2g	3.00	29.42
2b	2.40	36.78

3.3.2 Discussion

The synthesis of the amphiphilic Schiff base Zn^{II} complexes **2**-**4**, which are relatively soluble even in low-polarity solvents, allowed us to perform a systematic study of their spectroscopic properties that, in turn, can be related to the aggregation/deaggregation process in solution.

For complexes **3g** and **4g**, ^{1}H NMR and DOSY studies indicate the existence of defined dimeric species in solutions of non-coordinating solvents. In fact, the existence of sharp peaks independent of the concentration and the observed upfield shift of some signals, on switching from coordinating to non-coordinating solvents, are in accordance with definite aggregate species. In particular, the observed relevant upfield shift for H_1, H_4 and H_6 signals, which does not involve the H_2 protons, indicates that these hydrogens lie under the shielding zone of the π electrons of a conjugated system. Moreover, the different $\Delta\delta$ values observed for H_1, H_4 and H_1', H_4' protons in complexes **4b**, **4g** and **4h** indicate that they lie under the shielding zone of the salicylidene and pyridine aromatic rings, respectively. This view supports the formation of defined dimer species, *e.g.*, in a facial arrangement,[7d] in which both Zn atoms mutually interact through the Zn···O axial coordination, thus fulfilling the coordination sphere of the Zn^{II} ion (Chart 3.6).

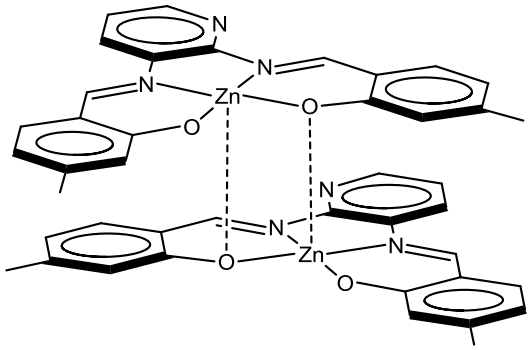

Chart 3.6 Proposed structure for dimeric aggregate of **4g**.

In the case of **2g**, the ^{1}H NMR spectra indicate a general peak broadening. Accordingly, this involves the existence of oligomeric species, as previously observed for **1a** (see paragraphs **3.2.1.1** and **3.2.2**).[4d] In fact, the formation of oligomeric aggregates causes a broadening due to a significant decrease in the T_2 relaxation time.[24]

The effect of the alkyl chain length on the aggregation properties has been analysed for the complex **4** alkyl derivatives. Actually, the alkyl chain length for compounds **4b**, **4g** and **4h** is expected to play a very minor role. In fact, on switching from coordinating to non-coordinating solvents, the observed constancy of the relevant chemical shifts and, hence, of $\Delta\delta$ values (Table 3.5), indicates that around the Zn^{II} ion of the aggregate species the same chemical and magnetic environment in solution is present.

The optical absorption and fluorescence emission data are in agreement with the above view. In fact, the absorption spectra of **2g-4g** in dilute solutions of non-coordinating solvents are consistent with the existence of aggregate species in solution. Optical absorption features are concentration-independent, as they remain substantially unaltered up to concentrations 5.0×10^{-4} M. Moreover, the alkyl chains length does not affect optical absorption and fluorescence spectra, as they remain almost unaltered in coordinating and non-coordinating solvents within the complexes **4b**, **4g** and **4h**.

On switching to coordinating solvents, independently of their degree of polarity, *e.g.*, DMSO and THF, is observed a red-shift of the longer wavelength feature. These significant changes are all indicative of monomeric species in solution upon axial coordination of the coordinating solvent to the Zn^{II} metal center.

Actually, these changes can be achieved by the addition of defined amounts of a coordinating species, such as DMSO, to $CHCl_3$ solutions of complexes **2g-4g**. In fact, upon progressive addition of DMSO, the optical absorption and ^1H NMR spectra of the resulting solutions are comparable to those recorded in the coordinating solvents, indicating a complete deaggregation of the complexes with formation of the related 1:1 DMSO adducts. However, while the formation of related **3g** and **4g** adducts involves the presence of multiple isosbestic points, further supporting the existence of defined aggregate species in dilute $CHCl_3$ solutions, the optical absorption spectra of **2g** do not show clear isosbestic points upon titration (Figure 3.31a), according to the presence of various aggregate species.

Films of complexes **2h**, **2g** and **2b** obtained by drop-casting from THF solutions on Si(100) substrates exhibit a fibrillar nanostructure.[8b,10a,c] Considering that THF is not a strong Lewis base (see paragraph **4.4.1.2**) and its high vapour pressure, these complexes, even if present in THF solution as monomeric axially coordinated species, upon solvent evaporation during the casting process, are stabilized through

intermolecular Zn···O interactions with formation of nanofibrillar aggregates. This is a plausible mechanism because these nanostructures are not observed from chloroform solutions (Figure 3.35), where the pre-assembled aggregates cannot organize in nanofibers.[10a]

The formation and the morphology of nanofibers are independent from the concentration and side alkyl chain length of complexes. Therefore the driving force for the aggregation is likely dominated by intermolecular Zn···O interactions and not by other intermolecular interactions such as CH-π or π-π.

Overall, from SEM and XRD data a representation of nanofibers is proposed in Chart 3.7.

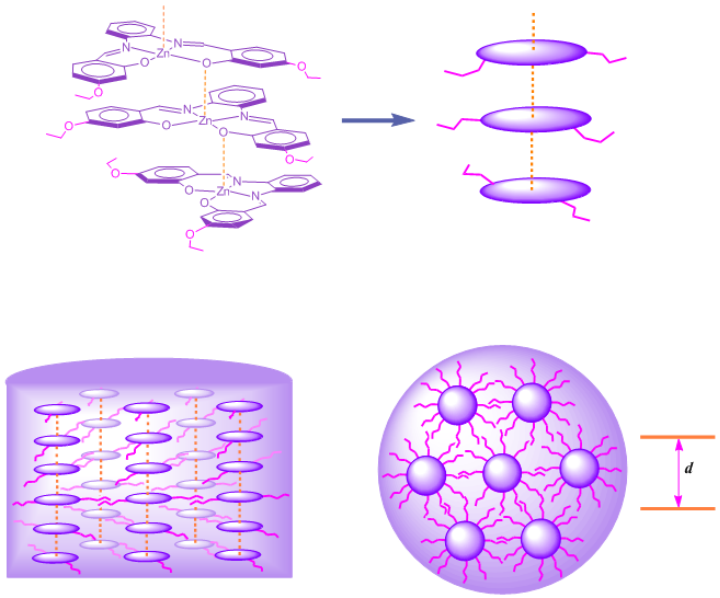

Chart 3.7 *(Top)* Representation of a single nanofiber of complexes **2h**, **2g** and **2b**. *(Bottom)* Axial and cross section representations of a nanofibers bundle.

Tangled bundle nanofibers are formed by interdigitation of the alkyl side chains of complexes that compose a single fiber through intermolecular Zn···O interactions.

The degree of interdigitation of side alkyl chains in the nanofibers is reflected in the XRD-derived interplanar spacing and influences their width, as observed in the SEM images. In particular, wider nanofibers are observed for **2g**, being characterized by larger interplanar spacing than those of **2h** because of the longer alkyl length. Conversely, despite the longer alkyl chains in **2b**, the observed width and interplanar spacing variation *vs.* **2g** is less affected with respect to the difference found between **2h** and **2g** nanofibers, presumably related to a larger degree of interdigitation.

3.4 Zn^{II} (salen) complexes

In this section, the complexes **5b**, **5g**, **5h** and **5i** are investigated (Chart 3.8). It has been studied this kind of complexes to highlight any analogies and differences, in terms of aggregation properties, respect to complexes having conjugated bridging diamine previously explored (see sections **3.2** and **3.3**).

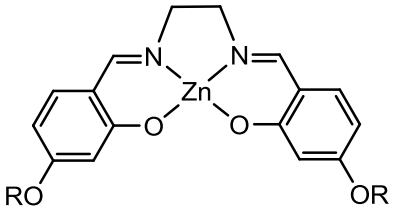

R = C_2H_5	**5h**
R = $C_{10}H_{21}$	**5g**
R = $C_{16}H_{33}$	**5b**
R = $C_{20}H_{41}$	**5i**

Chart 3.8 Structure of investigated complexes.

3.4.1 Results

Complexes **5g** and **5b** are moderately soluble in low-polarity solvents, such as chloroform, and in coordinating solvents, such as DMSO. On the other hand, complex **5h** is soluble in DMSO but shows very low solubility in $CHCl_3$, while derivative **5i**, which possesses longer alkyl chains, has good solubility in $CHCl_3$ but is almost insoluble in DMSO. This different solubility for alkyl derivatives **5h** and **5i** allows exploration of their behaviour in solution at higher concentrations, in coordinating and non-coordinating solvents, respectively, which is otherwise inaccessible for derivatives **5g** and **5b**.

The amphiphilic Zn(salen) complexes **5h**, **5g**, **5b** and **5i** have been characterized by ESI mass spectrometry and ^1H NMR spectroscopy. Mass spectrometry analysis always indicates the presence of defined signals corresponding to the protonated dimer.

3.4.1.1 ^{1}H NMR studies

^{1}H NMR spectra of Zn^{II} Schiff base complexes **5h**, **5g**,and **5b** in a dilute solution of coordinating solvents (DMSO-d_6, ~1×10^{-4} M) indicate the presence of sharp signals with the expected multiplicity, according to their molecular structures and consistent with the existence of monomeric species. The ^{1}H NMR spectrum of derivative **5b**, chosen as a reference compound, is reported in Figure 3.38. As expected, the ^{1}H NMR features in DMSO are concentration-independent, as can be verified using derivative **5h** (Figure 3.39) and remain unaltered for the **5h**, **5g** and **5b** complexes (Figure 3.40). In the case of complex **5i**, because of its insolubility in DMSO, the spectrum in DMSO-d_6 has been extrapolated from that in $CDCl_3$ upon the addition of a 5000-fold mole excess of DMSO-d_6.

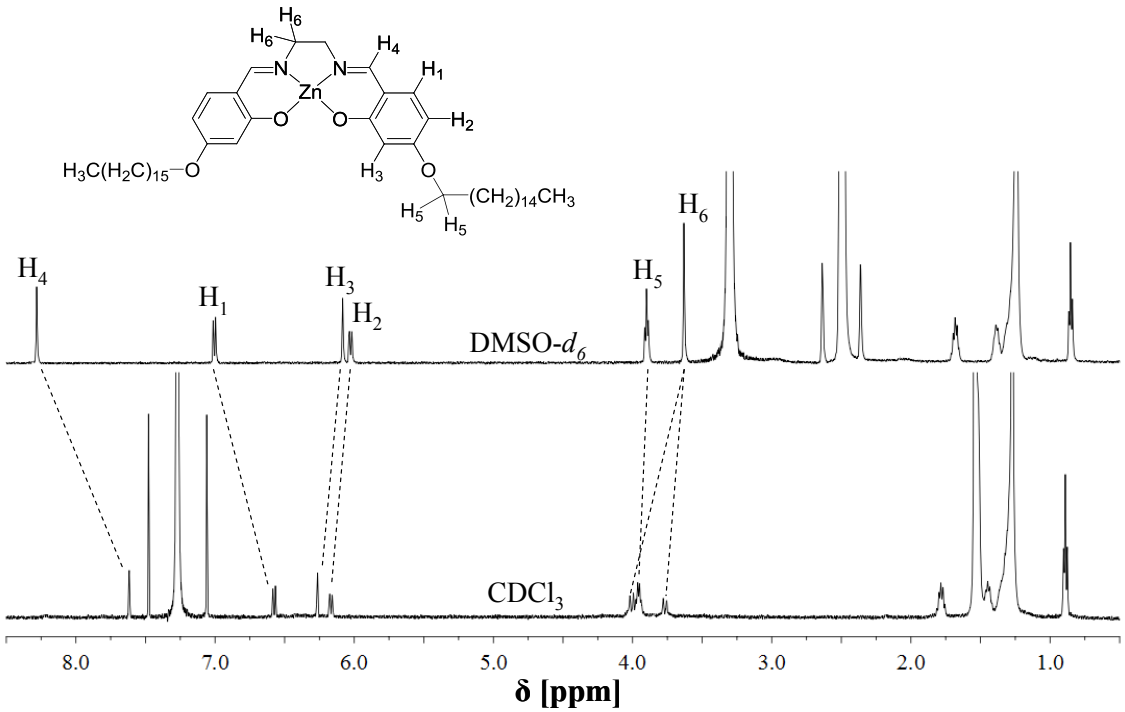

Figure 3.38 Comparison of ^{1}H NMR spectra of **5b** in DMSO-d_6 and $CDCl_3$ solutions (≈1×10^{-4} M).

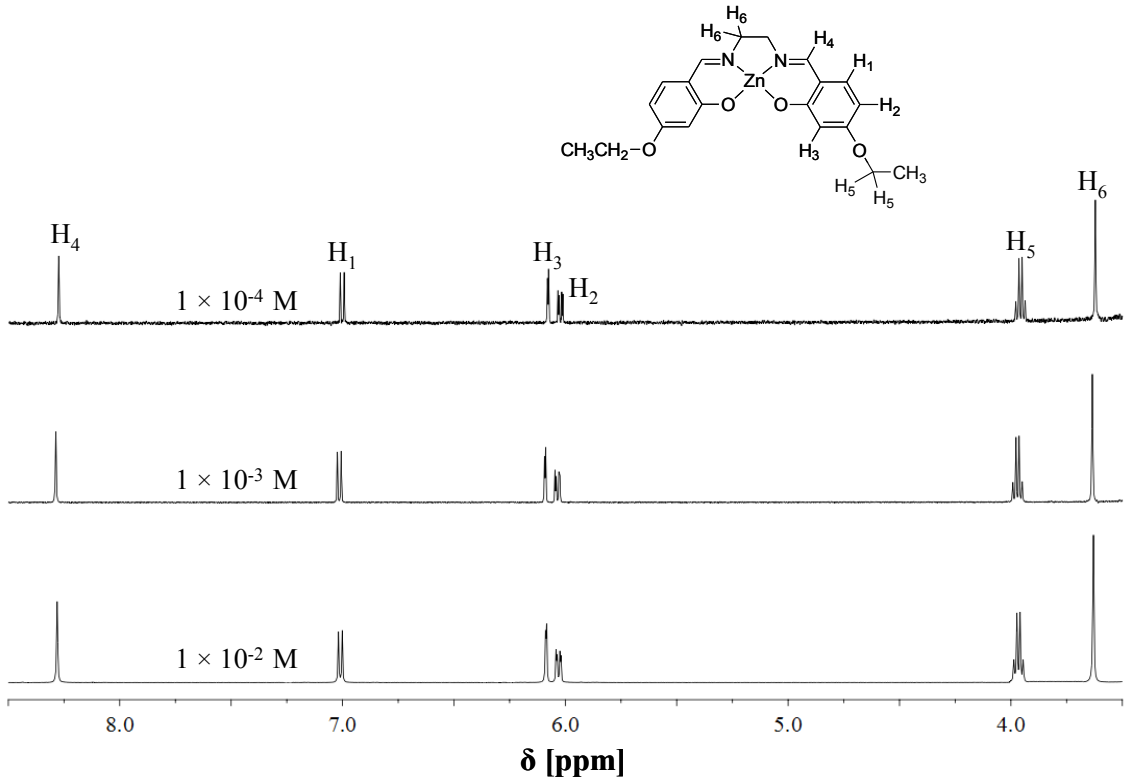

Figure 3.39 ^{1}H NMR spectra of **5h** in DMSO-d_6 at various concentrations.

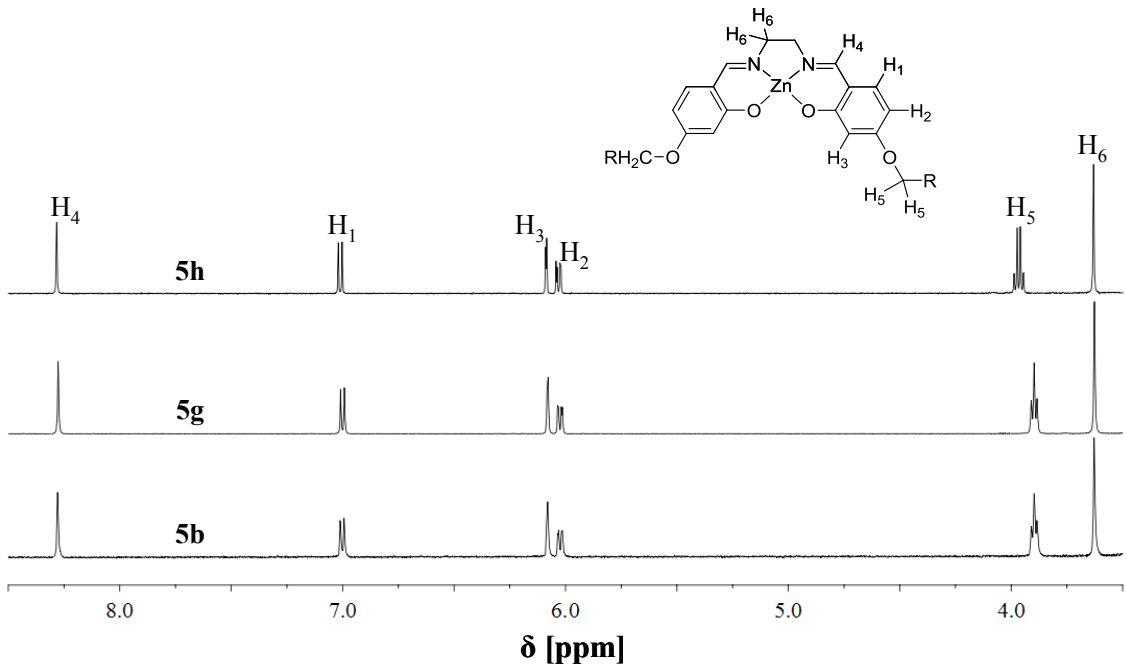

Figure 3.40 Comparison of ^{1}H NMR spectra of **5h**, **5g** and **5b** in DMSO-d_6 solutions at the same concentration (≈1 × 10^{-4} M).

On switching on non-coordinating solvents ($CDCl_3$, ~1 × 10^{-4} M, the maximum concentration achievable for complexes **5g** and **5b**), a substantial change in the ^1H NMR spectra is noted (Figure 3.38). In particular, a strong upfield shift, with respect to the coordinating solvent, of the H_4 (0.67 ppm) and H_1 (0.43 ppm) signals is found, while the H_2 and H_3 signals are shifted slightly downfield (*ca.* 0.15 ppm). Finally, H_6 signals, which are equivalent in DMSO-d_6, are split into two different signals, one of which is shifted substantially downfield (0.38 ppm). These relevant upfield shifts upon switching from coordinating to non-coordinating solvents indicate that the involved hydrogens lie under the shielding zone of the π electrons of a conjugated system (see paragraphs **3.2.1.1**, **3.2.2**, **3.3.1.1** and **3.3.2**),[4d,15] and the slight downfield shifts for some other hydrogen signals are consistent with the existence of aggregate species in solutions of non-coordinating solvents.

The alkyl side chains length is expected to play a very minor role in the aggregation properties, as the chemical shifts for all the aromatic, CH=N and the -OCH_2 hydrogens remain unaltered along the **5g**, **5b** and **5i** series ($CDCl_3$, ~1 × 10^{-4} M) (Figure 3.41).

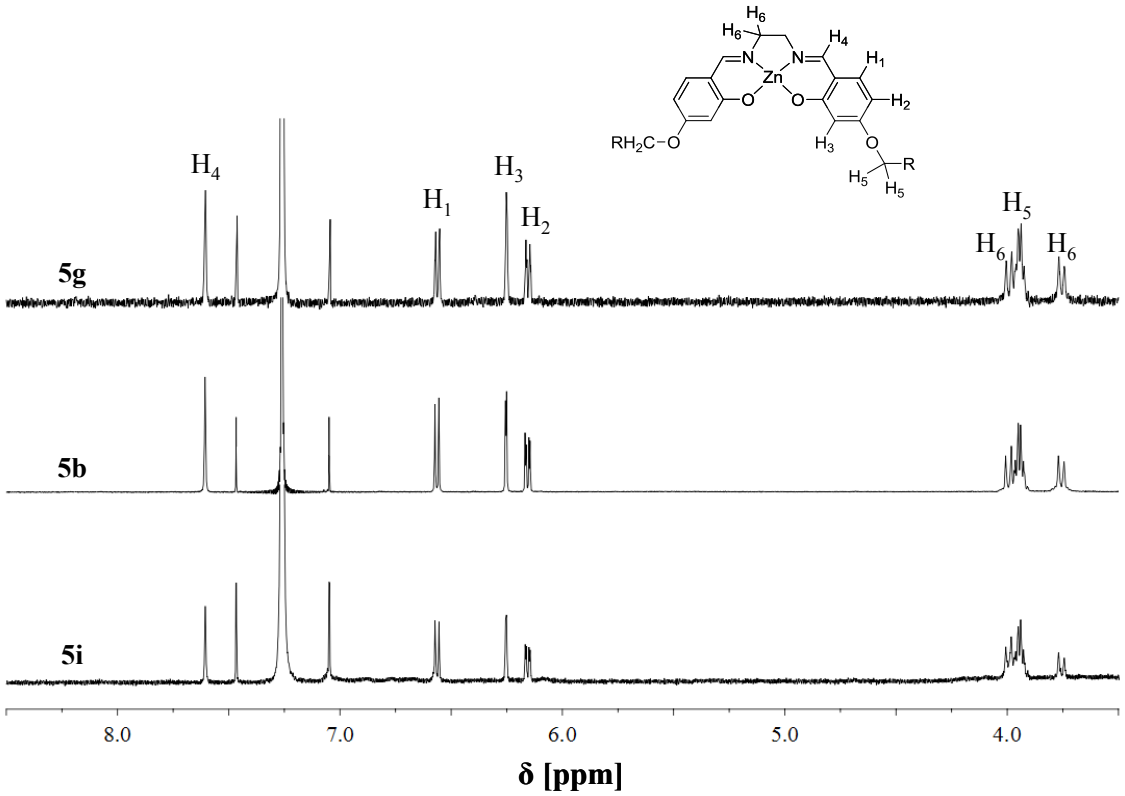

Figure 3.41 ^1H NMR spectra of **5g**, **5b** and **5i** in $CDCl_3$ solutions at the same concentration (1 × 10^{-4} M).

^{1}H NMR studies of complex **5b** in mixtures of non-coordinating/coordinating ($CDCl_3$/DMSO-d_6) solvents further support the existence of aggregates in the former solvent. In fact, the addition of defined amounts of DMSO-d_6 to $CDCl_3$ solutions of complex **5b** leads to substantial spectral changes. In particular, upon the addition of a 5000-fold mole excess of DMSO-d_6, the resulting solution shows a ^{1}H NMR spectrum that can be compared to that recorded in DMSO-d_6 (Figure 3.42).

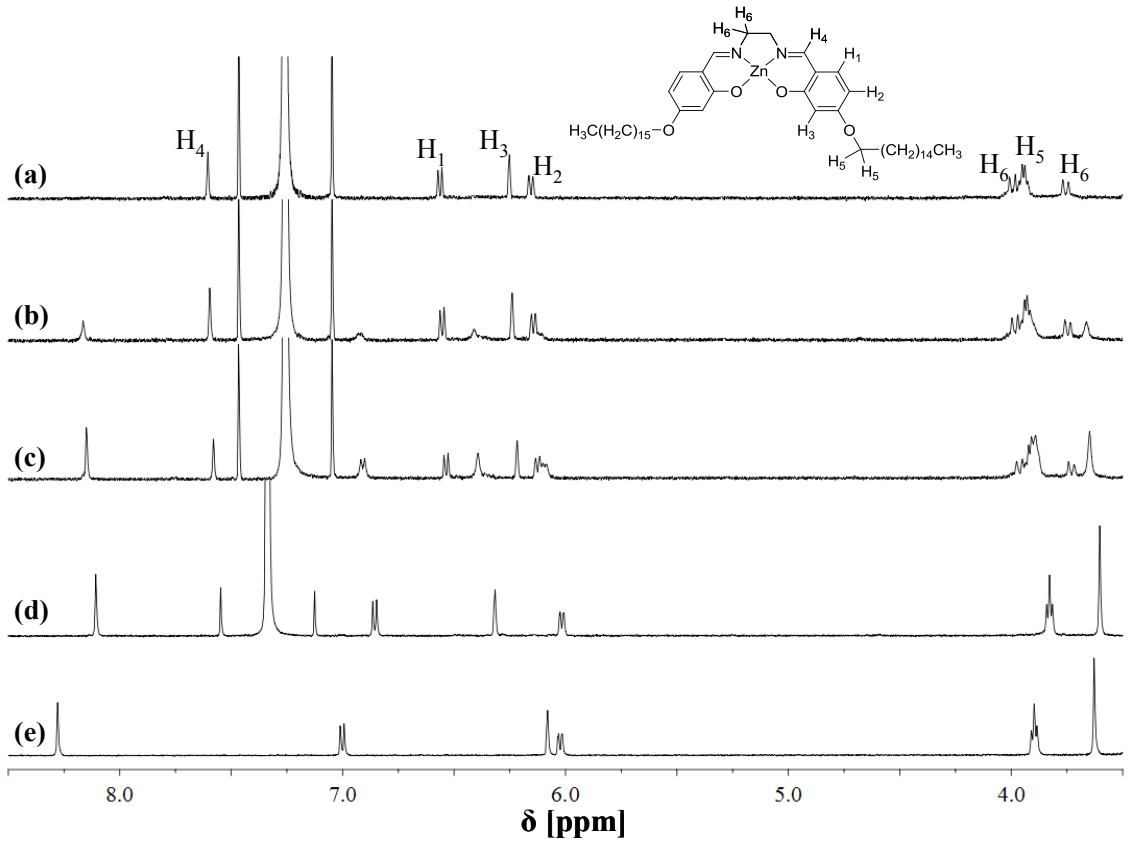

Figure 3.42 ^{1}H NMR spectra of **5b** in *(a)* $CDCl_3$ (1.0×10^{-4} M; 6.0×10^{-8} mol)**,** and with addition of *(b)* 1.8×10^{-5} mol, *(c)* 4.5×10^{-5} mol and *(d)* 3.0×10^{-4} mol of DMSO-d_6. *(e)*The ^{1}H NMR spectrum of **5b** in DMSO-d_6 is reported for comparison.

^{1}H NMR investigation of derivative **5i** to higher concentrations in solution of non-coordinating solvents shows an unexpected behaviour. In fact, the increase of the concentration ($CDCl_3$, up to 5×10^{-3} M) leads to the appearance of a new set of broad signals, which become progressively more intense with the increase of the concentration, while the sharp signals observed in dilute solutions undergo a parallel decrease (Figure 3.43). This behaviour is reversible, as demonstrated by dilution ^{1}H NMR experiments using stock solutions of **5i** (5×10^{-3} M) in $CDCl_3$.

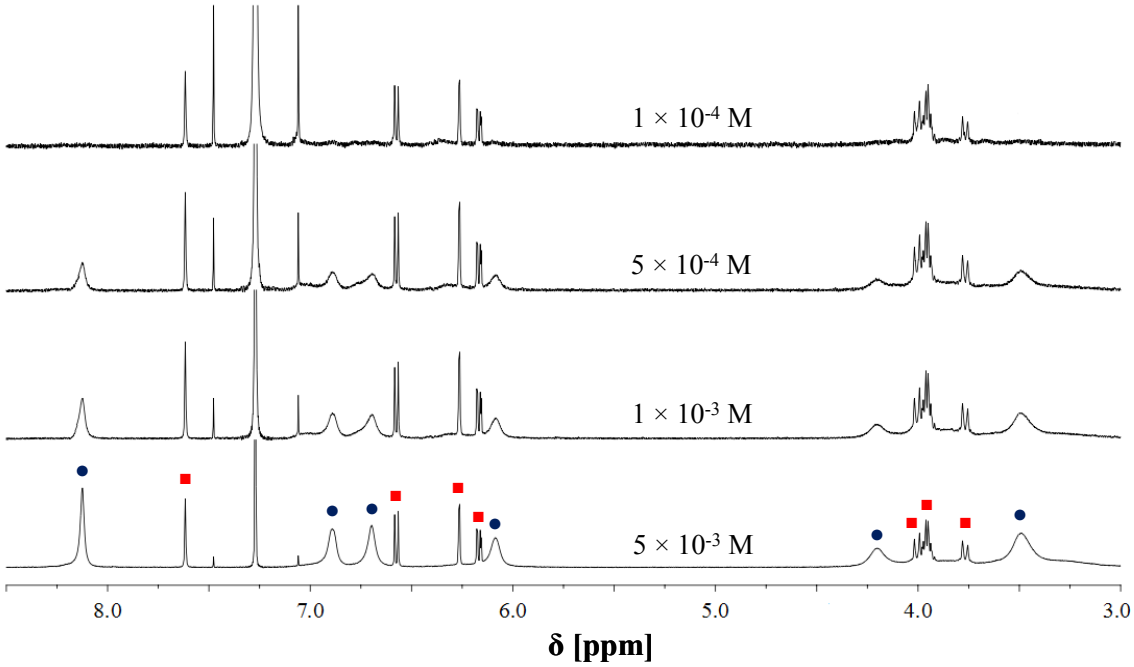

Figure 3.43 Concentration dependence of ^{1}H NMR spectra of **5i** in $CDCl_3$. The labelling of ^{1}H NMR signals related to the 5×10^{-3} M solution refers to species **A** (■) and **B** (●).

This new set of broad signals is still consistent with the molecular structure of **5i**. The detailed assignment of aromatic hydrogen signals has been made by means of selected 1D T-ROESY experiments, which indicate that the H_1 protons are spatially close to the H_4 and H_2 protons (Figure 3.44). Therefore, chloroform solutions of the derivative **5i** for concentrations greater than 1×10^{-4} M show evidence of the formation of a new species in slow equilibrium, with respect to the NMR time scale, with the species predominantly observed at lower concentrations. For confidence, the species prevalent at $\approx 1 \times 10^{-4}$ M will be noted as **A** whereas the other will be noted as **B**. At the concentration of *ca.* 5×10^{-3} M, the maximum concentration achievable in $CDCl_3$, the species **B** becomes prevalent (*ca.* 70%, calculated by integration of ^{1}H NMR signals) (Figure 3.43).

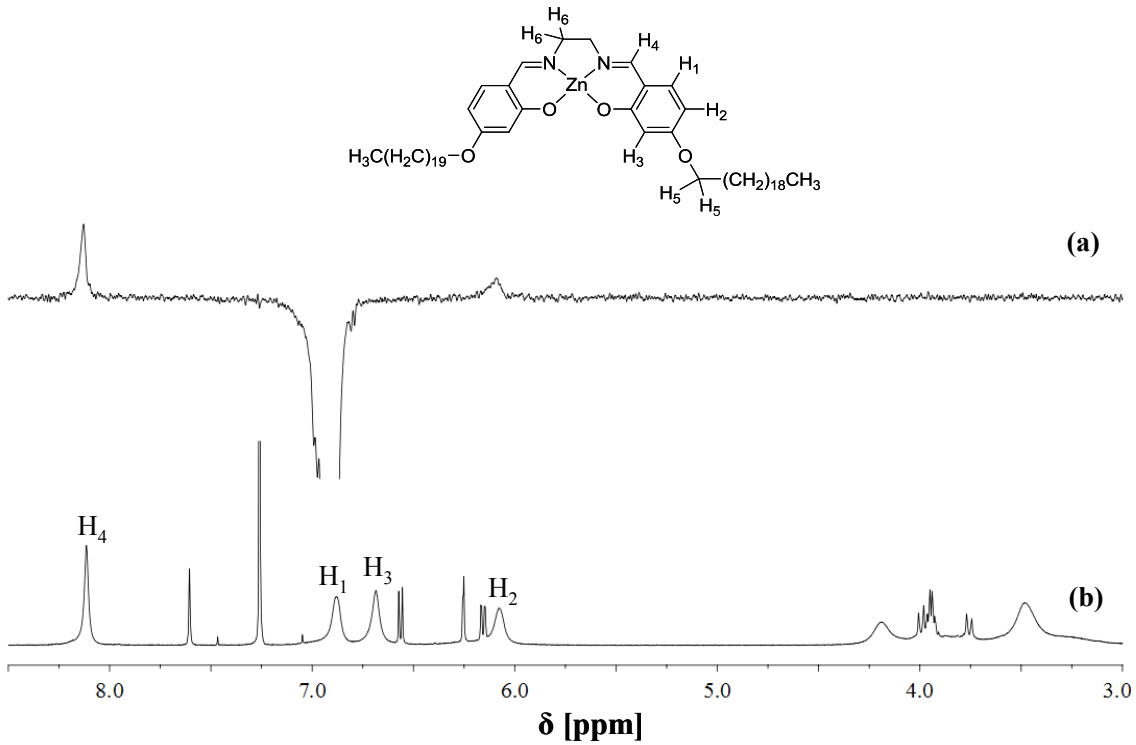

Figure 3.44 *(a)* 1D T-ROESY spectra upon selective irradiation of H_1 *(b)* and ^1H NMR of **5i** in $CDCl_3$ solution (5.0×10^{-3} M).

To further investigate this apparent concentration dependence behaviour, a series of ^1H NMR experiments have been performed on $CDCl_3$ solutions of **5i** (1.0×10^{-3} M) containing different concentration of water. Actually, upon passing from an unsaturated solution to a water-saturated $CDCl_3$ solution, a decrease of the **B**/**A** concentration ratio and an incipient demetallation are observed. The successive addition of D_2O, with the formation of a two-phase system, results in a progressive disappearance of species **B** and the appearance of a set of new ^1H NMR signals related to the demetallation of the complex. After 12 h, a complete disappearance of ^1H NMR signals of **5i** is observed, and the ^1H NMR spectrum corresponds to that of the uncomplexed ligand **5'** (Figure 3.45). Moreover, under these conditions, a white suspension in the NMR sample, is observed. An insoluble white precipitate then was isolated and characterized as $Zn(OH)_2$ by IR analysis. Analogous results are obtained from water-saturated $CDCl_3$ solutions after standing for several days. Analogous results are observed by even adding water or a DCl solution to $CDCl_3$ solutions of **5i**. In this last case, however, demetallation becomes faster.

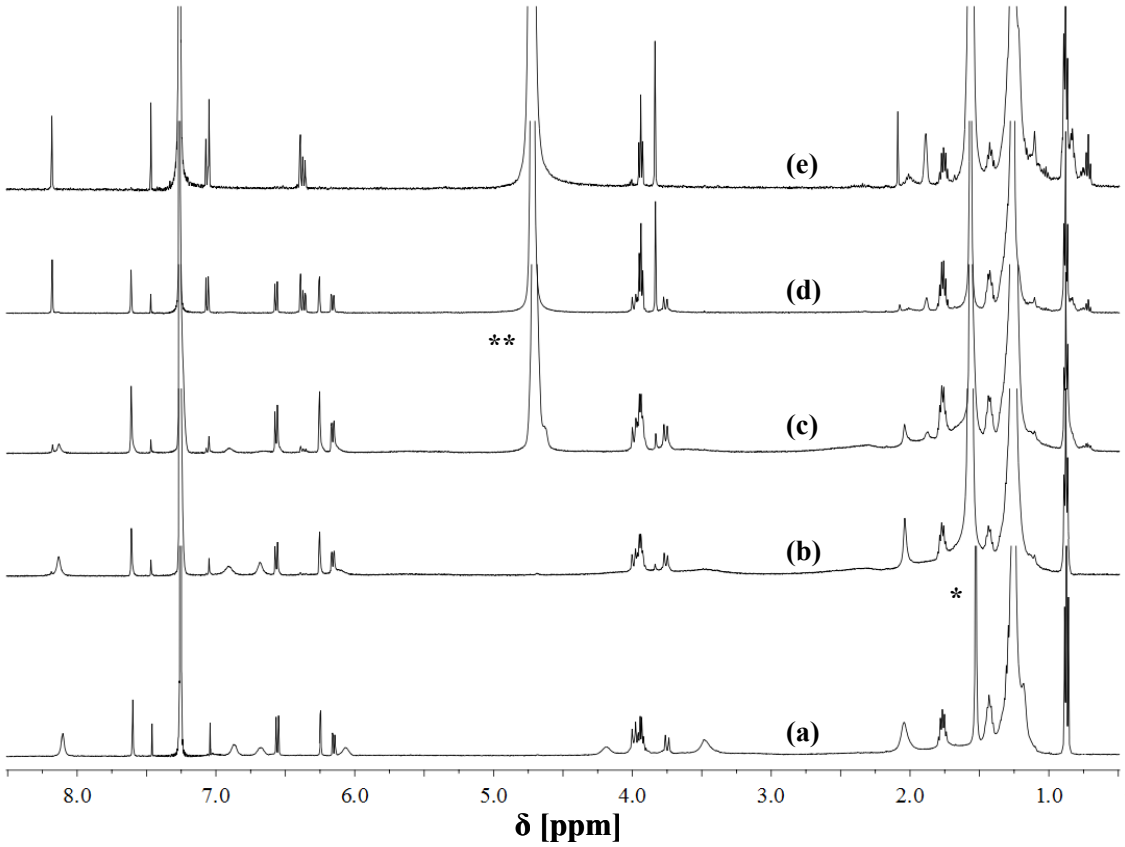

Figure 3.45 ^{1}H NMR spectra of **5i** in $CDCl_3$ solutions (1.0×10^{-3} M) containing different concentrations of water. *(a)* 3×10^{-3} M of water; **B**/**A** = 1.5. *(b)* water-saturated $CDCl_3$ solution (5×10^{-2} M); **B**/**A** = 1.0. *(c)* Recorded just after the addition of 2 μL of D_2O (formation of a two-phase system); **B**/**A** = 0.4. *(d)* Recorded after 1.5 h; **B**/**A** = 0. *(e)* Recorded after 12 h; the spectrum corresponds to that of the free ligand **5′**. The concentration of water in $CDCl_3$ and the **B**/**A** concentration ratio, have been estimated by integration of ^{1}H NMR signals. Single and double asterisked peaks refer to the signals of water in chloroform and water in suspension, respectively.

These data indicate a role of the amount of water dissolved in chloroform in determining the equilibrium between the two species **A** and **B**. Despite this, we do not observe evidence for coordinated water in the ^{1}H NMR spectra, presumably due to facile exchange. On the other hand, dimeric X-ray structures of bis(salicylaldiminato)Zn^{II} Schiff base derivatives always involve pentacoordinated Zn^{II} ions through intermolecular Zn···O axial interactions,[7] while no dimeric structures with hexacoordination around the Zn^{II} ion are reported for tetradentate Schiff base derivatives.[32] Monomeric structures that have axially coordinated water have been reported, for example, for the unsubstituted Zn(salen) derivative.[33] Moreover, it has been recently demonstrated theoretically that starting from the monomeric Zn(salen)·H_2O adduct, the formation of the dimer $[Zn(salen)]_2$ involves a negative Gibbs energy.[34]

These observations suggest that the species **A** is stabilized by the concentration of water dissolved in chloroform, although experimental data and the above observations suggest that the water is presumably involved in an intermediate species.

As far as species **B** is concerned, the broad nature of related ^{1}H NMR signals would suggest the presence of oligomeric aggregates or, alternatively, the existence of a slow (in the NMR time scale) conformational equilibrium involving species **B**. Therefore, we have used diffusion-ordered NMR spectroscopy (DOSY) to estimate the molecular mass of the species present in solution.[16,17] The ^{1}H NMR DOSY spectrum of **5i** in $CDCl_3$ (5.0×10^{-3} M) is separated into two components in the diffusion dimension, associated to the set of signals related to species **A** and **B**, in addition of signals at larger D values, because of the presence of the uncomplexed ligand **5'** used as reference. For both species, the estimated molecular mass clearly indicates the existence of dimers, although to the set of broad signals, species **B** is associated with a slightly larger D value and, hence, a smaller molecular mass (Table 3.9; Figure 3.46).

Table 3.9 Diffusion coefficients, *D*, and estimated molecular mass, *m*, for **5i** and **5i**·DMSO-d_6 adduct at 27°C in $CDCl_3$ (5.0×10^{-3} M).

	D (**5i**) ($\times 10^{-10}$ m^2 s^{-1})	*D* (**5′**) ($\times 10^{-10}$ m^2 s^{-1})	m^a (Da)	m^b (Da)	*% error*
A	4.50	6.80	1967	1849.5	6.3
B	4.80	6.80	1729	1849.5	6.5
5i·DMSO-d_6 [c]	5.55	5.80	958	1008.9	5.0

[a]Estimated molecular mass with eq 5 using **5′** as internal reference species (see paragraph **7.12** for details). [b]Expected molecular mass. [c]Obtained upon addition of 5000-fold mole excess of DMSO-d_6 to a $CDCl_3$ solution 5.0×10^{-3} M.

^{1}H NMR studies of **5i** in mixtures of non-coordinating/coordinating ($CDCl_3$/DMSO-d_6) solvents further support the existence of equilibrium between the two species (**A** and **B**). In fact, the progressive addition of defined amounts of DMSO-d_6 to $CDCl_3$ solutions (5.0×10^{-4} M) of **5i** leads to the predominant disappearance of signals associated with species **A**, with respect to those associated with species **B**. Finally, via the addition of a 5000-fold mole excess of DMSO-d_6 to a $CDCl_3$ solution of **5i**, both sets (**A** and **B**) of the proton signals merge in a unique set of signals (Figure 3.47), comparable to that recorded for complexes **5h-5b** in DMSO-d_6 (Figure 3.40).

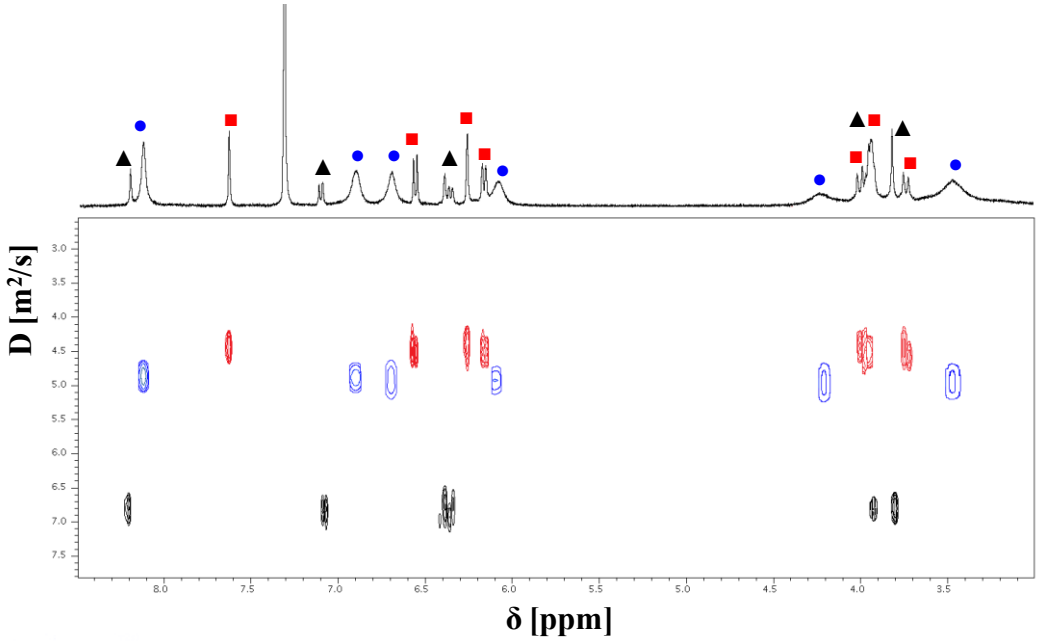

Figure 3.46 ^{1}H NMR DOSY spectrum of **5i** in $CDCl_3$ (5.0×10^{-3} M) in the presence of the free Schiff base ligand **5′** (5.0×10^{-3} M). The labelling of ^{1}H NMR signals refers to species **A** (■), **B** (●), and the free ligand (▲).

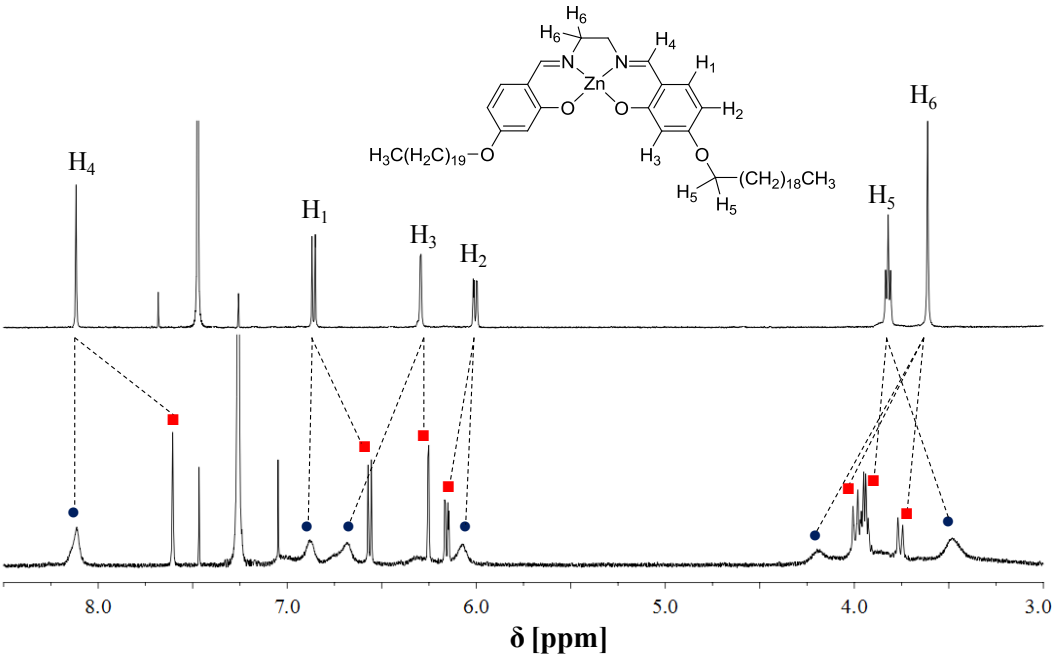

Figure 3.47 ^{1}H NMR spectra of **5i** in *(bottom)* $CDCl_3$ (5.0×10^{-4} M; 3.0×10^{-7} mol) and *(top)* with addition of 1.5×10^{-3} mol of DMSO-d_6. The labelling of ^{1}H NMR signals related to the $CDCl_3$ solution refers to species **A** (■) and **B** (●).

^{1}H NMR studies on changing the polarity of the non-coordinating solvent further insights into the equilibrium between species **A** and **B**. In particular, upon switching from chloroform to the slightly more polar tetrachloroethane solvent, a decrease of the

B/**A** concentration ratio is observed. Conversely, in the non polar tetrachloromethane solvent, **B** becomes the only observed species (Figure 3.48).

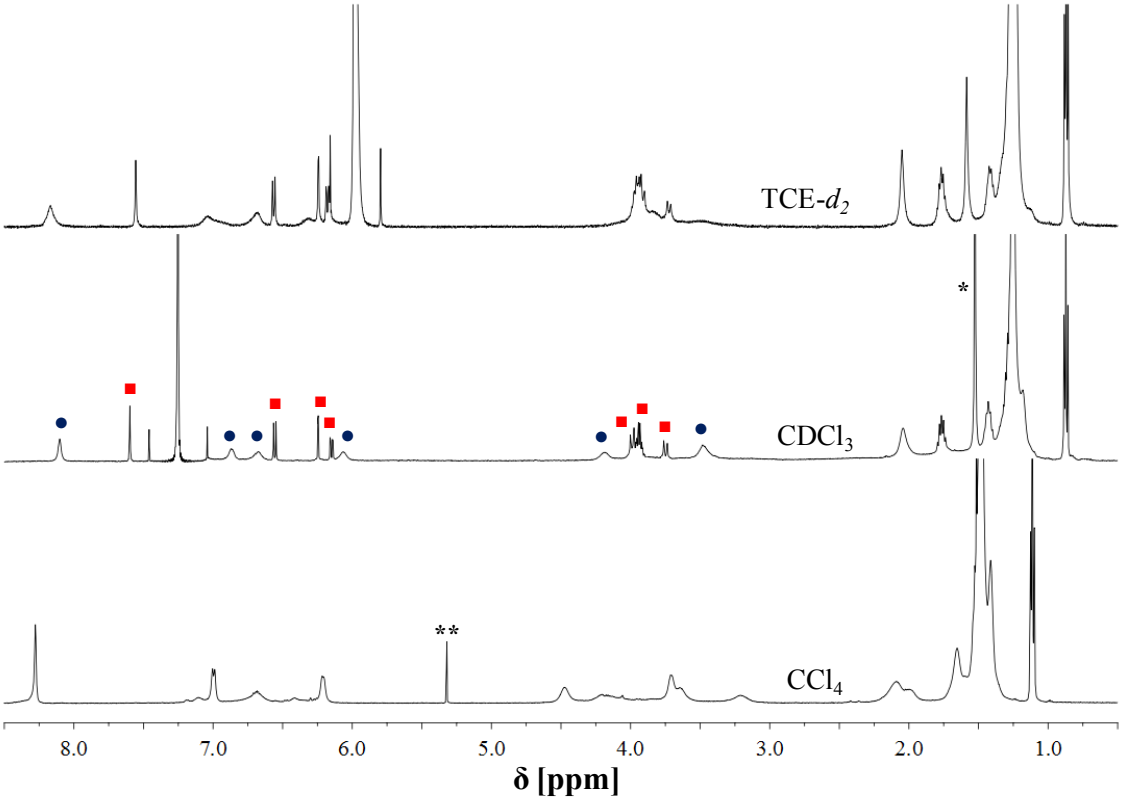

Figure 3.48 ^{1}H NMR spectra of **5i** (1.0×10^{-3} M) in various non-coordinating solvents. *(a)* 1.5×10^{-3} M of water; **B**/**A** = 1.3. *(b)* 3×10^{-3} M of water; **B**/**A** = 1.5. *(c)* water-saturated CCl_4 solution (1.15×10^{-2} M, Holbrook, M. T. "Carbon Tetrachloride"; *Kirk-Othmer Encyclopedia of Chemical Technology*, Wiley, 2000). The spectrum remains unchanged even in the dried (over molecular sieves) solvent or even recorded after 24 h. The concentration of water in *(a)* and *(b)* and the **B**/**A** concentration ratio, were estimated by integration of ^{1}H NMR signals. The labelling of ^{1}H NMR signals related to the $CDCl_3$ solution refers to species **A** (■) and **B** (●). The asterisked peak in the $CDCl_3$ and TCE-d_2 spectra refer to the signal of water in the solvents. The double asterisked peak in the CCl_4 spectrum is related to the residual solvent signal of DCM-d_2 external reference.

Variable-temperature ^{1}H NMR studies deserve further interesting investigations. Two non-coordinating solvents, $CDCl_3$ and TCE-d_2, have been considered. In particular, the latter solvent allows exploring at a higher temperature. Thus, ^{1}H NMR spectra of **5i** either in $CDCl_3$ or TCE-d_2 (5.0×10^{-3} M) indicate that, while the set of the sharp signals related to species **A** is almost temperature-independent in the investigated range, the broad signals related to species **B** are dependent on the temperature (Figure 3.49).

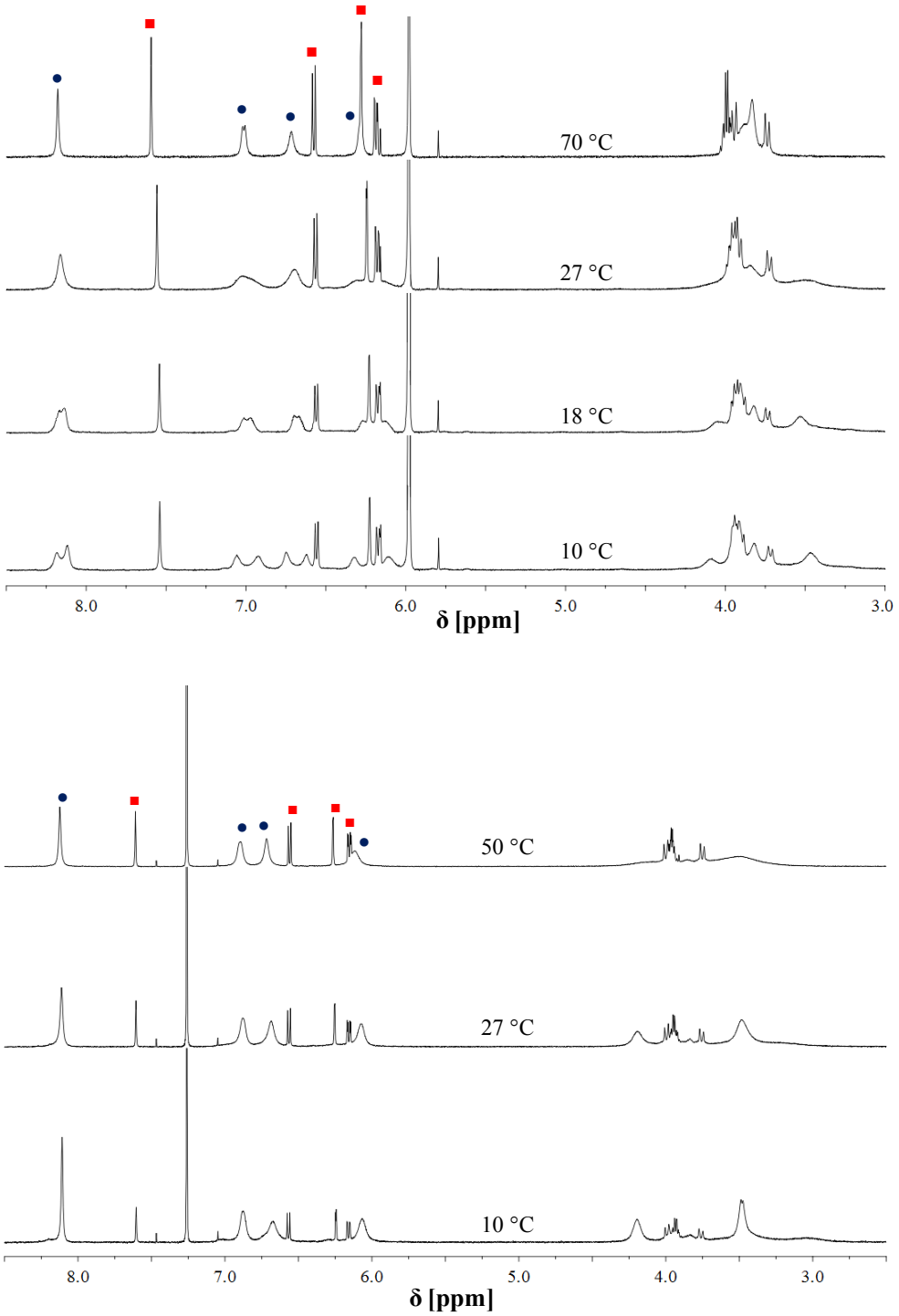

Figure 3.49 Variable temperature ^{1}H NMR spectra of **5i** (5.0×10^{-3} M) in *(top)* TCE-d_2 and *(bottom)* $CDCl_3$. The labelling of ^{1}H NMR signals refers to species **A** (■) and **B** (●).

In particular, in TCE-d_2, the broad signals recorded at room temperature, upon going down to 10°C, split into two sets of signals. On the other hand, exceeding the coalescence temperature (18°C), the broad signals become sharper as the temperature increases up to 70°C, and then remain unchanged up to 120°C. This is consistent with the existence of dimers of monomeric fragments that have magnetically equivalent protons, thus ruling out the formation of mixed SP-TBP dimeric species. Actually, the presence of mixed SP-TBP dimers would lead to a more complex ^{1}H NMR spectrum, including signals related to the TBP-TBP dimer. Moreover, the concentration ratio **B**/**A** increases as the temperature decreases, in both $CDCl_3$ and TCE-d_2 solvents.

3.4.1.2 Optical absorption studies

The absorption spectrum of complex **5b** in dilute solutions of non-coordinating solvents ($CHCl_3$, 1.0×10^{-4} M) consists of two main bands, at 297 nm and ~365nm (Figure 3.50a). On switching to DMSO, unlike to preceding studies on Zn^{II} having conjugated diamine bridge (see paragraphs **3.2.1.2**, **3.2.2**, **3.3.1.2** and **3.3.2**),[4d] a blue shift (~18 nm) of both absorption bands is observed. The addition of definite amounts of DMSO to $CHCl_3$ solutions of **5b** leads to optical changes analogous to those observed on switching to solutions of DMSO. In particular, by addition of 1.5×10^4-fold mole excess, the optical absorption spectrum of the resulting solution is comparable to that recorded in the coordinating DMSO solvent (Figure 3.50a).

UV-vis absorption spectra of complex **5i** in $CHCl_3$ are concentration-dependent (Figure 3.50b). While the absorption spectrum of the dilute solution (1.0×10^{-4} M) is almost identical to that recorded for complex **5b** at the same concentration (Figure 3.50b), more concentrated solutions are characterized by the progressive appearance of a new, blue shifted band at ~338 nm, while the band at 365 nm becomes a shoulder. Moreover, the presence of multiple isosbestic points clearly indicates the existence of an equilibrium between two different species.

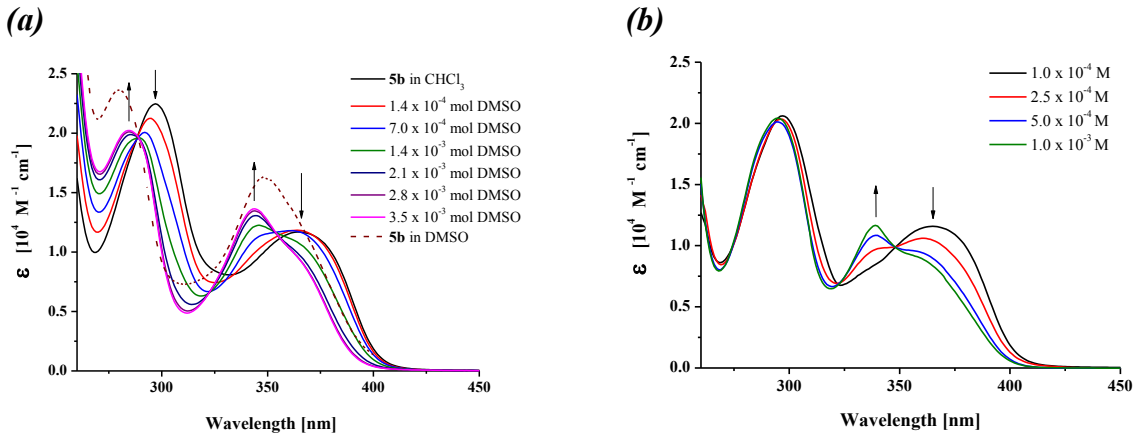

Figure 3.50 *(a)* UV-vis absorption spectra of **5b** (1.0×10^{-4} M; 2.0×10^{-7} mol) in $CHCl_3$, and with the addition of DMSO. The absorption spectrum of **5b** in DMSO (dotted line) is reported for comparison. *(b)* Concentration dependence of UV-vis absorption spectra of **5i** in chloroform. Absorption spectra were recorded on the solutions used for concentration dependence ^{1}H NMR experiments in Figure 3.43.

3.4.2 Discussion

The synthesis of the amphiphilic Schiff base Zn^{II} complexes **5h**, **5g**, **5b** and **5i**, which are relatively soluble even in low-polarity solvents, allowed us to perform a systematic study of their spectroscopic properties that, in turn, can be related to the aggregation/deaggregation process in solution.

For concentration ~1×10^{-4} M, optical absorption and ^{1}H NMR spectroscopic studies indicate that the behaviour in solutions of non-coordinating solvents for complexes **5h**, **5g** and **5b** seems to be analogous to that previously found for derivatives having conjugated bridging diamine. In particular, on switching from non-coordinating to coordinating solvents, the presence of sharp ^{1}H NMR signals and the observed ^{1}H NMR and optical absorption shifts are consistent with the existence of defined aggregate dimeric species (for example, in a pseudo-centrosymmetric fashion of the Zn(salen) units, twisted in opposite directions to each other). In particular, the lacking of conjugation between the salicylidene moieties, leads to a J-type coupling between the salicylidene groups of each unit in the dimer and, hence, a red shift of the optical absorption bands on switching from the monomer to the dimer.[35] In such an arrangement, both Zn^{II} atoms mutually interact through a Zn···O axial coordination, thus adopting a square-base pyramidal structure (**A**; Chart 3.9). This is consistent with the dimeric X-ray[7e] or the optimized[34] structure found for the unsubstituted Zn(salen) complex. A similar dimeric structure has been previously proposed in solution of non-

coordinating solvents for analogous Zn^{II} complexes having conjugated bridging diamines (see sections **3.2** and **3.3**).[4d]

In the case of complex **5i**, chloroform solutions at concentrations greater than 1×10^{-4} M show evidence of the formation of a new species **B** in slow equilibrium, with respect to the NMR time scale, with the species **A** predominantly observed at lower concentrations. This equilibrium is driven by the concentration of water dissolved in chloroform. In particular, it is proposed that the equilibrium between **A** and **B** presumably implies the interconversion of an intermediate monomer from a square pyramidal (SP) to a trigonal bipyramidal (TBP) structure,[36,37] through a pseudo-rotation[38] (Scheme 3.1). The water is likely involved in the intermediate monomeric SP species, which rapidly evolves toward the formation of the more-stable dimer, **A**.[34,39] On the other hand, water-saturated $CDCl_3$ solutions lead to demetallation with the formation of the free ligand **5'**. Thus, for species **B**, it is possible to suggest a structure in which both Zn^{II} atoms mutually interact through a Zn···O equatorial coordination, in a TBP arrangement, in which the Zn(salen) units lie orthogonal to each other (**B**; Chart 3.10). An analogous TBP configuration has been found in the X-ray structure of related Zn^{II} diamino-aliphatic derivatives,[7g,h] thus supporting this proposed structure.

Scheme 3.1 Proposed equilibrium involving the SP ⇄ TBP interconversion of complex **5i** in concentrate solutions of non-coordinating solvents.

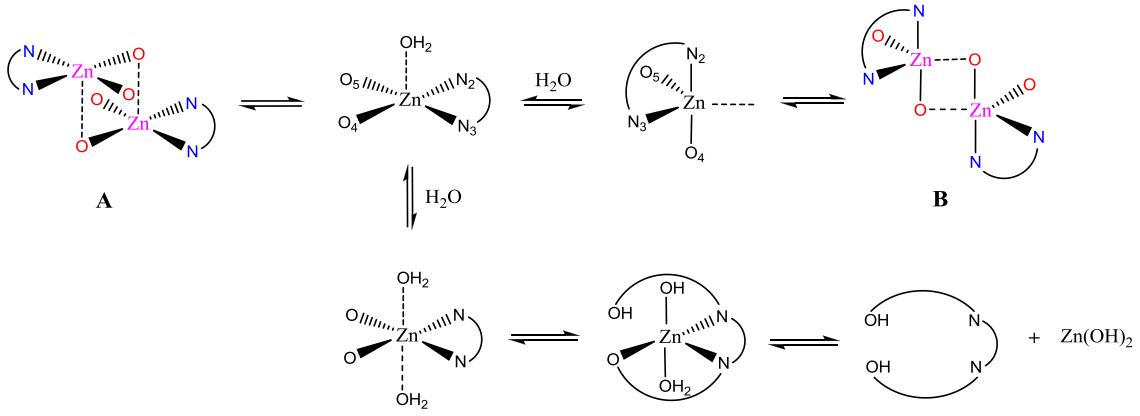

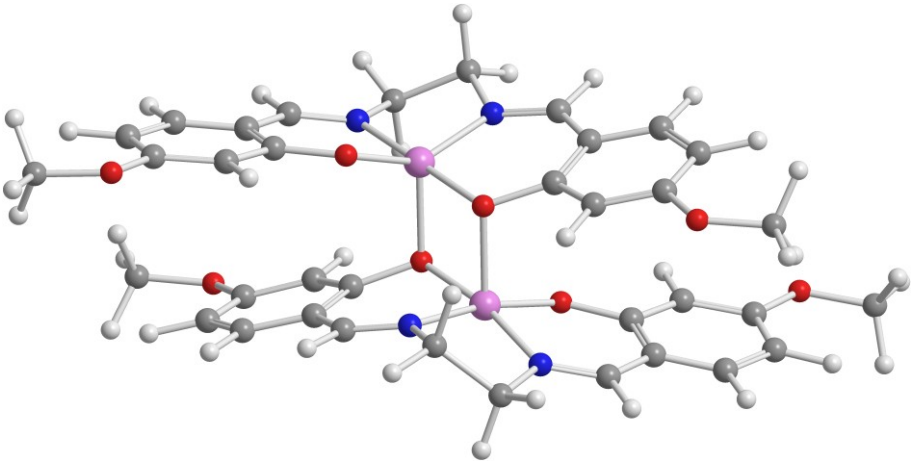

Chart 3.9 Modeling (MM+) of the proposed structure **A** for complexes **5h**, **5g**, **5b** and **5i** in dilute solutions of non-coordinating solvents. Side alkyl chains were replaced by methyl groups for clarity of representation. Side alkyl chains were replaced by methyl groups for clarity of representation.

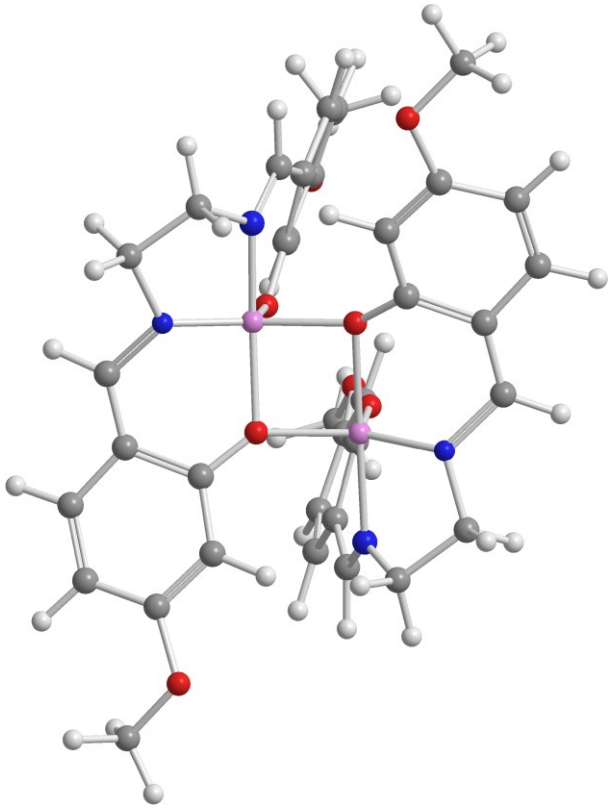

Chart 3.10 Modeling (MM+) of the proposed structure **B** for the complex **5i** in concentrated solutions of non-coordinating solvents. Side alkyl chains were replaced by methyl groups for clarity of representation. Side alkyl chains were replaced by methyl groups for clarity of representation.

The proposed structure **B** is consistent with UV-vis, ^{1}H NMR, DOSY NMR results, and deaggregation studies. In fact, the ^{1}H NMR chemical shifts of the broad signals related to species **B** ($CDCl_3$, 5.0×10^{-4} M), except the H_3 signals that are downfield shifted (0.40 ppm), are almost identical to those found upon the addition of a large mole excess of DMSO-d_6 (Figure 3.47). This is indicative that, at variance of the sharp signals related to species **A**, upon switching from species **B** to the monomer, these involved protons are almost in the same chemical and magnetic environment, thus excluding any structure in a twisted arrangement between the Zn(salen) units, as in the case of structure **A** (Chart 3.9). Accordingly, in structure **B**, except for H_3 hydrogens, which are deshielded, the remaining aromatic and CH=N hydrogens would not be influenced by the ring current effect of the salicylidene moieties of the other molecular unit (Chart 3.10).

The observed blue shift of the longer wavelength band in UV-vis absorption spectra of concentrated $CHCl_3$ solutions of **5i** (Figure 3.50b) is also consistent with a structure in which the two Zn(salen) units of the dimer are barely interacting. Actually, these UV-vis spectra resemble those achieved upon deaggregation of dilute $CHCl_3$ solutions of **5b** where species **A** is predominant.

Finally, the different molecular shape associated with the two (**A** and **B**) structures may account for the different observed diffusion coefficient values. In particular, the larger diffusion coefficient associated with structure **B** may be related to a more oblate spheroid shape of this dimeric aggregate (Chart 3.10), with respect that of structure **A** (Chart 3.9).[17]

^{1}H NMR studies on changing the polarity of the non-coordinating solvent may be of interest to get further insights into the nature of the involved species **A** and **B**. Actually, independent from the concentration, species **B** seems to be favoured upon decreasing the solvent polarity. This reflects a more hydrophobic nature of species **B**, with respect to **A**. Note that, independently from the amount of water dissolved in the solvent, CCl_4 solutions of complex **5i** are much more stable than those in $CDCl_3$, since no appreciable demetallation is observed after 24 h. This suggests that species **B** is not influenced by the presence of water, thus supporting the above involved equilibria (Scheme 3.1).

Overall, these results are in strict contrast to above studies in solution of non-coordinating solvents on related bis(salicylaldiminato)Zn^{II} derivatives having

conjugated bridging diamines (see sections **3.2** and **3.3**).[4d] In fact, we have found that they are always characterized as single dimeric species, while in the cases where a concentration dependence occurs, it affects the degree of aggregation. Thus, for present complexes, the existence of two different species, **A** and **B**, may be related to an improved conformation flexibility of the salen ligand, by virtue of the non-conjugated diamine bridge.

Variable-temperature ^{1}H NMR data further insight about aggregation behaviour of complex **5i**. In fact, these ^{1}H NMR data show the existence of a non equivalent species **B′** involved in a fluxional equilibrium with species **B**, through a Berry pseudorotation,[38,40] thus leading to two different sets of ^{1}H NMR signals. In particular, upon switching from **B** to **B′**, the Zn···O interactions change from mutually equatorial to mutually axial (Scheme 3.2).

By using the Gutowski-Holm approximation,[41] from the coalescence temperature and Δν values, a Gibbs free energy barrier of 14 kcal mol^{-1} is estimated for the **B** ⇄ **B'** interconversion. This Gibbs free energy barrier is consistent with that found for Berry pseudo-rotations in chelate metal complexes.[38b,42]

Scheme 3.2 Proposed Berry pseudorotation involving the **B** ⇄ **B′** interconversion of complex **5i**.

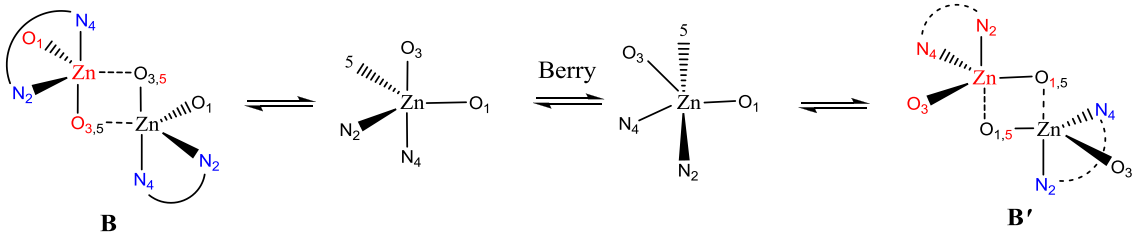

3.5 Conclusions

Amphiphilic dipolar Zn^{II} Schiff base complexes, relatively soluble in a wide variety of solvents, ranging from polar coordinating to non polar non-coordinating species, have allowed performing a detailed study on their spectroscopic properties, in relation to the aggregation/deaggregation process in solution.

These species always form aggregates in solutions of non-coordinating solvents and the degree and type of aggregation are related to the nature of the bridging diamine. The effect of the alkyl chain length seems to play a minor role in the aggregation properties, since ^1H NMR data, optical absorption and fluorescence spectra remain almost unaltered upon changing the chain lengths.

Solutions of the complexes where the bridging diamine contains the naphthalene or the pyridine nucleus are always characterized by the presence of defined dimer aggregates, whereas oligomeric aggregates are likely formed for complexes having the benzene bridge.

For complexes with the 2,3-diaminomaleonitrile as bridging diamine, the degree of aggregation is concentration dependence. Dilute solutions are likely characterized by the presence of defined dimer aggregates, whereas larger oligomeric aggregates are conceivably formed at higher concentrations. The threshold of concentration in which this is observed depends upon solvent polarity. Moreover, the NLO properties of this kind of complexes are concentration dependent. In particular, on passing from oligomeric to defined dimer aggregates upon dilution, the NLO response increase rapidly.

Among the amphiphilic Zn(salen) complexes, an unusual aggregation behaviour in solution of non-coordinating solvents which may be related to the non-conjugated, conformational flexible nature of the bridging diamine of the Schiff base is observed. Actually, a reversible equilibrium between two defined dimeric species is observed, driven by the concentration of water dissolved in chloroform. Dilute $CHCl_3$ solutions are characterized by the presence of defined dimers, presumably in a pseudo-centrosymmetric fashion of the Zn(salen) units, in which both Zn^{II} atoms mutually interact through a Zn···O axial coordination, thus adopting a square-base pyramidal structure (**A**). Investigations into higher concentrations of **5i** suggest the existence of a new dimeric species, **B**, which is in equilibrium with that observed at lower

concentrations. In particular, it has been proposed that the equilibrium between these two species involves a coordination mode interconversion of an intermediate monomer presumably from a SP to a TBP structure, in which the Zn(salen) units lie orthogonal to each other. The water is likely involved in the intermediate monomeric SP species, which rapidly evolves toward the formation of the more stable dimer (**A**). Variable-temperature ^{1}H NMR studies are consistent with the existence of a nonequivalent species **B′** involved in a fluxional equilibrium with species **B**, through a Berry pseudo-rotation. Solutions of **5i** in the non polar tetrachloromethane solvent are always characterized as species **B**, in agreement with its more hydrophobic nature.

Complexes having benzene ring bridge form fibrillar nanostructures by drop-casting of THF solutions on substrates of Si(100). In the drop-casting process, the Zn···O interactions allow the formation of stable, tangled fibrillar nanostructures whose morphology is concentration independent. Side alkyl chains influence the width of nanofibers because their length implies a different degree of interdigitation.

In coordinating solvents or in the presence of coordinating species, a complete deaggregation of all complexes occurs because of the axial coordination to the Zn^{II} ion, accompanied by considerable changes of the ^{1}H NMR and optical absorption, fluorescence and NLO properties. Thus, Zn^{II} Schiff base complexes represent suitable synthons for the design and development of new supramolecular architectures with large second-order NLO responses and of supramolecular fluorescent probes.

Finally, as the amount of coordinating species is dependent of Lewis character of Zn^{II} ion, the deaggregation data with DMSO for complexes **1**-**5** allows estimation of their relative tendency to deaggregation and, hence, their Lewis acidity. Thus, an order of the Lewis acidic character **1** > **4** > **3** > **2** > **5** can be established for the aggregate complexes in solution of non-coordinating solvents.

3.6 References

1. See, for example: *(a)* Steed, J. W.; Turner, D. R.; Wallace K. J. *Core Concepts in Supramolecular Chemistry and Nanochemistry*, Wiley, 2009. *(b)* Lehn, J.-M. *Supramolecular Chemistry*, VCH, Weinheim, 1995. *(c)* Balzani, V.; Scandola, F. *Supramolecular Photochemistry*, Horward, Chichester, U.K., 1991.
2. See, for example: Molecular Biology of Protein Folding, ed. M. Conn, in *Progress in Molecular Biology and Translational Science*, Academic Press, London, vol. 83, 2008.
3. For recent selected contributions of studies in solution see, for example: *(a)* Chen, Z.; Lohr, A.; Saha-Möller, C. R.; Würthner, F. *Chem. Soc. Rev.* **2009**, *38*, 564. *(b)* Lohr, A.; Grüne, M.; Würthner, F. *Chem. Eur. J.* **2009**, *15*, 3691. *(c)* Rösch, U.; Yao, S.; Wortmann, R.; Würthner, F. *Angew. Chem. Int. Ed.* **2006**, *45*, 7026. *(d)* Würthner, F. *Chem. Commun.* **2004**, 1564. *(e)* Würthner, F.; Yao, S.; Beginn, U. *Angew. Chem. Int. Ed.* **2003**, *42*, 3247. *(f)* Würthner, F.; Yao, S.; Debaerdemaeker, T.; Wortmann, R. *J. Am. Chem. Soc.* **2002**, *124*, 9431.
4. *(a)* Consiglio, G.; Failla, S.; Finocchiaro, P.; Oliveri, I. P.; Di Bella, S. *Inorg. Chem.* **2012**, *51*, 8409. *(b)* Consiglio, G.; Failla, S.; Finocchiaro, P.; Oliveri, I. P.; Di Bella, S. *Dalton Trans.* **2012**, *41*, 387. *(c)* Consiglio, G.; Failla, S.; Finocchiaro, P.; Oliveri, I. P.; Purrello, R.; Di Bella, S. *Inorg. Chem.* **2010**, *49*, 5134. *(d)* Consiglio, G.; Failla, S.; Oliveri, I. P.; Purrello, R.; Di Bella, S. *Dalton Trans.* **2009**, 10426.
5. For recent reviews see, for example: *(a)* Kleij, A. W. *Eur. J. Inorg. Chem.* **2009**, 193. *(b)* Kleij, A. W. *Chem. Eur. J.* **2008**, *14*, 10520. *(c)* Wezenberg, S. J.; Kleij, A. W. *Angew. Chem. Int. Ed.* **2008**, *47*, 2354. *(d)* Clever, G. H.; Carell, T. *Angew. Chem. Int. Ed.* **2007**, *46*, 250. *(e)* Cozzi, P. G. *Chem. Soc. Rev.* **2004**, *33*, 410. *(f)* Di Bella, S. *Chem. Soc. Rev.* **2001**, *30*, 355. *(g)* Lacroix, P. G. *Eur. J. Inorg. Chem.* **2001**, 339.
6. Kleij, A. W. *Dalton Trans.* **2009**, 4635.
7. *(a)* Martínez Belmonte, M.; Wezenberg, S. J.; Haak, R. M.; Anselmo, D.; Escudero-Adán, E. C.; Benet-Buchholz, J.; Kleij, A W *Dalton Trans.* **2010**, *39*, 4541. *(b)* Escudero-Adán, E. C.; Benet-Buchholz, J.; Kleij, A. W. *Inorg. Chem.* **2008**, *47*, 4256. *(c)* Gallant, A. J.; Chong, J. H.; MacLachlan, M. J. *Inorg. Chem.* **2006**, *45*, 5248. *(d)* Kleij, A. W.; Kuil, M.; Lutz, M.; Tooke, D. M.; Spek, A. L.;

Kamer, P. C. K.; vanLeeuwen, P. W. N. M.; Reek, J. N. H. *Inorg. Chim. Acta.* **2006**, *359*, 1807. *(e)* Odoko, M.; Tsuchida, N.; Okabe, N. *Acta Crystallogr., Sect. E: Struct. Rep. Online* **2006**, *E62*, m708. *(f)* Kleij, A. W.; Kuil, M.; Tooke, D. M.; Lutz, M.; Spek, A. L.; Reek J. N. H. *Chem. Eur. J.* **2005**, *11*, 4743. *(g)* Matalobos, J. S.; García-Deibe, A. M.; Fondo, D. N.; Bermejo, M. R. *Inorg. Chem. Commun.* **2004**, *7*, 311. *(h)* Reglinski, J.; Morris S.; Stevenson, D. E. *Polyhedron* **2002**, *21*, 2175.

8. *(a)* Hui, J. K.-H.; Yu, Z.; MacLachlan, M. J. *Angew. Chem. Int. Ed.* **2007**, *46*, 7980. *(b)* Ma, C. T. L.; MacLachlan, M. J. *Angew. Chem. Int. Ed.* **2005**, *44*, 4178.
9. *(a)* Bhattacharjee, C. R.; Das, G.; Mondal, P.; Prasad, S. K.; Rao, D. S. S. *Eur. J. Inorg. Chem.* **2011**, 1418. *(b)* Wezenberg, S. J.; Escudero-Adán, E. C.; Benet-Buchholz, J.; Kleij, A. J. *Chem. Eur. J.* **2009**, *15*, 5695. *(c)* Leung, A. C. W.; MacLachlan, M. J. *J. Mater. Chem.* **2007**, *17*, 1923.
10. *(a)* Hui, J. K.-H.; MacLachlan, M. J. *Dalton Trans.* **2010**, *39*, 7310. *(b)* Elemans, J. A. A. W.; Wezenberg, S. J.; Coenen, M. J. J.; Escudero-Adán, E. C.; Benet-Buchholz, J.; den Boer, D.; Speller, S.; Kleij A. W.; De Feyter, S. *Chem. Commun.* **2010**, *46*, 2548. *(c)* Hui, J. K.-H.; Yu, Z.; Mirfakhrai, T.; MacLachlan, M. J. *Chem. Eur. J.* **2009**, *15*, 13456. *(d)* Jung, S.; Oh, M. *Angew. Chem. Int. Ed.* **2008**, *47*, 2049.
11. *(a)* Liuzzo, V.; Oberhauser, W.; Pucci, A. *Inorg. Chem. Commun.* **2010**, *13*, 686. *(b)* Bhattacharjee, C. R.; Das, G.; Mondal, P.; Rao, N. V. S. *Polyhedron* **2010**, *29*, 3089. *(c)* Kuo, K.-L.; Huang, C.-C.; Lin, Y.-C. *Dalton Trans.* **2008**, 3889. *(d)* Son, H.-J.; Han, W.-S.; Chun, J.-Y.; Kang, B.-K.; Kwon, S.-N.; Ko, J.; Han, S. J.; Lee, C.; Kim, S. J.; Kang, S. O. *Inorg. Chem.* **2008**, *47*, 5666. *(e)* Lin, H.-C.; Huang, C.-C.; Shi, C.-H.; Liao, Y.-H.; Chen, C.-C.; Lin, Y.-C; Liu, Y.-H. *Dalton Trans.* **2007**, 781. *(f)* Di Bella, S.; Leonardi, N.; Consiglio, G.; Sortino, S.; Fragalà, I. *Eur. J. Inorg. Chem.* **2004**, 4561. *(g)* Ma, C.; Lo, A.; Abdolmaleki, A.; MacLachlan, M. J. *Org. Lett.* **2004**, *6*, 3841. *(h)* Chang, K.-H.; Huang, C.-C.; Liu, Y.-H.; Hu, Y.-H.; Chou, P.-T.; Lin, Y.-C. *Dalton Trans.* **2004**, 1731. *(i)* La Deda, M.; Ghedini, M.; Aiello, I.; Grisolia, A. *Chem. Lett.* **2004**, *33*, 1060. *(l)* Wang, P.; Hong, Z.; Xie, Z.; Tong, S.; Wong, O.; Lee, C.-C.; Wong, N.; Hung, L.; Lee, S. *Chem. Commun.* **2003**, 1664.
12. *(a)* Cano, M.; Rodríguez, L.; Lima, J. C.; Pina, F.; Dalla Cort, A.; Pasquini, C.; Schiaffino, L. *Inorg. Chem.* **2009**, *48*, 6229. *(b)* Germain, M. E.; Knapp, M. J. *J. Am. Chem. Soc.* **2008**, *130*, 5422. *(c)* Germain, M. E.; Vargo, T. R.; Khalifah, G. P.;

Knapp, M. J. *Inorg. Chem.* **2007**, *46*, 4422. *(d)* Dalla Cort, A.; Mandolini, L.; Pasquini, C.; Rissanen, K.; Russo, L.; Schiaffino, L. *New J. Chem.* **2007**, *31*, 1633.

13. *(a)* Di Bella, S.; Consiglio, G.; Sortino, S.; Giancane, G.; Valli, L. *Eur. J. Inorg. Chem.* **2008**, 5228. *(b)* Di Bella, S.; Consiglio, G.; La Spina, G.; Oliva, C.; Cricenti, A. *J. Chem. Phys.* **2008**, *129*,114704.
14. *(a)* Di Bella, S.; Oliveri, I. P.; Colombo, A.; Dragonetti, C.; Righetto, S.; Roberto, D. *Dalton Trans.* **2012**, *41*, 7013. *(b)* Di Bella, S.; Dragonetti, C.; Pizzotti, M.; Roberto, D.; Tessore F.; Ugo, R. *Top. Organomet. Chem.*, **2010**, *28*, 1. *(c)* Lacroix, P. G.; Di Bella, S.; Ledoux, I. *Chem. Mater.*, **1996**, *8*, 541.
15. See, for example: *(a)* Branchi, B.; Ceroni, P.; Balzani, V.; Cartagena, M. C.; Klämer, F.-G.; Schrader, T.; Vogtle, F. *New. J. Chem.* **2009**, *33*, 397. *(b)* Zhang, F.; Bai, S.; Yap, G. P. A.; Tarwade, V.; Fox, J. M. *J. Am. Chem. Soc.* **2005**, *127*, 10590. *(c)* Barnard, P. J.; Vagg, R. S. J. *Inorg. Biochem.* **2005**, *99*, 1009. *(d)* Gunter, M. J.; Farquhar, S. M. *Org. Biomol. Chem.* **2003**, *1*, 3450. *(e)* Chen, M. J.; Rathke, J. W. J. *Porphyrins Phthalocyanines* **2001**, *5*, 528. *(f)* Montaudo, G.; Caccamese, S.; Finocchiaro, P. *J. Am. Chem. Soc.* **1971**, *93*, 4202.
16. *(a)* Johnson Jr., C. S. *Prog. Nucl. Magn. Reson.* **1999**, *34*, 203. *(b)* Morris, K. F.; Johnson Jr., C. S.; *J. Am. Chem. Soc.* **1992**, *114*, 3139.
17. *(a)* Macchioni, A.; Ciancaleoni, G.; Zuccaccia, C.; Zuccaccia, D. in *From Supramolecular Chemistry: From Molecules to Nanomaterials;* Steed, J. W.; Gale, P. A.; Wiley: New York, 2012; Vol. 2, pp 319. *(b)* Macchioni, A.; Ciancaleoni, G.; Zuccaccia, C.; Zuccaccia, D. *Chem. Soc. Rev.* **2008**, *37*, 479. *(c)* Pregosin, P. S. *Prog. Nucl. Magn. Reson. Spectrosc.* **2006**, *49*, 261. *(d)* Song, F.; Lancaster, S. J.; Cannon, R. D.; Schormann, M.; Humphrey, S. M.; Zuccaccia, C.; Macchioni, A.; Bochmann, M. *Organometallics* **2005**, *24*, 1315.
18. *(a)* Gil, V. M. S.; Oliveira, N. C. *J. Chem. Educ.* **1990**, *67*, 473. *(b)* Hill, Z. D.; MacCarthy, P. *J. Chem. Educ.* **1986**, *63*, 162. *(c)* Job, P. *Ann. Chem.* **1928**, *9*, 113.
19. For recent reviews, see for example: *(a)* Maury, O.; Le Bozec, H. in *Molecular Materials*, ed. D. W. Bruce, D. O'Hare and R. I. Walton, Wiley, Chichester, 2010, pp. 1. *(b)* Humphrey, M. G.; Samoc, M. *Adv. Organomet. Chem.* **2008**, *55*, 61. *(c)* Coe, B. J. *Acc. Chem. Res.* **2006**, *39*, 383. *(d)* Cariati, E.; Pizzotti, M.; Roberto, D.; Tessore, F.; Ugo, R. *Coord. Chem. Rev.* **2006**, *250*, 1210. *(e)* Maury, O.; Le Bozec,

H. *Acc. Chem. Res.* **2005**, *38*, 691. *(f)* Powell, C. E.; Humphrey, M. G. *Coord. Chem. Rev.* **2004**, *248*, 725. *(g)* Coe, B. J.; Curati, N. R. M. *Comments Inorg. Chem*. **2004**, *25*, 147. *(h)* Coe, B. J. in *Comprehensive Coordination Chemistry II*, ed. J. A. McCleverty and T. J. Meyer, Elsevier Pergamon, Oxford, U.K., 2004, vol. 9, pp. 621.

20. Guggenheim, E. A. *Trans. Faraday Soc.* **1949**, *45*, 714.
21. Ledoux, I.; Zyss, J. *Chem. Phys.* **1982**, *73*, 203.
22. Di Bella, S. *New J. Chem.* **2002**, *26*, 495.
23. See, for example: *(a)* Bilakhiya, A. K.; Tyagi, B.; Paul, P.; Natarajan, P. *Inorg. Chem.* **2002**, *41*, 3830. *(b)* Tominaga, T. T.; Yushmanov, V. E.; Borissevitch, I. E.; Imasato, H.; Tabak, M. J. *Inorg. Biochem.* **1997**, *65*, 235.
24. See, for example: *(a)* Sasaki, H.; Arai, H.; Cocco, M. J.; White, S. H. *Biophys. J.* **2009**, *96*, 2727. *(b)* Da Costa, G.; Chevance, S.; Le Rumeur, E.; Bondon, A. *Biophys. J.* **2006**, *90*, L55. *(c)* Evertsson, H.; Nilsson, S.; Welch, C. J.; Sundelöf, L.-O. *Langmuir* **1998**, *14*, 6403.
25. Lacroix, P. G.; Di Bella, S.; Ledoux, I. *Chem. Mater.* **1996**, *8*, 541.
26. Wezenberg, S. J.; Escudero-Adán, E. C.; Benet-Buchholz, J.; Kleij, A. W. *Org. Lett.* **2008**, *10*, 3311.
27. *(a)* Vitalini, D.; Mineo, P.; Di Bella, S.; Fragalà, I.; Maravigna, P.; Scamporrino, E. *Macromolecules* **1996**, *29*, 4478. *(b)* Kanis, D. R.; Lacroix, P. G.; Ratner, M. A.; Marks, T. J. *J. Am. Chem. Soc.* **1994**, *116*, 10089.
28. *(a)* Trujillo, A.; Fuentealba, M.; Carrillo, D.; Manzur, C.; Ledoux-Rak, I.; Hamon, J.-R.; Saillard, J.-Y. *Inorg. Chem.* **2010**, *49*, 2750. *(b*) Gradinaru, J.; Forni, A.; Druta, V.; Tessore, F.; Zecchin, S.; Quici, S.; Garbalau, N. *Inorg. Chem.* **2007**, *46*, 884. *(c)* Rigamonti, L.; Demartin, F.; Forni, A.; Righetto, S.; Pasini, A. *Inorg. Chem.* **2006**, *45*, 10976. *(d)* Costes, J. P.; Lamère, J. F.; Lepetit, C.; Lacroix, P. G.; Dahan, F.; Kakatani, K. *Inorg. Chem.* **2005**, *44*, 1973. *(e)* Lacroix, P. G.; Averseng, F.; Malfant, I.; Nakatani, K. *Inorg. Chim. Acta* **2004**, *357*, 3825. *(f)* Di Bella, S.; Fragalà, I. *New. J. Chem.* **2002**, *26*, 285. *(g)* Di Bella, S.; Fragalà, I.; Ledoux, I.; Zyss, J. *Chem. Eur. J.* **2001**, *7*, 3738. *(h)* Di Bella, S.; Fragalà, I. *Synth. Met.* **2000**, *115*, 191. *(i)* Averseng, F.; Lacroix, P. G.; Malfant, I.; Lenoble, G.; Cassoux, P.; Nakatani, K.; Maltey-Fanton, I.; Delaire, J. A.; Aukauloo, A. *Chem. Mater.* **1999**,

11, 995. *(j)* Di Bella, S.; Fragalà, I.; Ledoux, I.; Diaz-Garcia, M. A.; Marks, T. J. *J. Am. Chem. Soc.* **1997**, *119*, 9550. *(k)* Di Bella, S.; Fragalà, I.; Marks, T. J.; Ratner, M. A. *J. Am. Chem. Soc.* **1996**, *118*, 12747. *(l)* Di Bella, S.; Fragalà, I.; Ledoux, I.; Marks, T. J. *J. Am. Chem. Soc.* **1995**, *117*, 9481.

29. Singer, K. D.; Sohn, J. E.; King, L. A.; Gordon, H. M.; Katz, H. E.; Dirk, C. W. *J. Opt. Soc. Am. B* **1989**, *6*, 1339.
30. *(a)* Montaudo; G.; Finocchiaro, P. *J. Am. Chem. Soc.* **1972**, *94*, 6745. *(b)* Johnson, C. E.; Bovey, F. A. *J. Chem. Phys.* **1958**, *29*, 1012.
31. In the case of complex **5i**, because of its insolubility in DMSO, the spectrum in DMSO-d_6 has been extrapolated from that in $CDC1_3$ upon the addition of a 5000-fold mole excess of DMSO-d_6 (see infra).
32. Actually, hexacoordinated Zn^{II} complexes are common for tridentate Schiff base ligands. See, for example: *(a)* Samanta, B.; Chakraborty, J.; Shit, S.; Batten, S. R.; Jensen, P.; Masuda, J. D.; Mitra, S. *Inorg. Chim. Acta* **2007**, *360*, 2471. *(b)* Basak, S.; Sen, S.; Banerjee, S.; Mitra, S.; Rosair, G.; Garland Rodriguez, M. T. *Polyhedron* **2007**, *26*, 5104. *(e)* Correia, V. R.; Bortoluzzi, A. J.; Neves, A.; Joussef, A. C.; Vieira, M. G. M.; Batista, S. C. *Acta Crystallogr., Sect. E: Struct. Rep. Online* **2003**, *E59*, m464.
33. Hall, D.; Moore, F. H. *J. Chem. Soc. A* **1966**, 1822.
34. Vladimirova, K. G.; Freidzon, A. Y.; Kotova, O. V.; Vaschenko, A. A.; Lepnev, L. S.; Bagatur'yants, A. A.; Vitukhnovskiy, A. G.; Stepanov, N. F.; Atfimov; M. V. *Inorg. Chem.* **2009**, *48*, 11123.
35. See, for example: *(a)* Beletskaya, I.; Tyurin, V. S.; Tsivadze, A. Y.; Guilard, R.; Stern, C. *Chem. Rev.* **2009**, *109*, 1659. *(b)* Di Bella, S.; Ratner, M. A.; Marks, T. J. *J. Am. Chem. Soc.* **1992**, *114*, 5842.
36. Holmes, R. R. *Prog. Inorg. Chem.* **1984**, *32*, 119.
37. See, for example: *(a)* Blagg, R. J.; Adams, C. J.; Charmant, J. P. H.; Connelly, N. G.; Haddow, M. F.; Hamilton, A.; Knight, J.; Orpen, A. G.; Ridgway, B. M. *Dalton Trans.* **2009**, 8724. *(b)* Casares, J. A.; Espinet, P. *Inorg. Chem.* **1997**, *36*, 5428.
38. For recent, general accounts on pseudo-rotation see, for example: *(a)* Moberg, C. *Angew. Chem., Int. Ed.* **2011**, *50*, 10290. *(b)* Couzijn, E. P. A.; Slootweg, J. C.; Ehlers, A. W.; Lammertsma, K. *J. Am. Chem. Soc.* **2010**, *132*, 18127.

39. Geometry optimization by semiempirical (MP3) calculations on the Zn(salen)·H_2O monomeric adduct in a SP or TBP structure indicates a more-stable structure in the former case.
40. Berry, R. S. *J. Chem. Phys.* **1960**, *32*, 933.
41. Gutowsky, S. H.; Holm, C. H. *J. Chem. Phys*. **1956**, *25*, 1228.
42. See, for example *(a)* Zhang, J, Pattaccini, R, Braunstein, P. *Inorg. Chem.* **2009**, *48*, 11954. *(b)* Nakazawa, H.; Kawamura, K.; Kubo, K.; Miyoshi, K. *Organometallics* **1999**, *18*, 2961.

4 *Zn^{II} Schiff Base Complexes: Molecular Probes for Alkaloids and Amines, Lewis Reference Acids and Vapochromic Materials*

4.1 Introduction

A molecular system can be definite as *"molecular probe"* if its properties are sensitive to environment. The affinity of a molecular probe for one or more microregions of a supramolecular species or macromolecular system depends on its chemical structure. There are different classes of molecular probes, in relation of the type of detection, material, application etc., and certainly optical molecular probes are nowadays extremely popular in many research fields. Their applications range from medicine, as labels for antibodies and proteins, or as fluorophores for imaging,[1] to biology as molecular tracers for in vivo processes, to chemical engineering as active dyes for smart polymeric materials[2] etc. The spectral parameters that generally respond to environmental conditions include excitation and emission wavelength, molar absorptivity, and fluorescence intensity.

Among the different kind of interactions useful to design a molecular probe, the Lewis acid-base interaction is one of most important. The Lewis acidity/basicity can be defined as the capability of a species to accept/donate a lone pair of electrons, with formation of an acid-base adduct.[3,4]

Bis(salicylaldiminato)Zn^{II} Schiff base complexes are tetracoordinated species in which the Zn^{II} ion is a Lewis acid, which saturate its coordination sphere by coordinating a large variety of neutral and anionic substrates or in their absence, can be stabilized through intermolecular Zn···O axial coordination involving the phenolic oxygen atoms of the ligand framework.[5] As reported in the chapter **3**, these species always form aggregates in solutions of non-coordinating solvents. The type and the degree of aggregation are related to the nature of the bridging diamine and to the concentration. In particular, complexes where the bridging diamine contains the naphthalene or the pyridine nucleus are always characterized by the presence of defined dimer aggregates, oligomeric aggregates are likely formed for complexes having the

benzene bridge, whereas for complexes with the 2,3-diaminomaleonitrile, the degree of aggregation is concentration dependence. Finally, for the complexes having as bridging diamine the ethane group, the existence of an equilibrium between two different types of dimers is observed, related to the non-conjugated, conformational flexible nature of the 1,2-ethylendiamine. In coordinating solvents or in the presence of coordinating species, a complete deaggregation of all complexes occurs because of the axial coordination to the Zn^{II} ion, accompanied by considerable changes of the ^{1}H NMR and optical absorption and fluorescence spectra.[6]

As the deaggregation process occurs because of the axial coordination to the acidic Zn^{II} ion, it is expected to be selective and sensitive upon Lewis basicity of the coordinating species, thus, allowing the study of these complexes as molecular probes, both in solution and in the solid state, and Lewis reference acids.[7]

In this chapter, the molecular probing, reference Lewis acid, and vapochromic properties of Zn^{II} Schiff base complexes upon coordination of various Lewis bases are investigated. For this purpose, the Zn^{II} complexes with the 2,3-diaminomaleonitrile as bridging diamino group, in particular the complex **1a**, have been chosen because show the highest optical absorption and fluorescence variations upon deaggregation (see section **3.2**).[6d]

This chapter is divided in four main sections. In the first two sections, it will be discussed the probing and the Lewis acid properties in solution of the Zn^{II} Schiff base complex **1a** with respect to the most common classes of alkaloids and to a series of primary, secondary and tertiary aliphatic amines. In the third section, it will be discussed how **1a** can been used as reference acid to build-up a reliable Lewis basicity scale in dichloromethane (DCM) for amines and common non-protogenic solvents, including ethanol. In the last section, it will be discussed the vapochromic properties of cast films of **1a** before and after the exposure to saturate amine vapours for applications as chemosensor in the solid state.

The investigation of probing properties of Zn^{II} Schiff base complexes has been carried out essentially through fluorescence titrations between the complex **1a** and the various Lewis bases, because of the higher sensitivity of detection.[8] Instead, the evaluation of binding constants, useful to obtain the Lewis basicity scale, has been achieved from spectrophotometric titrations, upon formation of **1a**·base adducts, in a

low-polarity, non-protogenic solvent medium such as DCM, by the least-squares nonlinear regression of multiwavelength spectrophotometric data.[9] Finally the vapochromic properties of **1a** films have been investigated through UV-vis analysis before and after exposure to vapours of volatile Lewis bases.

4.2 Sensing of alkaloids

Alkaloids are natural organic compounds, generally secondary plant metabolites, containing basic nitrogen atoms. They are easily isolable, soluble both in polar and non polar solvents, and characterized by a powerful physiological activity.[10] Actually, because of their pharmacological effects they are used as antibacterials[11] (berberine), vasodilators[12] (papaverine), anesthetics[13] (morphine, atropine), antimalarials[14] (quinine), and as stimulant[15] (nicotine, caffeine) or psychoactive[16] (cocaine) drugs, with a consequent considerable interest to medicine and society. More recently, alkaloids have attracted growing interest in synthesis and catalysis.[17]

Due to this broad range of applications, the molecular probing of alkaloids is certainly of relevance. In particular, the development of selective methods for sensitive detection of alkaloids is highly desirable. Among the different techniques utilized for developing chemical sensors, molecular fluorescence is one of most powerful because of the high sensitivity of detection.[8] However, literature on fluorescent chemosensors for alkaloids is rather limited. Except for a recent contribution on a cross-reactive array capable of classifying alkaloids,[18] literature data on fluorescent chemosensors are related to the detection of single alkaloids,[19] or a distinct class of them.[20]

In this section, the sensor properties of Zn^{II} Schiff base complex **1a** in DCM with respect to the most common classes of alkaloids, by investigating the optical changes and binding properties upon their basic structures (**2**-**5**) and related representative prototypes (**2a**-**6a**) (Chart 4.1) is reported.

It is found that the chromogenic and fluorogenic complex **1a** is selective between these classes of alkaloids, with excellent detection sensitivity. Since isolation and/or purification of alkaloids generally involve extractions with non polar solvents,[10] for example, as in the case of tobacco alkaloids,[21] the present approach represents a useful method for detection of alkaloids in non polar solvents.

4.2.1 Results and discussion

4.2.1.1 Binding constants The binding interaction between **1a** and the investigated alkaloids **2-5** and **2a-6a** always involves the formation of 1:1 adducts, as established by Job's plot analysis using the continuous variation method[22] (Figure 4.1), and as demonstrated by ^{1}H NMR measurements in the case of formation of the **1a**·pyridine adduct (see paragraphs **3.2.1.1** and **3.2.2**).[6d] Moreover, it is characterized by appreciable optical variations and naked-eye observation of fluorescence intensity enhancement.

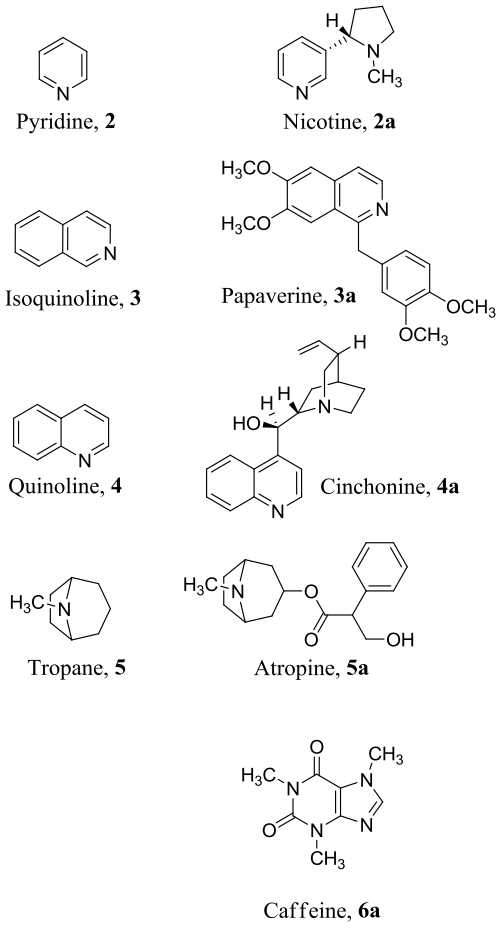

Chart 4.1 Structure of investigated alkaloids.

Spectrophotometric and spectrofluorimetric titrations of 10 μM DCM solutions of **1a** have been performed using DCM solutions of the alkaloids **2-5** and **2a-6a** as titrants. As representative example, the titration with nicotine, **2a**, is reported in Figure 4.2. They involve appreciable optical variations and an enhancement of the fluorescence emission, by almost an order of magnitude. In particular, on switching from **1a** to

1a·alkaloid adducts, the optical absorption spectra show the appearance of a new, more intense band at ≈550 nm, indicative of the axial coordination of the alkaloid to the Zn^{II} metal center (see paragraphs **3.2.1.2** and **3.2.2**).[5b,6d] Moreover, the existence of multiple isosbestic points upon spectrophotometric titrations (Figure 4.2) further confirms the formation of defined 1:1 **1a**·alkaloid adducts.

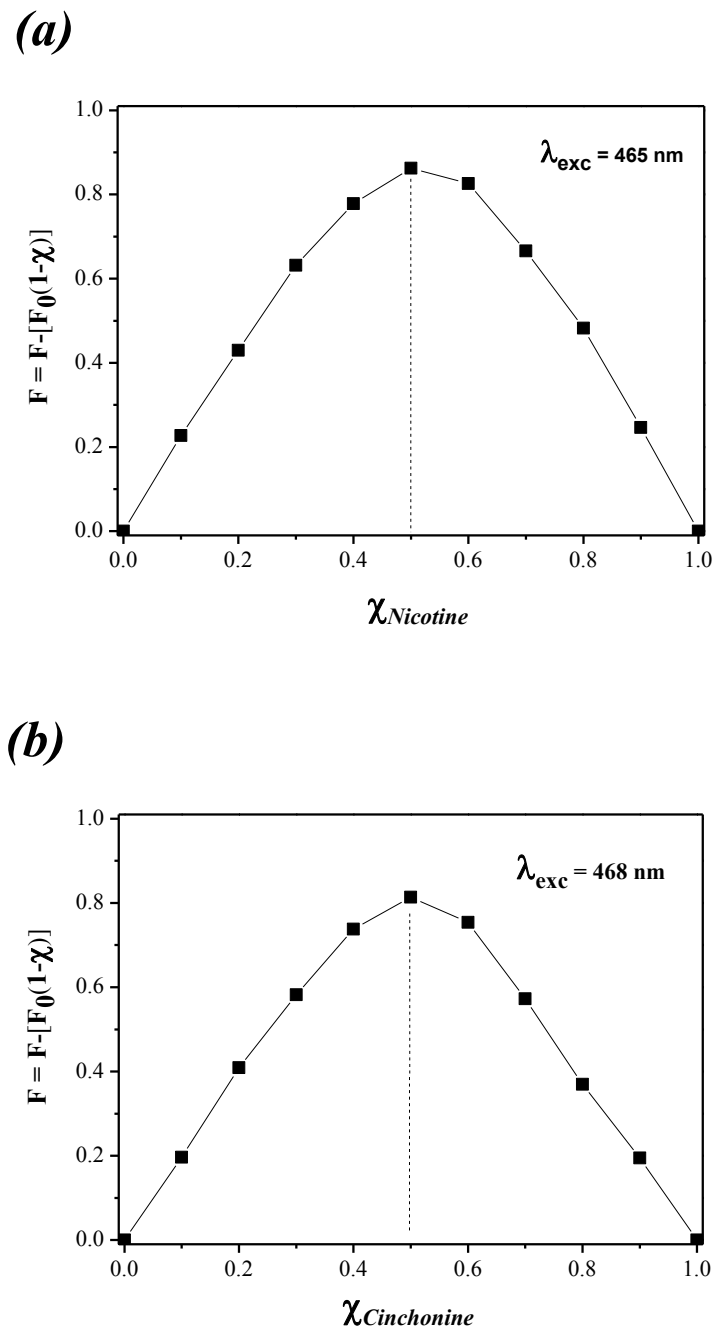

Figure 4.1 Job's plot for the binding of **1a** with *(a)* nicotine and *(b)* cinchonine in DCM. The total concentration of **1a** and alkaloid is 10 μM. F and F_0 (the initial fluorescence intensity of **1a**) are the fluorescence intensities at 597 nm for nicotine and 592 nm for cinchonine.

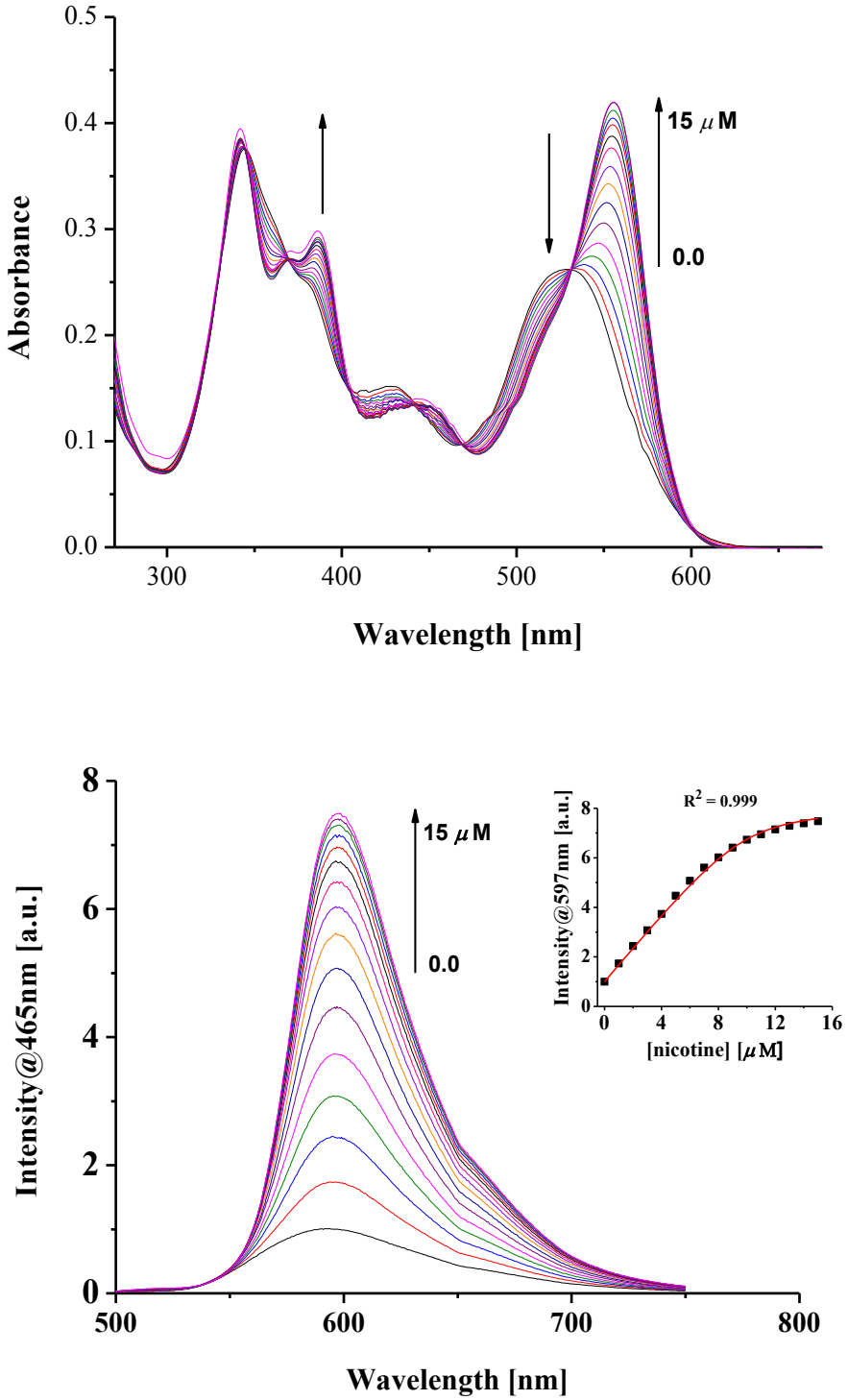

Figure 4.2 UV/vis absorption *(top)* and fluorescence *(bottom)* (λ_{exc} = 465 nm) titration curves of **1a** (10 μM solution in DCM) with addition of nicotine. The concentration of nicotine added varied from 0 to 15.0 μM. Inset: variation of fluorescence intensity at 597 nm as a function of the concentration of nicotine added. The solid line represents the curve fitting analysis with eq. 1 (see paragraph **7.3**).

The fluorescence emission wavelength (Table 4.1) is rather constant for all adducts (λ_{max} ≈600 nm), except for cinchonine (λ_{max} ≈592 nm) and tropane (λ_{max} ≈606 nm) adducts, and is independent of the excitation wavelength.

Table 4.1 Fluorescence emission, binding constants, and limits of quantification (LoQ) for the 1:1 **1a**·alkaloid adducts.

Adduct	λ_{max} (nm)	Alkaloid added[a] (μM)	log K	LoQ[b] (μM)
2, Pyridine	598	18	5.4 ± 0.1	0.49 (39)
2a, Nicotine	597	15	5.6 ± 0.1	0.40 (64)
3, Isoquinoline	596	19	6.1 ± 0.2	0.46 (60)
3a, Papaverine	603	70	5.1 ± 0.1	1.3 (4.3×10^2)
4, Quinoline	600	130	4.5 ± 0.3	3.6 (4.7×10^2)
4a, Cinchonine	592	14	6.4 ± 0.2	0.43 (1.3×10^2)
5, Tropane	606	140	4.6 ± 0.1	4.0 (3.4×10^2)
5a, Atropine	599	650	3.8 ± 0.3	15 (4.3×10^3)
6a, Caffeine	597	11×10^3	2.6 ± 0.2	1.8×10^2 (3.6×10^4)

[a]At saturation point. [b]Values in parentheses refer to LoQs in μgL^{-1}.

The **1a**·alkaloid binding constants, K, estimated from fluorescence titration data by the nonlinear curve fitting analysis of fluorescence intensity *vs.* alkaloid concentration,[23] are rather large, log K >4, except for **5a** and **6a** (Table 4.1), indicating strong binding interactions. The order is isoquinoline > pyridine >> tropane ≈ quinoline for the basic structures **2-5**, and cinchonine > nicotine > papaverine >> atropine > caffeine for the representative alkaloids **2a-6a**, in spite of the stronger Lewis basicity[24] of the tertiary **5** and **5a** amines with respect to the pyridine-like **2-4** and **2a-4a** species, thus indicating that the binding interaction is strongly influenced by steric hindrance.[25]

Within the **2a-6a** series, the largest **1a**·cinchonine binding constant suggests that of the two nitrogen atoms of cinchonine, the stronger Lewis basic and less encumbered quinuclidine nitrogen, rather than the quinoline one, is presumably involved in the formation of the 1:1 adduct (Figure 4.1b). Actually, fluorimetric titrations of DCM solutions of **1a** using quinuclidine as titrant give a **1a**·quinuclidine log K = 6.9 ± 0.3, comparable to that calculated for cinchonine (Table 4.1). This explains the larger binding constant value, by almost two orders of magnitude, on switching from quinoline to cinchonine, as previously found in the formation of diiodine·base adducts.[26] On the

other hand, the stronger Lewis basicity of quinuclidine, in comparison to tropane, can be related to the less sterically encumbered nature of the former.[25]

4.2.1.2 Selective properties The plots of relative fluorescence changes *vs.* concentration of alkaloids in the micromolar range clearly indicate the selectivity of **1a** within the investigated classes of alkaloids (Figure 4.3).

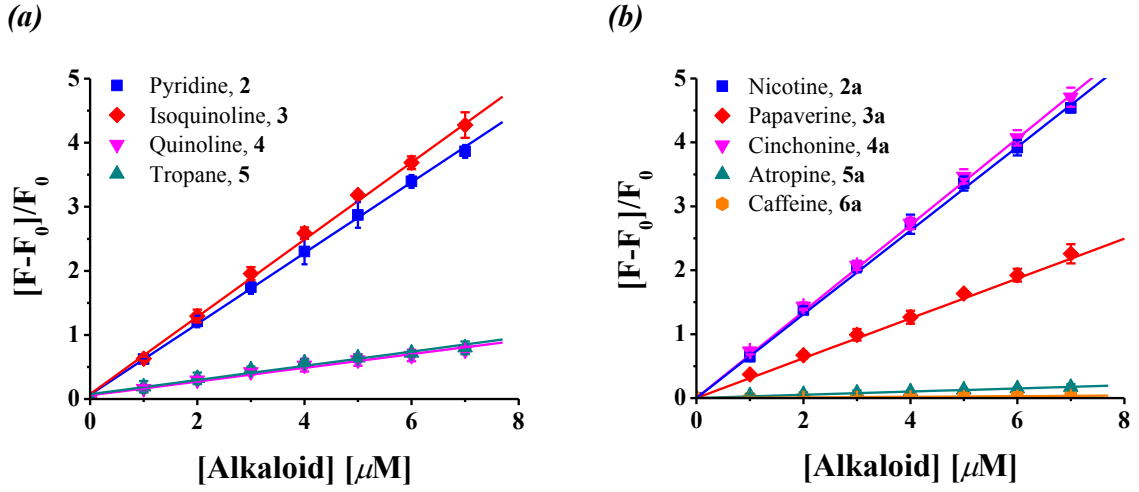

Figure 4.3 Plots of relative fluorescence changes *vs.* concentration of *(a)* basic structures **2-5** and *(b)* representative prototypes of alkaloid **2a-6a** in DCM added to **1a** (10 μM solution in DCM), monitored at 597 nm.

Thus, among the basic structures **2-5**, pyridines and isoquinolines can be selectively detected over the quinoline and tropane series. This can be easily verified by competitive experiments. For example, fluorimetric titrations of **1a** with isoquinoline performed with and without the presence of an equimolar concentration of quinoline, indicate negligible variations of fluorescence intensity (Figure 4.4). To observe a fluorescence response analogous to that for isoquinoline a concentration of quinoline one order of magnitude larger is required (Figure 4.5). Within the **2a-6a** alkaloids, nicotine, cinchonine, and papaverine can selectively be detected, in the micromolar range, which respect atropine and caffeine, as can be also easily verified by competitive titration experiments. Again, to observe an analogous fluorescence response to nicotine or cinchonine, a concentration of atropine almost two orders of magnitude larger is required; while in the case of papaverine a concentration of atropine 15 times larger is required. Overall, the present results indicate high selectivity of **1a** for pyridine-,

isoquinoline-based, and cinchona alkaloids, as cinchonine possesses the quinuclidine group common to the cinchona family.[10]

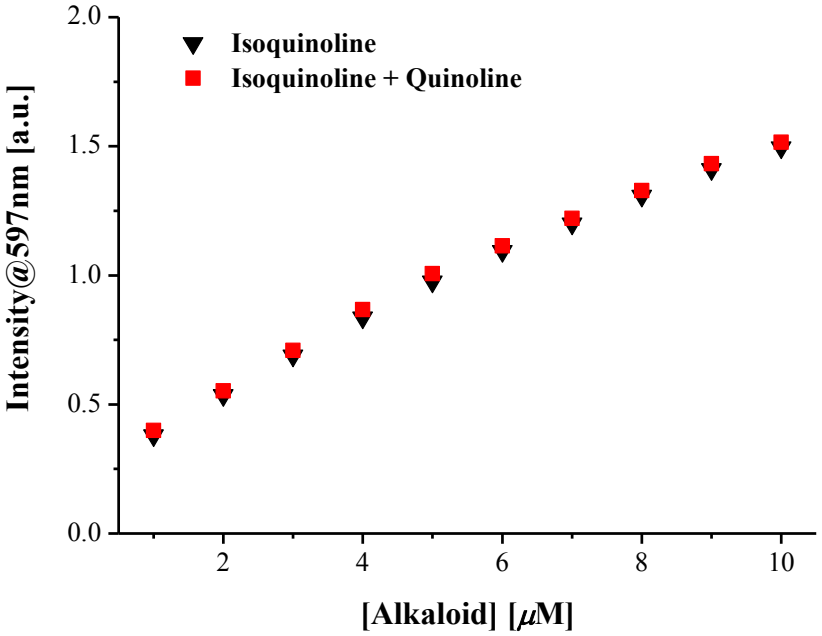

Figure 4.4 Variation of fluorescence intensity of **1a** (10 μM solution in DCM) at 597 nm as a function of the concentration of isoquinoline added, with (■) and without (▼) the presence of an equimolar amount of quinoline.

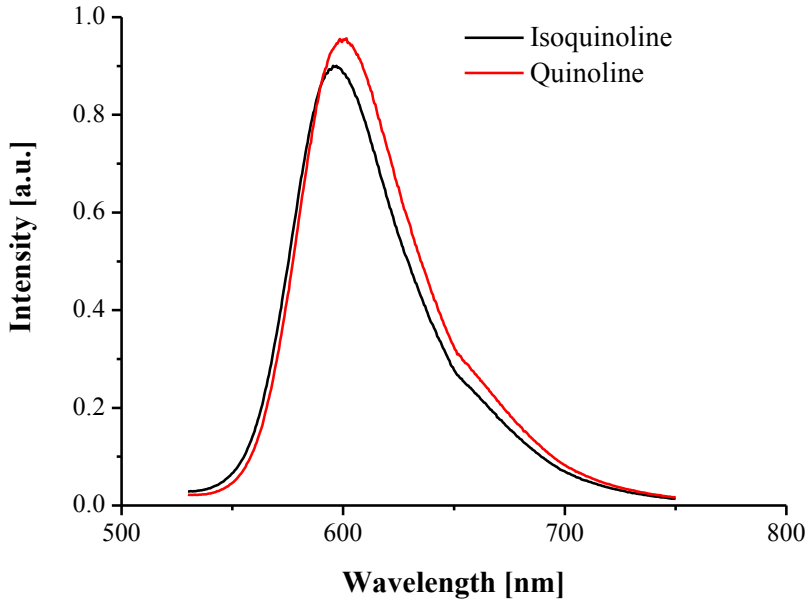

Figure 4.5 Fluorescence intensity of **1a** (10 μM solution in DCM) upon addition of isoquinoline (8.0 μM) (—) and quinoline (80 μM) (—).

4.2.1.3 Limit of quantification (LOQ) The limit of quantification (LOQ) of a 10 μM DCM solution of **1a**, calculated according to IUPAC recommendations,[27] indicates very low values for the series of investigated alkaloids, below the micromolar range for **2**, **3** and **2a**, **4a** (Table 4.1). When compared to literature fluorescent chemosensors of alkaloids,[18-20] the complex **1a** is definitely more sensitive. Actually, even if in these investigations limits of detection are not reported, the investigated range of concentrations is generally higher[18-20] than that explored in this study. Moreover, the present LoQ values rival or exceed those reported in literature for detection of alkaloids using hyphenated analytical methods.[21b,c,28] Thus, complex **1a** is useful for fast detection of pyridine-, isoquinoline-based, and cinchona alkaloids in trace amounts (μg L^{-1}), with a linear dynamic range spanning almost two orders of magnitude (Figure 4.3), up to 10 μM.

4.3 Sensing of aliphatic amines

Aliphatic amines are widespread compounds in nature.[29] They are also involved in many organic syntheses and catalysis.[17b, 30] In this view, the molecular recognition and sensitive optical detection of low-molecular-weight amines[31] is critical in the medical field, in environmental science, in food safety, and in organic chemistry.[32]

In this section, the sensing properties of the Zn^{II} complex, **1a**, with respect a series of primary, secondary and tertiary aliphatic amines, by changing the steric hindrance of *N*-alkyl substituents (Chart 4.2), through the study of optical absorption and fluorescence changes upon amine coordination to the Lewis acidic Zn^{II} metal center, are reported.

Various chromogenic[33] and fluorogenic[34] approaches are reported in the literature for the selective detection of aliphatic amines. These approaches are generally based on either Brønsted basicity of amines or formation of guest-host adducts. In this case, detection of investigated amines is based on their actual Lewis basicity in the low-polarity, non-protogenic, non-coordinating solvent medium such as DCM, hence avoiding relevant specific solvation effects.

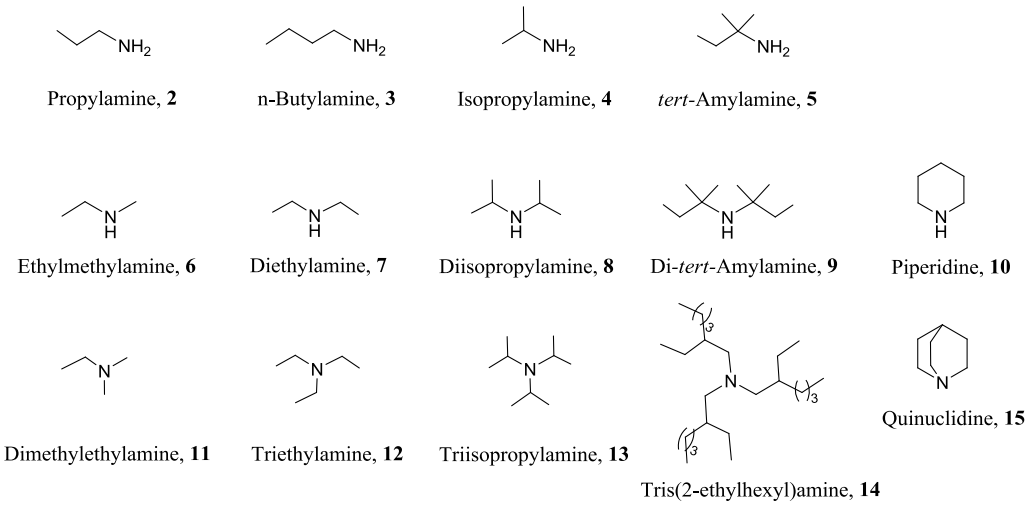

Chart 4.2 Structure of the investigated amines.

4.3.1 Results and discussion

4.3.1.1 Binding constants The binding interaction between **1a** and the involved amines always implies formation of 1:1 adducts, as established by Job's plot analysis (Figure 4.6),[22] ^{1}H NMR spectroscopy (Figure 4.7), and ESI mass spectrometry (see paragraph **4.2.1.1**). Because this process is accompanied by appreciable optical variations, it can be investigated on a quantitative ground simply by means of spectrophotometric and spectrofluorimetric titrations.

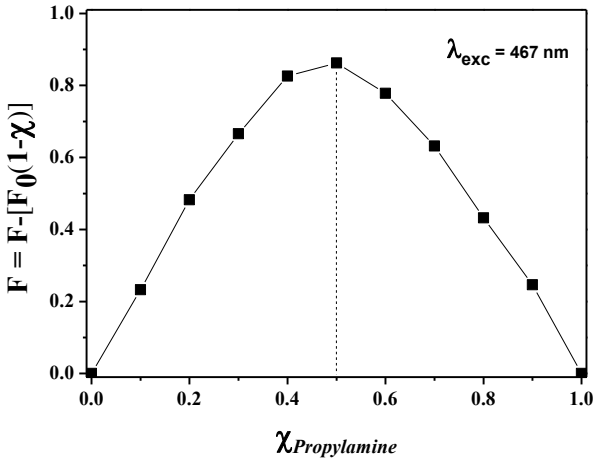

Figure 4.6 Job's plot for the binding of **1a** with propylamine in DCM. The total concentration of **1a** and propylamine is 10 μM. F and F_0 (the initial fluorescence intensity of **1a**) are the fluorescence intensities at 600 nm.

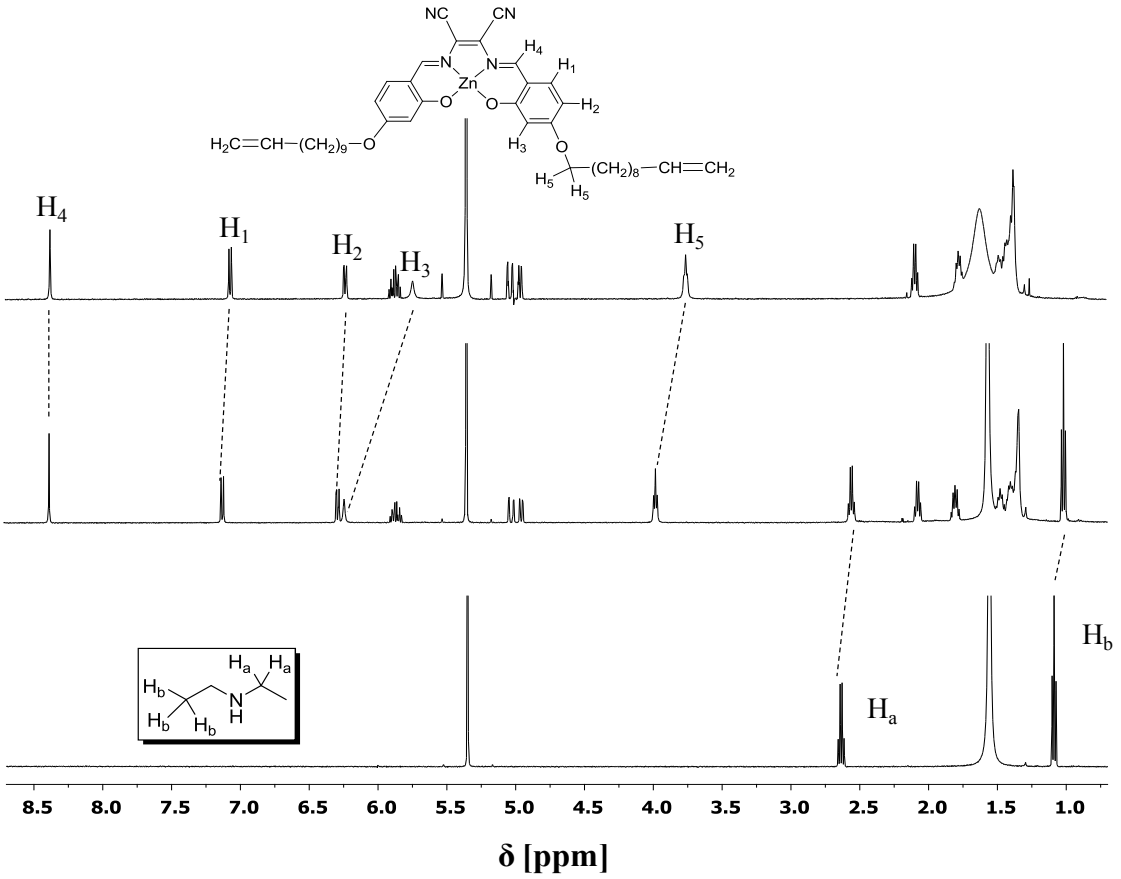

Figure 4.7 *(Top)* ^{1}H NMR spectra of **1a** (5.0×10^{-4} M) in DCM-d_2, and *(middle)* upon addition an equimolar amount of diethylamine. *(Bottom)* The ^{1}H NMR spectrum of diethylamine in DCM-d_2 is reported as reference. The addition of an equimolar amount of diethylamine to a DCM-d_2 solution of **1a** (5.0×10^{-4} M) results in a downfield shift of H_1, H_3 and the -OCH_2 signals, according to the deaggregation of the complex (see paragraphs **3.2.1.1** and **3.2.2**).[6d] Moreover, the observed upfield shift of the hydrogens of the diethylamine clearly indicates its axial coordination to the complex.

Spectrophotometric and spectrofluorimetric titrations of 10 μM DCM solutions of **1a** have been performed using DCM solutions of the amines **2-15** as titrants. As a representative example, the titration with propylamine, **2**, is reported in (Figure 4.8). Optical absorption spectra upon titration indicate some absorbance changes in the UV/vis region with the existence of multiple isosbestic points and an appreciable increase of the absorbance (λ_{max} = 557 nm) in the region between 530 and 600 nm. Spectrophotometric titrations of all investigated amines show almost identical optical changes in the region >330 nm, in terms of intensity, λ_{max} values (Table 4.2), and isosbestic points, thus indicating that coordination of the amine to the Zn^{II} atom similarly affects the low-lying electronic states of **1a**. Moreover, the existence of multiple isosbestic points in optical absorption spectra upon titration is in agreement with the formation of defined adducts (see paragraph **4.2.1.1**).

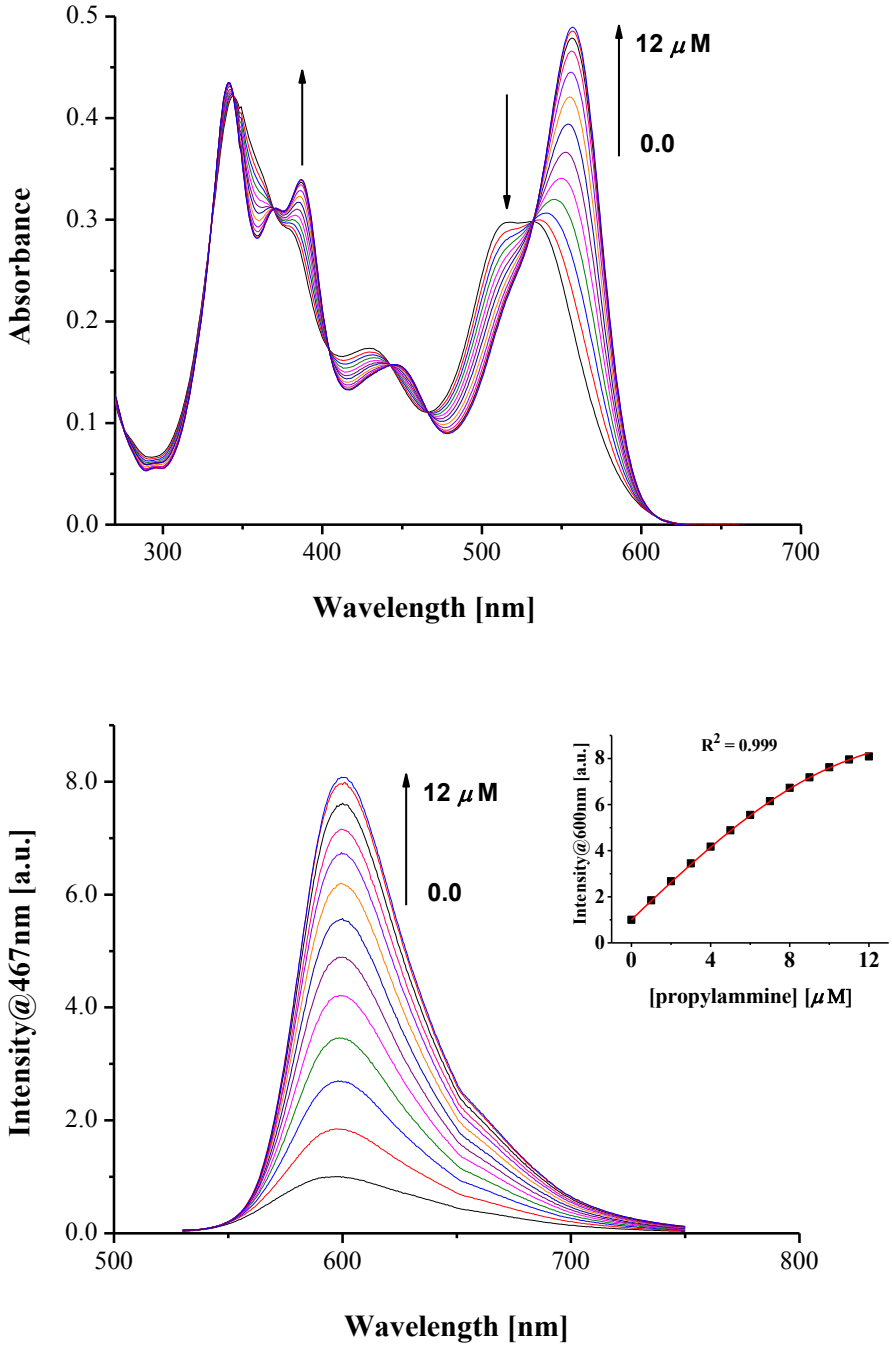

Figure 4.8 *(Top)* UV/vis absorption and *(bottom)* fluorescence (λ_{exc} = 467 nm) titration curves of **1a** (10 μM solution in DCM) with the addition of propylamine. The concentration of propylamine added varied from 0 to 12.0 μM. (Inset) Variation of the fluorescence intensity at 600 nm as a function of the concentration of propylamine added. The solid line represents the curve fitting analysis with eq.1 (see paragraph **7.3**).

Table 4.2 Optical absorption and fluorescence emission maxima, concentration of amine at saturation point, binding constants, and limits of detection (LODs) for the **1a**·amine adducts.

Adduct	$\lambda_{max, abs}$ (nm)	$\lambda_{max, em}$ (nm)	Amine added[a] (μM)	log K	LOD[b] (μM)
2, Propylamine	557	600	12	6.1 ± 0.2	0.17 (10)
3, *n*-Butylamine	557	600	13	6.1 ± 0.2	0.17 (12)
4, Isopropylamine	557	600	14	6.3 ± 0.3	0.19 (11)
5, *tert*-Amylamine	556	599	20	6.3 ± 0.2	0.21 (18)
6, Ethylmethylamine	557	600	13	6.1 ± 0.2	0.18 (11)
7, Diethylamine	557	600	22	5.7 ± 0.1	0.27 (20)
8, Diisopropylamine	554	599	1.9×10^3	3.0 ± 0.2	5.0 (506)
9, Di-*tert*-amylamine	556	598	3.6×10^3	2.8 ± 0.1	27 (420)
10, Piperidine	558	599	14	6.1 ± 0.2	0.16 (14)
11, Dimethylethylamine	557	599	18	6.0 ± 0.1	0.21 (16)
12, Triethylamine	558	603	4.6×10^2	3.7 ± 0.1	4.8 (480)
13, Triisopropylamine	558	602	9.1×10^3	2.3 ± 0.1	27 (380)
14, Tris(2-ethylhexyl)amine	558	602	5.5×10^4	1.7 ± 0.3	50 (18×10^3)
15, Quinuclidine	558	600	16	6.9 ± 0.3	0.19 (21)

[a]At saturation point. [b]Values in parentheses refer to LODs in μgL^{-1}.

Titration with propylamine is accompanied by an enhancement of the fluorescence emission, almost an order of magnitude larger. Spectrofluorimetric titrations of all investigated amines involve rather constant fluorescence emission λ_{max} values (Table 4.2), independent from the excitation wavelength, and almost the same fluorescence enhancement upon reaching of the saturation point. Analogously to optical absorption data, the almost constant fluorescence λ_{max} values upon formation of **1a**·amine adducts indicate that the same excited electronic state is involved for all of the investigated aliphatic amines. Although both optical absorption and fluorescence emission changes can be easily detected upon titration of **1a** with the involved amines, it has been chosen the latter observable because of the higher sensitivity of detection.[8] Thus, fluorescence titration data are used to calculate the limit of detection[27] (LOD) of **1a** for the investigated aliphatic amines and, eventually, to explore its selective sensing. Moreover, as we are interested to variations of **1a**·amine binding constants along the considered series, rather than in their absolute values, we have estimated them from fluorescence titration data by the nonlinear curve fitting analysis of fluorescence intensity *vs.* amine

concentration (see paragraph **4.2.1.1**).[23] Relevant optical absorption and fluorescence emission data, calculated binding constants, and LODs are collected in Table 4.2.

The calculated binding constants for **1a**·amine adducts span over several orders of magnitude (Table 4.2; Figure 4.9).

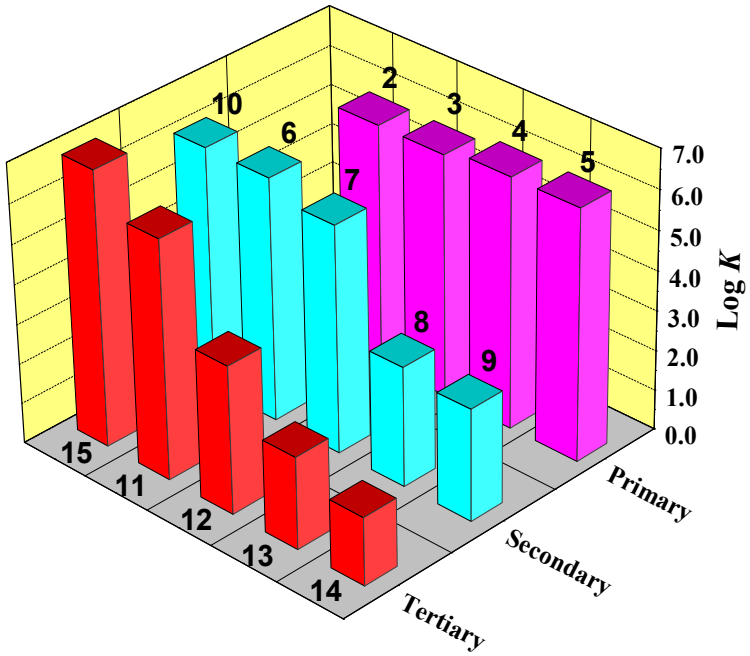

Figure 4.9 Profile of the calculated binding constants for the investigated amines.

In particular, while binding constants are almost invariable along primary amines, exhibiting the largest values among the considered acyclic species, they show a distinct decrease along the series of secondary or tertiary amines, strictly related to the increasing steric hindrance at the nitrogen amine atom. In line with this view, the alicyclic piperidine, **10**, having a low steric hindrance within the series of secondary amines, possesses a binding constant comparable to that of the ethylmethylamine, **6**, the latter of which is the least sterically encumbered species within the series secondary acyclic amines. Analogously, quinuclidine, **15**, representing the least sterically encumbered tertiary amine,[35] exhibits the largest binding constant value, even with respect primary amines (Table 4.2). Moreover, from calculated binding constants, a relative order, primary > secondary > tertiary, is found for amines having an analogous

N-alkyl chain, especially for those with more branched *N*-alkyls (*e.g.* **5**, **9**, **14**), while a levelling effect is observed for amines with linear *N*-alkyls (*e.g.* **2**, **6**, **11**).

4.3.1.2 Selective properties The plots of the relative fluorescence change *vs.* the amine concentration, in the micromolar range can be related to the selectivity of **1a** with respect to the investigated amines. As expected, **1a** is not selective within primary amines, according to the aforementioned almost identical estimated binding constants (see paragraph **4.2.1.2**). In contrast, a distinct selectivity is observed along the series of secondary or tertiary amines and parallels the increasing steric hindrance at the nitrogen atom (Figure 4.10).

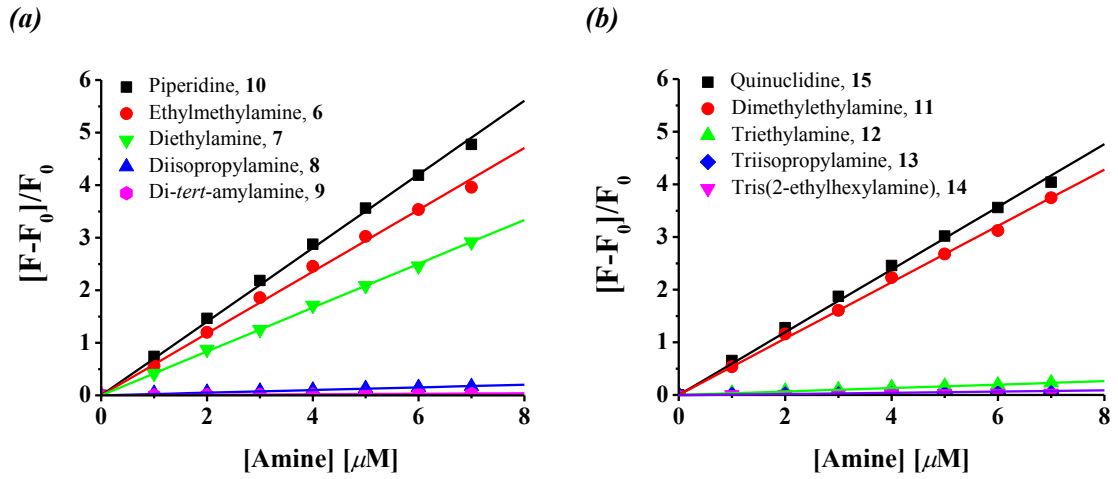

Figure 4.10 Plots of the relative fluorescence changes *vs.* the concentration of the *(a)* secondary amines **6-10** and *(b)* tertiary amines **11-15** in DCM added to **1a** (10 μM solution in DCM), monitored at 600 nm.

Thus, among the secondary amines **6-10**, piperidine and ethylmethylamine can selectively be detected with respect to the remaining amine series. This can be easily verified by competitive experiments. For example, fluorimetric titrations of **1a** with piperidine performed with and without the presence of an equimolar concentration of diisopropylamine indicate negligible variations of fluorescence intensity (Figure 4.11). To observe an analogous fluorescence response to that of piperidine, it needs a concentration of diisopropylamine more than 2 orders of magnitude larger (Figure 4.12). Analogously, quinuclidine and dimethylethylamine can selectively be detected with respect to any other more sterically encumbered tertiary amine, as can be also easily verified by competitive titration experiments. Again, to observe an analogous fluorescence response to that of quinuclidine or dimethylethylamine, it needs, for

example, a concentration of triisopropylamine about 600 times larger, while for triethylamine, a concentration 50 times larger is required.

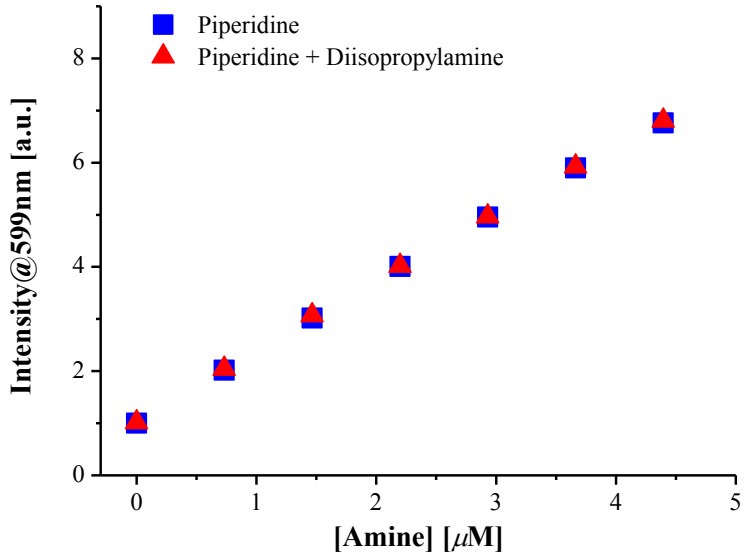

Figure 4.11 Variation of fluorescence intensity of **1a** (10 μM solution in DCM) at 599 nm as a function of the concentration of piperidine added without (▲) and with (■) the presence of an equimolar amount of diisopropylamine.

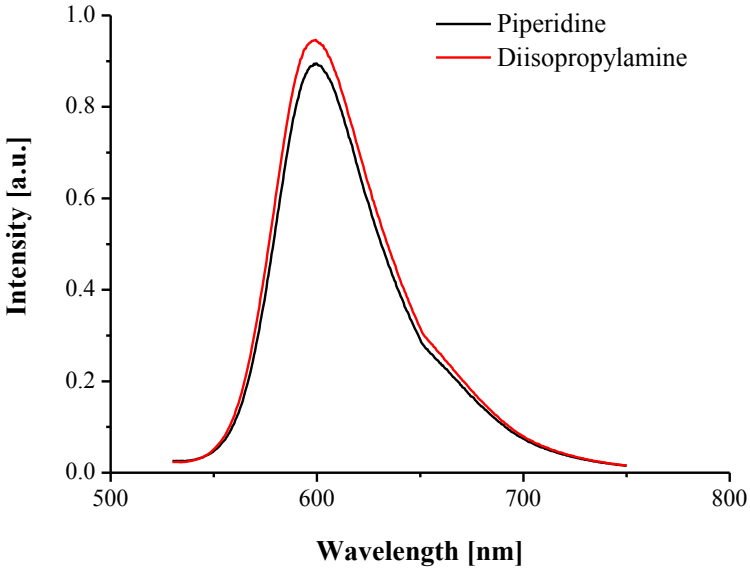

Figure 4.12 Fluorescence intensity of **1a** (10 μM solution in DCM) upon addition of piperidine (5.0 μM) (—) or diisopropylamine (0.9 mM) (—).

Selectivity of **1a** becomes also evident upon comparing the fluorescence response, again in the micromolar range, of primary *vs.* secondary and tertiary acyclic amines having an analogous *N*-alkyl chain (Figure 4.13). For example, within the amines **4**, **8**, and **13**, to observe an analogous fluorescence response to that of isopropylamine, it needs a concentration of diisopropylamine more than 1 order of magnitude larger, while for triisopropylamine, a concentration almost 2 orders of magnitude larger is required. Therefore, except for the secondary and tertiary linear *N*-alkyl amines, **6** and **11**, primary amines can selectively be detected over acyclic secondary and tertiary amines, especially those with branched *N*-alkyl chains.

4.3.1.3 Limit of detection (LOD) The limit of detection (LOD) of a 10 μM DCM solution of **1a**, calculated according to IUPAC recommendations,[27] indicates very low values for the series of investigated amines, falling into the nanomolar range for primary and alicyclic amines (Table 4.2). Thus, complex **1a** is useful for fast detection in solutions of low-polarity solvents of primary and alicyclic amines in the range of trace amounts (μg L^{-1}). For secondary and tertiary amines, even if LOD values are definitely higher, they again evidence an appreciable sensitivity of **1a** for all involved amines. The sensitivity of complex **1a** for primary and alicyclic amines exceeds that reported in the literature for the selective chromogenic[33a,b,f] or fluorogenic[34a-c,h] detection of aliphatic amines, rivalling that reported for fluorescent sensors of aliphatic amines in traces.[36]

4.3.1.4 Detection in water solution Preliminary data suggest that complex **1a** can potentially be applied for the detection of amines even in aqueous solutions. However, given the insolubility of **1a** in water, a two-phase (DCM/H_2O) system should be used. Thus, the addition of defined amounts of amine in aqueous solution to a DCM solution of **1a** produces a fluorescence response that can be compared to that achieved for addition of the same mole amounts of amine in DCM (Figure 4.14).

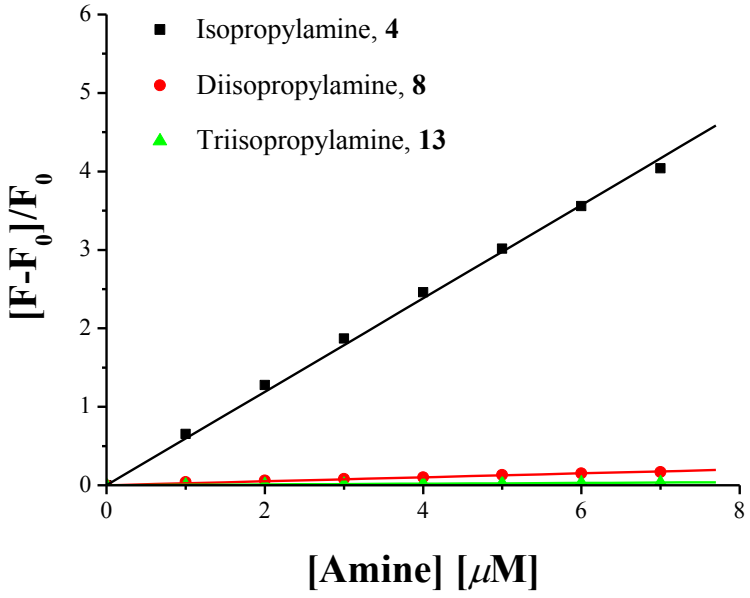

Figure 4.13 Plots of the relative fluorescence changes *vs.* the concentration of the amines **4**, **8**, and **13** in DCM added to **1a** (10 μM solution in DCM), monitored at 600 nm.

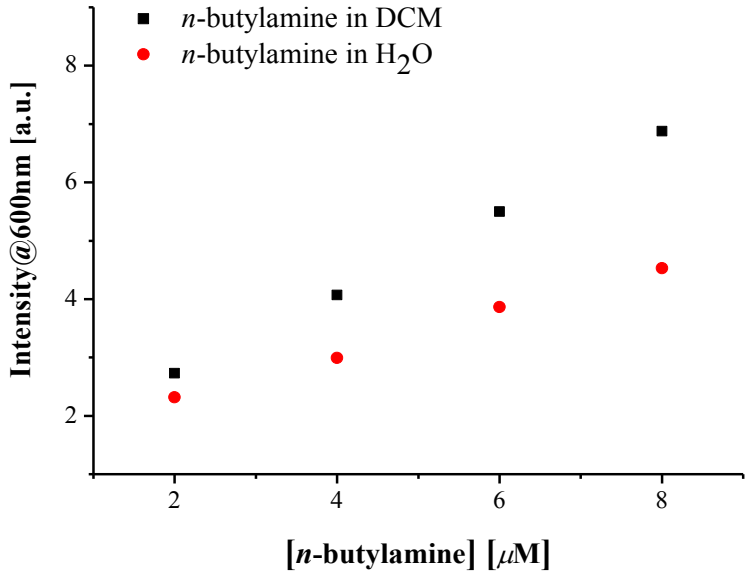

Figure 4.14 Comparison of the fluorescence intensity of **1a** (10 μM solution in DCM) at 600 nm as a function of the concentration of *n*-butylamine added in DCM (■) or in aqueous (●) solution. The fluorescence intensity related to addition of the amine in aqueous solution was corrected by the fluorescence signal increase of **1a** upon addition of water.

4.4 Lewis basicity scale

The Lewis theory of acids and bases represents one of most important concepts of modern chemistry, as it allows rationalizing most of the general chemical behaviour of these involved species. The Lewis acidity/basicity can be defined as the capability of a species to accept/donate a lone pair of electrons, with formation of an acid-base adduct.[3] It can be referred in the gas-phase or in solvent media; however, its evaluation in solvent media is certainly of relevance for the effective properties and chemical behaviour of a species in solution.

The acid/base strength, either in the gas-phase or in solution, cannot be determined by a direct measurement; therefore, it is indirectly referred to the bond strength of the formed adduct. To this end, a variety of methods, including optical UV-vis, IR absorption, fluorescence emission, NMR spectroscopy, electrical conductance, calorimetry, etc. can be found in the literature.[4] Nevertheless, not always the acid-base adduct bond strength deduced from these methods correlates with the Lewis base/acid strength and, hence, to the Lewis acidity/basicity.

Another drawback associated with Lewis acidity/basicity is the choice of the reference Lewis base/acid, to achieve reliable acidity/basicity scales. Actually, as the Lewis acidity/basicity is a relative concept, there are in principle as many possible Lewis basicity scales as there are Lewis acids. It therefore turns out that the definition of a reliable scale of general validity still represents an unsolved issue.[4a]

Although various attempts can be found in the literature about methods capable to establish reliable Lewis basicity scales, two main approaches are commonly involved to estimate Lewis basicity for solvents: the donor number (DN) first developed by Gutmann in the early seventies,[37] and reviewed by Jensen in 1978,[24b] and a Lewis basicity scale deduced by Maria, Gal et al. in 1985.[24a,38] The DN is a quantitative measure of the Lewis basicity and is defined as the negative enthalpy for the 1:1 adduct formation between $SbCl_5$, used as reference acid, and a Lewis base, both in a dilute solution in the non-coordinating 1,2-dichoroethane solvent. Analogously, Maria, Gal et al. established a solvent Lewis basicity scale in dichloromethane for various non-protogenic solvents by measuring calorimetrically their enthalpies of complexation with boron trifluoride, representing the archetypical Lewis acid. A further relevant scale of basicity involving diiodine or 1-iodoacetylenes has been compiled by Laurence et al.[39]

in eighties. More recently, an extensive scale of hydrogen bond basicity involving 4-fluorophenol as reference acid, has been developed by Graton, Laurence et al.[40] However, unlike the previous examples, the resulting hydrogen-bonded complexes can be considered as a special case of Lewis acid-base interactions.[4a]

Without bringing into question about the reliability of these basicity scales, they cannot be considered of general validity, as they generally refer to less sterically encumbered reference Lewis acids. On the other hand, a Lewis basicity scale of more general validity should necessarily be referred also to "*real world*", sterically encumbered, Lewis acids, such as most acidic organometallics involved in organic synthesis and catalysis,[41] excluding of course frustrated Lewis pairs.[42]

In this section, the use, for the first time, of the Lewis acidic Zn^{II} Schiff base complex, **1a**, as reference acid, to build up a reliable Lewis basicity scale in dichloromethane for amines and common non-protogenic solvents, including ethanol, in the "*real world*" of most Lewis acidic species is reported.

4.4.1 Results and discussion

4.4.1.1 Method According to the IUPAC definition of the Lewis basicity[3] as "*the thermodynamic tendency of a substance to act as a Lewis base*", the development of suitable methods whose "*comparative measures of this property are provided by the equilibrium constants for Lewis adduct formation for a series of Lewis bases with a common reference Lewis acid,*" become compulsory to achieve reliable basicity scales.

Additionally, some requirements in choosing the reference Lewis acid and the solvent medium should be fulfilled in order to design a suitable method, spectroscopic in our case, which correlates with the base strength and, hence, the Lewis basicity.

The reference acid should be a sufficient strong Lewis acid, capable to react with most common bases. It should form defined 1:1 adducts, without side reactions, always involving the same spectroscopic variations, thus avoiding specific effects on the acid-base adduct bond strength and, hence, on the Lewis basicity. In other terms, the adduct formation should be not family dependent. A suitable solvent should ensure adequate solubility for the acid/base and the formed adduct and, most important, it should not be involved in specific solvation effects.

In the paragraphs **3.2.1.2**, **3.2.2** and sections **4.2** and **4.3**, it has reported that the amphiphilic Zn^{II} Schiff base complex **1a** in solution of dichloromethane (DCM) upon

addition of a coordinating species, *i.e.* a Lewis base, leads to the formation of **1a**·base (1:1) adducts and involves substantial optical variations.[6d] As this process occurs because of the axial coordination to the Zn^{II} ion, it is expected to be sensitive upon Lewis basicity of the coordinating species.

Given its strong Lewis acidic character, hence fast to react with any base in solution of non-protogenic solvents, dichloromethane in our case, complex **1a** fulfils the primary requirement to be an appropriate reference Lewis acid. Moreover, the formation of defined 1:1 adducts, without side reactions, always involving the same UV-vis optical absorption variations, independent from the Lewis base (vide infra), avoids specific effects on the acid-base adduct bond strength, and hence upon the Lewis basicity.

Binding constants are then achieved by the least-squares nonlinear regression of multiwavelength spectrophotometric titrations data (see paragraph **7.4**),[9] upon formation of the (1:1) **1a**·base adducts, involving the following equilibrium:

$$\mathbf{1a}(\text{soln}) + \text{base}(\text{soln}) \rightleftarrows \mathbf{1a}\cdot\text{base}(\text{soln}) \qquad (1)$$

Therefore, according to the Lewis basicity definition,[3] the calculated binding constants upon equilibrium 1 can properly be related to the relative Lewis basicity of the involved species. The use of the Zn^{II} complex **1a** as reference Lewis acid would allow a better estimation of the Lewis basicity of most Lewis acidic species.[41] Actually, the complex **1a**, in addition to be a sufficient strong Lewis acid leading to stable adducts with any common Lewis base, is a sufficiently hindered molecule so that the formation of adducts will be influenced even of the steric hindrance of the base. Therefore, relative basicity values deduced from this reference Lewis acid will reflect the actual, *i.e.*, effective, basicity with respect this "*real world*" Lewis acidic species.

4.4.1.2 Binding constants The complex **1a** represents a suitable Lewis acidic system capable of axially coordinating Lewis bases. This binding interaction leads to formation of stable 1:1 adducts, as established by Job's plot analysis,[22] ^{1}H NMR spectroscopy, and ESI mass spectrometry (see paragraphs **3.2.1.1**, **3.2.2**, **4.2.1.1** and **4.3.1.1**).[6d] Moreover, this process is accompanied by appreciable optical absorption variations, therefore it has been investigated on a quantitative ground by means of spectrophotometric titrations,

followed by an accurate data analysis[9] to get binding constants. Calculated binding constants for the **1a**·base adducts are reported in Table 4.3.

Table 4.3 Calculated binding constants for the **1a**·base adducts.

	Lewis base	log K
2	Quinuclidine	6.73 ± 0.03
3	Pyridine	6.67 ± 0.03
4	Isopropylamine	6.66 ± 0.01
5	*n*-Butylamine	6.35 ± 0.02
6	Ethylmethylamine	6.31 ± 0.07
7	Propylamine	6.30 ± 0.04
8	*tert*-Amylamine	6.21 ± 0.01
9	Piperidine	6.18 ± 0.02
10	Isoquinoline	5.92 ± 0.02
11	Pyrrolidine	5.8 ± 0.1
12	Dimethylethylamine	5.75 ± 0.03
13	Diethylamine	5.48 ± 0.02
14	Tropane	4.59 ± 0.01
15	Quinoline	4.50 ± 0.01
16	DMSO	4.20 ± 0.01
17	DMF	3.55± 0.01
18	Triethylamine	3.45 ± 0.01
19	Diisopropylamine	3.30 ± 0.01
20	Aniline	3.08 ± 0.01
21	Triisopropylamine	2.89 ± 0.02
22	Di-*tert*-Amylamine	2.75 ± 0.02
23	THF	2.46 ± 0.01
24	Ethanol	1.83 ± 0.02
25	Tris-(2-ethylhexyl)amine	1.61 ± 0.01
26	Acetonitrile	1.32 ± 0.03
27	Acetone	1.18 ± 0.02

Spectrophotometric titrations of 10 μM DCM solutions of **1a** have been performed using DCM solutions of the Lewis bases **2**-**27** as titrants. As representative example, the titration with pyridine is reported in Figure 4.15. Optical absorption spectra upon titration indicate some absorbance changes in the UV-vis region with the existence of multiple isosbestic points, and an appreciable increase of the absorbance in the region between 530 and 600 nm. Spectrophotometric titrations of all investigated Lewis bases, upon reaching the saturation point, show almost identical optical absorption changes in the region >330 nm, in terms of intensity, λ_{max} values, and isosbestic points, thus

indicating that the coordination of the Lewis base to the Zn^{II} atom similarly affects the low-lying electronic states of **1a**. In other terms the formation of **1a**·base adducts is not family dependent. Moreover, the existence of multiple isosbestic points in optical absorption spectra upon titration is in agreement with the formation of defined 1:1 adducts (see paragraphs **4.2.1.1** and **4.3.1.1**).

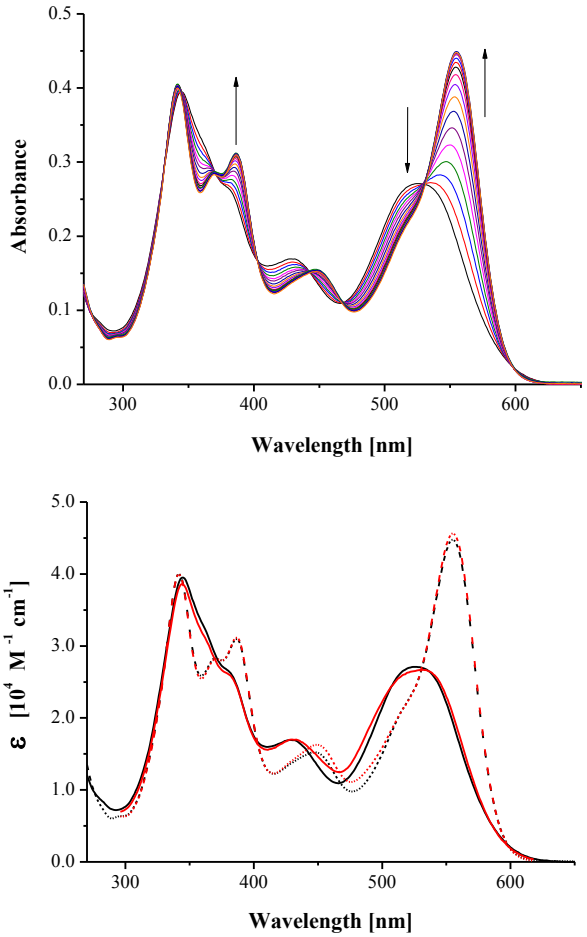

Figure 4.15 *(Top)* UV-vis absorption titration curves of **1a** (10 μM solution in DCM) with addition of pyridine. The concentration of pyridine added varied from 0 to 18.0 μM. *(Bottom)* Comparison of experimental (black lines) UV-vis absorption spectra for **1a** (—) and **1a**·pyridine adduct (---) with calculated values (red lines).

The almost identical absorptivity values upon comparison of experimental *vs.* calculated optical absorption data for **1a** and **1a**·base adduct (Figure 4.15), indicate the goodness of the least-squares nonlinear regression of multiwavelength spectrophotometric titration data.

4.4.1.3 Lewis basicity From binding constants for the **1a**·base adducts reported in Table 4.3, it is possible drawing some general trends about relative basicity of the involved species. Within acyclic amines, with exception of the less sterically encumbered secondary ethylmethylamine, primary amines always represent the strongest bases. On the other hand, the basicity of secondary and tertiary amines apparently does not show a regular trend, except if we consider amines having the same alkyl substituent, in this case secondary amines are stronger bases than tertiary amines. Thus, diethylamine is a stronger Lewis base than triethylamine, and diisopropylamine is stronger than triisopropylamine. Among alicyclic amines, the trend is opposite: the tertiary quinuclidine is a stronger base than the secondary piperidine or pyrrolidine. The tropane is the weaker base within this series.

In general, present data indicate a relative order of the Lewis basicity for acyclic amines, primary > secondary > tertiary, in agreement with the Lewis basicity deduced from the relative enthalpies of formation for some amineborane adducts,[43] or by competition experiments using $B(CH_3)_3$ as reference acid,[44] although gas-phase basicities indicate the opposite.[45,46] This order is, however, inverted, tertiary > secondary ≈ primary (acyclic), in the case of alicyclic amines, with exception of tropane, being a bicyclic tertiary amine but having a *N*-methyl.

These comparisons suggest that the relative Lewis basicity of involved aliphatic amines, with respect to the reference Lewis acid **1a**, is governed by steric effects, and can be attributed to poorer overlap of orbitals because of the additional steric constraints in the case more encumbered species.[47] In fact, the less sterically crowded primary amines show the highest, almost unchanging binding constants. The progressively lower binding constant for secondary and tertiary amines parallels the increasing steric hindrance at the nitrogen amine atom. Alicyclic amines, possessing a reduced sterical hindrance, exhibit larger binding constant values. Thus piperidine possesses a binding constant comparable to the ethylmethylamine, the latter of which being the least sterically encumbered species within the series secondary acyclic amines. Finally, quinuclidine, representing the least sterically encumbered tertiary amine,[35] exhibits the largest binding constant value, even with respect to primary amines (Table 4.3). An analogous trend for the relative binding ability of tertiary amines has recently been found in the formation of zinc-salophen amine adducts.[25]

The secondary alicyclic piperidine and pyrrolidine amines offer the opportunity for a further comparison, being the former a stronger base. This is in agreement with a larger Lewis basicity predicted on theoretical ground for cyclic amines, and can be related to degree of pyramidalization around the nitrogen donor atom.[48] The larger pyramidalization angle of pyrrolidine leads to a larger s-character of the nitrogen lone pair orbital and, hence, to a weaker Lewis basicity.

Prototype heterocyclic amines have been also considered. Again, within this series of amines the order of relative basicity, pyridine > isoquinoline > quinoline, can be related to the increasing steric hindrance at the heterocyclic nitrogen. Note that, pyridine is a stronger Lewis base than triethylamine, although gas-phase basicities indicate the opposite.[4a] However, it has been demonstrated that pyridine can displace trimethylamine from $(CH_3)_3N{\cdot}B(CH_3)_3$.[49] Again, the steric repulsion favour the less encumbered pyridine adduct over the triethylamine analogue.[47]

Among the involved solvents, calculated binding constants indicate that DMSO and DMF are stronger Lewis bases than acyclic tertiary amines and encumbered secondary amines, whereas acetonitrile and acetone represent the weakest bases within the investigated series.

4.4.1.4 Comparison with literature Lewis basicity scales Present Gibbs energy for the **1a**·base adducts can useful be compared with relevant scales reported in the literature,[24,37-39] although the latter refer to the Lewis affinity,[4] as they involve enthalpy measurements for the adduct formation.

In the case of the diiodine adducts, however, a comparison with Gibbs energy is possible (Figure 4.16) from available literature data.[26a,50] It shows a roughly linear correlation for most of the involved bases, with Gibbs energy for the **1a**·base adducts approximately twice than those found for diiodine adducts, thus indicating a stronger acid-base interaction in the former case. A clear divergence of this rough linearity is observed in the case of triethylamine, representing the most encumbered species among the bases involved in this comparison and, to a lesser amount, for the secondary amines **9** and **13**. It, therefore, turns out that these amines exhibit a lower Lewis basicity with the reference acid **1a** than that with the less sterically encumbered reference Lewis diiodine acid. An essentially analogous trend is observed on comparing Gibbs energy for the **1a**·base adducts with the enthalpy of formation for the diiodine analogues

(Figure 4.16). Again, triethylamine strongly deviates from the approximate linearity for the other bases. Note, however, that these comparisons should necessarily be considered just qualitative as the literature data[26a,50] refer to measurements in various laboratories, using different conditions and different data refinement.

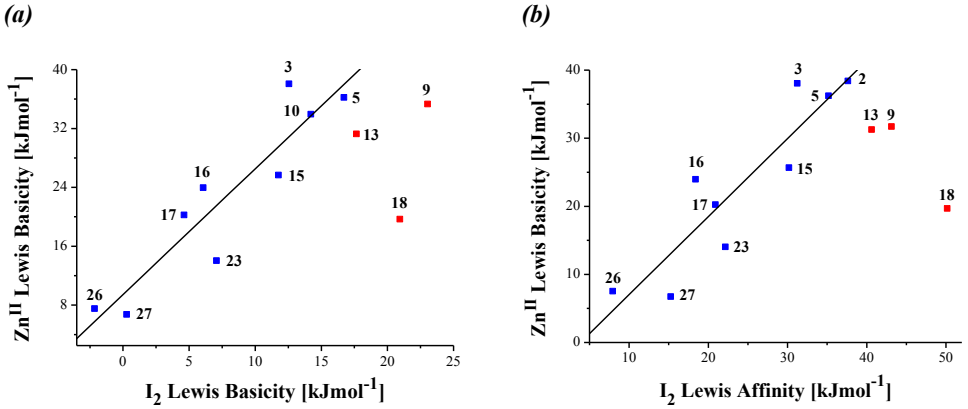

Figure 4.16 Comparison of Lewis basicity for **1a**·base adducts and *(a)* diiodine Lewis basicity or *(b)* diiodine Lewis affinity. Diiodine data are from references 26a and 50. Masked data (marked in red) are not included in the linear fit.

The comparison of the Gibbs energy for the **1a**·base adducts with available data from the $SbCl_5$[37] and BF_3[24a,38] Lewis affinity scales, the latter of which represents a homogeneous set of values, allows for a further assessment of present Lewis basicity scale. In both cases, linearity is apparent for involved solvents (Figure 4.17), whereas departure from linearity is evident for triethylamine and for isopropylamine.

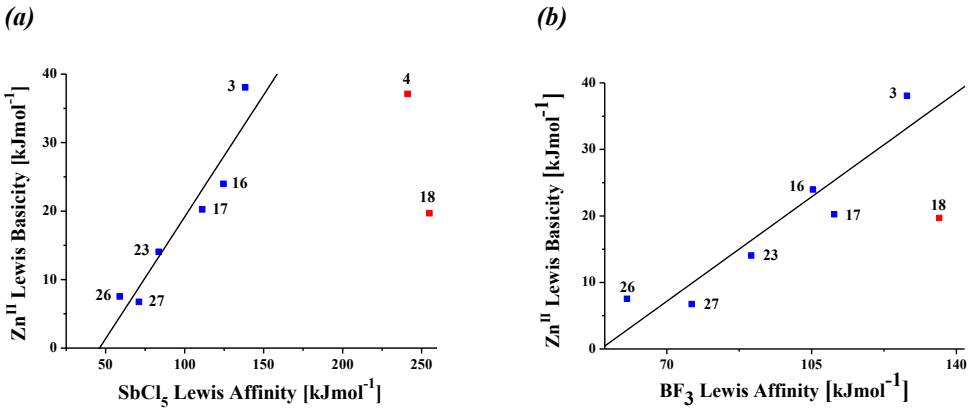

Figure 4.17 Comparison of Lewis basicity for **1a**·base adducts and *(a)* $SbCl_5$ Lewis affinity or *(b)* BF_3 Lewis affinity. $SbCl_5$ and BF_3 data are from references 24a, 37 and 38, respectively. Masked data (marked in red) are not included in the linear fit.

In particular, present data indicate a lower Lewis basicity for these aliphatic amines with respect that predicted considering $SbCl_5$ or BF_3 as reference acids. Again, it can be related to the greater steric hindrance at the nitrogen atom for these aliphatic amines.

In summary, the comparison of present Lewis basicity scale with data reported in the literature indicates that although the relative basicity for the involved solvents representing less sterically encumbered species is scarcely affected by the reference Lewis acid, for sterically encumbered amines, the Lewis basicity seems to be dependent from the reference acid. Actually, the reference Lewis acidic Zn^{II} complex **1a** involves very different relative Lewis basicities than those expected considering the less sterically encumbered $SbCl_5$, BF_3, or I_2 reference species. Thus, even the DMSO solvent is expected to be more basic than triethylamine, the latter of which is commonly considered as a strong base. On the other hand, THF possesses Lewis basicity comparable to that of various encumbered acyclic tertiary amines.

4.5 Vapochromism of 1a for detection of volatile organic compounds

A material is vapochromic if its colour changes reversibly upon exposure to vapours of a volatile chemical species.[53] This kind of materials have been recently investigated for the design and development of chemosensors,[54] useful for the selective and sensitive detection of volatile organic compounds (VOCs).[55]

The optical variations can be related to the:

- modulation of inter- or intramolecular metal-metal bonds[56]
- metal-solvent bonds[57]
- isomerization[53d,58]
- change of coordination geometry of metal centre[56b,57a,59]
- π-π interactions[60]
- host-guest interactions[61]

Lewis acid Zn^{II} Schiff base complexes tend to saturate their coordination sphere through axial coordination with a Lewis base or intermolecular Zn···O interactions both in solution and in the solid state.[5] Considering the ability to coordinate various Lewis bases, such as amines, alkaloids and solvents in solution, and the dramatic optical variations upon deaggregation (see sections **3.2**, **4.2-4.4**), the Zn^{II} Schiff base complex **1a** could be a potential vapochromic material useful for detection in the solid state of volatile Lewis base species.

In this section, the study of vapochromic properties of **1a** and the characterization of cast film for potential chemosensor application of volatile Lewis bases are reported. Through UV-vis absorption analysis, it is found that **1a** is a vapochromic material because of a dramatic reversible colour change upon exposure to isopropylamine vapours; hence it represents a useful potential chemosensor for detection of VOCs.

4.5.1 Results and Discussion

4.5.1.1 Vapochromic properties of 1a The idea to investigate the vapochromic properties of complex **1a** arose from the observed dramatic colour change of the precipitate solid **1a**, obtained by precipitation from ethanol in the synthesis procedure (see paragraph **2.4**), upon drying (80 °C, 10 mbar) (Figure 4.18).

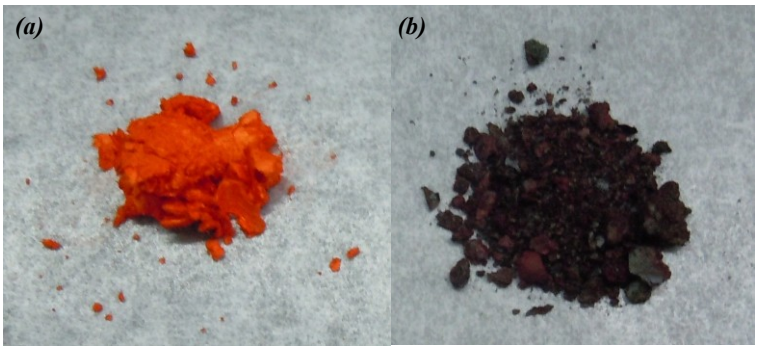

Figure 4.18 Solid complex **1a** *(a)* before and *(b)* after drying.

This colour change is consistent with the formation of aggregate species through intermolecular Zn···O interactions occurring by removal of the coordinated solvent to **1a** after the drying process. This hypothesis is in part supported by the spectral differences between the optical absorption spectra of the solid **1a** before and after drying in DCM solution (1.0×10^{-5} M) (Figure 4.19).

On passing from the spectrum of **1a** dried to that of **1a** obtained from ethanol, a hypochromism of the band centred at 345 nm, a shift of ~8 nm of the band at 429 nm and a split of the band centred at 529 nm into two bands at 511 nm and 539 nm are observed. These differences are consistent with the presence in solution of a small amount of ethanol axially coordinated to the Zn^{II} ion of **1a** (see Figures 3.16, 4.2, 4.8 and 4.15). Actually, since ethanol is a weak Lewis base (see section **4.4**), to achieve the typical optical variations observed in the formation of **1a**·Lewis base adduct, it is

required a stoichiometric excess amount of ethanol (see equilibrium 1 in the section **4.4**).

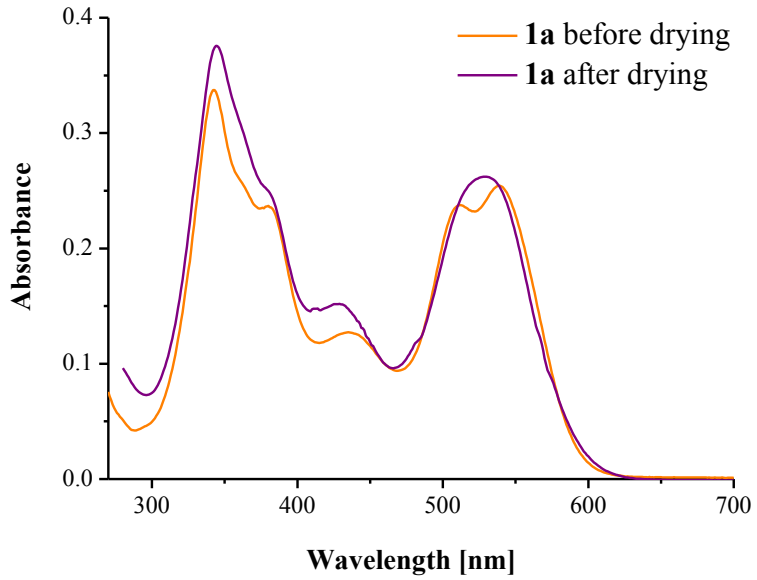

Figure 4.19 UV-vis spectra of **1a** in DCM (1.0×10^{-5} M) obtained solubilising the solid before (—) and after (—) the drying process.

However, to definite **1a** a vapochromic material, it is essential that the solid changes reversibly colour upon coordination of volatile Lewis bases. Thus, the dried solid **1a** has been exposed in an atmosphere of air saturated with vapours of isopropylamine, a highly volatile, strong Lewis base (see sections **4.3** and **4.4**), and then subsequently heated (Figure 4.20).

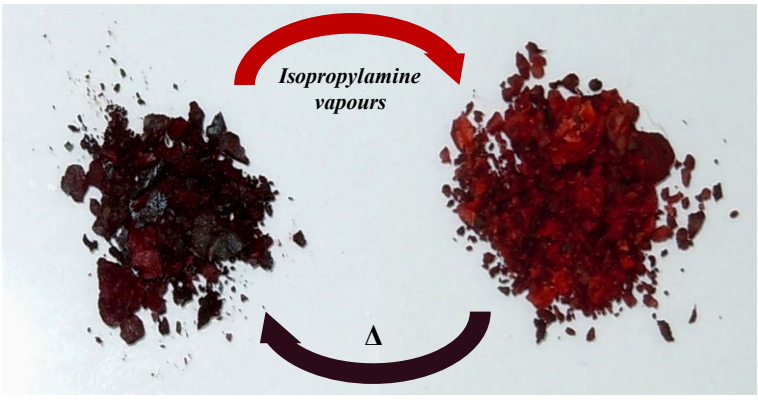

Figure 4.20 Reversible colour change of the dried solid complex **1a** upon exposure to saturate isopropylamine vapours and subsequent heating.

It is evident the reversible colour variation of the dried solid **1a** after exposure to saturate isopropylamine vapours. This colour variation resembles that observed for the solid **1a** obtained by precipitation from ethanol in the synthesis procedure (Figure 4.18) and is consistent with the amine coordination in the solid state. Therefore, **1a** possesses all features of a vapochromic material.

4.5.1.2 Vapochromic behaviour of drop cast films of 1a To investigate quantitatively the vapochromic properties of **1a**, films obtained by drop-casting on glass substrates from DCM solutions of **1a**, have been chosen. This is an easy, fast and cheap useful technique for the achievement of films. Moreover, considering that observed optical variations are in the visible spectrum, it is possible to use glass substrates for casting. The UV-vis spectrum of the film obtained by drop-casting from a DCM solution of **1a** (1.0×10^{-3} M) in reported in Figure 4.21.

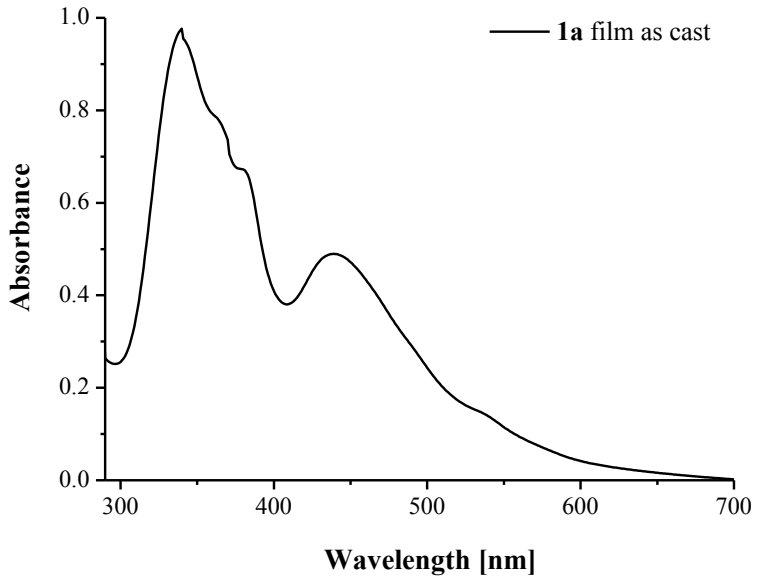

Figure 4.21 UV-vis spectrum of a film obtained by casting from a DCM solution of **1a** at 1.0×10^{-3} M.

The spectrum shows two main bands centred at 340 and 440 nm and it is deeply different with respect to the analogous spectrum of **1a** in DCM solution (see sections **3.2**, **4.2**-**4.4**). To rule out that these observed spectral differences are due to effects of the concentration, solvent, or method of preparation of the films, cast films of **1a** obtained from DCM and THF solutions at different concentration, and films obtained

through spin coating of **1a** DCM solutions (1.0×10^{-3} M) have been investigated (Figure 4.22-4.24).

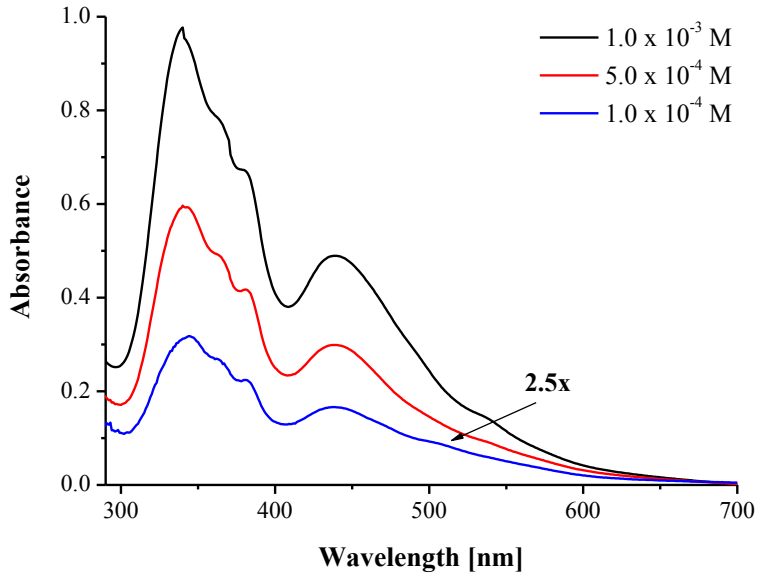

Figure 4.22 UV-vis spectra of films deposited by casting from **1a** DCM solutions at different concentrations.

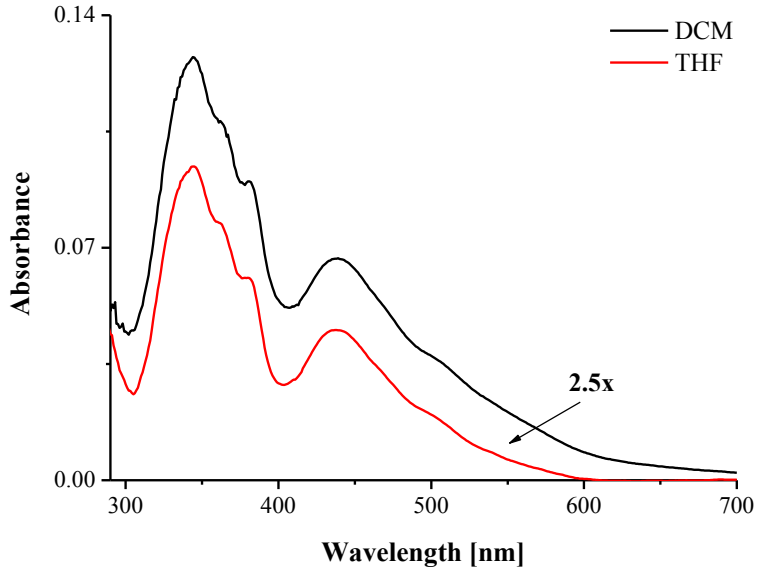

Figure 4.23 UV-vis spectra of films deposited by casting from a solution of **1a** at 1.0×10^{-4} M in DCM (—) and THF (—).

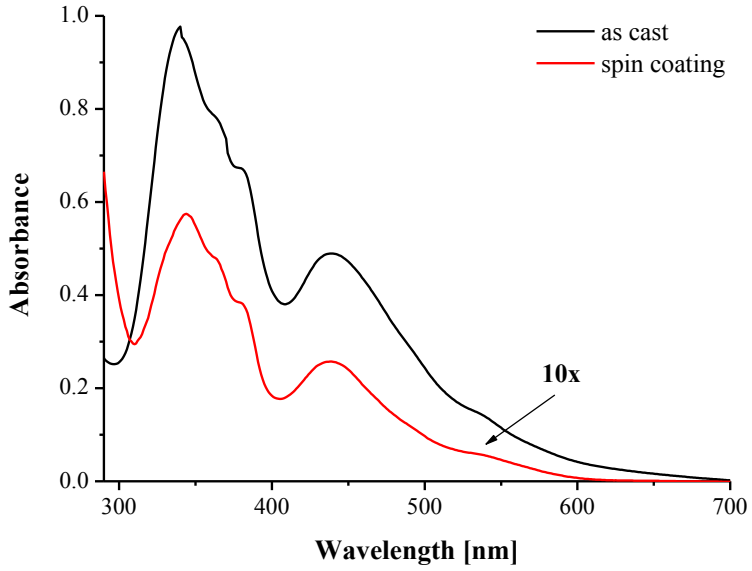

Figure 4.24 Comparison of UV-vis spectra of films obtained by casting (—) and spin coating (—) from a solution of **1a** at 1.0×10^{-3} M in DCM.

The comparison in Figure 4.22 shows that the UV-vis spectra of films of **1a** are unaffected from the concentration of the cast solution. However, no adherence to the Lambert-Beer law is observed, because the difference in terms of absorbance is related to the different amount of **1a** solution deposited in the casting process.

Films having analogous optical absorption properties are obtained even by casting from THF solutions. In fact, comparing the UV-vis spectra of **1a** films obtained by casting from THF and DCM solutions, no spectral differences, in terms of shape and position of the spectrum bands, are observed (Figure 4.23). As observed for the series of complexes having benzene ring bridge (see paragraph **3.3.2**), being the THF is a weak volatile Lewis base (see paragraph **4.4.1.2**), in the casting process, upon evaporation of the solvent, **1a** is stabilized through intermolecular Zn···O interactions with formation of the same aggregate species observed in the films obtained by casting from DCM solutions.

Finally, the formation of aggregate species **1a** is independent from the methodology used for the achievement of the films. In fact, the films obtained by spin coating from a 1.0×10^{-3} M DCM solution of **1a** possess a UV-vis spectrum analogous to those obtained by drop-casting (Figure 4.24).

Overall results demonstrate that the differences between the UV-vis spectrum of **1a** in solution and in the solid film are not related to the solvent, concentration or method

of preparation of the film, but are exclusively related to a different structure of aggregates in the two cases. Even if the molecular aggregation of Zn^{II} Schiff base complexes occurs through intermolecular Zn···O interactions both in solution and in the solid state,[5] in the latter case, secondary interactions may play a role in the stabilization of the aggregate structure.

To investigate the vapochromic effect upon coordination of a volatile Lewis base, a **1a** film obtained by drop-casting from a 1.0×10^{-3} M DCM solution has been exposed to saturate isopropylamine vapours and analyzed thought UV-vis spectroscopy.

The exposure to vapours of isopropylamine implies dramatic variations of the UV-vis spectrum of the film, accompanied by a naked-eye observation of the colour change (Figure 4.25). In particular, on passing from the UV-vis spectrum of the film as cast to that recorded after exposure to vapour of isopropylamine, a hypochromic shift of the band centred at 340 nm and a bathochromic shift of ~16 nm of the band centred at 440 nm, with the appearance of a shoulder at 503 nm, are observed. These variations are analogous to those observed in solution (see sections **3.2**, **4.2**-**4.4**) and are consistent with the chemisorption of isopropylamine.

To assess the reversibility of the vapochromic properties, **1a** films after exposure to vapours of isopropylamine, have been subjected to a heating process (80°C, 10 mbar, 15min), in order to desorb the coordinated amine to the Zn^{II} ion. Surprisingly, an unexpected behaviour upon the heating process is observed. In fact, the colour and, hence, the optical properties of the film, are dramatically different, compared to those of the film as cast. In particular, compared to the UV-vis spectrum of the as cast film, a hypochromic effect on the overall spectrum, a bathochromic shift of 15 nm of the band centred at 440 nm and the appearance of a new band at 568 nm, are observed. Therefore, the UV-vis spectrum of the as cast film upon heating is not restored (Figure 4.26). This observed unexpected behaviour is not due to the amine coordination. In fact, analogous optical absorption spectra are obtained upon a heating treatment “annealing” (80°C, 10 mbar, 15min), of the as cast films without any previous exposure to volatile Lewis bases (Figure 4.27).

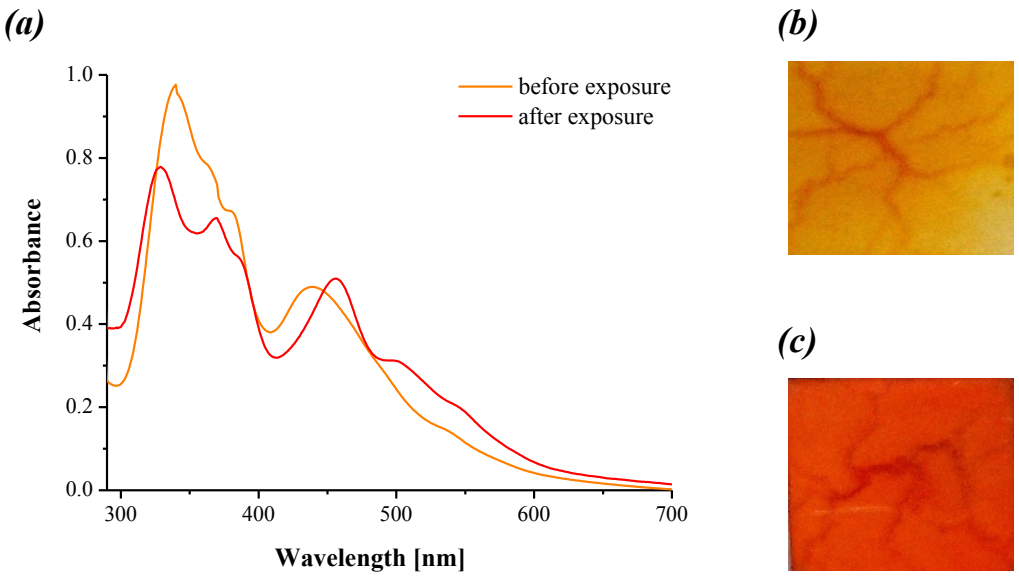

Figure 4.25 *(a)* UV-vis spectra of a **1a** film obtained by drop-casting of a 1.0×10^{-3} M DCM solution before (—) and after (—) exposure of saturate isopropylamine vapours. Visual colour change of a **1a** film as cast, before *(b)* and *(c)* after the exposure to isopropylamine vapours.

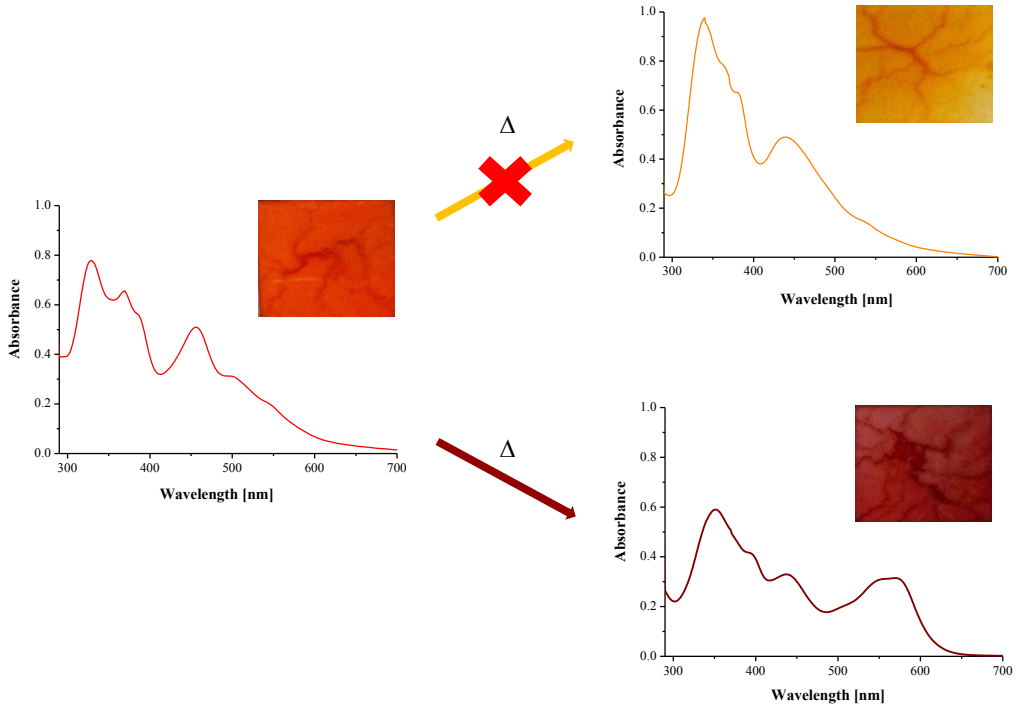

Figure 4.26 UV-vis spectra and visual colour change of a film after exposure to isopropylamine (—) upon the heating process (—).

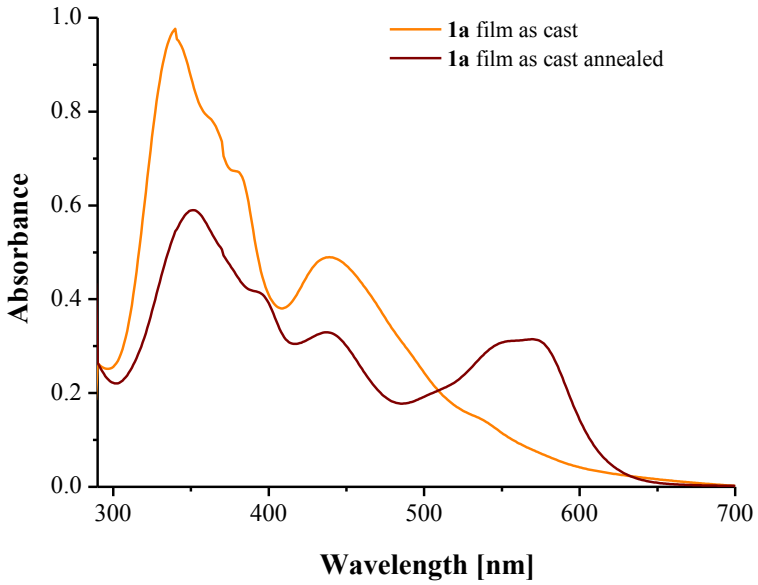

Figure 4.27 UV-vis spectra of films obtained by drop-casting from a **1a** solution (1.0×10^{-3} M) in DCM before (—) and after (—) annealing.

Since the colour and optical absorption variations of **1a** films upon this thermal treatment are independent from the exposure to volatile Lewis bases, an annealed film has been exposed to saturate isopropylamine vapours to verify whether the amine coordination implies optical absorption properties as those observed for the films as cast. Moreover, after exposure, the same film has been heated to verify or not the restoring of the UV-vis spectrum (Figure 4.28).

The exposure to isopropylamine vapours implies dramatic optical absorption variations accompanied by a naked-eye observation of the colour change. In particular, the UV-vis spectrum is formed by two bands at 332 and 369 nm in the 290-420 nm range, two bands at 460 and 504 nm and a shoulder at 547nm in the range 400-600 nm. These variations are consistent with the coordination of isopropylamine and are analogous to those observed for **1a** film as cast (Figure 4.29). In fact, in terms of band position, both UV-vis spectra are almost identical. The variations of the intensities of the bands are related to the two different initial conditions of cast-films. On the other hand, different spectroscopic shifts upon amine coordination are observed for the film as cast and heated. In particular, upon exposure to amine vapours, a red shift of the visible band for the as cast films (Figure 4.25), whereas a blue shift of the visible band for the films heated is observed (Figure 4.28).

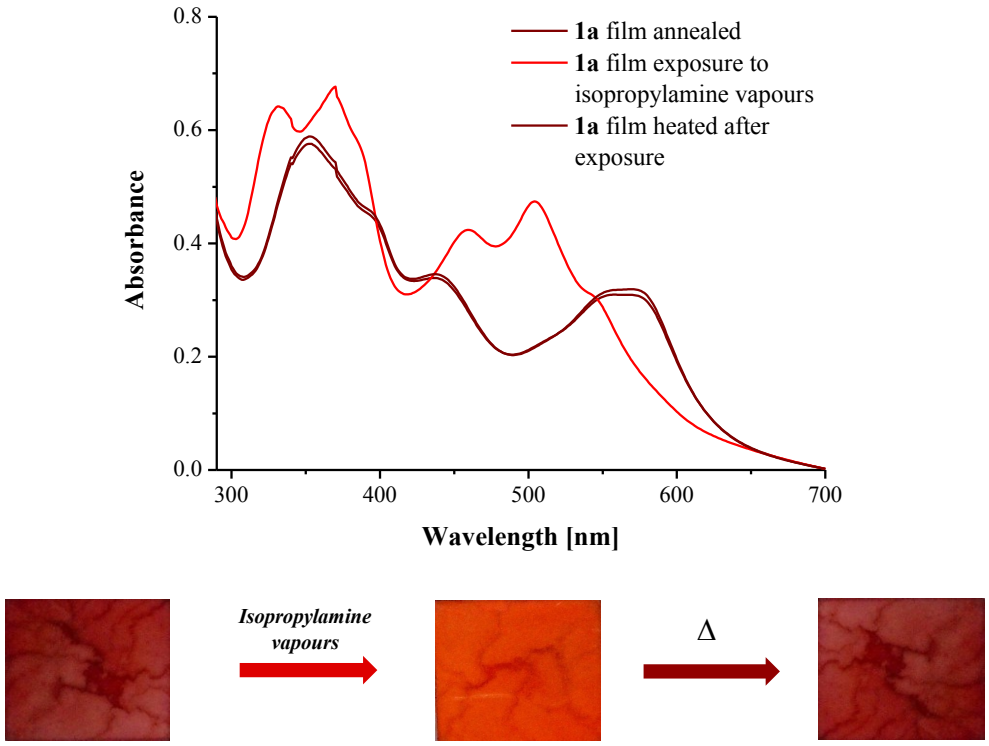

Figure 4.28 *(Top)* UV-vis spectra and *(bottom)* visual colour change of a **1a** film annealed (—), after exposure to isopropylamine vapours (—) and heated after exposure to isopropylamine vapours (—).

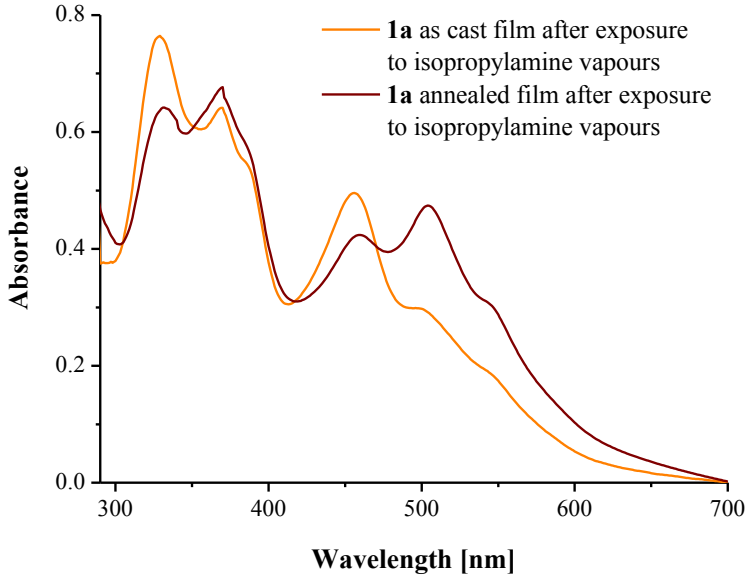

Figure 4.29 Comparison of UV-vis spectra of a **1a** film as cast (—) and annealed (—) after exposure to isopropylamine vapours.

In addition, in the case of the annealed films, the heating process after the exposure of isopropylamine vapours implies the complete restoring of Uv-vis spectrum recorded before the exposure (Figure 4.28), on contrary to that observed for the film as cast heated after exposure to amine vapours (Figure 4.26). This optical colour change is completely reversible in the chemisorption (ON)/desorption (OFF) cycles of the amine vapour (Figure 4.30).

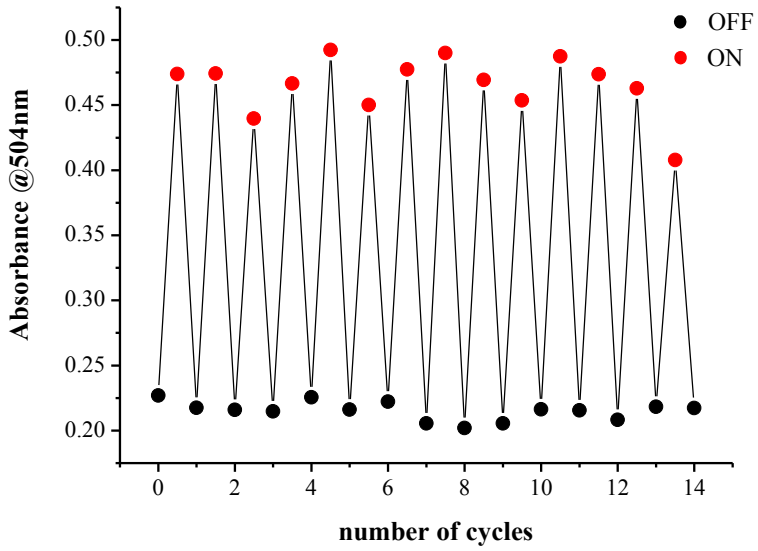

Figure 4.30 Absorbance values of **1a** film heated recorded at 504 nm in a series of the chemisorption (ON)/desorption (OFF) cycles of the saturate isopropylamine vapours.

The colour and the optical absorption property changes observed are consistent with a deep variation of the structure of the aggregate species in the solid state. This hypothesis is confirmed by X-ray diffraction (XRD) patterns of **1a** films as-cast, heated and exposed to saturate isopropylamine vapours (Figure 4.31).

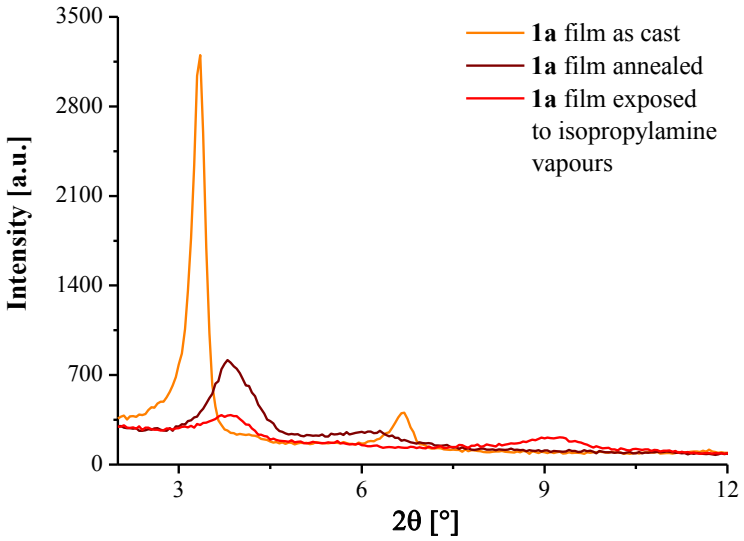

Figure 4.31 Comparison of X-ray diffraction (XRD) patterns of **1a** films as cast (—), annealed (—) and exposed to isopropylamine vapours (—).

The XRD patters are deeply different, thus indicating a different molecular structure in three cases.

Overall data indicate that presumably **1a** forms two different kinds of aggregate structures in the solid state. In particular, H-aggregates can be associated to as-cast films, whereas J-aggregates are likely formed upon heating (Chart 4.3). This is in agreement with the observed blue-shift of the visible optical absorption band on switching from the as cast to the heated films. Upon exposure to saturate isopropylamine vapours, the amine coordination to both aggregate species occurs, leading to identical final species. The structural transition H- → J-aggregates is irreversible because J-aggregates are more stable than H-aggregates. In fact, once J-aggregates are obtained through annealing of the as-cast films, the ON/OFF cycles to the amine vapours always leads to the restoring of J-aggregates. Therefore, the completely reversibility of amine coordination allows the application of **1a** as a vapochromic material for the sensing of volatile Lewis bases in the solid state.

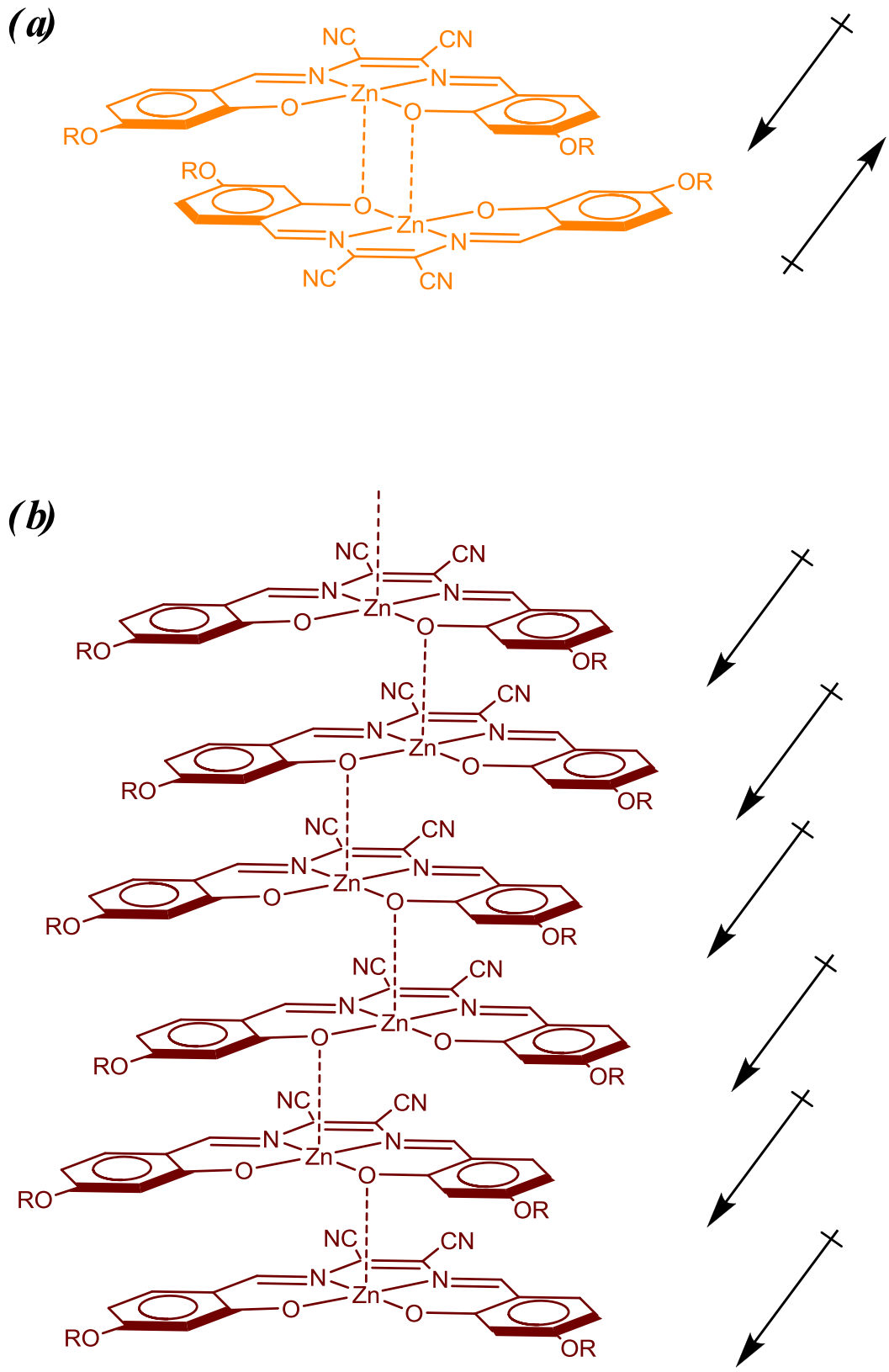

Chart 4.3 Representations of *(a)* H and *(b)* J-aggregates in **1a** films as cast and heated respectively.

4.6 Conclusions

On the basis of the results discussed, the Zn^{II} complex **1a** can be considered a sensitive fluorescent probe for alkaloids and amines in DCM, which exhibits fluorescence enhancement upon formation of 1:1 adducts. Its binding interaction can be related to Lewis basicity, strongly influenced by the steric characteristics of the coordinating nitrogen based species, leading to high selectivity, in the micromolar range, and sensitivity for pyridine-based, cinchona alkaloids, primary and alicyclic amines. Moreover, a distinct selectivity is also observed along the series of secondary or tertiary amines, paralleling the increasing steric hindrance at the nitrogen atom.

The use of the Lewis acidic Zn^{II} complex **1a** has successfully allowed the achievement of a consistent, reliable scale of Lewis basicity for amines and non-protogenic solvents. It represents a unique set of data reflecting the actual Lewis basicity with respect this "*real world*" Lewis acidic species.

The comparison of present Lewis basicity scale with data reported in the literature indicates that although the relative basicity of the involved solvents is scarcely affected by the reference Lewis acid, for sterically encumbered amines, the Lewis basicity seems to be dependent from the reference species. Actually, even if $SbCl_5$, BF_3, or I_2 are considered good reference Lewis acids, they represent simple model systems given their less sterically encumbered nature. In these cases, relative Lewis basicities take into account almost exclusively for electronic effects alone,[51] but not for sterical effects, which significantly contribute to the actual basicity of a species.

For the present reference Lewis acidic Zn^{II} complex **1a**, Lewis basicity is governed by the steric hindrance at the donor atom and involves very different relative basicities than those predicted considering typical reference Lewis acids. Thus, even the DMSO solvent is more basic than triethylamine, commonly considered as a strong base, whereas THF possesses Lewis basicity comparable to that of various encumbered acyclic tertiary amines. This is expected to have a major involvement in the organic synthesis and catalysis, given the sterically encumbered nature of commonly involved Lewis acidic organometallic complexes.

Modeling calculations for **1a**·base adducts in fluctuating polar solvent remains a challenge for the future, for example, by using QM/MM methodology[52] to generalize the present Lewis basicity scale to other solvent media.

Drop-casting of solutions of **1a** carries out to the formation of H-aggregate films which change colour upon exposure to saturate isopropylamine vapours according to amine coordination. Anneling of as cast films implies an irreversible structural transition H- → J-aggregates. On contrary to H-aggregates, J-aggregate films of **1a** possess vapochromic properties because the chemisorption/desorption process of the isopropylamine vapours is completely reversible, thus allowing the application of **1a** as potential chemosensor of volatile Lewis bases in the solid state.

4.7 References

1. *(a)* Kobayashi, H.; Ogawa, M.; Alford, R.; Choyke, P. L.; Urano, Y. *Chem. Rev.* **2010**, *110*, 2620. *(b)* Bates, M.; Huang, B.; Dempsey, G. T.; Zhuang, X. W. *Science* **2007**, *317*, 1749. *(c)* Becker, A.; Hessenius, C.; Licha, K.; Ebert, B.; Sukowski, U.; Semmler, W.; Wiedenmann, B.; Grotzinger, C. *Nat. Biotechnol.* **2001**, *19*, 327.
2. *(a)* Caruso, M. M.; Davis, D. A.; Shen, Q.; Odom, S. A., Sottos, N. R.; White, S. R.; Moore, J. S. *Chem. Rev.* **2009**, *109*, 5755. *(b*) Sagara, Y.; Kato, K. *Nat. Chem.* **2009**, *1*, 605.
3. Muller, P. *Pure Appl. Chem.* **1994**, *66*, 1077.
4. *(a)* For an excellent, general book on the Lewis basicity, see for example: Laurence, C.; Gal, J.-F. *Lewis Basicity and Affinity Scale: Data and Measurements*, Wiley: Chichester, U.K., 2010. *(b)* Persson, I.; Sadström, M.; Goggin, P. L. *Inorg. Chim. Acta* **1987**, *129*, 183.
5. *(a)* Kleij, A. W. *Dalton Trans.* **2009**, 4635. *(b)* Escudero-Adán, E. C.; Benet-Buchholz, J.; Kleij, A. W. *Inorg. Chem.* **2008**, *47*, 4256. *(c)* Hui, J. K.-H.; Yu, Z.; MacLachlan, M. J. *Angew. Chem. Int. Ed.* **2007**, *46*, 7980. *(d)* Gallant, A. J.; Chong, J. H.; MacLachlan, M. J. *Inorg. Chem.* **2006**, *45*, 5248. *(e)* Kleij, A. W.; Kuil, M.; Lutz, M.; Tooke, D. M.; Spek, A. L.; Kamer, P. C. K.; vanLeeuwen, P. W. N. M.; Reek, J. N. H. *Inorg. Chim. Acta* **2006**, *359*, 1807. *(f)* Kleij, A. W.; Kuil, M.; Tooke, D. M.; Lutz, M.; Spek, A. L.; Reek, J. N. H. *Chem. Eur. J.* **2005**, *11*, 4743. *(g)* Ma, C. T. L.; MacLachlan, M. J. *Angew. Chem. Int. Ed.* **2005**, *44*, 4178. *(h)* Matalobos, J. S.; García-Deibe, A. M.; Fondo, D. N.; Bermejo, M. R. *Inorg. Chem. Comm.* **2004**, *7*, 311. *(i)* Reglinski, J.; Morris S.; Stevenson, D. E. *Polyhedron* **2002**, *21*, 2175.

6. *(a)* Consiglio, G.; Failla, S.; Finocchiaro, P.; Oliveri, I. P.; Di Bella, S. *Inorg. Chem.* **2012**, *51*, 8409. *(b)* Consiglio, G.; Failla, S.; Finocchiaro, P.; Oliveri, I. P.; Di Bella, S. *Dalton Trans.* **2012**, *41*, 387. *(c)* Consiglio, G.; Failla, S.; Finocchiaro, P.; Oliveri, I. P.; Purrello, R.; Di Bella, S. *Inorg. Chem.* **2010**, *49*, 5134. *(d)* Consiglio, G.; Failla, S.; Oliveri, I. P.; Purrello, R.; Di Bella, S. *Dalton Trans.* **2009**, 10426.
7. *(a)* Oliveri, I. P.; Di Bella, S. *Tetrahedron* **2011**, *67*, 9446. *(b)* Oliveri, I. P.; Di Bella, S. *J. Phys. Chem. A* **2011**, *115*, 14325. *(c)* Oliveri, I. P.; Maccarrone, G.; Di Bella, S. *J. Org. Chem.* **2011**, *76*, 8879.
8. Selected general reviews:*(a)* Basabe-Desmonts, L.; Reinhoudt, D. N.; Crego-Calama, M. *Chem. Soc. Rev.* **2007**, *36*, 993. (b) Bell, T. W.; Hext, N. M. *Chem. Soc. Rev.* **2004**, *33*, 589.
9. *(a)* Gans, P.; Sabatini, A.; Vacca, A. *Talanta* **1996**, *43*, 1739. *(b)* Sabatini, A.; Vacca, A.; Gans, P. *Coord. Chem. Rev.* **1992**, *120*, 389.
10. *(a)* Aniszewski, T. *Alkaloids – Secrets of life*; Elsevier: Amsterdam, 2007. *(b)* Manfred, H. *Alkaloids. Nature's Curse or Blessing*; Wiley-VCH: Weinheim, 2002. *(c)* Roberts, M. F; Wink, M. *Alkaloids: Biochemistry, Ecology, and Medicinal Applications*; Plenum Press: New York, 1998.
11. *(a)* Bremner, J. B. *Pure Appl. Chem.* **2007**, *79*, 2143. *(b)* Grycová, L.; Dostál, J.; Marek, R. *Phytochemistry* **2007**, *68*, 150.
12. Karatas, A.; Gokce, F.; Demir, S.; Ankarali, S. *Neurosci. Lett.* **2008**, *445*, 58.
13. Grynkiewicz, G.; Gadzikowska, M. *Pharmacol. Rep.* **2008**, *60*, 439.
14. Wright, C. W. *Phytochem. Rev.* **2005**, *4*, 55.
15. *(a)* Wonnacott, S.; Sidhpura, N.; Balfour, D. J. K. *Curr. Opin. Pharmacol.* **2005**, 5, 53. *(b)* Waldvogel, S. R. *Angew. Chem. Int. Ed.* **2003**, *42*, 604.
16. Steketee, J. D. *Crit. Rev. Neurobiol.* **2005**, *17*, 69.
17. *(a)* Tálas, E.; Margitfalvi, J. L. *Chirality* **2010**, *22*, 3. *(b)* Song, C. E. *Cinchona Alkaloids in Synthesis & Catalysis: Ligands, Immobilization and Organocatalysis*; Wiley-VCH: Weinheim, 2009. (c) Kim, J.; Movassaghi, M. *Chem. Soc. Rev.* **2009**, *38*, 3035. *(d)* Jew, S.-s.; Park, H.-g. *Chem. Commun.* **2009**, 7090. *(e)* Tian, S.-K.; Chen, Y.; Hang, J.; Tang, L.; McDaid, P.; Deng, L. *Acc. Chem. Res.* **2004**, *37*, 621.
18. Pei, R.; Shen, A.; Olah, M. J.; Stefanovic, D.; Worgall, T.; Stojanovic, M. N. *Chem. Commun.* **2009**, 3193.

19. *(a)* Megyesi, M.; Biczók, L. *J. Phys. Chem. B* **2010**, *114*, 2814. *(b)* Mahapatra, A. K.; Sahoo, P.; Goswami, S.; Fun, H.-K.; Yeap, C. s. *J. Incl. Phenom. Macrocycl. Chem.* **2010**, *67*, 99. *(c)* Li, C.; Li, J.; Jia, X. *Org. Biomol. Chem.* **2009**, *7*, 2699. *(d)* Siering, C.; Kerschbaumer, H.; Nieger, M.; Waldvogel, S. R. *Org. Lett.* **2006**, *8*, 1471. *(e)* Deviprasad, G. R.; D'Souza, F. *Chem. Commun.* **2000**, 1915.

20. *(a)* Matsushita, M.; Yoshida, K.; Yamamoto, N.; Wirsching, P.; Lerner, R. A.; Janda, K. D. *Angew. Chem. Int. Ed.* **2003**, *42*, 5984. *(b)* Liu, Y.; Li, L.; Zhang, H.-Y.; Fan, Z.; Guan, X.-D. *Bioorg. Chem.* **2003**, *31*, 11. *(c)* Ueno, A.; Suzuki, I.; Osa, T. *Anal. Chem.* **1990**, *62*, 2461.

21. *(a)* Liu, B.; Chen, C.; Wu, D.; Su, Q. *J. Chromatogr. B* **2008**, *865*, 13. *(b)* Zhang, J.; Ji, H.; Sun, S.; Mao, D.; Liu, H.; Guo, Y. *J. Am. Soc. Mass Spectrom.* **2007**, 18, 1774. *(c)* Shen, J.; Shao, X. *Anal. Chim. Acta* **2006**, *561*, 83.

22. *(a)* Gil, V. M. S.; Oliveira, N. C. *J. Chem. Educ.* **1990**, *67*, 473. *(b)* Hill, Z. D.; MacCarthy, P. *J. Chem. Educ.* **1986**, *63*, 162. *(c)* Job, P. *Ann. Chem.* **1928**, *9*, 113.

23. Bourson, J.; Pouget, J.; Valeur, B. *J. Phys. Chem.* **1993**, *97*, 4552.

24. *(a)* Maria, P. C.; Gal, J. F. *J. Phys. Chem.* **1985**, *89*, 1296. *(b)* Jensen, W. B. *Chem. Rev.* **1978**, *78*, 1.

25. *(a)* Dalla Cort, A.; Mandolini, L.; Pasquini, C.; Rissanen, K.; Russo, L.; Schiaffino, L. *New J. Chem.* **2007**, *31*, 1633.

26. *(a)* Krishna, V. G.; Bhowmik, B. B. *J. Am. Chem. Soc.* **1968**, *90*, 1700. *(b)* Halpern, A. M.; Weiss, K. *J. Am. Chem. Soc.* **1968**, *90*, 6297.

27. *(a)* Currie, L. A. *Anal. Chim. Acta* **1999**, *391*, 127. *(b)* Analytical Methods Committee *Analyst* **1987**, *112*, 199.

28. *(a)* Li, L.; Sun, H. *Anal. Methods* **2010**, *2*, 1270. *(b)* Chen, Y.-Z.; Liu, G.-Z.; Shen, Y.; Chen, B.; Zeng, J.-Z. *J. Chromatogr. A* **2009**, *1216*, 2104. *(c)* Beyer, J.; Peters, F. T.; Kraemer, T.; Maurer, H. H. *J. Mass Spectrom.* **2007**, *42*, 621. *(d)* Reddy, M. M.; Suresh, V.; Jayashanker, G.; Rao, B. S.; Sarin, R. K. *Electrophoresis* **2003**, *24*, 1437. *(e)* Zheng, W.; Wang, S.; Barnes, L. F.; Guan, Y.; Louis, E. D. *Anal. Biochem.* **2000**, *279*, 125. *(f)* Lin, L. A. *J. Chromatogr.* **1993**, *632*, 69. *(g)* Gong, Z.; Zhang, Z.; Yang, X. *Analyst* **1997**, *122*, 283.

29. See, for example: Lawrence, S. A. *Amines: Synthesis, Properties and Applications*; Cambridge, University Press, 2004.

30. See, for example: *(a)* Nugent, T. C. *Chiral Amine Synthesis*; Wiley-VCH, Weinheim, 2010. *(b)* France, S.; Guerin, D. J.; Miller, S. J.; Lectka, T. *Chem. Rev.* **2003**, *103*, 2985.
31. Selected general reviews: *(a)* Mohr, G. J. *Anal. Bioanal. Chem.* **2006**, *386*, 1201. *(b)* Wright, A. T.; Anslyn, E. V. *Chem. Soc. Rev.* **2006**, *35*, 14.
32. Selected general reviews: *(a)* Al Bulushi, I.; Poole, S.; Deeth, H. C.; Dykes, G. A. *Crit. Rev. Food Sci. Nutr.* **2009**, *49*, 369. *(b)* Silva, P. J.; Erupe, M. E.; Price, D.; Elias, J.; Malloy, Q. G. J.; Li, Q.; Warren, B.; Cocker, D. R. III *Environ. Sci. Technol.* **2008**, *42*, 4689. *(c)* Ruiz-Capillas, C.; Jimenez-Colmenero, F. *Crit. Rev. Food Sci. Nutr.* **2004**, *44*, 489. *(d)* Schipper, R. G.; Penning, L. C.; Verhofstad, A. A. J. *Semin. Cancer Biol.* **2000**, *10*, 55. *(e)* Greim, H.; Bury, D.; Klimisch, H.-J.; Oeben-Negele, M.; Ziegler-Skylakakis, K. *Chemosphere* **1998**, *36*, 271.
33. Selected recent examples: *(a)* Ajayakumar, M. R.; Mukhopadhyay, P. *Chem. Commun.* **2009**, 3702. *(b)* Montes-Navajas, P.; Baumes, L. A.; Corma, A.; Garcia, H. *Tetrahedron Lett.* **2009**, *50*, 2301. *(c)* Reinert, S.; Mohr, G. J. *Chem. Commun.* **2008**, 2272. *(d)* Jung, J. H.; Lee, H. Y.; Jung, S. H.; Lee, S. J.; Sakata, Y.; Kaneda, T. *Tetrahedron* **2008**, *64*, 6705. *(e)* Kim, J. S.; Lee, S. J.; Jung, J. H.; Hwang, I.-C.; Singh, N. J.; Kim, S. K.; Lee, S. H.; Kim, H. J.; Keum, C. S.; Lee, J. W.; Kim, K. S. *Chem. Eur. J.* **2007**, *13*, 3082. *(f)* Nelson, T. L.; O'Sullivan, C.; Greene, N. T.; Maynor, M. S.; Lavigne, J. J. *J. Am. Chem. Soc.* **2006**, *128*, 5640. *(g)* Basurto, S.; Torroba, T.; Comes, M.; Martínez-Máñez, R.; Sancenón, F.; Villaescusa, L.; Amorós, P. *Org. Lett.* **2005**, *7*, 5469. *(h)* Comes, M.; Marcos, M. D.; Martínez-Máñez, R.; Sancenón, F.; Soto, J.; Villaescusa, L. A.; Amorós, P.; Beltrán, D. *Adv. Mater.* **2004**, *16*, 1773.
34. *(a)* Cörstern, S.; Morh, G. J. *Chem. Eur. J.* **2011**, *17*, 969. *(b)* McGrier, P. L.; Solntsev, K. M.; Miao, S.; Tolbert, L. M.; Miranda, O. R.; Rotello, V. M.; Bunz, U. H. F. *Chem. Eur. J.* **2008**, *14*, 4503. *(c)* García-Acosta, B.; Comes, M.; Bricks, J. L.; Kudinova, M. A.; Kurdyukov, V. V.; Tolmachev, A. I.; Descalzo, A. B.; Marcos, M. D.; Martínez-Máñez, R.; Moreno, A.; Sancenón, F.; Soto, J.; Villaescusa, L. A.; Rurack, K.; Barat, J. M.; Escriche, I.; Amorós, P. *Chem. Commun.* **2006**, 2239. *(d)* Lu, G.; Grossman, J. E.; Lambert, J. B. *J. Org. Chem.* **2006**, *71*, 1769. *(e)* Chung, Y. M.; Raman, B.; Ahn, K. H. *Tetrahedron* **2006**, *62*, 11645. *(f)* Secor, K.; Plante, J.;

Avetta, C.; Glass, T. *J. Mater. Chem.* **2005**, *15*, 4073. *(g)* Secor, K. E.; Glass, T. E. *Org. Lett.* **2004**, *6*, 3727. *(h)* Fabbrizzi, L.; Francese, G.; Licchelli, M.; Perotti, A.; Taglietti, A. *Chem. Commun.* **1997**, 581.

35. Wann, D. A.; Blockhuys, F.; Van Alsenoy, C.; Robertson, H. E.; Himmel, H.-J.; Tang, C. Y.; Cowley, A. R; Downs, A. J.; Rankin, D. W. H. *Dalton Trans.* **2007**, 1687.
36. See, for example: *(a)* Takagai, Y.; Nojiri, Y.; Takase, T.; Hinze, W. L.; Butsugan, M.; Igarashi, S. *Analyst* **2010**, *135*, 1417. *(b)* Bao, B.; Yuwen, L.; Zheng, X.; Weng, L.; Zhu, X.; Zhan, X.; Wang, L. *J. Mater. Chem.* **2010**, *20*, 9628.
37. See, for example: *(a)* Gutmann, V. *Coord. Chem. Rev.* **1976**, *16*, 225. *(b)* Gutmann, V. *Coord. Chem. Rev.* **1975**, *15*, 207. *(c)* Gutmann, V.; Schmid, R. *Coord. Chem. Rev.* **1974**, *12*, 263.
38. *(a)* Maria, P. C.; Gal, J.-F.; de Franceschi, J.; Fargins, E. *J. Am. Chem. Soc.* **1987**, *109*, 483.
39. See, for example: Laurence, C.; Queignec-Cabanetos, M.; Dziembowska, T.; Queignec, R.; Wojtkowiak, B. *J. Am. Chem. Soc.* **1981**, *103*, 2567.
40. See, for example: *(a)* Laurence, C.; Graton, J.; Berthelot, M.; Besseau, F.; Le Questel, J.-Y.; Luçon, M.; Ouvrad, C.; Plachat, A.; Renault, R. *J. Org. Chem.* **2010**, *75*, 4105. *(b)* Graton, J.; Berthelot, M.; Besseau, F.; Laurence, C. *J. Org. Chem.* **2005**, *70*, 7892.
41. See, for example: *(a)* Yamamoto, H.; Ishihara, K. *Acid catalysis in modern organic synthesis*; Eds.; Wiley-VCH: Weinheim, 2008. *(b)* Astruc, D. *Organometallic Chemistry and Catalysis*; Springer-Verlag: Berlin, 2007. *(c)* Fu, G. C. *J. Org. Chem.* **2004**, *69*, 3245. *(d)* Focante, F.; Mercandelli, P.; Sironi, A.; Resconi, L. *Coord. Chem. Rev.* **2006**, *250*, 170.
42. See, for example: *(a)* Erker, G. *Dalton Trans.* **2011**, *40*, 7475. *(b)* Geier, S. J.; Gille, A. L.; Gilbert, T. M.; Stephan, D. W. *Inorg. Chem.* **2009**, *48*, 10466.
43. Flores-Segura, H.; Torres, L. A. *Struct. Chem.*, **1997**, *8*, 227.
44. Brown, H. C. *J. Am. Chem. Soc.* **1945**, *67*, 1452.
45. As can be deduced by the first ionization energy,[46] or by proton affinity[4a] of relevant aliphatic amines.

46. *(a)* Noffsinger, J. B.; Danielson, N. D. *Anal. Chem.*, **1987**, *59*, 865. *(b)* Campbell, S.; Beauchamp, J, L.; Rembe, M.; Lichtenberger, D. L. *Int. J. Mass Spectrom. Ion Processes* **1992**, *117*, 83.
47. Staubitz, A.; Robertson, A. P. M.; Sloan, M. E.; Manners, I. *Chem. Rev.* **2010**, *110*, 4023.
48. Ohwada, T.; Hirao, H.; Ogawa, A. *J. Org. Chem.* **2004**, *69*, 7486.
49. Izutsu, K.; Nakamura, T.; Takizawa, K.; Takeda, A. *Bull. Chem. Soc. Jpn.* **1985**, *58*, 455.
50. *(a)* Laurence, C.; Guiheneuf, G.; Wojtkowiak, B. *J. Am. Chem. Soc.* **1979**, *101*, 4793. *(b)* Drago, R. S.; Vogel, G. C.; Needham, T. E. *J. Am. Chem. Soc.* **1971**, *93*, 6014. *(c)* Drago, R. S.; Wayland, B.; Carlson, R. L. *J. Am. Chem. Soc.* **1963**, *85*, 3125. *(d)* Person, W. B.; Golton, W. C.; Popov, A. I. *J. Am. Chem. Soc.* **1963**, *85*, 891. *(e)* Brandon, S. M.; Tamres, M.; Searles Jr., S. *J. Am. Chem. Soc.* **1960**, *82*, 2129. *(f)* Nagakura, S. *J. Am. Chem. Soc.* **1958**, *80*, 520.
51. See, for example: *(a)* Orozco, M.; Luque, F. J. *Chem. Rev.* **2000**, *100*, 4187. *(b)* Cramer, C. J.; Truhlar, D. G. *Chem. Rev.* **1999**, *99*, 2161.
52. For a theoretical discussion about the electron pair density involved in the Lewis model, see for example: Fradera, X.; Austen, M. A.; Bader, R. F. W. *J. Phys. Chem. A* **1999**, *103*, 304.
53. For recent works about vapochromic materials: *(a)* Zhang, X.; Li, B.; Chen, Z.-H.; Chen, Z.-N. *J. Mater. Chem.* **2012**, *22*, 11427. *(b)* Kumpfer, J. R.; Taylor, S. D.; Connick, W. B.; Rowan, S. J. *J. Mater. Chem.* **2012**, *22*, 14196. *(c)* Huang, X.; Hu, N.; Gao, R.; Yu, Y.; Wang, Y.; Yang, Z.; Kong, E. S.-W.; Wei, H.; Zhang, Y. *J. Mater. Chem.* **2012**, *22*, 22488. *(d)* Kobayashi, A.; Fukuzawa, Y.; Chang, H.-C.; Kato, M. *Inorg. Chem.* **2012**, *51*, 7508. *(e)* Naka, K.; Kato, T.; Watase, S.; Matsukawa, K. *Inorg. Chem.* **2012**, *51*, 4420. *(f)* Malwitz, M. A.; Lim, S. H.; White-Morris, R. L.; Pham, D. M.; Olmstead, M. M.; Balch, A. L. *J. Am. Chem. Soc.* **2012**, *134*, 10885. *(g)* Liu, X.; Xu, Y., Jiang, D. *J. Am. Chem. Soc.* **2012**, *134*, 8738. *(h)* Koshevoy, I. O.; Chang, Y.-C.; Karttunen, A. J.; Haukka, M.; Pakkanen, T.; Chou, P.-T. *J. Am. Chem. Soc.* **2012**, *134*, 6564. *(i)* de Miguel, G.; Ziółek, M.; Zitnan, M.; Organero, J. A.; Pandey, S. S.; Hayase, S.; Douhal, A. *J. Phys. Chem. C* **2012**, *116*, 9379.

54. *(a)* He, X.; Yam, V. W. *Coord. Chem. Rev.* **2011**, *255*, 2111. *(b)* Zhao, Q.; Li, F.; Huang, C. *Chem. Soc. Rev.* **2010**, *39*, 3007. *(c)* Fiddler, M. N.; Begashaw, I.; Mickens, M. A.; Collingwood, M. S.; Assefa, Z.; Bililign, S. *Sensors* **2009**, *9*, 10447.

55. Lin, H.; Jang, M.; Suslick, K. S. *J. Am. Chem. Soc.* **2011**, *133*, 16786.

56. *(a)* Lasanta, T.; Olmos, M. E.; Laguna, A.; López-de-Luzuriaga, J. M.; Naumov, P. *J. Am. Chem. Soc.* **2011**, *133*, 16358. *(b)* Strasser, C. E.; Catalano, V. J. *J. Am. Chem. Soc.* **2010**, *132*, 10009. *(c)* Ito, H.; Saito, T.; Oshima, N.; Kitamura, N.; Ishizaka, S.; Hinatsu, Y.; Wakeshima, M.; Kato, M.; Tsuge, K.; Sawamura, M. *J. Am. Chem. Soc.* **2008**, *130*, 10044. *(d)* Lee, Y.-A.; Eisenberg, R. *J. Am. Chem. Soc.* **2003**, *125*, 7778.

57. *(a)* Laguna, A.; Lasanta, T.; López-de-Luzuriaga, J. M.; Monge, M.; Naumov, P.; Olmos, M. E. *J. Am. Chem. Soc.* **2010**, *132*, 456. *(b)* Fernández, E. J.; López-de-Luzuriaga, J. M.; Monge, M.; Montiel, M.; Olmos, M. E.; Pérez, J.; Laguna, A.; Mendizabal, F.; Mohamed, A. A.; Fackler, J. P., Jr. *Inorg. Chem.* **2004**, *43*, 3573.

58. Cariati, E.; Bu, X.; Ford, P. C. *Chem. Mater.* **2000**, *12*, 3385.

59. *(a)* Forniés, J.; Sicilia, V.; Casas, J. M.; Martín, A.; López, J. A.; Larraz, C.; Borja, P.; Ovejero, C. *Dalton Trans.* **2011**, *40*, 2898. *(b)* Boonmak, J.; Nakano, M.; Chaichit, N.; Pakawatchai, C.; Youngme, S. *Dalton Trans.* **2010**, *39*, 8161. *(c)* Osawa, M.; Kawata, I.; Igawa, S.; Hoshino, M.; Fukunaga, T.; Hashizume, D. *Chem. Eur. J.* **2010**, *16*, 12114. *(d)* Bencini, A.; Casarin, M.; Forrer, D.; Franco, L.; Garau, F.; Masciocchi, N.; Pandolfo, L.; Pettinari, C.; Ruzzi, M.; Vittadini, A. *Inorg. Chem.* **2009**, *48*, 4044. *(e)* Baho, N.; Zargarian, D. *Inorg. Chem.* **2007**, *46*, 299.

60. *(g)* Ni, J.; Zhang, X.; Wu, Y.-H.; Zhang, L.-Y.; Chen, Z.-N. *Chem. Eur. J.* **2011**, *17*, 1171. *(d)* Rawashdeh-Omary, M. A.; Rashdan, M. D.; Dharanipathi, S.; Elbjeirami, O.; Ramesh, P.; Dias, H. V. R. *Chem. Commun.* **2011**, *47*, 1160. *(d)* Chang, M.; Kobayashi, A.; Nakajima, K.; Chang, H.-C.; Kato, M. *Inorg. Chem.* **2011**, *50*, 8308. *(d)* Dou, C.; Chen, D.; Iqbal, J.; Yuan, Y.; Zhang, H.; Wang, Y. *Langmuir* **2011**, *27*, 6323. *(c)* Kobayashi, A.; Dosen, M.; Chang, M.; Nakajima, K.; Noro, S.; Kato, M. *J. Am. Chem. Soc.* **2010**, *132*, 15286. *(b)* Yoon, S.-J.; Chung, J. W.; Gierschner, J.; Kim, K. S.; Choi, M.-G.; Kim, D.; Park, S. Y. *J. Am. Chem. Soc.* **2010**, *132*, 13675.

(c) Takahashi, E.; Takaya, H.; Naota, T. *Chem. Eur. J.* **2010**, *16*, 4793. *(b)* Kobayashi, A.; Hara, H.; Noro, S.; Kato, M. *Dalton Trans.* **2010**, *39*, 3400. *(f)* Field, J. S.; Grimmer, C. D.; Munro, O. Q.; Waldron, B. P. *Dalton Trans.* **2010**, *39*, 1558. *(g)* Mathew, I.; Sun, W. *Dalton Trans.* **2010**, *39*, 5885. *(c)* Forniés, J.; Fuertes, S.; López, J. A.; Martín, A.; Sicilia, V. *Inorg. Chem.* **2008**, *47*, 7166. *(b)* Kui, S. C. F.; Chui, S. S.-Y.; Che, C.-M.; Zhu, N. *J. Am. Chem. Soc.* **2006**, *128*, 8297. *(e)* Grate, J. W.; Moore, L. K.; Janzen, D. E.; Veltkamp, D. J.; Kaganove, S.; Drew, S. M.; Mann, K. R. *Chem. Mater.* **2002**, *14*, 1058.

61. *(a)* Hudson, Z. M.; Sun, C.; Harris, K. J.; Lucier, B. E. G.; Schurko, R. W.; Wang, S. *Inorg. Chem.* **2011**, *50*, 3447. *(b)* Lee, C.-S.; Zhuang, R. R.; Sabiah, S.; Wang, J.-C.; Hwang, W.-S.; Lin, I. J. B. *Organometallics* **2011**, *30*, 3897. *(c)* Abe, T.; Suzuki, T.; Shinozaki, K. *Inorg. Chem.* **2010**, *49*, 1794. *(d)* Stylianou, K. C.; Heck, R.; Chong, S. Y.; Bacsa, J.; Jones, J. T. A.; Khimyak, Y. Z.; Bradshaw, D.; Rosseinsky, M. J. *J. Am. Chem. Soc.* **2010**, *132*, 4119.

5 *Zn^{II} Schiff Base Complexes: Suitable Building Blocks for New Supramolecular Architectures*

5.1 Introduction

The design of new supramolecular architectures through the intermolecular interactions between various tailored molecular units is a topic which implies a multidisciplinary approach, such as chemistry, biology, and materials science. The new supramolecular structures achieved, possess properties tunable in relation to the self-assembly of the molecular units. In fact, a wide variety of nanostructures such as particles, fibers, rods, sheets, cubes, and tubes can be obtained in relation of the kind of interaction. These features allow a wide variety of applications in the field of sensors,[1] field-effect transistors,[2] and photovoltaics.[3]

Tetracoordinated Zn^{II} complexes, in particular Schiff base derivatives, are suitable substrates to achievement of new supramolecular architectures through intermolecular interactions. In the previous chapter **3** and **4** of PhD thesis, it has been discussed that these systems are Lewis acids capable to saturate their coordination sphere by coordinating a large variety of neutral[4] and anionic species,[5] whose binding constants are strongly dependent of Lewis basicity of donor species, thus allowing their application such molecular probes (see sections **4.2** and **4.3**).[6] Moreover, Zn^{II} Schiff base complexes have been used as Lewis reference acids to build up a reliable Lewis basicity scale in dichloromethane for amines and common non-protogenic solvents, including ethanol (see section **4.4**).[7] On the other hand, in absence of coordinating species, these Zn^{II} complexes saturate their coordination through intermolecular Zn···O interaction, with formation of different kinds of aggregates species in relation of molecular structures of the complex (see chapter **3**).[8] This allows for a different control of the supramolecular architecture and, a variety of aggregate molecular architectures,[9] supramolecular assemblies[10] and nanostructures[11] have been found. Zn^{II} Schiff base complexes have also been investigated for their fluorescent features, which are related

to the structure of the salen template[12] and the axial coordination,[8,13] and second-order nonlinear optical properties.[14]

The demand for the axial binding to the Zn^{II} ion to saturate its coordination sphere in these complexes is the driving force that allows the design of new molecular architectures through intermolecular interactions. A possible approach useful to driven the self assembly of these species is, for example, the use of interconnecting ditopic Lewis donor[10a] or anionic[10c] species capable to coordinate the Zn^{II} ion of this species (see paragraph **1.4**). Alternatively, another approach to achieve new tailored Zn^{II} supramolecular architectures is the appropriated design of ligands possessing flexible Lewis donor atoms as side substituents, suitable to axially coordinate the Zn^{II} atom of another molecular unit.

In this chapter, the synthesis and characterization, through ^1H NMR, absorption and fluorescence spectroscopy and scanning electron microscopy (SEM), of a Zn^{II} Schiff base complex, **1d**, having dipodal alkyl side chains in the salicylidene rings, bearing an alkyl ammonium bromide is discussed. Considering the bromide ion is expected to be a suitable Lewis base to coordinate the Zn^{II} ion, competing with the phenolic oxygen donor atoms of salicylaldehyde, the aim of this study is to investigate the aggregation properties of this derivatized alkyl-ammonium bromide complex in comparison with simpler amphiphilic species, **1a**.[8]

5.2 Results and discussion

5.2.1 Comparison of spectroscopic properties between 1d and 1a ^1H NMR spectra of **1d** in a solution of DMSO-d_6 show the presence of sharp signals with the expected multiplicity, according to its molecular structure and consistent with the existence of monomeric species, having the axially coordinated solvent. In fact, ^1H NMR signals related to the aromatic, $-OCH_2$ and CH=N hydrogens are identical to those found in DMSO-d_6 solutions of **1a** (Figure 5.1) (see paragraphs **3.2.1.1** and **3.2.2**).[8d]

With the exception of DMSO and DMF, compound **1d** is very low soluble in most common coordinating (*e.g.*, acetonitrile, THF, methanol) or low-polarity non-coordinating (*e.g.*, DCM) solvents, while is almost insoluble in non polar solvents. The substantial higher solubility in DMSO and DMF indicates the existence of monomeric species of **1d** in these solvent media, as suggested by ^1H NMR analysis (vide supra).

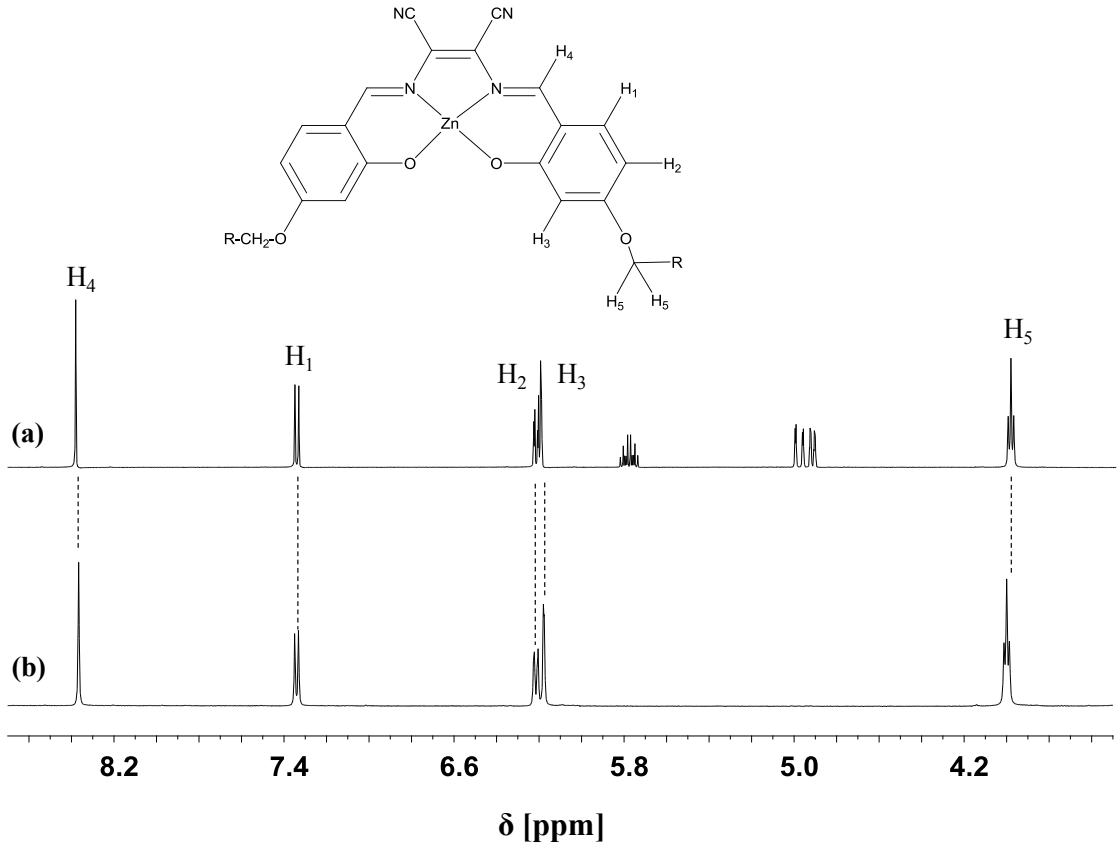

Figure 5.1 ^{1}H NMR spectra of *(a)* **1a** and *(b)* **1d** in DMSO-d_6. Unassigned peaks refer to -C*H*=CH_2 signals of the 4-(undec-10-enyloxy)-derivative, **1a**, complex.

Surprisingly, in strict contrast to previous studies on **1a** (see paragraphs **3.2.1.2** and **3.2.2**),[8d] optical absorption spectral features of **1d** are independent from the nature of the solvent. In fact, either in coordinating (THF, DMSO) or non-coordinating (DCM) solvents optical spectra are identical to each other, except for a red-shift of the longer wavelength band in the case of the more polar DMSO solvent (Figure 5.2).

The optical absorption features of **1d** resemble those of the parent complex **1a** in coordinating solvents or in DCM upon axial coordination of a Lewis base (see paragraphs **3.2.1.2** and **3.2.2** and chapter **4**).[8d] In other words, optical absorption properties of **1d** in solution, independently of the presence or not of a Lewis base, indicate the existence of an axially coordinated species to the Zn^{II} ion. Moreover, complex **1d** exhibits a moderate fluorescence emission ($\Phi \approx 0.08$), with the presence of an unstructured band, λ_{max} between 602 and 620 nm, independent from the excitation wavelength.

Therefore, present data suggest the existence of Zn···Br interactions in **1d** in a solution of DCM, thus satisfying the coordination sphere of the Zn^{II} ion and avoiding intermolecular Zn···O interactions, as usually occur in the absence of other coordinating species.[9]

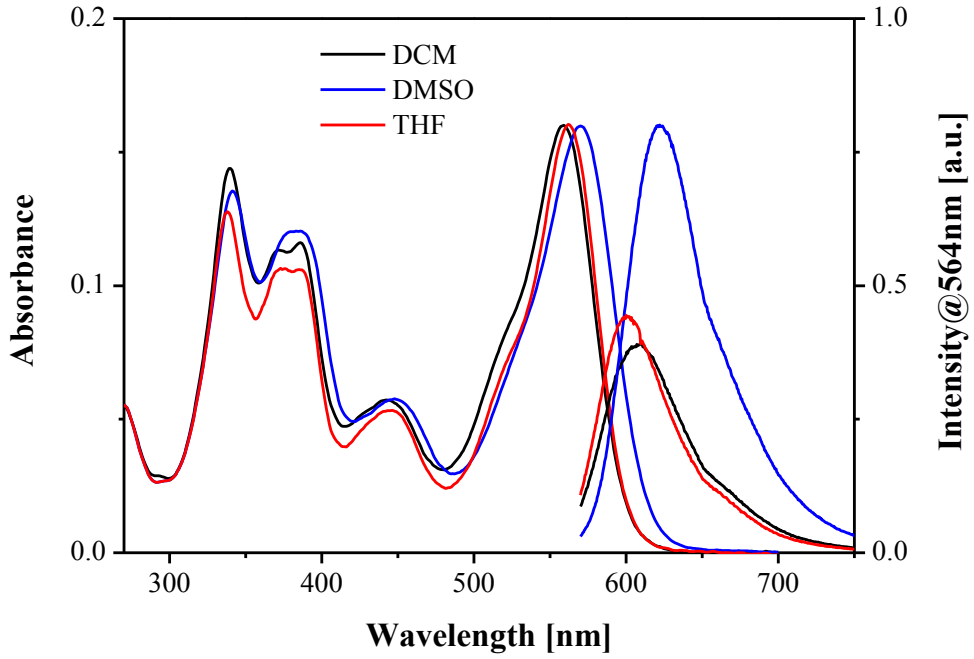

Figure 5.2 UV-vis absorption and fluorescence (λ_{exc} = 564 nm) spectra of **1d** in DMSO (5.0×10^{-6} M) (—), DCM(—) and THF (—). Absorption spectra in DCM and THF were recorded with an absorbance of the longer wavelength band equal to that recorded in DMSO.

To verify this hypothesis, we performed a series of experiments using DCM solutions of **1a**, as reference species, by adding DCM solutions of a bromide, and compared the results with those achieved for the complex **1d**.

As previously found for treatment of DCM solutions of **1a** with neutral Lewis bases (see paragraphs **3.2.1.1**, **3.2.2** and **4.3.1.1**),[8d] the addition of a stoichiometric amount of tetrabutylammonium (TBA) bromide to a DCM-d_2 solution of **1a** results in a sizable downfield shift of aromatic H_3 and the -OCH_2 signals, in agreement with the deaggregation process and formation of the **1a**·BrTBA adduct (Table 5.1; Figure 5.3). Moreover, the resulting ^{1}H NMR spectrum is similar to that found for the **1a**·pyridine adduct in DCM-d_2 solutions (Figure 5.4), thus suggesting an analogous axially coordination mode of the bromide to the Zn^{II} ion.

Table 5.1 ^{1}H NMR chemical shifts (ppm) of selected protons for **1d**, **1a** and **1a**·BrTBA.

Complex	H_4	H_1	H_2	H_3	H_5	Solvent
1d	8.36	7.33	6.21	6.17	3.99	DMSO-d_6
1a	8.38	7.35	6.23	6.20	4.00	DMSO-d_6
1d	8.31	7.12	6.23	6.25	4.01	DCM-d_2
1a·BrTBA	8.24	7.04	6.17	6.28	3.96	DCM-d_2
1a	8.35	7.04	6.20	5.71	3.73	DCM-d_2

The ^{1}H NMR spectrum of **1d** in DCM-d_2 solution is almost identical, in terms of chemical shift and multiplicity of the signals, to that found for the above **1a**·BrTBA adduct (Figure 5.3; Table 5.1). Moreover, the evidence of a single signal for H_1-H_5 protons of the two salicylidene moieties indicates that in both species a local C_2 axis passing through the central Zn^{II} ion and perpendicular to the chelate ring is present. These data suggest in both cases an analogous coordination mode of the alkyl-ammonium bromide to the Zn^{II} ion, ruling-out the existence of intramolecular Zn···Br interactions in **1d**.

In order to study the optical properties of the **1a**·BrTBA adduct, spectrophotometric and spectrofluorimetric titrations of 10 μM DCM solutions of **1d** were performed using DCM solutions of TBA bromide as titrant (Figure 5.5). The resulting optical absorption spectra of the **1a**·BrTBA adduct upon reaching the saturation point, except for a slightly red-shift (~6 nm) of the longer wavelength band, are equivalent to those of **1d** in DCM (Figure 5.6). Moreover, Job's plot analysis[16] clearly indicates the formation of 1:1 adducts (Figure 5.7).

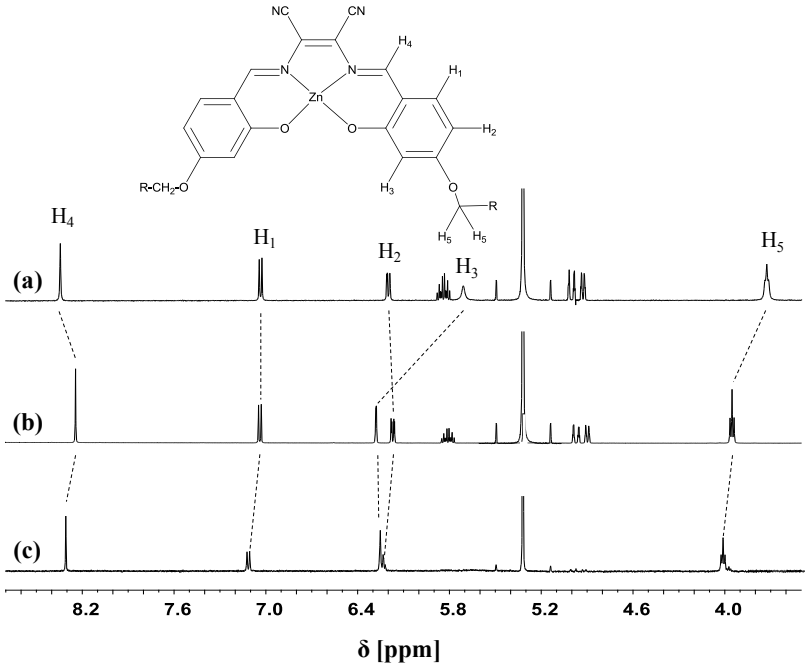

Figure 5.3 ^{1}H NMR spectra in DCM-d_2 of **1d** *(a)* and *(b)* **1a**·BrTBA adduct (obtained upon addition of an equimolar amount of TBA bromide to a DCM-d_2 solution of **1a**). *(c)* The ^{1}H NMR spectrum of **1d** in DCM-d_2 is reported for comparison.

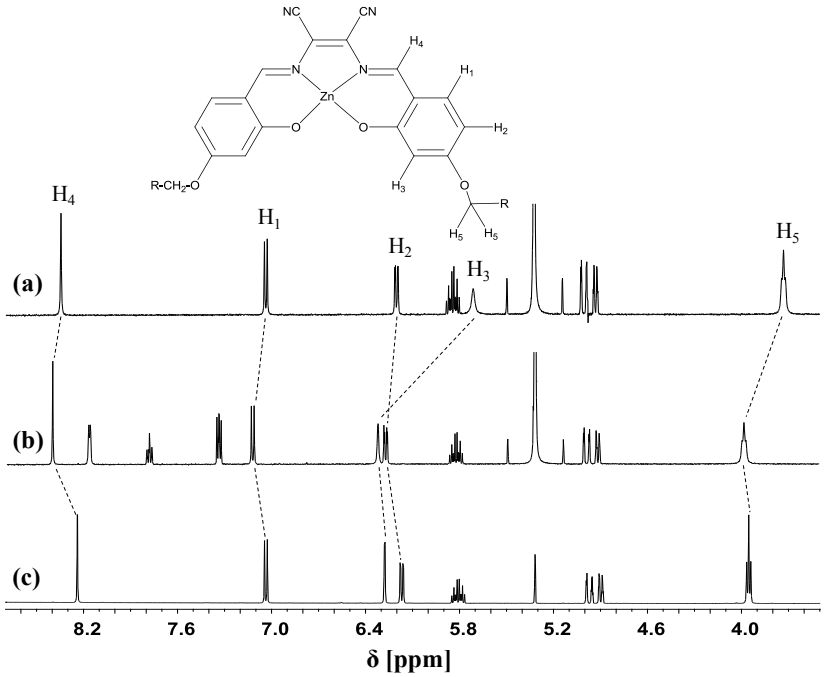

Figure 5.4 Comparison of ^{1}H NMR spectra of *(a)* **1a**, *(b)* **1a**·pyridine adduct, and *(c)* **1a**·BrTBA adduct in DCM-d_2. Note that, the ^{1}H NMR spectrum of the **1a**·BrTBA adduct differs significantly from that of the **1a**·pyridine adduct, as far as the upfield shift of the proton aromatic and CH=N signals are concerned. However, this shielding effect is in agreement with an increased negative charge on the conjugated ligand framework upon bromide coordination to the Zn^{II} ion.[11b]

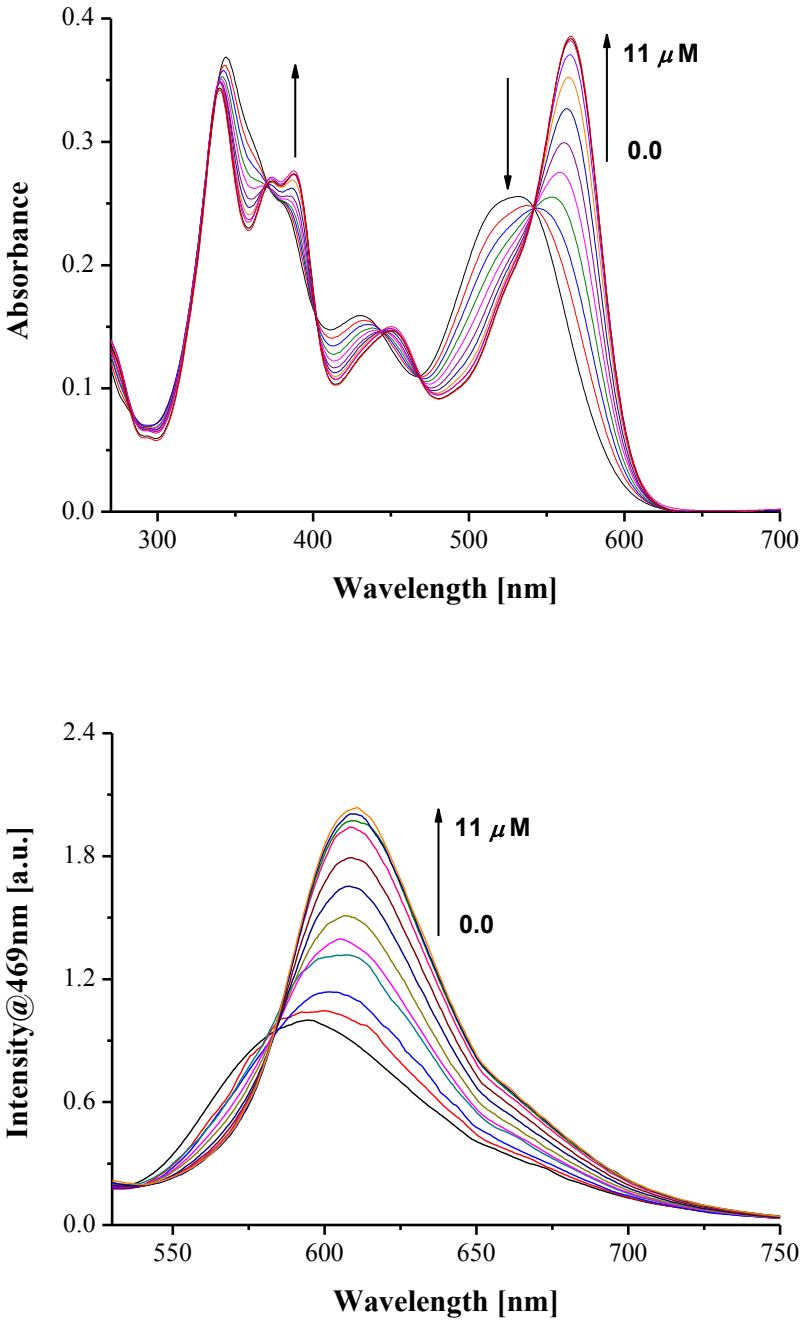

Figure 5.5 *(Top)* UV-vis absorption and *(bottom)* fluorescence (λ_{exc} = 469 nm) titration curves of **1a** (10 μM solution in DCM) with addition of TBA bromide. The concentration of TBA bromide added varied from 0 to 11.0 μM.

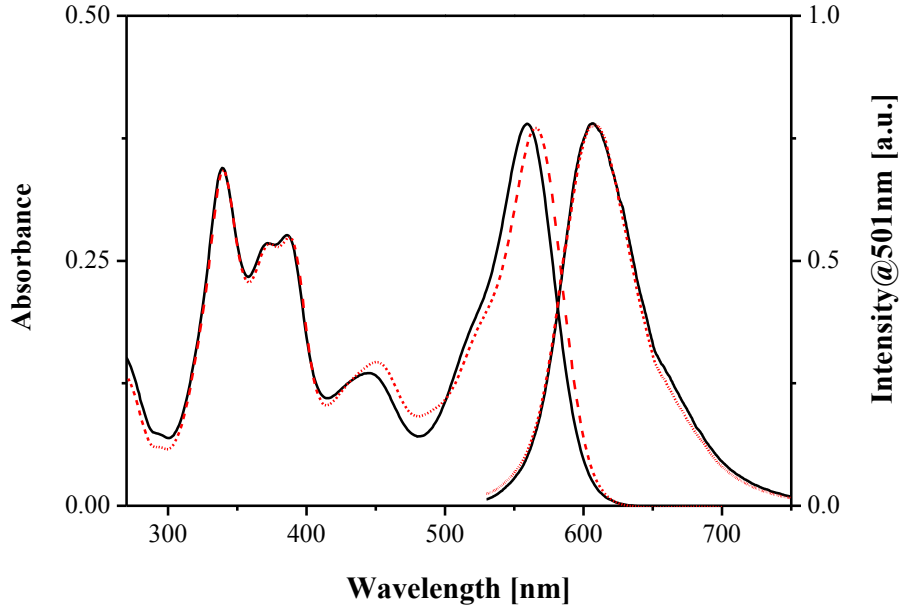

Figure 5.6 UV-vis absorption and fluorescence (λ_{exc} = 501 nm) spectra in DCM of **1d** (—) and the **1a**·BrTBA adduct (– –) (1.0 × 10^{-5} M). The absorption spectrum of **1d** has been recorded with an absorbance of the longer wavelength band equal to that recorded for the **1a**·BrTBA adduct.

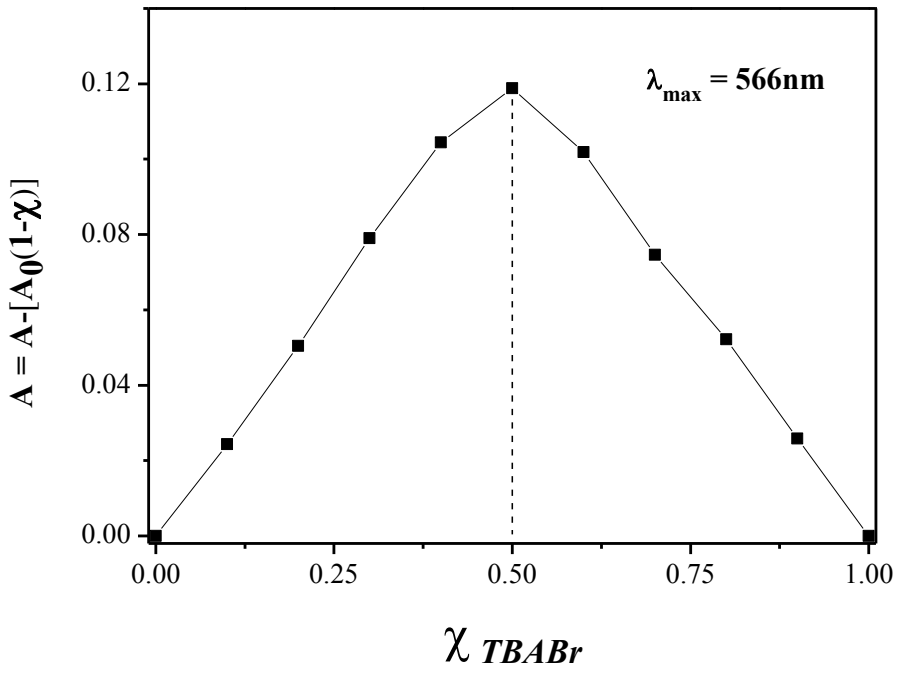

Figure 5.7 Job's plot for the binding of **1a** with TBA bromide in DCM. The total concentration of **1a** and TBA bromide is 10 μM. *A* and A_0 (the initial absorbance of **1d**) are the absorbances at 566 nm.

Analogously, a comparison of fluorescence spectra for the **1a**·BrTBA adduct and **1d** indicates an identical emission, in terms of intensity and fluorescence maxima. Note however that, while optical absorption spectra of the **1a**·BrTBA adduct do not significantly differ from those obtained for 1:1 adducts with neutral Lewis bases (see paragraphs **4.2.1.1** and **4.3.1.1**),[8d] the fluorescence enhancement upon formation of the **1a**·BrTBA adduct is lower. Actually, starting from DCM solutions of **1a**, the formation of 1:1 adducts with neutral Lewis bases, *e.g.*, pyridine, involves a fluorescence enhancement of almost one order of magnitude (see paragraphs **3.2.1.2** and **3.2.2**).[8d] Conversely, in the case of the **1a**·BrTBA adduct, about a two-fold increase of the fluorescence intensity is observed (Figure 5.5). This lower fluorescence enhancement for the **1a**·BrTBA adduct can be related to a quenching effect due to the heavy bromide ion.[17] As expected, analogous titrations of DCM solutions of **1d** with TBA bromide or using non-coordinating anion species, *e.g.*, TBA hexafluorophosphate, do not involve appreciable optical absorption or fluorescence variations.

In summary, the comparison of optical absorption and fluorescent properties of **1d** in DCM solution with those for the **1a**·BrTBA adduct, analogously to ^{1}H NMR studies, indicates the existence of Zn···Br interactions. Although on statistical ground both intra- or intermolecular Zn···Br interactions or a combination of them are possible, however, spectroscopic data and the very low solubility of **1d** in DCM in comparison to that of the **1a**·BrTBA adduct[18] suggest the occurrence of intermolecular Zn···Br interactions and, hence, aggregate structures, *e.g.*, dimeric (Chart 5.1) or oligomeric species, in solution.[19,20]

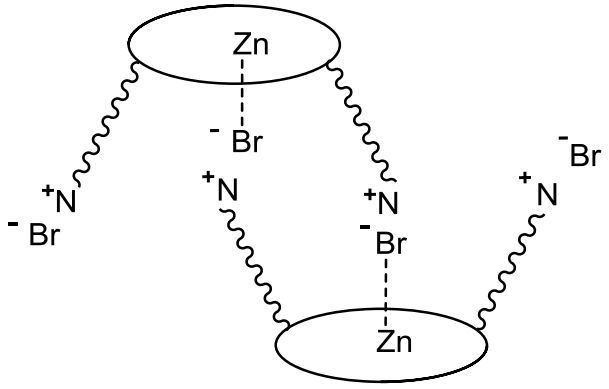

Chart 5.1 A possible aggregation mode of **1d** in DCM solution.

These species are very stable in DCM and do not exhibit bromide displacement even with the addition of stoichiometric amounts of strong Lewis bases, *e.g.*, pyridine. To observe an appreciable **1d**·pyridine adduct formation it needs adding 2000-fold mole excess of pyridine, as can be monitored by a significant increase of the fluorescence intensity. A complete bromide displacement is achieved by addition of ca. 10^5-fold mole excess of pyridine (Figure 5.8). Conversely, the addition of ca. 10^3-fold mole excess of pyridine is required for a complete bromide displacement in the case of the **1a**·BrTBA adduct, in agreement with its simpler monomer nature.

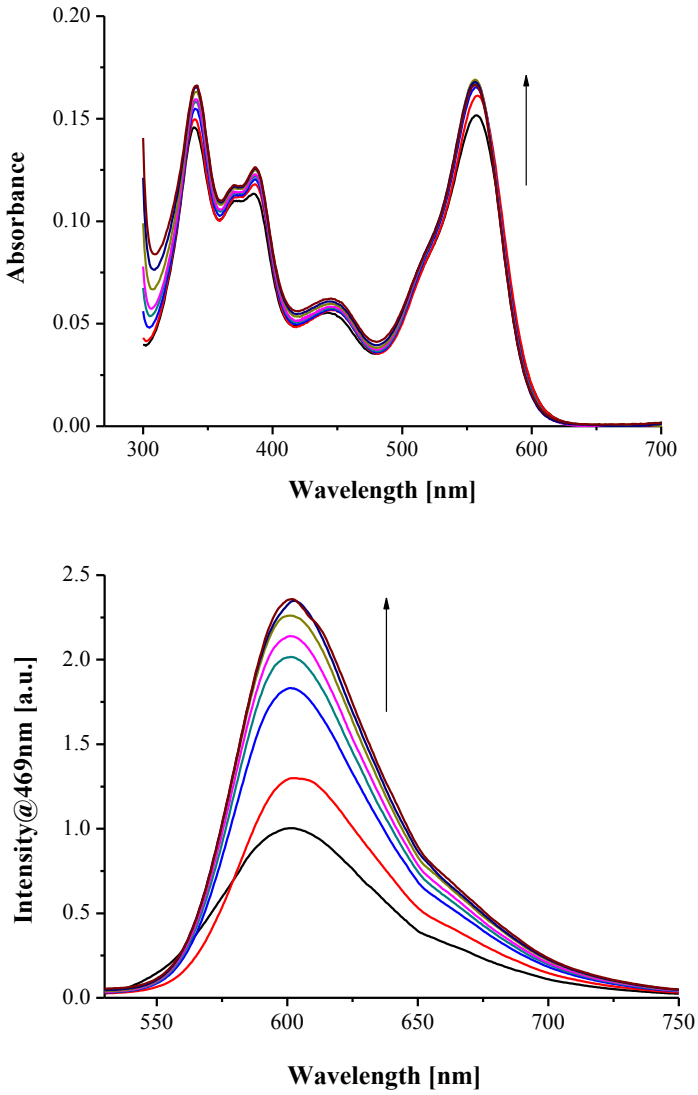

Figure 5.8 *(a)* UV-vis absorption and *(b)* fluorescence (λ_{exc} = 481 nm) titration curves of **1d** (*ca.* 4 μM solution in DCM, estimated assuming a molar absorbance equal to that of the **1a**·BrTBA adduct) with addition of pyridine. The concentration of pyridine added was 0, 0.008, 0.05, 0.09, 0.13, 0.21, 0.3, 0.4 M. The increase of the fluorescence emission can be related to the formation of the **1d**·pyridine adduct (see text).

5.2.2 Scanning electron microscopy (SEM) studies Field emission scanning electron microscopy images (FE-SEM) of samples obtained by drop-casting from dilute DCM solutions of **1d** indicate the existence of coral-like nanostructures (Figure 5.9) whose structural motif may be related to an aggregate structure as sketched in Chart5.2.

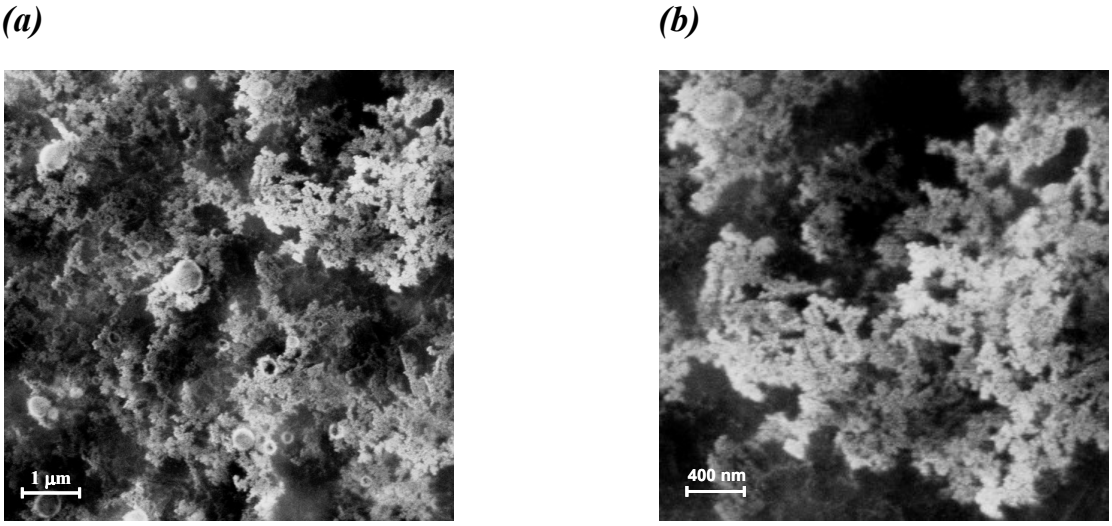

Figure 5.9 *(a)* Low and *(b)* high magnification FE-SEM images of **1d** deposited by casting from a dilute DCM solution.

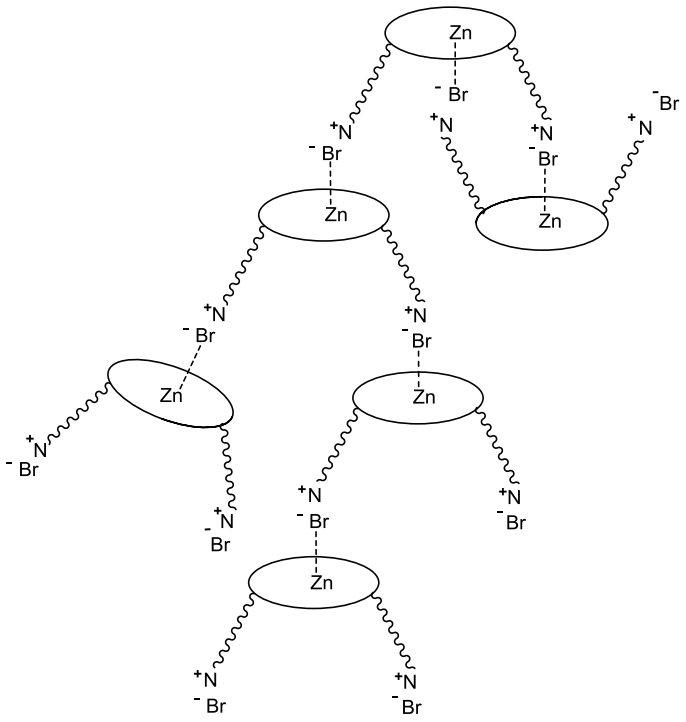

Chart 5.2 A potential aggregation motif of **1d** in the coral-like nanostructures.

In fact, considering intermolecular Zn···Br interactions and given the presence of the flexible side alkyl chains, a branched nanostructure can be envisaged. Although branched nanostructures are rather common among inorganic materials,[21] there are only a few molecular materials showing such a structure.[22] In this view, the present investigation represents a unique example of a metal-organic coordination complex exhibiting a branched nanostructure. On the other hand, FE-SEM images of samples achieved by drop-casting from dilute DMSO solutions of **1d** (Figure 5.10) indicate a very different, nanorod structure, in which **1d** is presumably axially coordinated to the DMSO, thus avoiding any intermolecular branched aggregation.

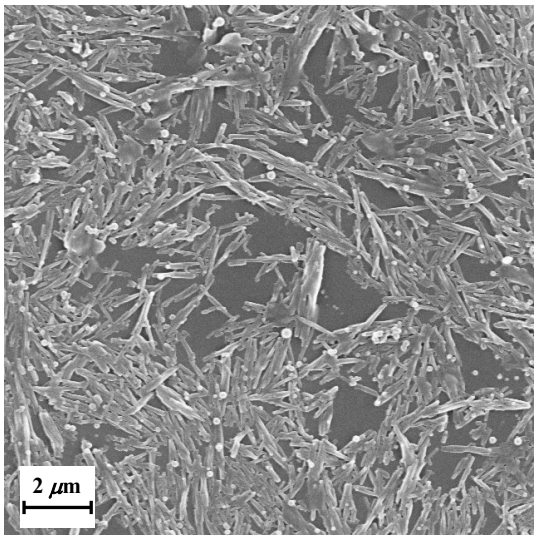

Figure 5.10 FE-SEM image of **1d** nanorods deposited by casting from a dilute DMSO solution.

5.3 Conclusions

The comparison of ^{1}H NMR and optical spectroscopic properties of the tailored bis(salicylaldiminato)Zinc(II) Schiff base complex, **1d**, having dipodal, alkyl ammonium bromide derivatized chains in the salicylidene rings, with those of the reference complex **1a**, through the study of the 1:1 **1a**·BrTBA adduct, allowed getting insights into the nature of species in solutions.

In strict contrast to studies on **1a** (see section **3.2**), ^{1}H NMR and optical absorption spectral features of **1d** are independent from the coordinating or non-coordinating nature of the solvent. With the exception of DMSO and DMF, in which 1:1 adducts with the solvent are likely to occur, present data suggest the existence of Zn···Br

interactions in **1d** in solution, thus satisfying its coordination sphere. This avoids intermolecular Zn···O interactions, as usually occur in the absence of other coordinating species.

SEM analysis of samples obtained by drop-casting from DCM solutions of **1d** reveals the existence of branched nanostructures, whose structural motif is consistent with the existence of intermolecular Zn···Br interactions. These results represent an unprecedented example of a coordination complex exhibiting a branched nanostructure.

5.4 References

1. *(a)* Grimsdale, A. C.; Müllen, K. *Angew. Chem. Int. Ed.* **2005**, *44*, 5592. *(b)* Holman, M. W.; Liu, R.; Zang, L.; Yan, P.; DiBenedetto, S. A.; Bowers, R. D.; Adams, D. M. *J. Am. Chem. Soc.* **2004**, *126*, 16126. *(c)* Liu, R.; Holman, M. W.; Zang, L.; Adams, D. M. *J. Phys. Chem. A* **2003**, *107*, 6522. *(d)* Sauer, M. *Angew. Chem. Int. Ed.* **2003**, *42*, 1790.
2. *(a)* Guo, Y.; Li, Y.; Xu, J.; Liu, X.; Xu, J.; Lv, J.; Huang, C.; Zhu, M.; Cui, S.; Jiang, L.; Liu, H.; Wang, S. *J. Phys. Chem. C* **2008**, *112*, 8223. *(b)* Li, R.; Ma, P.; Dong, S.; Zhang, X.; Chen, Y.; Li, X.; Jiang, J. *Inorg. Chem.* **2007**, *46*, 11397. *(c)* Chen, Y.; Su, W.; Bai, M.; Jiang, J.; Li, X.; Liu, Y.; Wang, L.; Wang, S. *J. Am. Chem. Soc.* **2005**, *127*, 15700. *(d)* Xu, B. Q.; Xiao, X.; Yang, X.; Zang, L.; Tao, N. J. *J. Am. Chem. Soc.* **2005**, *127*, 2386.
3. *(a)* Li, Y.; Xiao, S.; Li, H.; Li, Y.; Liu, H.; Lu, F.; Zhuang, J.; Zhu, D. *J. Phys. Chem. B* **2004**, *108*, 6256. *(b)* Gregg, B. A. *J. Phys. Chem. B* **2003**, *107*, 4688. *(c)* Peeters, E.; Van Hal, P. A.; Meskers, S. C. J.; Janssen, R. A. J.; Meijer, E. W. *Chem. Eur. J.* **2002**, *8*, 4470. *(d)* Schmidt-Mende, L.; Fechtenkotter, A.; Mullen, K.; Moons, E.; Friend, R. H.; MacKenzie, J. D. *Science* **2001**, *293*, 1119. *(e)* Gregg, B. A. *J. Phys. Chem.* **1996**, *100*, 852. *(f)* Tamizhmani, G.; Dodelet, J. P.; Cote, R.; Gravel, D. *Chem. Mater.* **1991**, *3*, 1046.
4. Germain, M. E.; Vargo, T. R.; Khalifah, G. P.; Knapp, M. J. *Inorg. Chem.* **2007**, *46*, 4422. *(b)* Dalla Cort, A., Mandolini, L.; Pasquini, C.; Rissanen, K.; Russo, L.; Schiaffino, L. *New J. Chem.* **2007**, *31*, 1633. *(c)* Ma, C. T. L.; MacLachlan, M. J. *Angew. Chem. Int. Ed.* **2005**, *44*, 4178. *(d)* Salter, M. H. Jr.; Reibenspies, J. H.; Jones, S. B.; Hancock, R. D. *Inorg. Chem.* **2005**, *44*, 2791. *(e)* Subat, M.; Borovik, A. S.; König, B. *J. Am. Chem. Soc.* **2004**, *126*, 3185.

5. *(a)* Wezenberg, S. J.; Anselmo, D., Escudero-Adán, E. C.; Benet-Buchholz, J.; Kleij, A. W. *Eur. J. Inorg. Chem.* **2010**, 4611. *(b)* Cano, M.; Rodríguez, L.; Lima, J. C.; Pina, F.; Dalla Cort, A.; Pasquini, C.; Schiaffino, L. *Inorg. Chem.* **2009**, *48*, 6229. *(c)* Khatua, S.; Choi, S. H.; Lee, J.; Kim, K.; Do, Y.; Churchill, D. G. *Inorg. Chem.* **2009**, *48*, 2993.
6. *(a)* Oliveri, I. P.; Di Bella, S. *Tetrahedron* **2011**, *67*, 9446. *(b)* Oliveri, I. P.; Di Bella, S. *J. Phys. Chem. A* **2011**, *115*, 14325.
7. Oliveri, I. P.; Maccarrone, G.; Di Bella, S. *J. Org. Chem.* **2011**, *76*, 8879.
8. *(a)* Consiglio, G.; Failla, S.; Finocchiaro, P.; Oliveri, I. P.; Di Bella, S. *Inorg. Chem.* **2012**, *51*, 8409. *(b)* Consiglio, G.; Failla, S.; Finocchiaro, P.; Oliveri, I. P.; Di Bella, S. *Dalton Trans.* **2012**, *41*, 387. *(c)* Consiglio, G.; Failla, S.; Finocchiaro, P.; Oliveri, I. P.; Purrello, R.; Di Bella, S. *Inorg. Chem.* **2010**, *49*, 5134. *(d)* Consiglio, G.; Failla, S.; Oliveri, I. P.; Purrello, R.; Di Bella, S. *Dalton Trans.* **2009**, 10426.
9. Kleij, A. W. *Dalton Trans.* **2009**, 4635.
10. *(a)* Martínez Belmonte, M.; Wezenberg, S. J.; Haak, R. M.; Anselmo, D.; Escudero-Adán, E. C.; Benet-Buchholz, J.; Kleij, A W *Dalton Trans.* **2010**, *39*, 4541. *(b)* Escudero-Adán, E. C.; Benet-Buchholz, J.; Kleij, A. W. *Inorg. Chem.* **2008**, *47*, 4256. *(c)* Gallant, A. J.; Chong, J. H.; MacLachlan, M. J. *Inorg. Chem.* **2006**, *45*, 5248. *(d)* Kleij, A. W.; Kuil, M.; Lutz, M.; Tooke, D. M.; Spek, A. L.; Kamer, P. C. K.; vanLeeuwen, P. W. N. M.; Reek, J. N. H. *Inorg. Chim. Acta.* **2006**, *359*, 1807. *(e)* Odoko, M.; Tsuchida, N.; Okabe, N. *Acta Crystallogr. Sect. E: Struct. Rep. Online* **2006**, *E62*, m708. *(f)* Kleij, A. W.; Kuil, M.; Tooke, D. M.; Lutz, M.; Spek, A. L.; Reek J. N. H. *Chem. Eur. J.* **2005**, *11*, 4743. *(g)* Malandrino, G.; Blandino, M.; Perdicaro, L. M. S.; Fragalà, I. L.; Rossi, P.; Dapporto, P. *Inorg. Chem.* **2005**, *44*, 9684. *(h)* Matalobos, J. S.; García-Deibe, A. M.; Fondo, D. N.; Bermejo, M. R. *Inorg. Chem. Commun.* **2004**, *7*, 311. *(i)* Reglinski, J.; Morris S.; Stevenson, D. E. *Polyhedron* **2002**, *21*, 2175.
11. *(a)* Bhattacharjee, C. R.; Das, G.; Mondal, P.; Prasad, S. K.; Rao, D. S. S. *Eur. J. Inorg. Chem.* **2011**, 1418. *(b)* Wezenberg, S. J.; Escudero-Adán, E. C.; Benet-Buchholz J.; Kleij, A. W. *Chem. Eur. J.* **2009**, *15*, 5695. *(c)* Leung, A. C. W.; MacLachlan, M. J. *J. Mater. Chem.* **2007**, *17*, 1923.

12. *(a)* Hui, J. K.-H.; MacLachlan, M. J. *Dalton Trans.* **2010**, *39*, 7310. *(b)* Elemans, J. A. A. W.; Wezenberg, S. J.; Coenen, M. J. J.; Escudero-Adán, E. C.; Benet-Buchholz, J.; den Boer, D.; Speller, S.; Kleij A. W.; De Feyter, S. *Chem. Commun.* **2010**, *46*, 2548. *(c)* Hui, J. K.-H.; Yu, Z.; Mirfakhrai, T.; MacLachlan, M. J. *Chem. Eur. J.* **2009**, *15*, 13456. *(d)* Jung, S.; Oh, M. *Angew. Chem. Int. Ed.* **2008**, *47*, 2049. *(e)* Hui, J. K.-H.; Yu, Z.; MacLachlan, M. J .*Angew. Chem. Int. Ed.* **2007**, *46*, 7980.
13. *(a)* Liuzzo, V.; Oberhauser, W.; Pucci, A. *Inorg. Chem. Commun.* **2010**, *13*, 686. *(b)* Bhattacharjee, C. R.; Das, G.; Mondal, P.; Rao, N. V. S. *Polyhedron* **2010**, *29*, 3089. *(c)* Kuo, K.-L.; Huang, C.-C.; Lin, Y.-C.; *Dalton Trans.* **2008**, 3889. *(d)* Son, H.-J.; Han, W.-S.; Chun, J.-Y.; Kang, B.-K.; Kwon, S.-N.; Ko, J.; Han, S. J.; Lee, C.; Kim, S. J.; Kang, S. O. *Inorg. Chem.* **2008**, *47*, 5666. *(e)* Lin, H.-C.; Huang, C.-C.; Shi, C.-H.; Liao, Y.-H.; Chen, C.-C.; Lin, Y.-C; Liu, Y.-H. *Dalton Trans.* **2007**, 781. *(f)* Di Bella, S.; Leonardi, N.; Consiglio, G.; Sortino, S.; Fragalà, I. *Eur. J. Inorg. Chem.* **2004**, 4561. *(g)* Ma, C.; Lo, A.; Abdolmaleki, A.; MacLachlan, M. J. *Org. Lett.* **2004**, *6*, 3841. *(h)* Chang, K.-H.; Huang, C.-C.; Liu, Y.-H.; Hu, Y.-H.; Chou, P.-T.; Lin, Y.-C. *Dalton Trans.* **2004**, 1731. *(i)* La Deda, M.; Ghedini, M.; Aiello, I.; Grisolia, A. *Chem. Lett.* **2004**, *33*, 1060. *(j)* Wang, P.; Hong, Z.; Xie, Z.; Tong, S.; Wong, O.; Lee, C.-C.; Wong, N.; Hung, L.; Lee, S. *Chem. Commun.* **2003**, 1664.
14. *(a)* Germain, M. E.; Knapp, M. J. *J. Am. Chem. Soc.* **2008**, *130*, 5422. *(b)* Di Bella, S.; Consiglio, G.; Sortino, S.; Giancane, G.; Valli, L. *Eur. J. Inorg. Chem.* **2008**, 5228. *(c)* Di Bella, S.; Consiglio, G.; La Spina, G.; Oliva, C.; Cricenti, A. *J. Chem. Phys.* **2008**, *129*, 114704.
15. *(a)* Di Bella, S.; Oliveri, I. P.; Colombo, A.; Dragonetti, C.; Righetto, S.; Roberto, D. *Dalton Trans.* **2012** *41*, 7013. *(b)* Di Bella, S.; Dragonetti, C.; Pizzotti, M.; Roberto, D.; Tessore, F.; Ugo, R. *Top. Organomet. Chem.* **2010** *28*, 1. *(c)* Coe, B. J. in *Comprehensive Coordination Chemistry II*, ed. J. A. McCleverty and T. J. Meyer, Elsevier Pergamon, Oxford, U.K., 2004, vol. 9, pp. 621. *(d)* Di Bella, S. *Chem. Soc. Rev.* **2001**, *30*, 355. *(e)* Lacroix, P. G.; Di Bella, S.; Ledoux, I. *Chem. Mater.* **1996**, *8*, 541.
16. *(a)* Gil, V. M. S.; Oliveira, N. C. *J. Chem. Educ.* **1990**, *67*, 473. *(b)* Hill, Z. D.; MacCarthy, P. *J. Chem. Educ.* **1986**, *63*, 162. *(c)* Job, P. *Ann. Chem.* **1928**, *9*, 113.
17. Lakowicz, J. R. *Principles of Fluorescence Spectroscopy*, Springer, 2006.

18. In fact, despite the salt nature of the **1a**·BrTBA adduct, it is possible achieving relatively high concentrated DCM solutions (up to 5×10^{-3} M), in contrast to the very low solubility ($\leq 5 \times 10^{-5}$ M) of **1d** in DCM.
19. Note that, quaternary ammonium compounds when dissolved in low permittivity organic solvents, such as THF and DCM, form tight ion pairs.[17] Therefore, the occurrence of intermolecular Zn···Br interactions necessarily implies the formation of aggregate structures.
20. See, for example: *(a)* Mo, H.; Wang, A.; Wilkinson, P. S.; Pochapsky, T. C. *J. Am. Chem. Soc.* **1997**, *119*, 11666. *(b)* Kraus, C. A. *J. Phys. Chem.* **1956**, *60*, 129.
21. For some recent contributions, see for example: *(a)* Chockla, A. M.; Harris, J. T.; Korgel, B. A. *Chem. Mater.* **2011**, *23*, 1964. *(b)* Chen, Y.-H.; Hung, H.-H.; Huang, M. H. *J. Am. Chem. Soc.* **2009**, *131*, 9114. *(c)* Gou, X.; Wang, G.; Kong, X.; Wexler, D.; Horvat, J.; Yang, J.; Park, J. *Chem. Eur. J.* **2008**, *14*, 5996. *(d)* Zhong, H.; Zhou, Y.; Yang, Y.; Yang, C.; Li, Y. *J. Phys. Chem. C* **2007**, *111*, 6538. *(e)* Chu, Y.; Hu, J.; Yang, W.; Wang, C.; Zhang, J. Z. *J. Phys. Chem. B* **2006**, *110*, 3135.
22. *(a)* Neelakandan, P. P.; Pan, Z.; Hariharan, M.; Zheng, Y.; Weissman, H.; Rybtchinski, B.; Lewis, F. D. *J. Am. Chem. Soc.* **2010**, *132*, 15808. *(b)* Ryu, J.-H.; Lee, E.; Lim, Y.-b.; Lee, M. *J. Am. Chem. Soc.* **2007**, *129*, 4808. *(c)* Guler, M. O.; Hsu, L.; Soukasene, S.; Harrington, D. A.; Hulvat, J. F.; Stupp, S. I. *Biomacromolecules* **2006**, *7*, 1855. *(d)* Witte, T.; Decker, B.; Mattay, J.; Huber, K. *J. Am. Chem. Soc.* **2004**, *126*, 9276.

6 *Conclusions*

The research activity discussed in this PhD thesis has been focused on the synthesis, characterization and study of aggregation/deaggregation properties of Lewis acidic Zn^{II} Schiff base complexes **1a-5i** and their application as molecular probes for amines and alkaloids, NLO and vapochromic materials, and building blocks to formation of fibrillar and branched nanostructures in the solid state. Moreover, these complexes have been investigated to build up a new reliable Lewis acidity scale for amines and solvents.

The achievement of the amphiphilic complexes **1a-5i**, having conjugated and non-conjugated diamines as bridging groups and side alkyl chain with different length, has allowed the study of how the ligand framework influences the aggregation of these complexes in a variety of polar coordinating and non polar, non-coordinating solvents.

In absence of Lewis bases, the aggregation of Zn^{II} Schiff base complexes always occurs through intermolecular Zn···O interactions. However, it is found that the type and the degree of aggregation are strongly influenced by the bridging diamino group, independently from the side alkyl chains length. In particular, solutions of the complexes of naphthalene and pyridine series are always characterized by the presence of defined dimer aggregates, whereas oligomeric aggregates are likely formed for complexes of benzene series. In addition, the latter complexes in the solid state form fibrillar nanostructures through intermolecular Zn···O interactions, whose width is influenced by the different degree of interdigitation of side alkyl chains. For complexes of having the 2,3-diaminomaleonitrile bridge, the degree of aggregation is concentration dependence. Dilute solutions are likely characterized by the presence of defined dimer aggregates, whereas larger oligomeric aggregates are conceivably formed at higher concentrations. Finally, among of series of salen complexes, a reversible equilibrium between two defined dimeric species is observed, driven by the concentration of water dissolved in $CHCl_3$, which may be related to the non-conjugated, conformational flexible nature of salen bridge.

On the other hand, in coordinating solvents or upon addition of Lewis bases, a complete deaggregation of all complexes occurs through the axial Lewis acid/base interaction. This process is accompanied by considerable changes of their optical properties and the amount of Lewis base needed to a complete deaggregation is related to their Lewis acidic character. Thus, an order of the Lewis acidic character, **1** > **4** > **3** > **2** > **5**, can be established for the aggregate complexes in solution of non-coordinating solvents. In addition, the deaggregation process implies a switch-on of NLO properties of **1a**, allowing the possibility to use this molecular material for specific NLO applications.

The sensing properties of complex **1a** have been investigated for application as molecular probe, since its dramatic optical variations upon deaggregation. It has been found that the Zn^{II} complex **1a** is a sensitive fluorescent probe for alkaloids and amines in DCM, upon formation of 1:1 adducts. Its binding interaction can be related to Lewis basicity, strongly influenced by the steric characteristics of the coordinating nitrogen-based species, leading to high selectivity, in the micromolar range, and sensitivity for pyridine-based, cinchona alkaloids, primary and alicyclic amines. Moreover, the use of the Lewis acidic Zn^{II} complex **1a** has successfully allowed the achievement of a consistent, reliable scale of Lewis basicity for amines and solvents. It represents a unique set of data reflecting the actual Lewis basicity with respect this "*real world*" Lewis acidic species. In addition, vapochromic properties of **1a** upon coordination of volatile Lewis base vapours allowed the possibility to apply this complex as chemosensor in the solid state for coordinating volatile organic compounds (VOCs).

Finally, the design of complex **1d** having the bromide ion as peripheral groups, allowed obtaining branched nanostructures in the solid state. The mechanism of aggregation of **1d** is driven by intermolecular Zn···Br interactions because the Lewis base bromide ion of the ligand framework coordinates the Zn^{II} ion of another unit, thus allowing the formation of coral-like, branched nanostructures in the solid state.

7 *Experimental Section*

7.1 Materials and general procedures

All chemicals (Aldrich) have been used without purification, with the exception of:

- 2,3-diaminomaleonitrile: has been purified by recrystallization from an ethanol solution.
- 1,2-diaminobenzene: has been purified by crystallization from aqueous 1% sodium hydrosulphite.
- Papaverine: has been obtained from papaverine hydrochloride by extraction with a 3M solution of NaOH saturated with Na_2CO_3 in diethyl ether.

DCM and $CHCl_3$ stabilized with amylene have been used. DCM-d_2 and TCE have been dried over anhydrous potassium carbonate overnight before using. $CDCl_3$ containing 0.5 wt % silver foil as stabilizer and TCE-d_2 have been dried over molecular sieves (3 Å). CCl_4 has been distilled before using.

Solutions of **1a** for spectrophotometric, and fluorimetric measurements have been obtained from stock solutions 1.0×10^{-3} M, except for acetonitrile, mesitylene (1.0×10^{-4} M), and toluene (5.0×10^{-5} M), because of the lower solubility of **1a** in these last three solvents. Fresh prepared DCM solutions and 24-h aged mesitylene and toluene solutions have been used for spectrophotometric and fluorimetric measurements.

Column chromatography has been performed on silica gel 60 (230-400 mesh), eluting with cyclohexane and EtOAc. TLC have been performed using silica gel 60 F254 plates with visualization by UV and standard staining.

7.2 Absorption and fluorescence measurements

Optical absorption spectra have been recorded at room temperature with a Varian Cary 500 UV-Vis-NIR spectrophotometer. Fluorescence spectra have been recorded at room temperature with a Fluorolog-3 (Jobin Yvon Horiba) spectrofluorimeter.

The fluorescence quantum yield has been obtained using fluorescein (Φ_F = 0.925) in 0.1 M NaOH as standard. The absorbance value of the samples at and above the excitation wavelength has been lower than 0.1 for 1 cm pathlength cuvettes.

Spectrophotometric and fluorimetric titrations have been performed using a 1 cm path length cuvette equipped with a magnetic stirrer. Typically, to record a spectrum the species has been delivered by a precision buret. At least three replicate titrations have been performed for each species. In each fluorimetric titration the wavelength of excitation is related to an isosbestic point.

7.3 Calculation of binding constant with fluorescence titrations data

The **1a**·alkaloid and **1a**·amine binding constants, K, have been calculated from fluorescence titration data by the nonlinear curve fitting analysis of F *vs.* c_p in eq 1[1]

$$F = F_0 + \frac{F_{\lim} - F_0}{2c_0}\left[c_0 + c_p + \frac{1}{K} - \left[\left(c_0 + c_p + \frac{1}{K}\right)^2 - 4c_0c_p\right]^{\frac{1}{2}}\right] \qquad (1)$$

where F_0 is the initial fluorescence of the solution of **1a** having a concentration c_0, F is the fluorescence intensity after addition of a given amount of alkaloid/amine at a concentration c_p, and $F_{\lim}$ is the limiting fluorescence reached in the presence of an excess of alkaloid/amine.

The **1a**·dpe binding constants, K_1 and K_2 for the 1:1 and 2:1 species, respectively, have been estimated from fluorescence titration data by the nonlinear curve fitting analysis of F *vs.* [*dpe*] in eq 2:[2]

$$F = \frac{F_0 + F_{\lim}K_1[dpe]\left(1 + aK_2[dpe]\right)}{1 + K_1[dpe] + K_1K_2[dpe]^2} \qquad (2)$$

where F_0 is the initial fluorescence of the solution of **1a**, F is the fluorescence intensity after addition of a given amount of dpe, and $F_{\lim}$ is the limiting fluorescence reached in the presence of an excess of dpe. The parameter a represents the relative contribution of the 1:1 and 2:1 species to the total fluorescence of the solution.

7.4 Calculation of binding constant with absorption titrations data

The stoichiometry of the **1a**·Lewis base adducts has been initially determined by the mole ratio[3] and Job's plot methods.[4] Both methods indicate the presence of 1:1 **1a**·base adducts. However, since the above methods are not sensitive enough to reveal the presence of minor species that may accompany the formation of the 1:1 adducts, the speciation of the systems has been carried out resorting to multiwavelength and multivariate treatments of the spectral data, by using two different softwares, *i.e.*, SPECFIT[5] and HYPERQUAD.[6] However, under the actual experimental conditions of spectrophotometric titrations, the system indicates the presence of only two absorption species. Spectrophotometric data have been collected over the range 270-650 nm for all the investigated Lewis bases. These data have been initially analyzed by the software SPECFIT, which makes use of a multiwavelength and multivariate treatment of spectral data, combining a chemometric analysis (factor analysis and evolving factor analysis)[7] with a nonlinear least-squares minimization procedure. However, as the data compression procedure used by SPECFIT might introduce some distortion into the data, for this reason, the data have been double checked by using the HYPERQUAD program, which follows a different strategy to deduce the number of light absorbing species, by adopting a procedure that eliminates the accumulation of errors inherent in the matrix compression procedure.[8] Furthermore, HYPERQUAD is able to refine simultaneously the data from different titration measurements.[8a] At least three replicate titrations data have been refined for each base. Therefore, data reported in Table 4.3 refer to those achieved by the HYPERQUAD program. However, the binding constants values obtained by using the two different software packages gave, within the standard deviations, almost equal values.

7.5 Calculation of the limit of detection (LOD)

The LOD has been calculated from fluorescence data, according to IUPAC recommendations.[9] In particular, they have been calculated using eq 3:

$$\mathrm{LOD} = K \times \left(\frac{S_b}{S} \right) \qquad (3)$$

where K= 3, S_b is the standard deviation of the blank solution, and S is the slope of the calibration curve. In our case, because the DCM solution of **1a** gives a fluorescence signal without the presence of the amine, this signal is taken as the blank. Fifteen blank replicates have been considered. The calibration curve has been obtained from plots of the fluorescence intensity of **1a** *vs.* the concentration of the amine added. Each point is related to the mean value obtained from at least three replicate measurements.

7.6 Calculation of the limit of quantification (LOQ)

The LOQ has been calculated from fluorescence data, according to IUPAC recommendations.[9] In particular, they have been calculated using eq 4:

$$\mathrm{LOQ} = K \times \left(\frac{S_b}{S} \right) \qquad (4)$$

where K= 10, S_b is the standard deviation of the blank solution, and S is the slope of the calibration curve. In our case, because the DCM solution of **1a** gives a fluorescence signal without the presence of the alkaloid, this signal is taken as the blank. Fifteen blank replicates have been considered. The calibration curve has been obtained from plots of the fluorescence intensity of **1a** *vs.* the concentration of the alkaloid added. Each point is related to the mean value obtained from at least three replicate measurements.

7.7 Dipole moments measurements

Dipole moments, μ, have been determined using a WTWDM01 dipolemeter coupled with a RX-5000 ATAGO digital refractometer in order to measure, respectively, the dielectric constant and the refractive index of the solutions in $CHCl_3$. From these experimental data the dipole moment can be calculated according to the Guggenheim method.[10]

7.8 EFISH measurements

All EFISH measurements have been carried out at the Dipartimento di Chimica Inorganica Metallorganica e Analitica "Lamberto Malatesta" at the Università degli Studi di Milano, in DCM solutions in concentration ranges of 10^{-4}-10^{-3} M. The

measurements have been performed working with a non-resonant incident wavelength of 1.907 μm, which has been obtained by Raman-shifting the fundamental 1.064 μm wavelength that has been produced by a Q-switched, mode-locked Nd^{3+}-YAG laser manufactured by Atalaser. The apparatus for the EFISH measurements has been a prototype made by SOPRA (France). The $\mu\beta_{EFISH}$ values reported are the mean values of 16 successive measurements performed on the same sample. The sign of $\mu\beta$ has been determined by comparison with the reference solvent (DCM).

7.9 Elemental analysis

Elemental analyses have been performed on a Carlo Erba 1106 elemental analyzer.

7.10 Field emission scanning electron microscopy measurements

The cast film surface morphology has been examined by field emission scanning electron microscopy (FE-SEM) using a ZEISS SUPRA VP 55 microscope. Samples have been sputtered with gold to avoid charging effects.

7.11 FT-IR measurements

FT-IR spectra have been recorded on a Spectrum 100 spectrometer (Perkin Elmer) using a NaCl-plaques liquid-sample holder.

7.12 ^{1}H NMR measurements

Solution NMR experiments have been carried out on a Varian Unity Inova 500 (499.88 MHz for 1H) spectrometer using an inverse-detection tunable triple-resonance pfg 5 mm $^1H^{13}C\{X\}$ probe capable of generating field strengths of 60 G/cm.

All 1D ^{1}H NMR experiments have been referenced to tetramethylsilane ($Si(CH_3)_4$, TMS). Samples have been not spinning during all the analyses. The working temperature is 27°C, with exception for variable temperature experiments.

For 1D T-ROESY experiments, the ^{1}H 90° pulse has been 7.300 μs, with a relaxation delay of 3.5 s. 1D T-ROESY spectra have been obtained using a spin-lock time of 250 ms.

^{1}H DOSY experiments have been carried out at 27 °C, and referenced to the residual solvent signals ($CDCl_3$: 7.27 ppm; $CDCl_2CDCl_2$: 5.98 ppm; DMSO-d_6: 2.50 ppm). The gradient strength has been calibrated by using the HDO signal at 25 °C ($D = 19.02 \times 10^-$

^{10} m^2/s). The bipolar pulse pair stimulated echo pulse-sequence with convection compensation (Dbppste-cc in the standard Varian pulse sequence library) has been used for acquiring diffusion data with a diffusion delay (Δ) of 35 ms, a diffusion gradient length of 2.0 ms, and 128 increments for gradient levels. Gradient strengths of 2% and 95% of maximum power have been used to obtain spectral pairs with acquisition times of 2 s and recycle delays of 3.5 s. The Varian DOSY package has been used for the acquisition and processing (VnmrJ version 2.2, revision C).

Because the studies of aggregation require an estimate of the degree of aggregation, and since the structure of present complexes in solution is far from the spherical one, thus precluding a straightforward application of the Stokes-Einstein equation,[11] the molecular mass in solution (*m*) has been simply estimated using Graham's law of diffusion: $D = K(T/m)^{1/2}$, where the constant K depends on geometric factors, including the area over which the diffusion is occurring. By assuming a constant temperature and that K is the same for both species in solution, the relative diffusion rate of two species A and B is given by

$$\frac{D_A}{D_B} = \left(\frac{m_B}{m_A}\right)^{1/2}$$

This allows for the calculation of an unknown molecular mass via eq 5:

$$m_B = m_A\left(\frac{D_A}{D_B}\right)^2 \qquad (5)$$

Therefore, the diffusion rate values obtained by DOSY can be used to estimate the molecular mass of a species, by comparison with the actual D value of a known internal reference.[12] As reference, in the case of complexes **1a** and **2g**-**4g** the solvent has been used, while for the complex **5i**, it has been used the uncomplexed ligand **5'**.

7.13 Mass spectrometry measurements

MALDI TOF mass spectra have been recorded in linear mode with Voyager-DE PRO (Perseptive Biosystem) mass spectrometer instrument, equipped with a nitrogen

laser emitting at 337 nm, with a 3-ns pulse width and working in positive ion mode. The accelerating voltage has been 25 KV, the grid voltage and delay time (delayed extraction, time lag) have been optimized to achieve a higher mass resolution, expressed as the molar mass of a given ion divided by the full width at half maximum (FWHM). The laser irradiance has been maintained slightly above the threshold. For the complex **1a**, [meso-Tetra(pentafluoro phenyl)porphine] 0.1 M in THF solvent has been used as matrice. The concentration of the sample has been 5 mg/mL in THF solvent. 10 µl of sample solution have been mixed with 10 or 30 µl of [meso-Tetra(pentafluoro phenyl)porphine] solution, and 1 µl of each sample/matrix mixture has been spotted on the MALDI sample holder and slowly dried to allow matrix crystallization. For the complex **1d**, the sample dissolved in DCM solvent has been mixed with malononitrile/DMF, used as a matrix.

ESI mass spectra have been recorded with a Finnigan LCQ-Duo ion trap electrospray mass spectrometer (Thermo).

7.14 Preparation of drop-cast films

Films for SEM and UV-vis analysis have been obtained respectively by drop casting onto cleaned Si(100) and glass substrates. All films have been obtained by evaporation at room temperature of three drops of solution.

7.15 X-ray diffraction measurements

θ-2θ X-ray diffraction (XRD) patterns were recorded in grazing incidence mode (0.5°) on a Bruker-AXS D5005 θ-θ X-ray diffractometer, using a Göebel mirror to parallel Cu-K_α radiation operating at 40 KV and 30 mA.

7.16 References

1. Bourson, J.; Pouget, J.; Valeur, B. *J. Phys. Chem.* **1993**, *97*, 4552.
2. *(a)* Shen, X.; Belletête, M.; Durocher, G. J. *Phys. Chem. B* **1997**, *101*, 8212. *(b)* Nigan, S.; Durocher, G. *J. Phys. Chem.* **1996**, *100*, 7135. *(c)* Kusumoto, Y. *Chem Phys. Lett.* **1987**, *136*, 535.
3. Yoe, J. H.; Harvey, A. E. *J. Am. Chem. Soc.* **1948**, *70*, 648.
4. *(a)* Gil, V. M. S.; Oliveira, N. C. *J. Chem. Educ.* **1990**, *67*, 473. *(b)* Hill, Z. D.; MacCarthy, P. *J. Chem. Educ.* **1986**, *63*, 162. *(c)* Job, P. *Ann. Chem.* **1928**, *9*, 113.

5. Binstead, R. A.; Zuberbühler, A. D. *SPECFIT, a Global Analysis System with Expanded Factor Analysis and Marquardt Least Squares Minimization*; Spectrum Software Associates; Chapel Hill: NC, 1993-1999.
6. *(a)* Gans, P.; Sabatini, A.; Vacca, A. *Talanta* **1996**, *43*, 1739. *(b)* Sabatini, A.; Vacca, A.; Gans, P. *Coord. Chem. Rev.* **1992**, *120*, 389.
7. Gampp, H.; Maeder, M.; Meyer, C. J.; Zuberbühler, A. D. *Talanta* **1986**, *33*, 943.
8. *(a)* Contino, A.; Cucinotta, V.; Giuffrida, A.; Maccarrone, G.; Messina, M.; Puglisi, A.; Vecchio, G. *Tetrahedron Lett.* **2008**, *49*, 4765. *(b)* Arena, G.; Contino, A.; Maccarrone, G.; Sciotto, D.; Sgarlata, C. *Tetrahedron Lett.* **2007**, *48*, 8274. *(c)* Conato, C.; Contino, A.; Maccarrone, G.; Magrì, A.; Remelli, M.; Tabbì, G. *Thermochim. Acta* **2000**, *362*, 13.
9. *(a)* Currie, L. A. *Anal. Chim. Acta* **1999**, *391*, 127. *(b)* Analytical Methods Committee. *Analyst* **1987**, *112*, 199.
10. Guggenheim, E. A. *Trans. Faraday Soc.* **1949**, *45*, 714.
11. *(a*) Macchioni, A.; Ciancaleoni, G.; Zuccaccia, C.; Zuccaccia, D. *Chem. Soc. Rev.* **2008**, *37*, 479. *(b)* Pregosin, P. S. *Prog. Nucl. Magn. Reson. Spectrosc.* **2006**, *49*, 261. *(c)* Song, F.; Lancaster, S. J.; Cannon, R. D.; Schormann, M.; Humphrey, S. M.; Zuccaccia, C.; Macchioni, A.; Bochmann, M. *Organometallics* **2005**, *24*, 1315.
12. *(a)* Kagan, G.; Li, W.; Hopson, R.; Williard, P. G. *J. Am. Chem. Soc.* **2011**, *133*, 6596. *(b)* Fielden, J.; Long, D.; Slawin, A. M. Z.; Kolgerler, P.; Cronin, L. *Inorg. Chem.* **2007**, *46*, 9090.

A1 *List of Publications and Proceedings*

Publications

1. G. Consiglio, S. Failla, **I. P. Oliveri**, R. Purrello, and S. Di Bella
   Controlling the Molecular Aggregation. An Amphiphilic Schiff-Base Zinc(II) Complex as Supramolecular Fluorescent Probe.
   Dalton Trans. **2009**, 10426-10428.
   (http://dx.doi.org/10.1039/b914930a)

2. G. Consiglio, S. Failla, P. Finocchiaro, **I. P. Oliveri**, R. Purrello, and S. Di Bella
   Supramolecular Aggregation/Deaggregation in Amphiphilic Dipolar Schiff-Base Zinc(II) Complexes.
   Inorg. Chem. **2010**, 49, 5134-5142.
   (http://pubs.acs.org/doi/abs/10.1021/ic100284r)

3. **I. P. Oliveri** and S. Di Bella
   Highly Sensitive Fluorescent Probe for Detection of Alkaloids.
   Tetrahedron **2011**, 67, 9446-9449.
   (http://dx.doi.org/10.1016/j.tet.2011.09.100)

4. **I. P. Oliveri**, G. Maccarrone, and S. Di Bella
   A Lewis Basicity Scale in Dichloromethane for Amines and Common Nonprotogenic Solvents Using a Zinc(II) Schiff-Base Complex as Reference Lewis Acid.
   J. Org. Chem. **2011**, 76, 8879-8884.
   (http://pubs.acs.org/doi/abs/10.1021/jo2016218)

5. **I. P. Oliveri**, S. Failla, G. Malandrino, and S. Di Bella
   New Molecular Architectures by Aggregation of Tailored Zinc(II) Schiff-Base Complexes.
   New J. Chem. **2011**, 35, 2826-2831.
   (http://pubs.rsc.org/en/Content/ArticleLanding/2011/NJ/c1nj20618d)

6. **I. P. Oliveri**, and S. Di Bella
Sensitive Fluorescent Detection and Lewis Basicity of Aliphatic Amines.
J. Phys. Chem. A **2011**, 115, 14325-14330.
(http://dx.doi.org/10.1021/jp2066265)

7. G. Consiglio, S. Failla, P. Finocchiaro, **I. P. Oliveri**, and S. Di Bella
Aggregation Properties of Bis(salicyaldiminato)zinc(II) Schiff-Base Complexes and their Lewis Acidic Character.
Dalton Trans. **2012**, 41, 387-395.
(http://pubs.rsc.org/en/content/articlelanding/2012/dt/c1dt11295c)

8. S. Di Bella, **I. P. Oliveri**, A. Colombo, C. Dragonetti, S. Righetto and D. Roberto
An unprecedented switching of the second-order nonlinear optical response in aggregate bis(salicylaldiminato)zinc(II) Schiff-base complexes.
Dalton Trans., **2012**, 41, 7013-7016.
(http://pubs.rsc.org/en/Content/ArticleLanding/2012/DT/c2dt30702b)

9. G. Consiglio, S. Failla, P. Finocchiaro, **I. P. Oliveri**, and S. Di Bella
An Unprecedented Structural Interconversion in Solution of Aggregate Zinc(II) Salen Schiff-Base Complexes.
Inorg. Chem. **2012**, 51, 8409-8418.
(http://dx.doi.org/10.1021/ic300954y)

Proceedings

1. **I. P. Oliveri**, G. Consiglio, S. Failla, R. Purrello, S. Di Bella
   An amphiphilic Schiff-base Zinc(II) Complex as Supramolecular Fluorescent Probe for *N*-Heterocycles.
   Convegno SAMIC 2009, INSTM-Bressanone, 30 November-3 December 2009 (Poster P14)

2. **I. P. Oliveri**, G. Consiglio, S. Failla, R. Purrello, S. Di Bella
   Studio dell'Aggregazione Molecolare di Complessi Anfifilici di Zinco(II) derivati da Basi di Schiff: "Probes" Supramolecolari Fluorescenti di Composti *N*-Eterociclici.
   Convegno SCI Sezioni Calabria e Sicilia 2009, Catania, 1-2 December 2009 (Oral O32)

3. S. Failla, P. Finocchiaro, G. Consiglio, **I. P. Oliveri**, R. Purrello, S. Di Bella
   Synthesis, Characterization and Aggregation/Deaggregation Properties of Amphiphilic Schiff-Base Zinc (II) Complexes.
   VII Convegno AICing 2010, Bressanone, 5-8 September 2010 (Poster P63)

4. **I. P. Oliveri**, and S. Di Bella
   Zn^{II} Schiff Base Molecular Materials: Highly Sensitive Fluorescent Probes for Detection of Alkaloids.
   VIII INSTM CONFERENCE, Catania, 26-29 June 2011 (Poster P67)

5. **I. P. Oliveri**, S. Di Bella and S. Failla
   Aggregation/deaggregation properties of Zn^{II} Schiff-Base complexes and their applications as molecular probes, nonlinear optical materials and building blocks for new supramolecular architectures.
   VIII Convegno AICIng 2012, Catania, 16-19 September 2012 (Oral O3)
   I. P. Oliveri, S. Di Bella, G. Consiglio, S. Failla, and P. Finocchiaro
   Zinc(II) salen Schiff-Base complexes: unprecedented aggregation behaviour in solution.
   VIII Convegno AICIng 2012, Catania, 16-19 September 2012 (Poster P27)

Ringraziamenti

La presente tesi di dottorato è il frutto di tre anni d'intenso lavoro di ricerca, durante i quali ho potuto consolidare il mio profondo amore per la chimica e per la ricerca scientifica. Nel corso della mia attività di ricerca, ho avuto modo di lavorare con diversi professori, avendo così la possibilità di crescere scientificamente e umanamente traendo il massimo vantaggio da questa esperienza lavorativa. Per questo, colgo l'occasione per ringraziarli singolarmente per tutto ciò che mi hanno dato in questi tre anni di dottorato.

Ringrazio di cuore il *Prof. Salvatore Failla* per avermi trasmesso l'amore per la chimica e per avermi guidato e consigliato nell'attività di sintesi organica svolta durante la mia attività di ricerca. Desidero ringraziarlo per i modi sempre gentili e pacati che ha utilizzato sia per gratificarmi, sia per correggermi. Inoltre lo ringrazio per avermi dato l'opportunità di lavorare nel suo laboratorio e di aiutarlo durante lo svolgimento dell'*VIII Convegno Nazionale dell'Associazione di Chimica per Ingegneria AICINg 2012*, di cui è stato il coordinatore scientifico.

Ringrazio il *Dott. Giuseppe Consiglio* per avermi trasmesso la sua esperienza e conoscenza nell'ambito della sintesi organica. Desidero ringraziarlo per la pazienza e la disponibilità con cui mi ha insegnato le varie tecniche utili per l'ottenimento di tutti i composti studiati. Inoltre lo ringrazio anche per il suo contributo sia umano che scientifico profuso durante tutta la mia attività di ricerca.

Ringrazio il *Prof. Giuseppe Maccarrone* per il suo contributo scientifico nella determinazione analitica delle costanti di formazione riportate nel mio lavoro di tesi. Desidero ringraziarlo per i suoi elogi riguardo ai dati analitici da me ottenuti e per i suoi utili consigli per poterli ulteriormente migliorare.

Ringrazio la *Prof.ssa Graziella Malandrino* per il suo contributo scientifico nelle misure SEM e XRD. La sua competenza e la sua sempre gentile disponibilità, mi hanno permesso di imparare molto riguardo queste tecniche di caratterizzazione.

Ringrazio la *Prof.ssa Dominique Roberto* (Università degli Studi di Milano) per avermi dato la possibilità di lavorare nel suo laboratorio e apprendere nuove conoscenze sulla tecnica EFISH. Inoltre, desidero ringraziarla anche per la sua disponibilità e calorosità con cui mi ha accolto durante tutto il periodo trascorso nel suo laboratorio.

Ringrazio il *Prof. Roberto Purrello* per avermi dato la possibilità di svolgere la mia attività scientifica nel suo laboratorio e per il suo contributo scientifico.

Ringrazio il *Prof. Paolo Finocchiaro* per il suo contributo scientifico profuso durante la mia attività di dottorato.

Desidero ringraziare affettuosamente il *Prof. Santo Di Bella*, il mio tutor di dottorato, nonché relatore delle mie tesi di laurea triennale e specialistica. Desidero ringraziarlo perché durante tutta la mia attività di ricerca, mi ha sempre seguito in modo attento e premuroso, trasmettendomi il corretto modo di condurre una ricerca scientifica, dalle misure sperimentali alla stesura di un articolo. È riuscito a infondermi tutto il suo amore per la ricerca scientifica e il bellissimo rapporto di stima e fiducia reciproca che si è instaurato in questi anni, mi ha permesso di svolgere nel migliore dei modi la mia attività lavorativa. Per me è un esempio da seguire per il suo spirito di dedizione e sacrificio nei confronti della ricerca. Lo ringrazio inoltre per tutto il sostegno umano donatomi in tutti i momenti in cui ne ho avuto davvero bisogno. Mi ha sempre trattato come un suo pari, e ciò mi ha permesso di acquisire più fiducia in me stesso e nelle mie capacità. Infine, lo ringrazio per tutti i suoi consigli e le sue correzioni, che hanno reso certamente migliore la mia tesi di dottorato. La sua guida mi ha permesso di crescere sia scientificamente sia umanamente e per questo non potrò mai ringraziarlo abbastanza.

Infine, con il seguente lavoro di tesi, colgo l'occasione per ringraziare tutta la mia famiglia, la mia ragazza, i miei colleghi e amici, poiché mi hanno sempre sostenuto in ogni momento del corso di dottorato e in tutta la mia carriera universitaria.

Grazie